Inner Piedmont geology in the South Mountains-Blue Ridge Foothills and the southwestern Brushy Mountains, central-western North Carolina

Carolina Geological Society
Annual Field Trip
October 19-20, 2002

Guidebook Editors:
Robert D. Hatcher, Jr. and Brendan R. Bream

Field Trip Leaders (in order of appearance):
Joseph C. Hill, Brendan R. Bream, Scott D. Giorgis, Scott T. Williams, James L. Kalbas, Arthur J. Merschat, and Russell W. Mapes

Acknowledgments and Credits

Sponsorship of CGS–2002 (received prior to printing) by:

Campbell and Associates, Inc., Columbia, South Carolina
Carolina Geological Conultants, Inc., Columbia, South Carolina
Central Savannah River Geological Society, Aiken, South Carolina
Steve Gurley, Consulting Soil Scientist, Lincolnton, North Carolina
Godfrey and Associates, Inc., Blythewood, South Carolina
Kubal and Furr, Greenville, South Carolina
Zemex Corporation, Spruce Pine, North Carolina

Vulcan Materials Company (Jim Stroud, Brad Allison) for access to the Lenoir Quarry.

Organization, registering participants, keeping financial records, and guidebook proofreading:
Nancy L. Meadows

The National Cooperative Mapping Program, EDMAP component grants (administered by the USGS), funded the detailed geologic mapping. Without these grants, none of the petrologic, geochronologic, or other research presented here would be meaningful.

Cooperation, encouragement, and field checking by North Carolina Geological Survey geologists:
Leonard S. Wiener
Carl E. Merschat
Mark W. Carter
and the cooperation of State Geologist (just retired):
Charles H. Gardner

Cover Photo:

Recording data on a traverse in the South Mountains, winter 1998. Scott T. Williams and Scott D. Giorgis in foreground. (Photo by Bob Hatcher.).

Adobe Pagemaker™ layout by Brendan R. Bream.

Inner Piedmont geology in the South Mountains-Blue Ridge Foothills and the southwestern Brushy Mountains, central-western North Carolina

Carolina Geological Society
Annual Field Trip
October 19-20, 2002

Guidebook Editors:
Robert D. Hatcher, Jr. and Brendan R. Bream

Field Trip Leaders (in order of appearance):
Joseph C. Hill, Brendan R. Bream, Scott D. Giorgis, Scott T. Williams, James L. Kalbas, Arthur J. Merschat, and Russell W. Mapes

Carolina Geological Society

http://carolinageologicalsociety.org/

2002 Officers

President.......Neil Gilbert
Vice-President.......Randy Cumbest
Secretary-Treasurer.......Duncan Heron

Board Members

Randy Cumbest
1015 Richardson Lake Rd.
Warrenville, SC 29851

Neil Gilbert
Zapata Engineering
1100 Kenilworh Avenue
Charlotte, NC 28204

Duncan Heron
Department of Earth and Ocean Sciences
Box 90230
Duke University
Durham, NC 27708-0230

Jim Hibbard
Box 8208 MEAS
NC State Univeristy
Raleigh, NC 27695

Bill Powell
Carolina Geological Consultants
619 Garmony Road
Columbia, SC 29212

Kevin Stewart
Department of Geological Sciences
University of North Carolina - Chapel Hill
Chapel Hill, North Carolina 27559

Doug Wyatt
118 Trailwood Ave.
Aiken, SC 29803

2002 Guidebook Contributors

Sara E. Bier
Department of Geosciences
Pennsylvania State University
503 Deike Building
University Park, PA 16802
sbier@geosc.psu.edu

Brendan R. Bream
Department of Geological Sciences
University of Tennessee–Knoxville
306 Geological Sciences Building
Knoxville, TN 37996-1410
bbream@utk.edu

John M. Garihan
Department of Earth and Environmental Sciences
Furman University
Greenville, SC 29613
Jack.Garihan@furman.edu

Scott D. Giorgis
Department of Geology and Geophysics
University of Wisconsin–Madison
1215 W. Dayton St.
Madison, WI 53706
scott@geology.wisc.edu

Robert D. Hatcher, Jr.
Department of Geological Sciences
University of Tennessee–Knoxville
306 Geological Sciences Building
Knoxville, TN 37996-1410
bobmap@utk.edu

Joseph C. Hill
Department of Geological Sciences
University of Missouri–Columbia
101 Geology Building
Columbia, MO 65211
jchill@tranquility.net

James L. Kalbas
Earth and Atmospheric Sciences
Purdue University
1397 Civil Engineering Building
West Lafayette, IN 47907-1397
jkalbas@purdue.edu

Russell W. Mapes
Department of Geological Sciences
University of North Carolina–Chapel Hill
CB 3315, Mitchell Hall
Chapel Hill, NC 275
mapes@email.unc.edu

Arthur J. Merschat
Department of Geological Sciences
University of Tennessee–Knoxville
306 Geological Sciences Building
Knoxville, TN 37996-1410
arthurmeschat@hotmail.com

Scott T. Williams
Rural Delivery 2
Box 74 J
Huntingdon, PA 16652
scottw@pennswoods.net

DEDICATION

Richard Goldsmith
William C. Overstreet

Two superb field geologists

CONTENTS

An Inner Piedmont primer

Robert D. Hatcher, Jr.
Department of Geological Sciences
University of Tennessee–Knoxville
306 Geological Sciences Building
Knoxville, TN 37996-1410
bobmap@utk.edu

INTRODUCTION

The Inner Piedmont is the focus of the 2002 Carolina Geological Society field trip for the fifth time in the history of the Society. The first was the 1963 meeting convened by Charles J. Cazeau and Charles Q. Brown to discuss Inner Piedmont geology near Clemson, South Carolina (Cazeau and Brown, 1963). Villard S. Griffin and I convened the 1969 CGS meeting again at Clemson, South Carolina (Griffin, 1969; Hatcher, 1969) to present new concepts and compare the geology of the Brevard fault zone, nonmigmatitic Chauga belt, and migmatitic western Inner Piedmont. This meeting presented the first detailed geologic mapping completed in the western Inner Piedmont The earlier work of Overstreet et al. 1963a, 1963b, in the North Carolina eastern Inner Piedmont set the standard for detailed geologic mapping in the southern Appalachians. The late 1960s-early 1970s work, particularly that of Villard Griffin (1969, 1971, 1974a), revealed the basic structural framework of large plastic thrust sheets that is still valid in both Carolinas (Fig. 1). A great deal of new information and a number of new ideas have appeared since the 1969 field trip. The purpose of this primer is mostly to summarize some of the implications and additional problems arising from the newer work that are not discussed in other papers in this guidebook. The familiar attributes and basic knowledge about the Inner Piedmont were summarized in my paper in the 1993 guidebook (Hatcher, 1993) and thus are not repeated here.

Timothy L. Davis and Gregory M. Yanagihara, with my assistance, convened the 1993 CGS meeting and field trip at Hendersonville, North Carolina (Hatcher and Davis, 1993) to discuss their detailed studies from the Columbus Promontory along the North Carolina-South Carolina border northeastward to beyond Lake Lure. Last year John M. Garihan and William. A. Ranson (Ranson and Garihan, 2001) convened the CGS meeting in Greenville, South Carolina, to examine the results of several years of detailed geologic mapping in northern Greenville and Pickens Counties. Their mapping filled the gap that ties the earlier work by Griffin and myself to the southwest to that of Davis and Yanagihara to the northeast. The purposes of the 2002 CGS field trip are: (1) to present the results of ten person-years of detailed (1:12,000- and 1:24,000-scale) geologic mapping northwest of and in the South Mountains near Marion and Morganton, North Carolina, by five of my M.S. students, Brendan R. Bream (Bream, 1999), Joseph C. Hill (Hill, 1999), Scott D. Giorgis (Giorgis, 1999), Scott T. Williams (Williams, 2000), and Sara E. Bier (Bier, 2001); and (2) the results of three person-years of detailed geologic mapping in the Brushy Mountains northeast of Lenoir, North Carolina, by two of my most recent M.S. students, James L. Kalbas (Kalbas, in progress) and Arthur J. Merschat (Merschat, in progress). The South Mountains work adjoins the earlier work of Davis (1993a) and Yanagihara (1994) to the southwest, and the detailed mapping to the southeast by Overstreet et al. (1963a) and in the Shelby, North Carolina, 15-minute quadrangle and the southern part of the Casar 7 1/2-minute quadrangle by Overstreet et al. (1963b). Only a small gap in detailed mapping exists between the South Mountains and the Brushy Mountains. This gap is partially filled by the geologic map of the Lenoir 15-minute quadrangle (Reed, 1964), part of the Grandfather Mountain window map (Bryant and Reed, 1970), and reconnaissance mapping in the Charlotte 1˚ x 2˚ sheet by Goldsmith et al. (1988). So, continuous detailed geologic mapping currently exists over a distance of greater than 250 km in the Inner Piedmont from the Alto allochthon in northeastern Georgia and northwestern South Carolina (Hopson and Hatcher,

Hatcher, R.D., Jr., 2002, An Inner Piedmont primer, *in* Hatcher, R.D., Jr., and Bream, B.R., eds., Inner Piedmont geology in the South Mountains-Blue Ridge Foothills and the southwestern Brushy Mountains, central-western North Carolina: North Carolina Geological Survey, Carolina Geological Society annual field trip guidebook, p. 1-18.

1988) through the South Mountains and across the small gap to the Brushy Mountains in central-western North Carolina. This fortunate circumstance in map data, coupled with structural analysis, and new geochemical and geochronologic data, now permits us to more precisely address questions about: (1) the age, depositional history, and correlations (or lack of) with eastern Blue Ridge metasedimentary and metavolcanic assemblages; (2) the fundamental nature and continuity of large faults; (3) the timing of deformation and metamorphism; (4) the distribution of plutons with regard to both composition and age; and (5) the possible existence of terrane boundaries within the Inner Piedmont.

The Inner Piedmont extends some 700 km southwestward from the frame of the Sauratown Mountains window in North Carolina to the Coastal Plain overlap in Alabama (Fig. 1). Its width is about 100 km from the Brevard fault zone on the northwest to the Central Piedmont suture to the

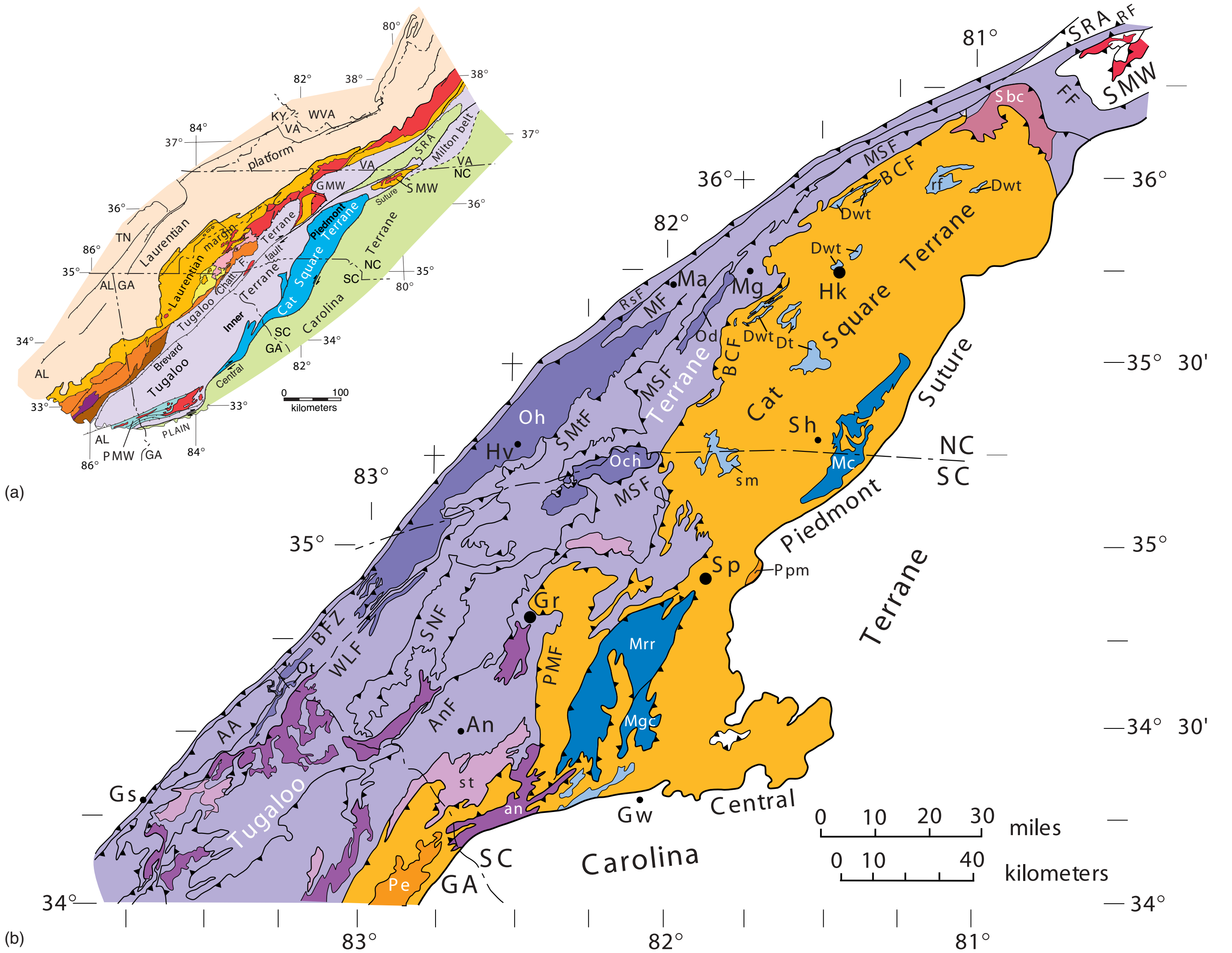

Figure 1. (a) Index map of the southern Appalachians showing the location of the Inner Piedmont and major tectonostratigraphic terranes. Chatt. F.–Chatahoochee fault. GMW–Grandfather Mountain window. PMW–Pine Mountain window. SMW–Sauratown Mountains window. SRA–Smith River allochthon. (b) Tectonic map of the Inner Piedmont in the Carolinas and northern Georgia, compiled and modified from numerous published sources cited herein and Hatcher (unpublished data). New age dates on several eastern Inner Piedmont granitoids are from Mapes (2002). Grenville basement (Sauratown Mountains window)–red. Faults: AA–Alto allochthon. AnF–Anderson. BCF–Brindle Creek. BFZ–Brevard. FF–Forbush. MF–Marion. MSF–Mill Spring. PMF–Paris Mountain. RF–Ridgeway. RsF–Rosman. SmtF–Sugarloaf Mountain. SNF–Six Mile-Seneca. WLF–Walhalla. Named Ordovician (purple) and Ordovician(?) (lighter purple) granitoids: Och–Caesars Head. Od–Dysartsville. Oh–Henderson. Ot–Toccoa. an–Antreville. st–Starr. Others in the western Inner Piedmont colored lighter shades of purple. Silurian granitoid: Sbc–Brooks Crossroads. Devonian and Devonian(?) granitoid plutons (light blue): Dt–Toluca. Dwt–Walker Top. rf–Rocky Face. sm– Sandy Mush. Mississippian granitoids: Mc–Cherryville Mgc–Gray Court. Mrr–Reedy River. Pennsylvanian granitoids: Pe–Elberton. Ppm–Pacolet Mills (Carolina terrane). Towns: An–Anderson. Gr–Greenville. Gs–Gainesville. Gw–Greenwood. Hk–Hickory. Hv–Hendersonville. Ma–Marion. Mg–Morganton. Sh–Shelby. Sp–Spartanburg.

southeast. Although the flanks are lower grade, its core comprises one of the largest areas of sillimanite grade metamorphism and migmatization in the world, comparable in extent to the Monashee complex in British Columbia (Greenwood, et al., 1991). As is discussed in greater detail below, the Inner Piedmont is linked stratigraphically to the eastern Blue Ridge (Hatcher, 1987; Hopson and Hatcher, 1988; Bream, 1999; Hill, 1999). Although it may have a Laurentian provenance and remains part of the Piedmont terrane of Williams and Hatcher (1983), its peculiar and unique structural style, kinematics, and uniformly extensive migmatitic character set the Inner Piedmont apart from the eastern Blue Ridge.

The structure of the western Inner Piedmont is dominated by a series of thrust sheets originally recognized by Griffin (1969, 1971, 1974a). The boundary of the migmatitic Inner Piedmont and the Chauga belt in South Carolina is formed by the Walhalla nappe, a Type F (fold-related; Hatcher and Hooper, 1992) thrust with a displacement that ranges from zero to a few kilometers. Within the Chauga belt in South Carolina is at least one major high temperature thrust and strike-slip fault, the Stumphouse Mountain fault (Hatcher and Acker, 1984; Liu, 1991). Southeast of the nonmigmatitic Chauga belt and migmatitic Walhalla nappe in South Carolina is the Six Mile nappe, and farther southeast is the Anderson nappe (Griffin, 1974a). Davis (1993a, 1993b) recognized the Tumblebug Creek, Sugarloaf Mountain, and Mill Spring thrusts in the Inner Piedmont in southern North Carolina. Based on their work in northern Greenville County and adjacent Pickens County, South Carolina, Garihan (2001), Ranson and Garihan (2001), and Garihan (this guidebook) concluded the Sugarloaf Mountain thrust in North Carolina is also recognizable in South Carolina, and represents the northern continuation of the Six Mile thrust sheet.

The dominant foliation in the Inner Piedmont was concluded by Hopson and Hatcher (1988) and Davis (1993a, 1993b) to be S_2 that formed close to the metamorphic peak. Osberg et al. (1989, their Fig. 2B) suggested and Davis also concluded that peak metamorphism and migmatization occurred during a mid-Paleozoic Acadian event. Dennis and Wright (1997) more recently determined U-Pb ages of monazite in the South Carolina Inner Piedmont, yielding 360 and 320 Ma ages; Carrigan et al. (2001) and Bream (this guidebook) have determined U-Pb ages of zircon rims using the ion microprobe, yielding 360-350 Ma, and a group of younger ages clustering about 325 Ma (Alleghanian). These data have confirmed that peak metamorphism in the Inner Piedmont and eastern Blue Ridge (Tugaloo terrane, Fig. 1a) was Acadian (or more properly, "Neoacadian").

FUNDAMENTAL AND RECENTLY DISCOVERED STRATIGRAPHIC, PLUTONIC, AND STRUCTURAL RELATIONSHIPS

The purpose here is to summarize some new solutions to old problems in light of some of the new field and laboratory data and to address some new problems that have arisen because of the accumulation of new data. These new problems constitute opportunities for future research on the nature and origin(s) of the Inner Piedmont and the terranes that comprise it.

Stratigraphic Relationships and the Henderson Gneiss Enigma

Tugaloo Terrane Stratigraphy. The most widespread unit in the Tugaloo terrane is the Tallulah Falls-Ashe Formation that occupies most of the outcrop area in the eastern Blue Ridge (Chattahoochee thrust sheet) and Inner Piedmont west of the Brindle Creek fault. The Tallulah Falls Formation, like Gaul (Caesar, 52 B.C.), comprises three parts: the lower graywacke-schist-amphibolite member that is separated from the upper graywacke-schist member by the aluminous schist member, the critical traceable marker unit for subdividing the formation. This stratigraphy was first recognized in the Whetstone quadrangle in the northwestern South Carolina, eastern Blue Ridge, by L. L. Acker and myself following a suggestion from H. S. Johnson, Jr., based on experience mapping the same units (now Ashe Formation) in the Spruce Pine pegmatite district, North Carolina (Brobst, 1962). We subsequently subdivided the Tallulah Falls Formation throughout the remainder of Oconee County, South Carolina, Rabun, and most of Habersham Counties, Georgia (with the assistance of J. E. Wright, Jr.) (Hatcher, 1971, in preparation).

The Tallulah Falls Formation in the area of the 2002 CGS field trip has been subdivided by Bream (1999) and Hill (1999) into the same tripartite stratigraphy at staurolite-kyanite, kyanite (Stop 1), and sillimanite grade (Stop 2) immediately southeast of the Brevard fault zone in the Marion-Sugar Hill area. To the southeast, the Tallulah Falls Formation is overlain by synclinally preserved sillimanite grade Poor Mountain Amphibolite and then Poor Mountain Quartzite in the footwall of the Mill Spring thrust. The entire sequence is repeated again in the Mill Spring thrust sheet where migmatization becomes intense in the immediate footwall of the Brindle Creek thrust (Giorgis, 1999; Williams, 2000). This stratigraphy was not recognized by Reed (1964) in the Lenoir quadrangle, although (Hill, 1999) easily mapped it into the portion of the Inner Piedmont shown on the map by Bryant and Reed (1970), nor were the subdivisions recognized by Rankin et al. (1972) or Espenshade et al. (1975) despite mapping an extensive area of Ashe Formation in the Inner Piedmont immediately southwest of the Sauratown Mountains window. Heyn (1984), however, did recognize the tripartite subdivision at staurolite-kyanite grade in this same area.

Stratigraphic relationships in the Inner Piedmont are best understood in the westernmost largely nonmigmatitic Chauga belt in South Carolina (Hatcher, 1972) and in the Marion-Sugar Hill area in North Carolina at the northeast end of the belt occupied by Early Ordovician Henderson Gneiss. The Brevard fault zone, with its mappable Chauga River Formation stratigraphy (Hatcher, 1969), occupies the northwestern flank of the Chauga belt. This stratigraphy is clearly mappable continuously (but not unbroken), despite complex faulting from northeastern Georgia (near Gainesville) at least to the latitude of Rosman, North Carolina, where Horton (1982) was able to recognize most of its components. From Rosman northeastward most of the Brevard fault zone occurs beneath the floodplains of major rivers thus limiting exposure.

The Chauga River Formation, and what was originally considered its southeastern equivalent, the Poor Mountain Formation (see Hatcher, 1993, his Fig. 2b), occupy most of the Chauga belt in western Oconee County, South Carolina (Hatcher, in preparation). Chauga River Formation rocks rest on metagraywacke in the Brevard fault zone in the Tugaloo Lake quadrangle along the Georgia-South Carolina border (Hatcher, in preparation) (Fig. 2), suggesting that these two units may rest on the upper Tallulah Falls Formation in the westernmost Chauga belt and eastern Blue Ridge (Fig. 2). There appears to be a locally unfaulted contact here between the Chauga River Formation and the main Tallulah Falls Formation sequence in the Blue Ridge at the western edge of the Brevard fault zone in the Tugaloo Lake quadrangle (Fig. 2). Chauga River Formation (Cambrian to Lower Ordovician?) metasiltstone and overlying Middle Ordovician (Bream, this guidebook) Poor Mountain Formation rocks, plus the overlying (by faulting) Early Ordovician (Vinson, 2001) Henderson Gneiss, are repeated in several thrust sheets at the southwest end of the Henderson Gneiss outcrop belt (Fig. 3). Ironically, at the northeastern end of the Henderson Gneiss outcrop belt southwest of Marion, North Carolina, instead of *younger* Chauga River and Poor Mountain rocks, the northeast-striking garnet-aluminous schist member (staurolite-kyanite-bearing) and the other two members of the *older* Tallulah Falls Formation are truncated against the northeastern contact of the main Henderson Gneiss body (Fig. 4).

The Brevard fault zone at the latitude of the 2002 Carolina Geological Society field trip contains elements of Chauga River Formation stratigraphy, but not enough based on current knowledge that a conclusive statement can be made about the continuity of that stratigraphy here. Poor Mountain Formation rocks do not occur in contact with the Henderson Gneiss in this area, but do occur sequentially above the Tallulah Falls Formation to the southeast in the Sugarloaf Mountain thrust sheet (Bream, 1999; Hill, 1999). Poor Mountain Formation here consists of: (1) the Poor Mountain (Cedar Creek) Amphibolite Member, a Middle Ordovician MORB metavolcanic sequence if standard tectonic discriminant diagrams are employed (Davis, 1993a) (Figs. 5, 6, and 7); and (2) the overlying Poor Mountain Quartzite, a Middle Ordovician (Bream, this guidebook) quartzite and interlayered silicified felsic tuff that contains marble in South Carolina (Shufflebarger, 1961; Hatcher 1969) (Fig. 3).

We will examine the well-exposed unconformable contact between the Tallulah Falls Formation and the overlying Poor Mountain Amphibolite at STOP 4 on the first day of the field trip. The recognition of Poor Mountain Formation units resting unconformably above the Tallulah Falls Formation provides another tie between western Inner Piedmont and eastern Blue Ridge assemblages, once more indicating the Brevard fault zone is not a suture joining separate accreted terranes (see Hatcher, 2001a, for a discussion of Brevard fault zone history). An additional ion microprobe date on detrital zircons from the Brevard-Poor Mountain transitional member metasiltstone in South Carolina reveals the dominant 1.1 Ga suite of the underlying Tallulah Falls Formation metasandstones, without any trace of younger components (Bream, this guidebook). Based on these new zircon data, the tie of the metasiltstone with the underlying Tallulah Falls Formation and lack of a tie to the overlying Poor Mountain Formation indicates that the original correlation of the Chauga River Formation with the Poor Mountain Formation by Hatcher (1969, his Fig. 7, upper diagram) is incorrect. The gradational and interlayered character of the Brevard phyllonite and Brevard-Poor Mountain transitional units with Poor Mountain Amphibolite and interlayering of the amphibolite in the other two units (Hatcher, 1969, 1993) remains problematic, but might be explained as an attribute of transposition. This interlayering, however, occurs to such a degree that separate pelitic interlayers may be present in the Poor Mountain Amphibolite and a different amphibolite component may be present in the Chauga River Formation. An unconformity below the Poor Mountain Amphibolite, however, helps explain the absence of the Brevard-Poor Mountain transitional metasiltstone unit beneath the amphibolite in the Marion-Morganton, North Carolina, area and its presence in the Columbus Promontory, and to the southwest.

A major revision of the stratigraphic relationships for the western Inner Piedmont (and remainder of the Tugaloo terrane in the eastern Blue Ridge) (Fig. 8) thus would have

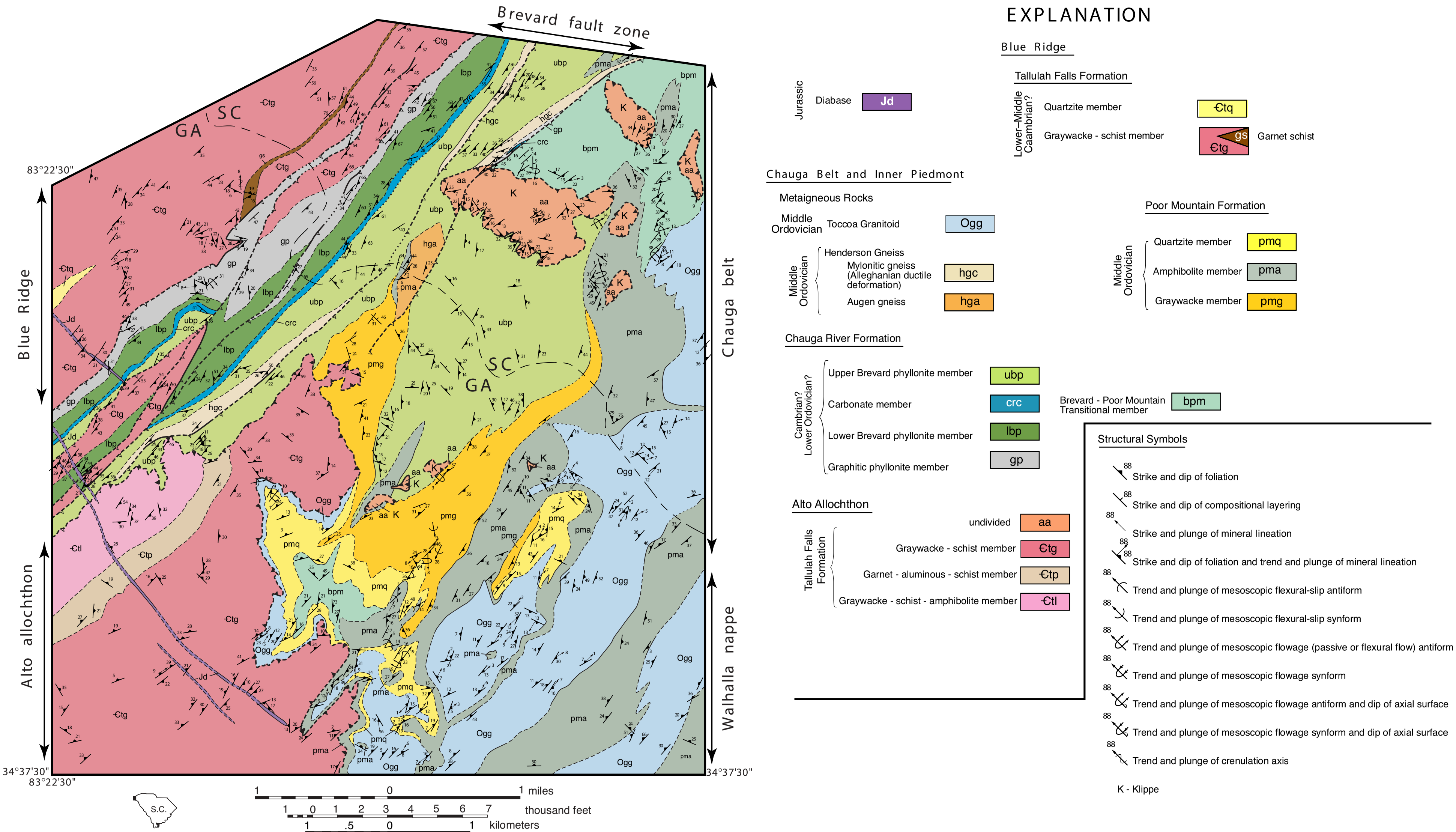

Figure 2. Detailed geologic map of the southwest part of the Tugaloo Lake quadrangle, South Carolina-Georgia (Hatcher, in preparation). Geology by RDH assisted by Louis L. Acker, William M. Rivers, D. Hoke Petrie, Stephen L. Wood and David E. Howell (1968-1976). Mylar drafting assisted by Teunis Heyn. Map editing by A. J. Zupan. Computer drafting by Scott D. Giorgis.

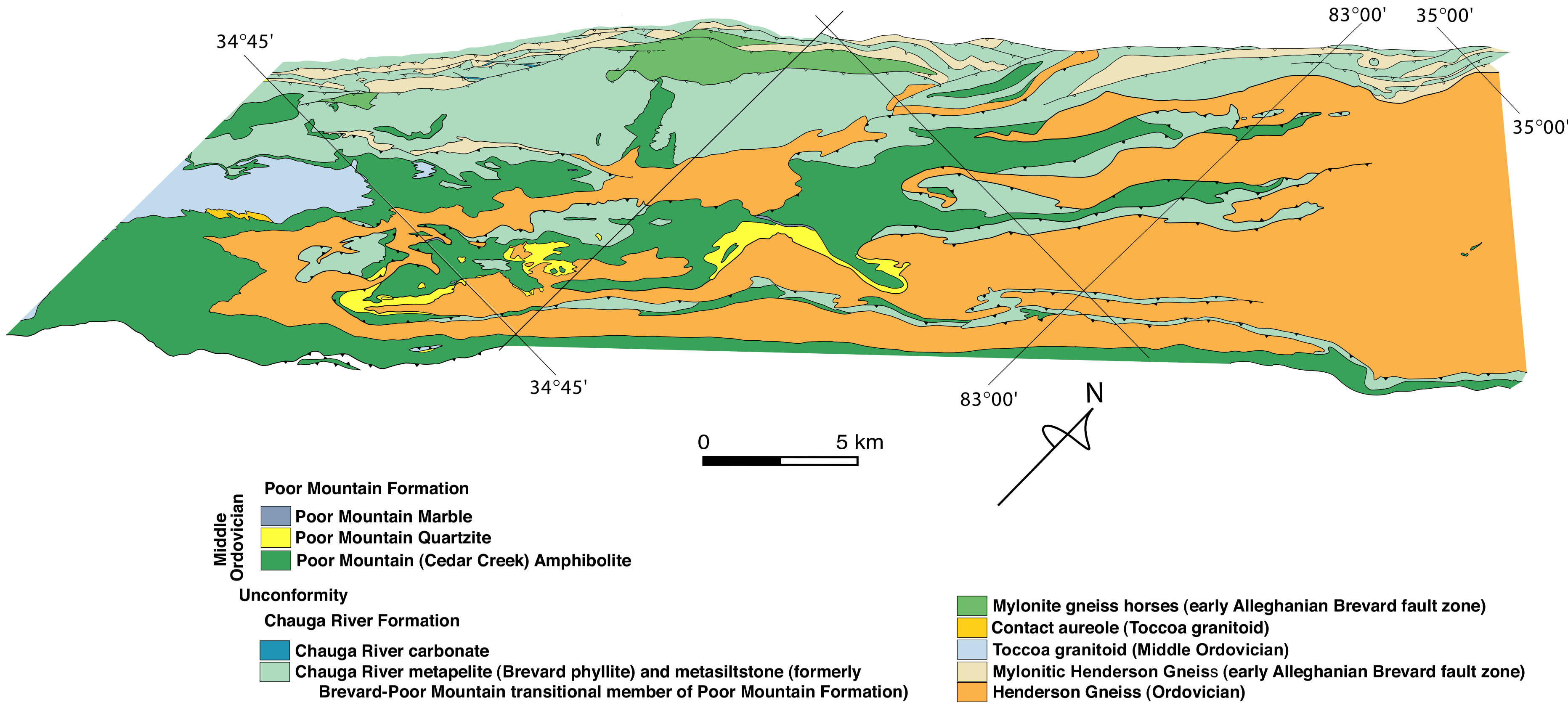

Figure 3. Detailed geologic map at the southwest end of the Henderson Gneiss in South Carolina. Note that there is an early set of thrusts (with solid teeth) and a later set (with open teeth) confined to the Brevard fault zone. Although the early faults have the map configurations of low-angle thrusts, shear-sense indicators and shallow plunge and strong NE orientation of the prominent high temperature mineral stretching lineation in the Chauga belt indicate the thrusts were moving southwest. Apparent NW verging early plastic (isoclinal-recumbent) folds are probably components of the NW limbs of SW-directed sheath folds. Macroscale patterns of interaction of the early folds and faults with the later early Alleghanian Brevard fault zone faults, coupled with the strong NE-trending, shallow plunging mineral stretching lineation and S–C fabric, suggest that the early Alleghanian faults are also dextral with a dip-slip component. Compiled and modified from Griffin (1973, 1974b), Hatcher and Acker (1984), Hatcher (in preparation), and Hatcher and Acker (unpublished data in the Tamassee quadrangle, South Carolina-Georgia). Electronic graphics at the southwest end of this figure by Scott. D. Giorgis.

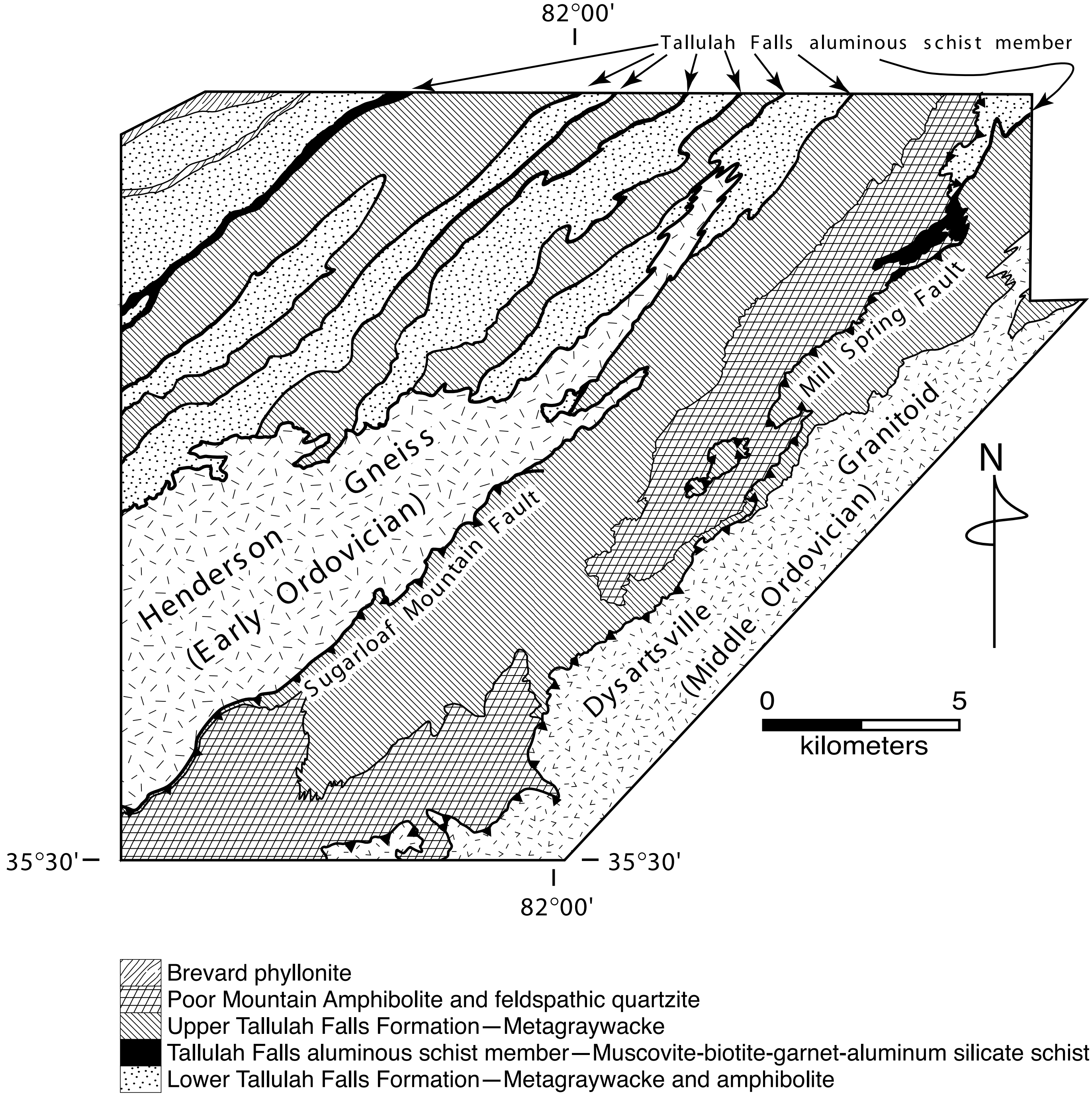

Figure 4. Detailed geologic map at the northeastern end of the main body of Henderson Gneiss. Note multiple truncations of folded Tallulah Falls Formation units by the Henderson Gneiss contact. From Hill (1999) and Bream (1999). Modified from a map compiled by Brendan R. Bream.

Tallulah Falls Formation (Lower to Middle Cambrian?) deposited on mostly oceanic crust and fragments of Grenvillian continental basement. The Chauga River Formation (Cambrian to Lower Ordovician?) would then be deposited on the Tallulah Falls, partial regional uplift occurred, and erosion removed part of the Chauga River Formation in the western Inner Piedmont in North Carolina. Subsidence would have occurred again and Middle Ordovician (~460 Ma) MORB volcanic rocks were extruded onto the sea floor that were succeeded by clean quartzite with felsic tuff and clean limestone (in South Carolina) interlayers. It is also interesting that the age of this unconformity is the same as the Middle Ordovician (Knox) unconformity throughout the Appalachian platform and into the North American cratonic interior. The Middle Ordovician plutonic-volcanic event in the Tugaloo terrane and Dahlonega

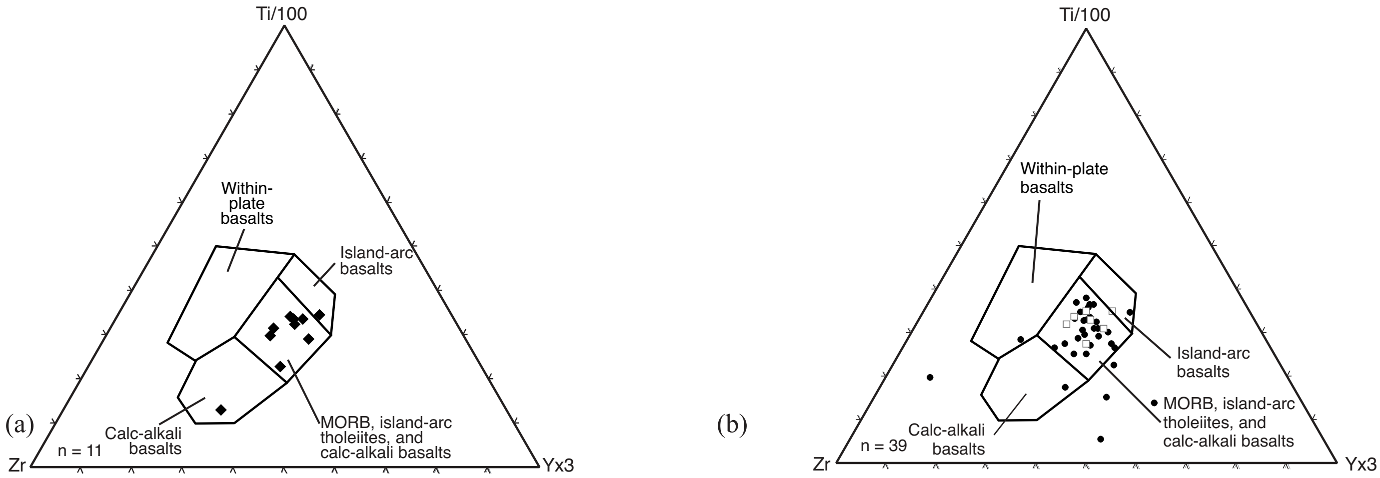

Figure 5. Ti-Zr-Y tectonic discrimination diagrams for Poor Mountain Amphibolite (after Pearce and Cann, 1973). (a) Plot of new South Mountains Poor Mountain Amphibolite data. ICP-MS analyses were performed by Activation Laboratories, Ancaster, Ontario. (b) Poor Mountain Amphibolite analyses from Davis (1993a), Yanagihara (1994), Bream (1999), and Kalbas (in preparation). Black dots–data from Davis (1993b) and Yanagihara (1994). Open squares–data from Bream (1999). Modified from plots by James L. Kalbas.

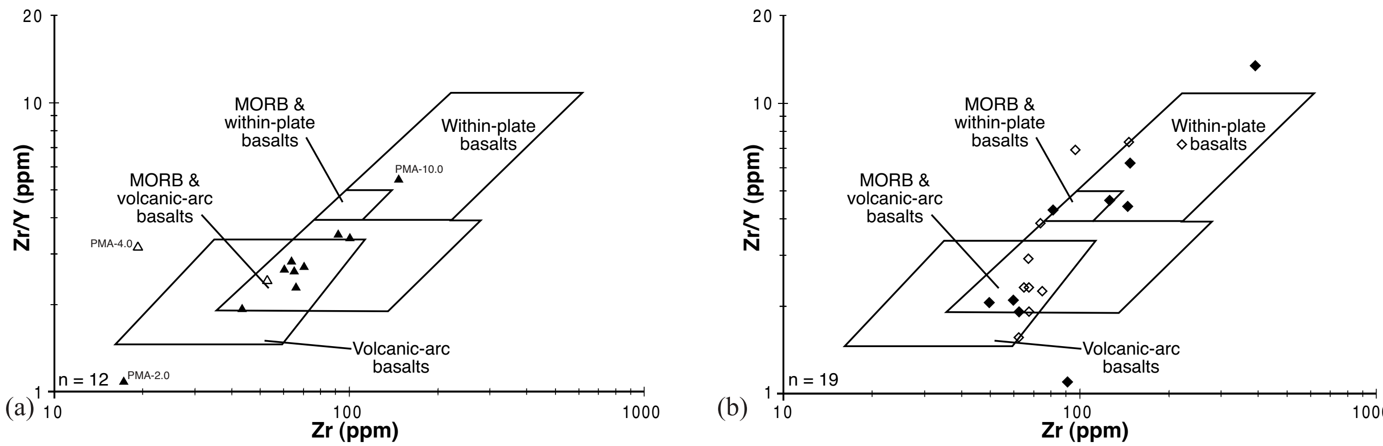

Figure 6. Zr vs. Y-Zr tectonic discrimination diagrams for Poor Mountain Amphibolite (after Pearce and Norry, 1979). (a) Plot of new South Mountains data. ICP-MS analyses were performed by Activation Laboratories, Ancaster, Ontario. (b) Plot of Poor Mountain Amphibolite samples from Davis (1993a), Yanagihara (1994), Bream (1999), and Kalbas (in preparation). Closed diamonds and triangles indicate CaO + MgO between 12-20%. Open triangles and diamonds indicate samples with CaO + MgO greater than, or less than 12-20%. Modified from plots by James L. Kalbas.

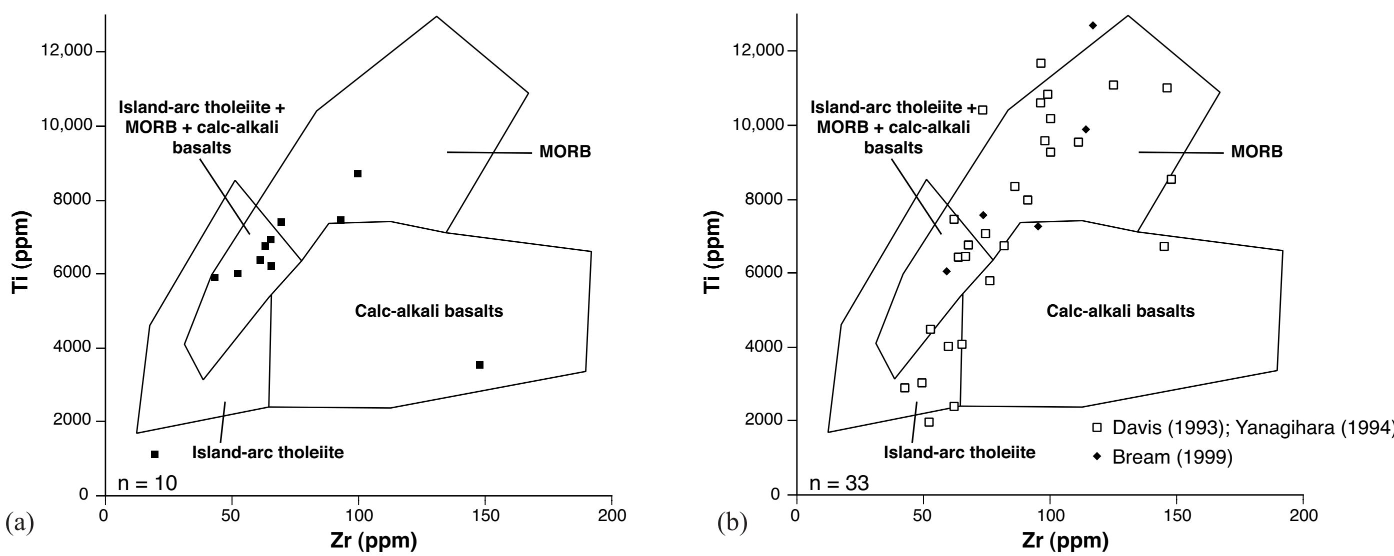

Figure 7. Ti/Zr tectonic discrimination diagrams for Poor Mountain Amphibolite (after Pearce and Cann, 1973). (a) Plots of new South Mountains data. ICP-MS analyses were performed by Activation Laboratories, Ancaster, Ontario. (b) Plots of Poor Mountain Amphibolite data from Davis (1993a), Yanagihara (1994), Bream (1999) and Kalbas (in preparation). Modified from plots by James L. Kalbas.

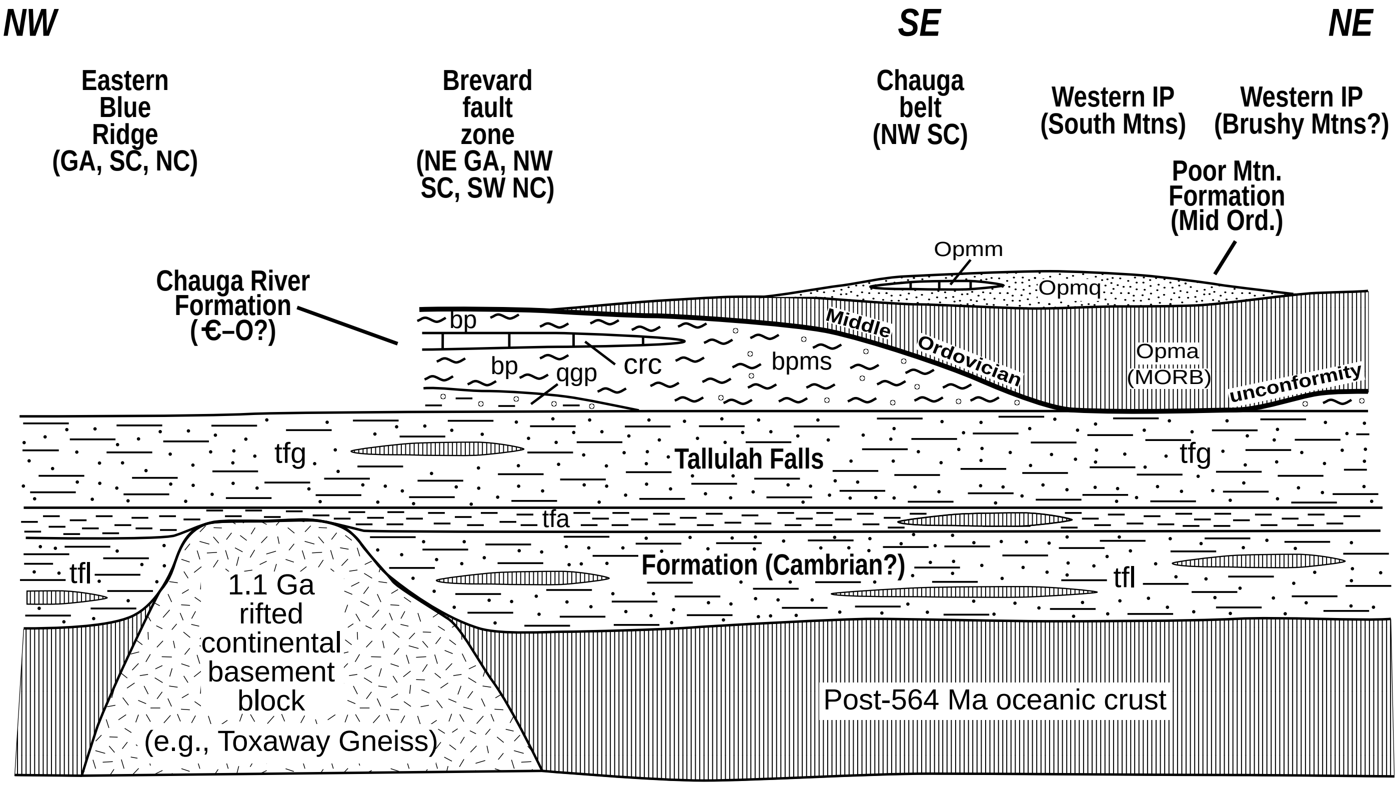

Figure 8. Revised stratigraphic relationships in the Tugaloo terrane based on Bream's (this guidebook) detrital and igneous zircon geochronologic data and field relationships. Both vertical and horizontal scales are approximate: the NW to SE segment is expanded relative to the compressed SE to NE segment. Tallulah Falls Formation members: tfl–Graywacke-schist-amphibolite member. tfa–Aluminous schist member. tfg–Graywacke-schist member. Note that, while amphibolite (vertical-ruled lenses) occurs in all members of the Tallulah Falls, it is most common in the lower member. Limited analyses of interlayered amphibolite indicate they have a more continental affinity (Bream, 1999), whereas definable mafic-ultramafic complexes have noncontinental affinities (Hatcher et al., 1984). Chauga River Formation subdivisions: qgp–Quartzite and graphitic phyllonite. bp–Brevard Phyllite Member. crc–Chauga River carbonate. bpms–interlayered Brevard phyllite and metasiltstone (formerly Brevard-Poor Mountain transitional member). Poor Mountain Formation members: Opma–Poor Mountain (Cedar Creek) Amphibolite. Opmq–Quartzite. Opmm–Marble.

gold belt may also be the source for the Middle Ordovician K-bentonites in the continental interior if the Tugaloo terrane was located adjacent to Laurentia at this time.

Henderson Gneiss Enigma. The Henderson Gneiss is one of the largest igneous bodies in the southern Appalachians (Figs. 1 and 9). The along-strike difference between the rock units that are in contact at the distal ends of the Henderson Gneiss outcrop belt is intriguing. The main Henderson body appears to climb section from the older Tallulah Falls Formation at the northeast end of its outcrop belt into the younger Poor Mountain Formation at the southwest end of the outcrop belt. One way to explain this relationship is to assume that the Henderson is simply a pluton that intruded the rocks with which it is presently in contact and the roots of the pluton lie near its northeastern terminus. No contact aureoles are known, however, in any part of the Henderson outcrop belt, even at the northeast end where the Henderson truncates folded Tallulah Falls aluminous schist and other metasedimentary rocks (Fig. 4) and at the southwest end where garnet grade rocks of a variety of compositions are in contact with the Henderson (Fig. 3). Henderson Gneiss, however, contains a strong high temperature mylonitic overprint (Davis, 1993a) such that very few domains of euhedral K-spar megacrysts survive. Southwest of the Keowee River in South Carolina the mylonitic overprint is so intense that most K-spar megacrysts are flattened into the dominant foliation forming S-tectonites or locally L-tectonites with Flinn's k values >10. A prominent northeast- (or southwest-) trending subhorizontal mineral lineation is present throughout this southwest domain. At the northeastern end of the body, the Henderson Gneiss is dominantly coarse augen gneiss containing the northeast-trending subhorizontal mineral lineation, but without the extreme flattening and elongation strain present at the southwestern end. The Henderson, however, is an S–C mylonite throughout (dextral motion), producing the augen fabric that characterizes most of the body, including the more extreme flattening, imbrication, and lineation that exists at its southwest end. The high temperature fabric is overprinted by the early Alleghanian ductile deformation and retrogressive metamorphism (to chlorite grade) along the northwestern part of the Henderson outcrop belt and in imbricates within the Brevard fault zone (Hatcher, 2001a) (Fig. 3).

Was the Henderson Gneiss body intruded into the Chauga belt, and later strongly deformed during Acadian peak metamorphism, or was the Henderson intruded elsewhere in the Ordovician, thrust over the Chauga belt later in the Taconian or during the Acadian orogeny, and then penetratively deformed and dextrally faulted during the Neoacadian, as described above? A partial answer could lie in the lenticular-shaped outcrops of Henderson Gneiss preserved northeast of the main body (Reed, 1964; Hill, 1999) (Fig. 9a). These could simply be interpreted as small satellite intrusions. Such bodies do not exist southeast or southwest of the main body of Henderson. The southwestern end is also imbricated (Fig. 3). Alternatively, these could be synformal outliers of sheath fold hinges that resulted from Acadian dextral noncoaxial deformation of the Chauga belt. One possibility is the original Henderson Gneiss pluton had a triaxial ellipsoid shape with the X (longest) axis either tilted slightly off the vertical or oriented subhorizontally NE-SW. Noncoaxial penetrative dextral Neoacadian deformation may have then changed the shape of the body to a flattened teardrop with the apex at the southwest end (Fig. 9b). Contacts of the Henderson with enclosing rocks, where exposed, are mylonitic, suggesting to Davis (1993b) that the contact is faulted. He named this the Tumblebug Creek fault (see CGS 1993 guidebook STOP 2) and concluded that it emplaced the Henderson Gneiss before D_2. A problem with this conclusion is that, while the Henderson Gneiss contact is probably everywhere faulted as Davis said, the contact truncates probable F_2 Neoacadian folds at the northeast end of the main body (Fig. 4). This truncation also prohibits the Henderson from being an *in situ* pluton, because the age of the pluton is Early Ordovician and it truncates Neoacadian (~350 Ma) folds.

EASTERN INNER PIEDMONT–THE BRINDLE CREEK FAULT

The staurolite-kyanite to sillimanite grade belt of Tallulah Falls Formation overlain by Poor Mountain Formation is truncated and overthrust (Mill Spring thrust) by sillimanite-bearing Tallulah Falls Formation that is again overlain in sequence by synclinally preserved Poor Mountain Amphibolite and Quartzite (Bream, 1999; Hill, 1999). This entire thrust sheet, however, is also migmatitic and becomes intensely migmatitic close to the Brindle Creek fault that bounds this sheet to the southeast (Giorgis, 1999; Williams, 2000; Kalbas, in preparation; Merschat and Kalbas, this guidebook).

Giorgis (1999) defined the Brindle Creek fault as a low-angle fault traceable across parts of the Morganton South and Dysartsville quadrangles in the South Mountains. Williams (2000) also traced the fault to the southwest across the remainder of the Dysartsville quadrangle. Although not indicated as a fault, this boundary was originally recognized and traced regionally throughout the Charlotte 1 x 2-degree sheet by Goldsmith et al. (1988). As mapped by Goldsmith et al. (1988), we now know that this boundary separates the western Inner Piedmont of recognizable Tallulah Falls and Poor Mountain Formation stratigraphy, and Ordovician granitoid plutons (Dysartsville–Caesars Head–Toccoa suite), from the eastern two-thirds of the Inner Piedmont composed predominantly of sillimanite schist and biotite gneiss, and Acadian granitoid plutons (Walker Top and Toluca granites), with some amphibolite. The fault has since been traced northeastward across the Kings Creek, Ellendale, and part of the Boomer quadrangles in the Brushy Mountains (Kalbas, in preparation; Merschat and Kalbas, this guidebook; Merschat, in preparation).

A major change in recognizable stratigraphy and plutons occurs at the Brindle Creek fault. The characteristic Tallulah Falls Formation stratigraphy is no longer recognizable, and no Poor Mountain Formation rocks have been recognized east of the Brindle Creek fault. Instead, the thick sillimanite schist that appears here may be overlain by the biotite gneiss (metagraywacke) unit. No Ordovician plutons have been recognized to date east of the fault, and none of the Acadian plutons occur west of the fault in North Carolina, except the Pink Beds, Looking Glass, Rabun, Yonah, Mount Airy, and Stone Mountain plutons in the eastern Blue Ridge.

A unit originally recognized by Goldsmith et al. (1988), a feldspar, quartz, biotite granitoid containing K-spar megacrysts with metamorphic myrmekite rims (that they identified as Rapakivi texture) was correlated with the Henderson Gneiss. This unit has been mapped throughout the Morganton South and Dysartsville quadrangles by Giorgis (1999) and Williams (2000). Giorgis (1999) gave it the informal name Walker Top orthogneiss and now Walker Top Granite (see Giorgis et al., this guidebook). The Walker Top orthogneiss has since yielded an ion probe date of ~370 Ma (Mapes et al., 2002; Giorgis et al., this guidebook), suggesting it is an Acadian pluton. It occurs only in the Brindle Creek thrust sheet. A mineralogical difference between the Henderson Gneiss and Walker Top Granite is the presence of both biotite and muscovite in the Henderson Gneiss, whereas the Walker Top contains an overwhelming dominance of biotite. The Toluca Granite (Overstreet et al., 1963a) also occurs in the Brindle Creek thrust sheet. It too has yielded a ~375 Ma Acadian ion microprobe age (Mapes et al., 2002).

The northern and southern extent of the Brindle Creek thrust is only speculative at present (Fig. 1b), but it may be the most fundamental boundary in the Inner Piedmont (Bream et al., 2001). A sinuous boundary separating biotite-

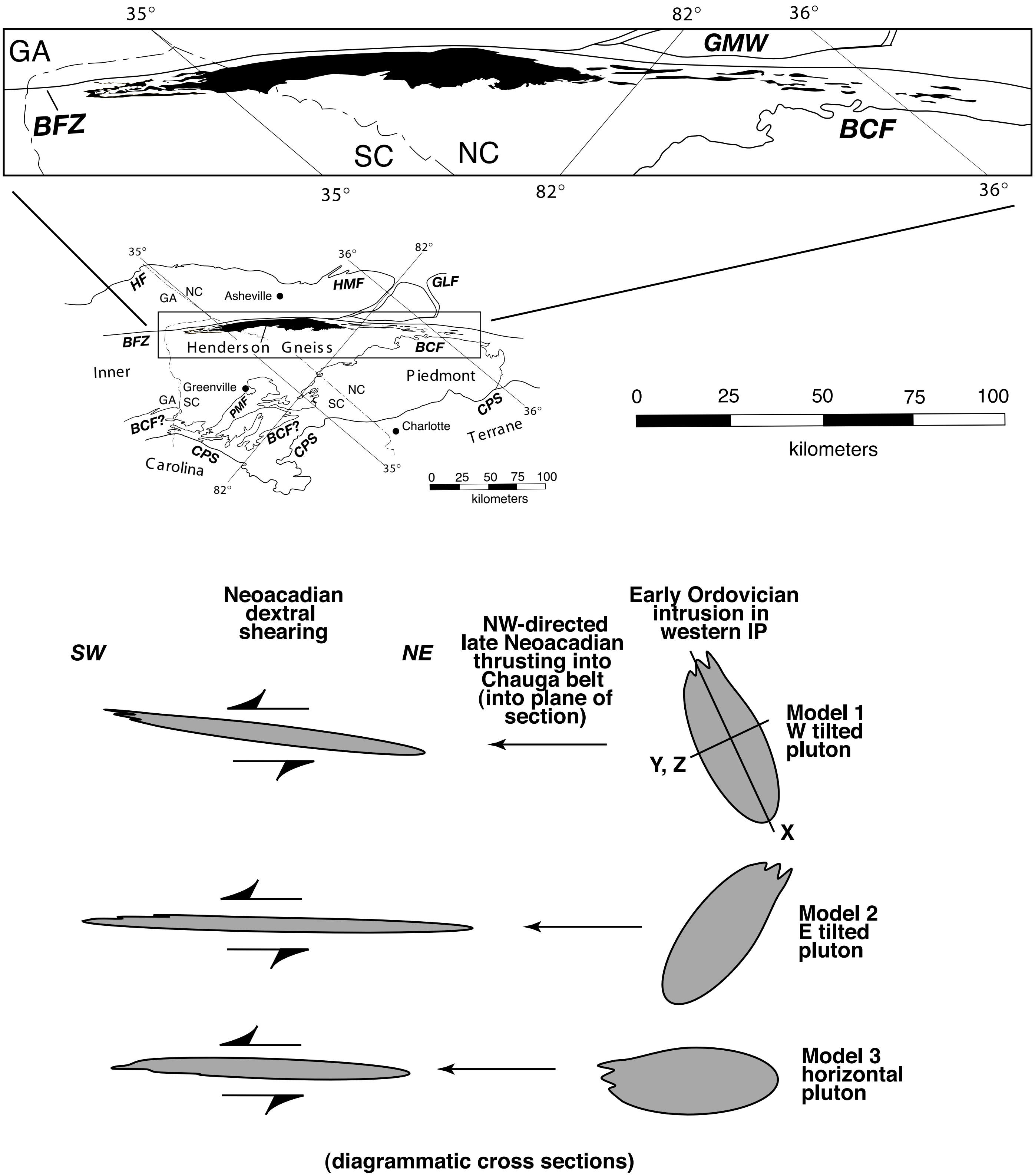

Figure 9. (a) Outcrop distribution of the Henderson Gneiss. Faults and other structural features: BCF–Brindle Creek. BFZ–Brevard. CPS–Central Piedmont suture. GLF–Gossan Lead. GMW–Grandfather Mountain window. HF–Hayesville. HMF–Holland Mountain. PMF–Paris Mountain. (b) Schematic cross sections illustrating possible shape and three alternative initial orientations of the Henderson Gneiss pluton before and after Neoacadian NW-directed thrusting and SW-directed dextral faulting. Area is not conserved in any of the three models.

gneiss/biotite-amphibolite gneiss (bag) to the southeast from Paleozoic (Pzg) granitoid to the northwest in the Winston Salem 1˚ x 2˚ sheet (Rankin et al., 1972; Espenshade et al., 1975) could trace the northeast continuation of the Brindle Creek thrust. This boundary continues to the northeast to the vicinity of the Sauratown Mountains window, then turns abruptly toward the east and is truncated by the western border fault of the Davie County Mesozoic basin (Espenshade et al., 1975). Farther south, it appears to also have a more due-southerly trend causing its outcrop trace to track toward the eastern parts of the Inner Piedmont into South Carolina. Such a boundary was not recognized by Nelson et al. (1998) in the Greenville 1˚ x 2˚ quadrangle, so its trace most likely occurs farther east. A possibility is that the Paris Mountain thrust sheet in the Greenville 1˚ x 2˚ sheet could represent an outlier of the Brindle Creek thrust sheet. More recent South Carolina Geological Survey work in the Paris Mountain quadrangle and mapping by MacLean and Blackwell (2001) in the Taylors quadrangle strongly indicate the Paris Mountain thrust does not exist as mapped by Nelson et al. (1998). A major fault mapped by Curl (1998) in the Reidville and Wellford 7 1/2-minute quadrangles southeast of Greenville, South Carolina, could represent the main southern continuation of the Brindle Creek thrust into South Carolina. If the boundary identified above in the Winston-Salem 1˚ x 2˚ sheet (Espenshade et al., 1975) represents the Brindle Creek thrust sheet, and the Brindle Creek thrust sheet indeed continues into South Carolina between Greenville and Spartanburg (Nelson et al., 1998), then both ends of its outcrop trace would terminate against the Central Piedmont suture, possibly as far southwestward as Central Georgia, and appear to be truncated by it (Fig. 1b). One implication of these truncations is that the Central Piedmont suture is a late Neoacadian structure as several have proposed (e.g., Dennis et al., 2000), or that the suture was reactivated as a thrust during the Alleghanian, making it no longer a suture, as proposed by Hibbard (2000) and Hibbard et al. (2002). The latter hypothesis is difficult to understand and reconcile because, once a suture joins two terranes, reactivation, low-angle crosscutting by a later thrust, or other modificaion does not make the boundary any less of a suture. U–Pb age dating of fault rocks that frame the Pine Mountain window (Box Ankle and Ocmulgee faults) yield consistent Alleghanian ages (Student and Sinha, 1992). Neither of these faults exhibit evidence of reactivation. The Ocmulgee fault is probably the southwest continuation of the Central Piedmont suture (Hooper and Hatcher, 1990). If the time of accretion of the Carolina terrane is early Alleghanian, what is the source of the 600 to 400+ Ma zircons discussed below and the age of the metasedimentary rocks that contain them?

The Brindle Creek thrust separates assemblages containing major differences: (1) in stratigraphy; (2) age of detrital zircons (1.1 Ga to the west from small populations of 2.7, 1.8, 1.4 Ga plus a major population of 1.1 Ga plus small populations of 600, 500, and 450 Ma old zircons; Bream et al., in review; Bream, this guidebook); and (3) age and character of granitoid plutonism (Mapes, 2002). It is possible that the rocks between the Brindle Creek fault and the Central Piedmont suture comprise a previously unrecognized suspect terrane (Bream, this guidebook) that was accreted during the Neoacadian event. If so, the 1.1 Ga detrital zircons in this terrane would have been derived either from the Laurentian margin or from a different 1.1 Ga source, e.g. Gondwana like the 600 Ma and younger zircons. Nevertheless, the older zircon population remains difficult to explain. Regardless, if this is either a suspect or an exotic terrane, I suggest that the rocks between the Brindle Creek fault and the Central Piedmont suture be called the Cat Square terrane, from the crossroads by that name northwest of Lincolnton, and south of Hickory, North Carolina. I earlier suggested (Hatcher, 2001b) that the rocks to the west between the Brindle Creek fault in the Inner Piedmont and the Chattahoochee fault in the eastern Blue Ridge be called the Tugaloo terrane for the Tugaloo River on the South Carolina-Georgia border, and that the central Blue Ridge complex (Soque River fault to the Hayesville fault) be called the Cartoogechaye terrane for a creek (and church) by that name west of Franklin, North Carolina (Fig. 1a). The stratigraphic assemblages and detrital zircon suites in each terrane justify separation into different tectonostratigraphic units.

Alternatively, the Brindle Creek fault may only juxtapose different facies of the same regional, time-transgressive stratigraphic assemblage. It would consist of equivalents of the Late Proterozoic (to early Paleozoic?) Ocoee Supergroup (and possible equivalent Mount Rogers and Grandfather Mountain Formations), along with latest Neoproterozoic to Cambrian Catoctin and Lynchburg Formations, deposited along the Laurentian rifted margin before and at the beginnings of the opening of the Iapetus ocean. The Tallulah Falls-Ashe Formation in the eastern Blue Ridge is intruded by the Middle Ordovician Whiteside Granite (466 Ma, Miller et al., 2000), and in the western Inner Piedmont by the Middle Ordovician Dysartsville pluton (~460 Ma, Bream, this guidebook), Late Ordovician Caesars Head biotite augen gneiss (Ranson et al., 1999), and other unnamed plutons in South Carolina and near Toccoa, Georgia (~460 Ma, Bream, this guidebook). The Tallulah Falls Formation in the western Inner Piedmont is overlain by the ~460 Ma Poor Mountain Amphibolite and Quartzite (Bream, this guidebook), probably a locally calcareous felsic tuff. The Tallulah Falls could thus range in age from Neoproterozoic to Early Ordovician. The stratigraphic assemblage east of the Brindle Creek fault could also be Ordovician or even Silurian, if the oldest plutonic rocks here are the Acadian Walker Top and Toluca granitoids. Detrital zircons ranging from 2.7, 1.8, 1.4, and 1.1 Ga, and 600 to 500 to ~450 Ma, however, have been found in the Brindle Creek sheet (Cat Square terrane). The 600 to ~425 Ma detrital zircons in the Cat Square terrane may indicate early Paleozoic (Silurian) approach of the Carolina terrane, as the exotic terrane shed zircons onto the easternmost seafloor off the Laurentian margin. This may, however, only indicate that the age of paragneisses in the Cat Square terrane are post-450 Ma, with the ~370 Ma age of the Walker Top and Toluca granitoids providing a minimum upper bound. The fact that the Walker Top and Toluca Granites are both catazonal plutons requires several millions to tens of millions of years for deposition and burial to depths where metamorphism at sillimanite-grade conditions and catazonal plutonism could occur (~15 km; Merschat and Kalbas, this guidebook). The maximum upper bound for the age of the paragneisses in the Brindle Creek thrust sheet thus may be 390 to 405 m.y. If so, this would prohibit early Paleozoic docking of the Carolina terrane (Hibbard, 2000), but would still permit docking to occur at ~350 Ma or possibly later at 325 to 330 Ma. Docking of the Carolina terrane shortly before 350 Ma and partial A subduction of the Tugaloo and Cat Square terranes beneath the Carolina terrane could provide the burial conditions needed to reach sillimanite-grade metamorphism by ~350 Ma and form the ~350 Ma plutonic suite (Cherryville of Kish, 1983). Renewed heating of the already warm Inner Piedmont could have set the younger 320 Ma ages reported by Dennis and Wright (1997), crystallization of ~325 Ma pegmatites at Zirconia, North Carolina (Bream, unpublished data), and emplacement of the nearby suite of 315 to 330 Ma plutons (e.g., the 317 Ma High Shoals Granite and the 325 Ma Elberton pluton; Horton et al., 1987; Goldsmith et al., 1988; Nelson et al., 1998). This would be the first shared thermal event between the Inner Piedmont and Carolina terrane (Dennis et al., 2000), indicating probable Neoacadian to early Alleghanian accretion of the Carolina terrane. Regardless of whether the Cat Square terrane was accreted during the Neoacadian or the early Alleghanian, the frequently invoked "Newfoundland" model of Ordovician accretion of the Carolina terrane and other terranes to the west (Williams, 1979; Hibbard, 2000; Hibbard et al., 2000, 2002) cannot be considered valid for the southern and central Appalachians (and, using other data, for southeastern New England).

THE INNER PIEDMONT BASEMENT PROBLEM

An attribute of the Inner Piedmont, and also an enigma, is to date no bodies of basement from a previous tectonic cycle (possible exception: Forbush Gneiss at the boundary of the Inner Piedmont with the Sauratown Mountains window; Heyn, 1984; McConnell, 1990) have been discovered here, and very little exists in the remainder of the Tugaloo terrane west of the Brevard fault zone (Hatcher et al., in review). Ironically, 1.1 Ga detrital zircons appear consistently throughout the Tugaloo and Cat Square terranes. The Cat Square assemblage contains zircons with older cores at 2.7, 1.8, and 1.4 Ga, whereas only 1.4 Ga cores have been found in the western Inner Piedmont (Bream, this guidebook). Several Paleozoic suites (Bream, this guidebook) are present in the Cat Square terrane that might be expected if the eastern Inner Piedmont were derived from a Gondwanan continent.

Several have suggested that the eastern Blue Ridge and, by implication the western Inner Piedmont as the other component of the Tugaloo terrane, were deposited on basement of mostly oceanic crust (Rankin, 1975, 1988; Hatcher, 1978, 1987, 1989). If so, this crust would have formed no earlier than 564 Ma as the Iapetus ocean opened in the southern Appalachians (Aleinikoff et al., 1995). The largest mafic-ultramafic complexes and best candidates for ophiolites, however, are in the Cartoogechaye terrane—not in the Tugaloo terrane. Numerous small ultramafic bodies occur in the Tugaloo terrane (Larrabee, 1966; Misra and Keller, 1978; Mittwede and Stoddard, 1989), and, if considered with their mafic components, attain greater size. At least one candidate for an ophiolite, the Laurel Creek mafic-ultramafic complex (Hatcher et al., 1984), occurs in the eastern Blue Ridge of northeastern Georgia, and others are present in the western Tugaloo terrane in North Carolina (east of Franklin, Spruce Pine synclinorium) where mafic-ultramafic complexes are most common. With the exception of the Soapstone Ridge body south of Atlanta, they are even smaller in the Inner Piedmont. Mittwede (1989) suggested the Hammett Grove metaigneous complex east of Spartanburg in the Cat Square terrane is ophiolitic mélange or a dismembered ophiolite (Mittwede, 1989). Mafic rocks are otherwise abundant in the Tugaloo terrane, but many appear as flows intercalated with the Tallulah Falls Formation and appear to have an intraplate to arc setting (with very limited geochemical data; see Bream, 1999). Poor Mountain Amphibolite has clear MORB affinity, however (Figs. 5, 6, 7, and 8) (Davis, 1993a; Yanagihara, 1994).

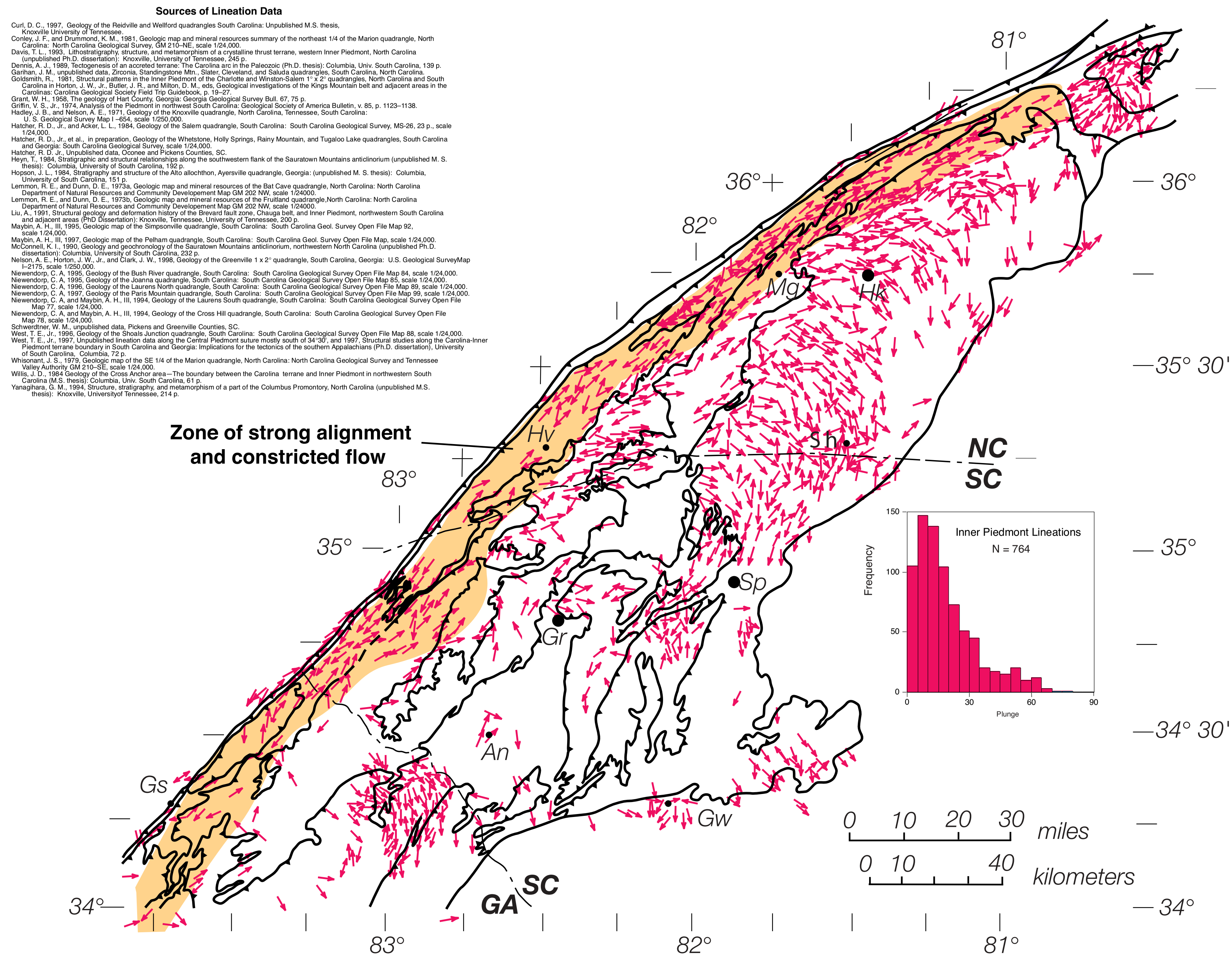

Figure 10. Mineral lineation pattern superimposed on the fault pattern in the Inner Piedmont in the Carolinas and part of northeastern Georgia. Note the systematic change in orientation of lineation. Lineation data is filtered to remove part of data in tight clusters. See Figure 1 for explanation of city abbreviations.

INNER PIEDMONT DEFORMATION PLAN AND FAULT KINEMATICS

Davis et al. (1991) suggested that the Inner Piedmont is a crustal shear zone based on the widespread occurrence of mylonitic fabrics in the paragneisses throughout much of the western Inner Piedmont. These fabrics are not as common in the eastern Inner Piedmont, however, possibly because of annealing by pervasive intense migmatization. Goldsmith (1981) recognized a systematic change in orientation of the subhorizontal mineral lineation and parallel early fold hinges in the Inner Piedmont in the Charlotte 1˚ x 2˚ sheet from northwest-southeast to the southeast to east-west in the eastern Inner Piedmont to strongly aligned northeast-southwest from the northwest hanging wall of the Brindle Creek thrust sheet across all of the western Inner Piedmont (Fig. 10). This strongly aligned high temperature fabric (Davis, 1993b) in the northwestern Inner Piedmont is strongly overprinted by retrogressive early Alleghanian Brevard fault zone fabrics. Davis (1993a), from c-axis determination of the quartz slip system, concluded the Inner Piedmont mineral lineation and associated folds are the product of high temperature deformation. The lineation pattern originally recognized by Goldsmith (1981) has been reconfirmed by detailed mapping in the South and Brushy Mountains (Bream, 1999; Hill, 1999; Giorgis, 1999; Williams, 2000; Bier, 2001; Kalbas, in preparation; Merschat, in preparation; Merschat and Kalbas, this guidebook) and by compilation of published and unpublished mineral lineation data in the Carolinas and northeastern Georgia (Fig. 10). Davis et al. (1991) and Davis (1993a, 1993b) concluded that this systematic change in orientation of the high temperature mineral lineation, and related fold hinges, tracks material flow and the motion of thrust sheets. If correct, thrusts in the southeastern part of the Inner Piedmont in the Carolinas and northeastern Georgia were northwest-directed. In the eastern Inner Piedmont, thrust motion and flow became west-directed. In the west-central and western Inner Piedmont motion was southwest-directed and likely the product of tightly constricted flow (Hatcher, 2001a). This zone of constricted flow is thought to be related to buttressing and southwest deflection of westward moving thrust sheets by the primordial Brevard fault zone (Davis, 1993a, 1993b). Recognition of the Brindle Creek thrust sheet has not changed Davis' kinematic model. Actually, the Brindle Creek, if it is a single thrust sheet, records all of the changes in flow pattern across the Inner Piedmont (Merschat and Kalbas, this guidebook) (Fig. 10).

ACKNOWLEDGMENTS

Support for the field work presented on this CGS trip has been provided by the National Cooperative Geologic Mapping Program EDMAP component (administered by the U.S Geological Survey) awards 1434HQ97AG01720, 98HQAG2026, and 99HQAG0026 for the South Mountains and 01HQAG0176 for the Brushy Mountains. The continuing cooperation of the North Carolina Geological Survey has also been a major factor in the success of this project. Support for high resolution ion probe and U-Pb analyses of detrital and igneous zircons cited herein has been provided by National Foundation grant EAR–9814800. Critical reviews by J. M. Garihan and B. R. Bream are very much appreciated; both resulted in corrections of several mistakes and an overall improvement of the manuscript. I remain culpable for all other uncorrected errors and misinterpretations.

REFERENCES CITED

Aleinikoff, J. N., Zartman, R. E., Rankin, D. W., and Burton, W. C., 1995, U-Pb ages of metarhyolites of the Catoctin and Mt. Rogers Formations, central and southern Appalachians: Evidence of two pulses of Iapetan rifting: American Journal of Science, v. 295, p. 428–454.

Bier, S. E., 2001, Geology of the southeastern South Mountains, North Carolina [unpublished M.S. thesis]: Knoxville, University of Tennessee, 162 p.

Bream, B. R., 1999, Geology of the Glenwood and Sugar Hill quadrangles, North Carolina, and the structure of the northeast end of the Henderson Gneiss [unpublished M.S. thesis]: Knoxville, University of Tennessee, 155 p.

Bream, B. R., Hatcher, R. D., Jr., Miller, C. F., and Fullagar, P. D., 2001, Geochemistry and provenance of Inner Piedmont paragneisses, NC and SC: Evidence for an internal terrane boundary?: Geological Society of America Abstracts with Programs, v. 33, p. 65.

Bream, B. R., Hatcher, R. D., Jr., Miller, C. F., and Fullagar, P. D., in review, Detrital zircon ages and Nd isotopic data from the southern Appalachian crystalline core, GA-SC-NC-TN: New provenance constraints for Laurentian margin paragneisses, *in* Tollo, R. P., and Bartholomew, M. J., eds., Proterozoic evolution of the Grenville orogen in North America: Boulder, Colorado, Geological Society of America Special Paper.

Brobst, D. A., 1962, Geology of the Spruce Pine district, Avery, Mitchell, and Yancey Counties, North Carolina: U.S. Geological Survey Bulletin 1122–A, 26 p.

Bryant, B., and Reed, J. C., Jr., 1970, Geology of the Grandfather Mountain window and vicinity: U.S. Geological Survey Professional Paper 615, 190 p.

Caesar, J., 52 B.C., The conquest of Gaul, Handford, S. A., 1951 trans.: Harmondsworth, Middlesex, England, Penguin Books, 283 p.

Carrigan, C. W., Bream, B. R., Miller, C. F., and Hatcher, R. D., Jr., 2001, Ion microprobe analyses of zircon rims from the eastern Blue Ridge and Inner Piedmont, NC-SC-GA: Implications for the timing of Paleozoic metamorphism in the southern Appalachians: Geological Society of America Abstracts with Programs, v. 33, p. A-7.

Cazeau, C. J., and Brown, C. Q., 1963, Guide to the geology of Pickens and Oconee Counties, South Carolina: South Carolina Division of Geology Geologic Notes, v. 7, p. 31–40.

Curl, D. C., 1998, Stratigraphy and structure of Wellford and Reidville quadrangles in part of the eastern Inner Piedmont, near Spartanburg, South Carolina [unpublished M.S. thesis]: Knoxville, University of Tennessee, 129 p.

Davis, T. L., 1993a, Lithostratigraphy, structure, and metamorphism of a crystalline thrust terrane, western Inner Piedmont, North Carolina [unpublished Ph.D. dissertation]: Knoxville, University of Tennessee, 245 p.

Davis, T. L., 1993b, Geology of the Columbus Promontory, western Inner Piedmont, North Carolina, southern Appalachians, *in* Hatcher, R. D. Jr., and Davis, T. L., eds., Studies of Inner Piedmont geology with a focus on the Columbus Promontory: North Carolina Geological Survey, Carolina Geological Society Guidebook, p. 17–43.

Davis, T. L., Hatcher, R. D., Jr., Liu, A., and Tabor, J. R., 1991, Southern Appalachian western Inner Piedmont: A progressive crustal–scale shear zone. Geological Society of America Abstracts with Programs, v. 23, p. A138.

Dennis, A. J., and Wright, J. E., 1997, Middle and late Paleozoic monazite U–Pb ages, Inner Piedmont, South Carolina: Geological Society of America Abstracts with Programs, v. 29, p. 12.

Dennis, A. J., Secor, D. T., and Shervais, J. W., 2000, Fault-bounding eclogite-bearing gneisses, Newberry, South Carolina: Geological Society of America Abstracts with Programs, v. 32, p. A–14.

Espenshade, G. H., Rankin, D. W., Shaw, K. W., and Neuman, R. B., 1975, Geologic map of the east half of the Winston-Salem quadrangle, North Carolina-Virginia: U.S. Geological Survey Map I-709-B, scale 1:250,000.

Garihan, J. M., 2001, Observations of the Seneca fault and their implications for thrust emplacement in the Inner Piedmont of the Carolinas, *in* Garihan, J. M., Ranson, W. A., and Clendinin, C. W., eds. Geology of the Inner Piedmont in the Caesars Head and Table Rock State Parks area, northwestern South Carolina: 2001 Carolina Geological Society Field Trip Guidebook, South Carolina Geology, v. 43, p. 1-13.

Giorgis, S. D., 1999, Inner Piedmont geology of the northwestern South Mountains near Morganton, North Carolina [unpublished M.S. thesis]: Knoxville, University of Tennessee, 191 p.

Goldsmith, R., 1981, Structural patterns in the Inner Piedmont of the Charlotte and Winston-Salem 2-degree quadrangles, North Carolina and South Carolina, *in* Horton, J. W., Jr., Butler, J. R., and Milton, D. M., eds., Geological investigations of the Kings Mountain belt and adjacent areas in the Carolinas: Carolina Geological Society Field Trip Guidebook, p. 19-27.

Goldsmith, R., Milton, D. J., and Horton, J. W., Jr., 1988, Geologic map of the Charlotte 1 degree x 2 degree quadrangle, North Carolina and South Carolina: U.S. Geological Survey Map I–1251–E, scale 1:250,000.

Greenwood, H. J., Woodsworth, G. J., Read, P. B., Ghent, E. D., and Evenchick, C. A., 1991, Chapter 16, Metamorphism, *in* Gabrielse, H., and Yorath, eds., Geology of the Cordilleran orogen in Canada: Boulder, Colorado, Geological Society of America Geology of North America, v. G–2, p. 533–570.

Griffin, V. S., Jr., 1969, Migmatitic Inner Piedmont belt of northwestern South Carolina: South Carolina Division of Geology, Geologic Notes, v. 13, p. 87–104.

Griffin V. S., Jr., 1971, Inner Piedmont belt of the southern crystalline Appalachians: Geological Society of America Bulletin, v. 82, p. 1885-1898.

Griffin, V. S., Jr., 1973, Geology of the Old Pickens quadrangle, S.C.: South Carolina Division of Geology MS–18, 54 p., scale 1:24,000.

Griffin, V. S., Jr., 1974a, Analysis of the Piedmont in northwest South Carolina: Geological Society of America Bulletin, v. 85, p. 1123–1138.

Griffin, V. S., Jr., 1974b, Geology of the Walhalla quadrangle, S.C.: South Carolina Division of Geology MS–19, 53 p., scale 1:24,000.

Hatcher, R. D., Jr., 1969, Stratigraphy, petrology and structure of the low rank belt and part of the Blue Ridge of northwesternmost South Carolina: South Carolina Division of Geology, Geologic Notes, v. 13, p. 105-141.

Hatcher, R. D., Jr., 1971, Geology of Rabun and Habersham Counties, Georgia: A reconnaissance study: Georgia Geological Survey Bulletin 83, 48 p.

Hatcher, R.D., Jr., 1972, Developmental model for the southern Appalachians: Geological Society of America Bulletin, v. 83, p. 2735-2760.

Hatcher, R. D., Jr., 1978, Tectonics of the western Piedmont and Blue Ridge: Review and speculation: American Journal of Science, v. 278, p. 276–304.

Hatcher, R. D., Jr., 1987, Tectonics of the southern and central Appalachian internides: Annual Review of Earth and Planetary Sciences, v. 15, p. 337-362.

Hatcher, R. D., Jr., 1989, Tectonic synthesis of the U.S. Appalachians, Chapter 14, *in* Hatcher, R. D., Jr., Thomas, W. A., and Viele, G. W., eds., The Appalachian–Ouachita orogen in the United States: Boulder, Colorado, Geological Society of America, The Geology of North America, v. F–2, p. 511–535.

Hatcher, R. D., Jr., 1993, Perspective on the tectonics of the Inner Piedmont, southern Appalachians, *in* Hatcher, R. D., Jr., and Davis, T. L., eds., Studies of Inner Piedmont geology with a focus on the Columbus Promontory: Carolina Geological Society Guidebook, North Carolina Geological Survey, p. 1–16.

Hatcher, R. D., Jr., 2001a, Rheological partitioning during multiple reactivation of the Paleozoic Brevard Fault Zone, Southern Appalachians, USA, *in* Holdsworth, R. E., Strachan, R. A., Macloughlin, J. F., and Knipe, R. J., eds., The nature and significance of fault zone weakening: Geological Society of London Special Publication 186, p. 255–269.

Hatcher, R. D., Jr., 2001b, Terranes and terrane accretion in the southern Appalachians: An evolved working hypothesis: Geological Society of America Abstracts with Programs, v. 33, p. A–65.

Hatcher, R. D., Jr., in preparation, Geology of the Whetstone, Holly Springs, Tugaloo Lake and Rainy Mountain quadrangles, South Carolina, Georgia: South Carolina Geological Survey, scale 1/24,000.

Hatcher, R. D., Jr., and Acker, L. L., 1984, Geology of the Salem quadrangle, South Carolina: South Carolina Geological Survey, MS–26, 23 p., scale 1/24,000.

Hatcher, R. D. Jr., and Davis, T. L., eds., 1993, Studies of Inner Piedmont geology with a focus on the Columbus Promontory: North Carolina Geological Survey, Carolina Geological Society Guidebook, 113 p.

Hatcher, R. D., Jr., and Hooper, R. J., 1992, Evolution of crystalline thrust sheets in the internal parts of mountain chains, *in* McClay, K. R., ed., Thrust tectonics: London, Chapman and Hall, p. 217–234.

Hatcher, R. D., Jr., Bream, B. R., Miller, C. F., Eckert, J. O., Jr., Fullagar, P. D., and Carrigan, C. W., in review, Paleozoic structure of southern Appalachian Blue Ridge Grenvillian internal basement massifs, *in* Tollo, R. P., and Bartholomew, M. J., eds., Proterozoic evolution of the Grenville orogen in North America: Boulder, Colorado, Geological Society of America Special Paper.

Hatcher, R. D., Jr., Hooper, R. J., Petty, S. M., and Willis, J. D., 1984, Structure and chemical petrology of three southern Appalachian mafic–ultramafic complexes and their bearing upon the tectonics of emplacement and origin of Appalachian ultramafic bodies: American Journal of Science, v. 284, p. 484–506.

Heyn, T., 1984, Stratigraphic and structural relationships along the southwestern flank of the Sauratown Mountains anticlinorium [unpublished M.S. thesis]: Columbia, University of South Carolina, 192 p.

Heyn, T., McConnell, K.I., Hatcher, R. D., Jr., and Godfrey, S. E., 1988, Geologic map of the western Sauratown Mountains window and vicinity, *in* Hatcher, R. D., Jr., ed., Structure of the Sauratown Mountains window, North Carolina: North Carolina Geological Survey, Carolina Geological Society Guidebook, scale 1:48,000.

Hibbard, J. P., 2000, Docking Carolina: Geology, v. 28, p. 127–130.

Hibbard, J. P., Stoddard, E.F., Secor, D. T., Jr., and Dennis, A. J., 2000, The Carolina realm: Overview of exotic terranes along the eastern flank of the southern Appalachians: Geological Society of America Abstracts with Programs, v. 32, p. A–26.

Hibbard, J. P., Stoddard, E.F., Secor, D. T., Jr., and Dennis, A. J., 2002, The Carolina zone: Overview of Neoproterozoic to early Paleozoic peri-Gondwanan terranes along the eastern flank of the southern Appalachians: Earth Science Reviews, v. 57, p. 299–339.

Hill, J. C., 1999, Geology of the Marion East quadrangle, North Carolina, and the stratigraphy of the Tallulah Falls Formation in the Chauga belt [unpublished M.S. thesis]: Knoxville, University of Tennessee, 188 p.

Hooper, R. J., and Hatcher, R. D., Jr., 1990, The Ocmulgee fault: The Piedmont–Avalon terrane boundary in central Georgia: Geology, v. 18, p. 708–711.

Hopson, J. L., and Hatcher, R. D., Jr., 1988, Structural and stratigraphic setting of the Alto allochthon, northeast Georgia: Geological Society of America Bulletin, v. 100, p. 339–350.

Horton, J. W., Jr., 1982, Geologic map and mineral resources of the Rosman quadrangle, North Carolina: North Carolina Department of Natural Resources and Community Development, Geological Survey GM 185–NE, scale 1/24,000.

Horton, J. W., Jr., Sutter, J. F., Stern, T. W., and Milton, D. J., 1987, Alleghanian deformation, metamorphism, and granite emplacement in the Central Piedmont of the southern Appalachians: American Journal of Science, v. 287, p. 635–660.

Kish, S. A., 1983, A geochronological study of deformation and metamorphism in the Blue Ridge and Piedmont of the Carolinas [Ph. D. dissertation]: Chapel Hill, University of North Carolina, 220 p.

Larrabee, D. M., 1966, Map showing distribution of ultramafic and intrusive mafic rocks from northern New Jersey to eastern Alabama: U.S. Geological Survey Miscellaneous Geologic Investigations Map I–476, scale 1:500,000.

Liu, A., 1991, Structural geology and deformation history of the Brevard fault zone, Chauga belt, and Inner Piedmont, northwestern South Carolina and adjacent areas [Ph.D. dissertation]: Knoxville, University of Tennessee, 200 p.

Maclean, J. S., and Blackwell, S. S., 2001, Paris Mountain project: Part 1, Geology of Taylors 7.5-minute quadrangle, Greenville County, South Carolina, *in* Garihan, J. M., Ranson, W. A., and Clendenin, C. W., eds., Geology of the Inner Piedmont in the Caesars Head and Table Rock state parks area, northwestern South Carolina: South Carolina Department of Natural Resources, Carolina Geological Society Guidebook, p. 15-24.

Mapes, R. W., 2002, Geochemistry and geochronology of mid-Paleozoic granitic plutonism in the southern Appalachian Piedmont terrane, North Carolina-South Carolina-Georgia [unpublished M. S. thesis]: Nashville, Tennessee, Vanderbilt University, 150 p.

Mapes, R. W., Maybin, A. H., III, Miller, C. F., Fullagar, P. D., and Bream, B. R., 2002, Geochronology and geochemistry of mid Paleozoic granitic magmatism, central and eastern Inner Piedmont, NC & SC: Geological society of America Abstracts with Programs, v. 34, p. A-92.

McConnell, K. I., 1990, Geology and geochronology of the Sauratown Mountains anticlinorium, northwestern North Carolina [unpublished Ph. D. thesis]: Columbia, University of South Carolina, 232 p.

Miller, C. F., Hatcher, R. D., Jr., Ayers, J. C., Coath, C. D., and Harrison, T. M., 2000, Age and zircon inheritance of eastern Blue Ridge plutons, southwestern North Carolina and Northeastern Georgia, with implications for magma history and evolution of the southern Appalachian orogen: American Journal of Science, v. 300, p. 142–172.

Misra, K. C., and Keller, F. B., 1978, Ultramafic bodies in the southern Appalachians: A review: American Journal of Science, v. 278, p.389–418.

Mittwede, S. K., 1989, The Hammett Grove Meta-igneous suite; a possible ophiolite in the northwestern South Carolina Piedmont, *in* Mittwede, S. K., and Stoddard, E. F., Ultramafic rocks of the Appalachian Piedmont: Geological Society of America Special Paper 231, p. 45–62.

Mittwede, S. K., and Stoddard, E. F., 1989, Ultramafic rocks of the Appalachian Piedmont: Geological Society of America Special Paper 231, 103 p.

Nelson, A. E., Horton, J. W., Jr., and Clarke, J. W., 1998, Geologic map of the Greenville 1˚ x 2˚ quadrangle, South Carolina, Georgia, and North Carolina: U. S. Geological Survey Map I–2175, scale 1/250,000.

Osberg, P. H., Tull, J. F., Robinson, P. Hon, R., and Butler, J. R., 1989, The Acadian orogen, *in* Hatcher, R. D., Jr., Thomas, W. A., and Viele, G. W., eds., The Appalachian–Ouachita orogen in the United States: Boulder, Colorado, Geological Society of America The geology of North America, v. F–2, p.179–232.

Overstreet, W. C., Yates, R. G., and Griffitts, W. R., 1963a, Geology of the Shelby quadrangle, North Carolina: U.S. Geological Survey Map I-384, scale 1/62,500.

Overstreet, W. C., Whitlow, J. W., White, A. M., and Griffitts, W. R., 1963b, Geologic map of the southern part of the Casar quadrangle, Cleveland, Lincoln, and Burke Counties, North Carolina, showing areas mined for monazite and mica: U.S. Geological Survey Map MF-257, scale 1/24,000.

Pearce J. A., and Cann, J. R., 1973, Tectonic setting of basic volcanic rocks determined using trace element analysis: Earth and Planetary Science Letters, v. 19, p. 956–983.

Pearce, J. A., and Norry, M. J., 1979, Petrogenetic implications of Ti, Zr, Y, and Nb variations in volcanic rocks: Contributions to Mineralogy and Petrology, v. 69, p.33–37.

Rankin, D. W., 1975, The continental margin of eastern North America in the southern Appalachians: The opening and closing of the Iapetus ocean: American Journal of Science, v. 255–A, p.298–336.

Rankin, D. W., 1988, The Jefferson terrane of the Blue Ridge tectonic province: An exotic accretionary prism: Geological Society of America Abstracts with Programs, v. 20, no. 4, p.310.

Rankin, D. W., Espenshade, G. H., and Neuman, R. B., 1972, Geologic map of the west half of the Winston-Salem quadrangle, North Carolina, Virginia, and Tennessee: U.S. Geological Survey Map I-709-A, scale 1/250,000.

Ranson, W. A., and Garihan, J. M., 2001, Geology of the Inner Piedmont in the Caesars Head and Table Rock State Parks area, northwestern South Carolina, *in* Garihan, J. M., Ranson, W. A., and Clendinin, C. W., eds. Geology of the Inner Piedmont in the Caesars Head and Table Rock State Parks area, northwestern South Carolina: Carolina Geological Society Field Trip Guidebook, South Carolina Geology, v. 43, p. 73-86.

Ranson, W. A., Williams, I. S., and Garihan, J. M., 1999, SHRIMP zircon U-Pb ages of granitoids from the Inner Piedmont of South Carolina: Evidence for Ordovician magmatism involving mid to Late Proterozoic crust: Geological Society of America Abstracts with Programs, v. 31, p. A–167.

Reed, J. C., Jr., 1964, Geology of the Lenoir quadrangle, North Carolina: U.S. Geological Survey Map GQ-242, scale 1/62,500.

Shufflebarger, T. E., 1961, Notes on relationships of Piedmont sedimentary rocks with emphasis on the Poor Mountain-Chauga River area, Oconee County, South Carolina: South Carolina Division of Geology, Geologic Notes, v. 5, p. 31–38.

Student, J. J., and Sinha, A. K., 1992, Carboniferous U-Pb ages of zircons from the Box Ankle and Ocmulgee fault zones, Central Georgia: Implications for accretionary models: Geological Society of America Abstracts with Programs, v. 24, p. 69.

Vinson, S., 2001, Ion probe geochronology of granitoid gneisses of the Inner Piedmont, North Carolina and South Carolina [unpublished M.S. thesis]: Nashville, Tennessee, Vanderbilt University, 84 p.

Williams, H., 1979, The Appalachian orogen in Canada: Canadian Journal of Earth Sciences, v. 16, p. 792–807.

Williams, H., and Hatcher, R.D., Jr., 1983, Appalachian suspect terranes, *in* Hatcher, R.D., Jr., Williams, H., and Zietz, I., eds., Contributions to the tectonics and geophysics of mountain chains: Geological Society of America Memoir 158, p. 33-53.

Williams, S. T., 2000, Structure, stratigraphy, and migmatization in the southwestern South Mountains, North Carolina [unpublished M.S. thesis]: Knoxville, University of Tennessee, 111 p.

Yanagihara, G. M., 1994, Structure, stratigraphy, and metamorphism of a part of the Columbus Promontory, North Carolina [M.S. thesis]: Knoxville, University of Tennessee, 214 p.

Carolina Geological Society
Annual Field Trip
October 19-20, 2002

Geology of Standingstone Mountain quadrangle, western Inner Piedmont, North and South Carolina

John M. Garihan
Department of Earth and Environmental Sciences
Furman University
Greenville, SC 29613
Jack.Garihan@furman.edu

ABSTRACT

Five major Paleozoic thrust sheets occur in the Inner Piedmont in Standingstone Mountain quadrangle. Northwest to southeast, they involve: 1) Henderson Gneiss, sheet I; 2) Brevard – Poor Mountain transitional member (muscovite-biotite-feldspar-quartz gneiss, or metasiltstone), sheet II; 3) Henderson Gneiss, sheet III; 4) Table Rock gneiss and associated rocks of the Walhalla nappe, sheet IV; and 5) Poor Mountain and Tallulah Falls Formations of the Six Mile thrust sheet, sheet V. Certain of these major thrusts are affected by younger episodes of superimposed folding (earlier northeast- and later northwest-striking folds) and thrust faulting. Ductile shear zones confined within Henderson Gneiss and Table Rock gneiss units resulted from thrusting or faulting during tight folding. The Mesozoic Green River and Gap Creek normal oblique faults of the Marietta-Tryon fault system offset the trace of the Paleozoic Seneca thrust, at the base of the Six Mile allochthon.

INTRODUCTION

Standingstone Mountain (SM) 7.5-minute quadrangle is situated within the rugged Columbus Promontory in the Inner Piedmont (Davis, 1993). Its southern portion lies across the North Carolina-South Carolina state line at the Eastern Continental Divide (~3000 ft elevation) (Fig. 1). With its lines of impressive exfoliation balds, the escarpment of the Blue Ridge Front winds its way across the southern margin of SM quadrangle. Local relief across this prominent mountain wall in the vicinity of Jones Gap State Park and the headwaters of the Middle Saluda River is 1400 - 2000 ft. The highest elevations in SM quadrangle (3600 - 3700 ft) lie along Stone Mountain and The Pinnacle, 10 km to the north of the Blue Ridge Front escarpment (Fig. 1). There resistant gneisses lie structurally above less resistant gneiss, forming an impressive north-facing escarpment above Crab Creek. Large aprons of colluvial blocks have been shed downslope from many steep cliffs across the map area.

Rugged topography and excellent rock exposure in the Piedmont are the result of modern stream incision along joints and faults produced by Holocene uplift of the order of several millimeters per year relative velocity in this part of the southern Appalachians (based on precise leveling surveys of Citron and Brown, 1979; Gable and Hatton, 1983). Incised meanders and stream capture phenomena are common features here and documented in Cleveland quadrangle immediately to the south (Haselton, 1974). Major east-northeast and northeast drainages at Green River

Garihan, J.M., 2002, Geology of Standingstone Mountain quadrangle, western Inner Piedmont, North and South Carolina, *in* Hatcher, R.D., Jr., and Bream, B.R., eds., Inner Piedmont geology in the South Mountains-Blue Ridge Foothills and the southwestern Brushy Mountains, central-western North Carolina: North Carolina Geological Survey, Carolina Geological Society annual field trip guidebook, p. 19-32.

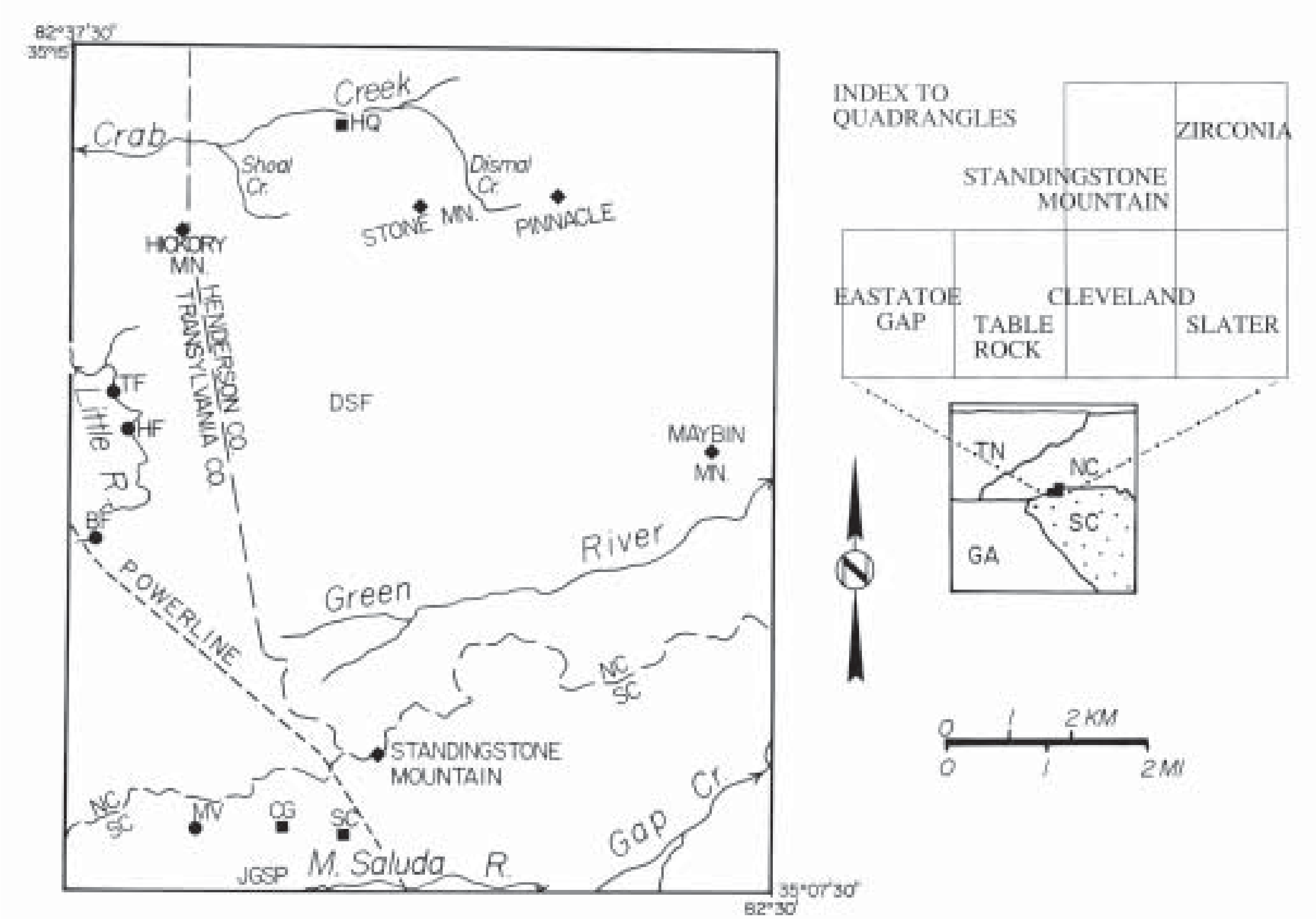

Figure 1. Selected features of Standingstone Mountain quadrangle, NC-SC, with index to quadrangles. BF-Bridal Veil Falls, DSF-Dupont State Forest, CG-Camp Greenville, HF-High Falls, HQ-Holmes Educational Forest Headquarters, JGSP-Jones Gap State Park, MV-Mulligan's View, SC-Symmes Chapel, TF-Triple Falls.

and Gap Creek appear structurally controlled by erosion along zones of brittle faulting. Similiar erosion along northeast brittle faults (Garihan et al., 1997) occurs in the linear Devils Fork and Cox Creek drainages in northeast Cleveland quadrangle just to the south of SM quadrangle (Garihan, 2000). A thorough discussion of regional geomorphology and landscape development in the Columbus Promontory area is provided by Clark (1993) in the 1993 Carolina Geological Society Field Trip Guidebook.

Ready access to spectacular mountain scenery and waterfalls in the past 40 years have attracted the development of eight or ten youth camps with large, permanent facilities in the area. Jones Gap State Park in South Carolina and the Dupont State Forest in North Carolina provide public access via extensive, well-maintained hiking and horseback riding trails. Utilization of these popular trails has facilitated access for geologic mapping in the southwest part of SM quadrangle. Field trip guides with geologic roadlogs to the area are provided by Garihan and Ranson (1999) and Ranson and Garihan (2001). The purpose of this paper is to provide a summary of the major geological features of SM quadrangle. In describing below the mineral assemblages of the various rocks, the convention used here is to place the most abundant mineral in the name to the right; therefore a muscovite-biotite gneiss generally contains more biotite than muscovite.

GEOLOGIC RELATIONSHIPS IN STANDINGSTONE MOUNTAIN QUADRANGLE

Regional thrust fault relationships within the Inner Piedmont have been described for the adjacent Greenville 1° x 2° sheet (Nelson et al., 1986, 1987, 1998). A recent discussion of the tectonic framework of the Inner Piedmont in the Caesars Head and Table Rock state parks area is provided in the volume for the 2001 Carolina Geological Society meeting (Garihan, 2001). Detailed geologic mapping at 1:24,000 scale within SM quadrangle indicates that four lithostratigraphic packages of metaigneous and metasedimentary rocks are caught up in a stack of five major Paleozoic thrust sheets (Garihan, 2002). The thrust sheets form clearly identifiable northeast-trending zones across

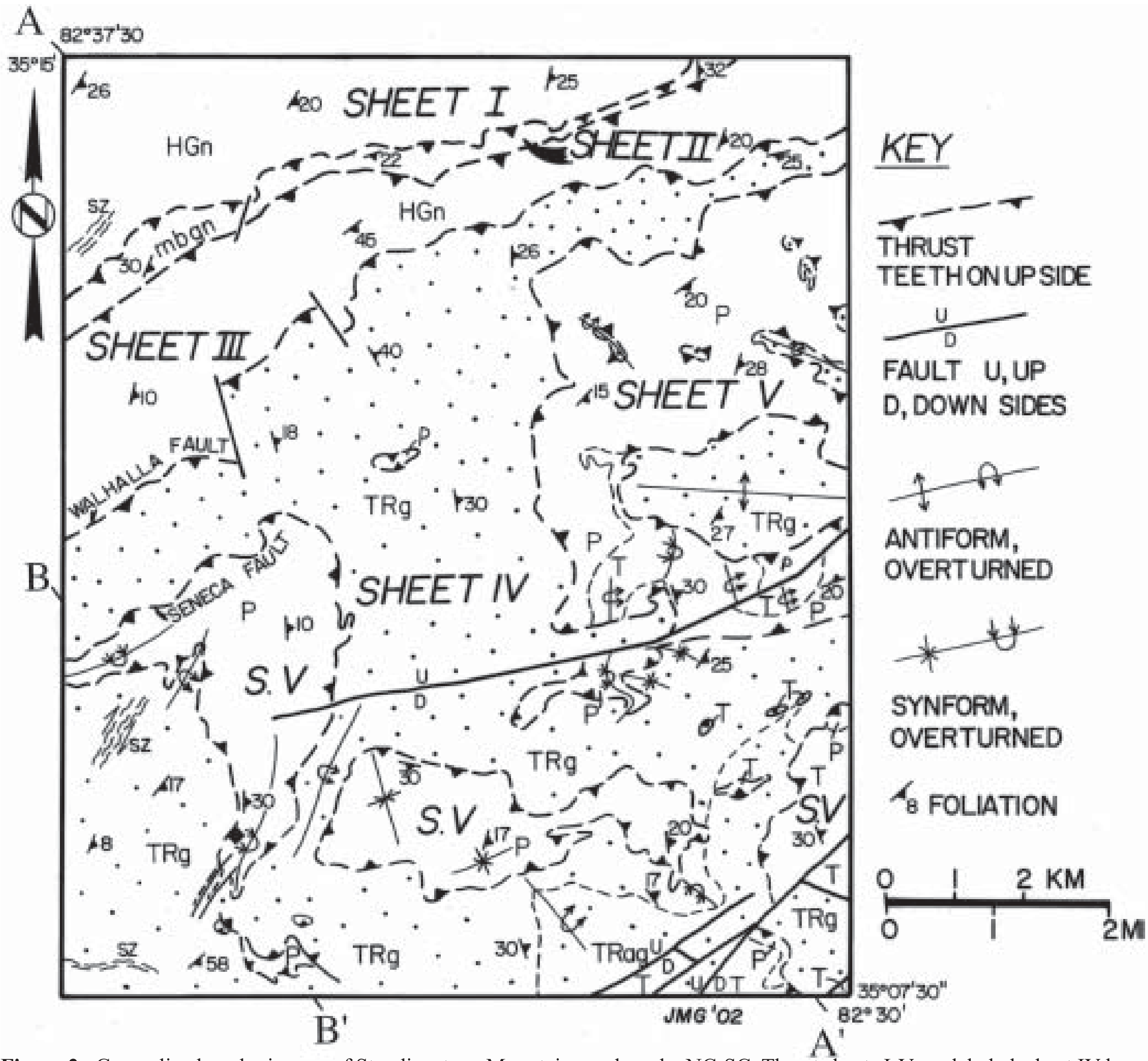

Figure 2. Generalized geologic map of Standingstone Mountain quadrangle, NC-SC. Thrust sheets I-V are labeled; sheet IV has a stippled pattern. HGn Henderson Gneiss, mbgn muscovite-biotite-feldspar-quartz gneiss, TRg Table Rock gneiss, TRag Table Rock augen gneiss, P Poor Mountain Formation, T Tallulah Falls Formation, sz shear zone, diamond is sphalerite-chalcopyrite-galena prospect.

the geologic map (Fig. 2). Each major thrust fault has transported a suite of metamorphic units in its hanging wall northwestward or westward (Fig. 3). Hanging wall rocks are distinctly different than the footwall lithologies. A group of less extensive thrust faults is present in the southwestern part of the region. These minor thrusts affect an earlier thrust and duplicate some of the metamorphic units found in two other thrust sheets.

The thrust stack in SM quadrangle is arranged with the structurally lowest thrust sheet to the northwest. The interpretation is based on compilation of geologic maps, including mapping in adjacent quadrangles (Fig. 4), and selected cross section information (Fig. 5). To facilitate the discussion, allochthonous rocks are labeled thrust sheets I through V on the SM geologic map (Fig. 2). The lowest sheet (sheet I) involves Henderson Gneiss. Structurally higher sheets progressively to the southeast are preserved at the higher elevations north of the Blue Ridge Front. In structural order upward, the major thrust sheets involve the following units: 1) Henderson Gneiss, sheet I; 2) Brevard – Poor Mountain transition member (muscovite-biotite-feldspar-quartz gneiss, or metasiltstone), sheet II; 3) Henderson Gneiss, sheet III; 4) Table Rock biotite quartzofeldspathic gneiss, biotite augen gneiss, granitoid gneiss, and amphibolite of the Walhalla nappe, sheet IV; and 5) Poor Mountain and Tallulah Falls Formations of the Six Mile

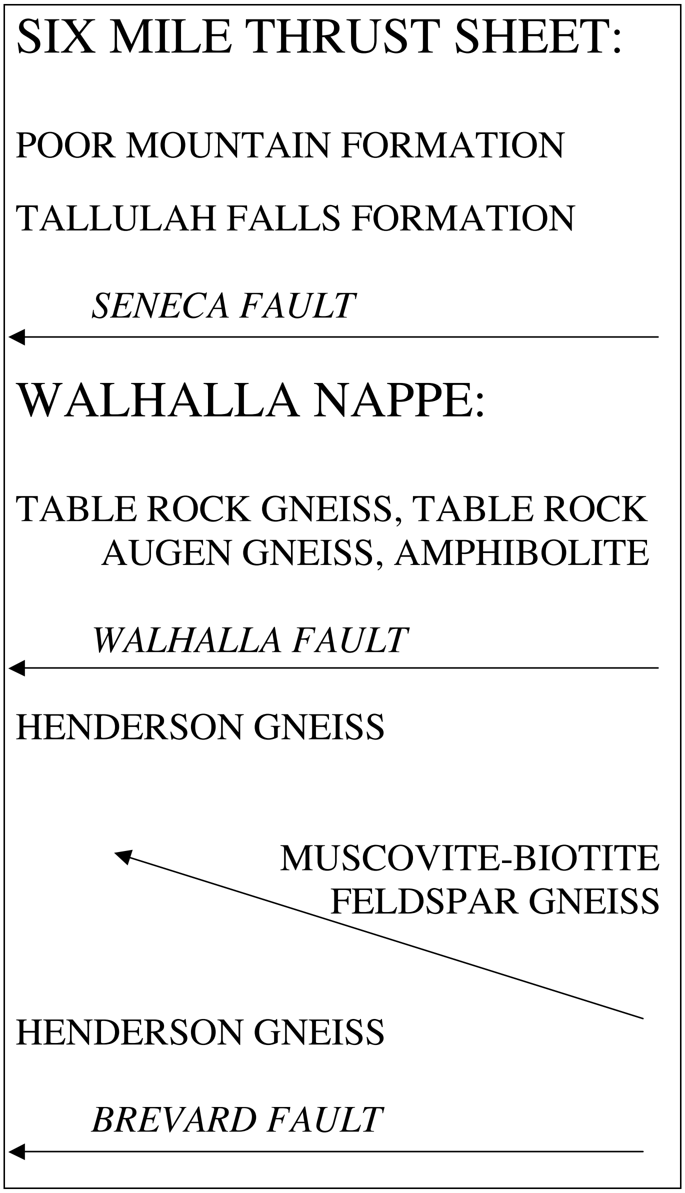

Figure 3. Lithotectonic summary for Standingstone Mountain quadrangle.

thrust sheet, sheet V. Nomenclature for the thrust sheets (sheet I, sheet II etc.) is for convenience of description only; it does not imply sequence of emplacement. The following is a general summary of the lithologic and structural features of each thrust sheet.

Thrust sheet I Henderson Gneiss

In northwest SM quadrangle, muscovite-biotite-two feldspar augen Henderson Gneiss underlies a belt 1-2 km wide along the Crab Creek drainage (Fig. 1). Leucocratic, poorly foliated, granitoid gneiss and pegmatite are subordinate lithologies in sheet I. Typical Henderson gneiss is saprolitic, fine- to medium-crystalline, and well foliated. It is moderately well layered compositionally (i.e., alternating more mafic and more felsic layers) on a scale of millimeters to tens of centimeters. Rounded to ovoid to lenticular microcline augen or porphyroclasts average 0.5 – 1 cm in long dimension; they may be sparsely distributed across an exposure. Henderson Gneiss is variably mylonitic. Many pink microcline augen in hand specimen have thin, gray margins of myrmekite ± fine-crystalline, recrystallized microcline. Augen margins are locally asymmetric (winged).

Stereoplot analysis indicates Henderson Gneiss foliation attitudes within sheet I ($n = 34$) are oriented approximately N37˚E, 19˚SE. Sparse mineral lineations on foliation plunge gently northeast (< 20˚). Sheared varieties of Henderson Gneiss contain abundant recrystallized muscovite. An example is a mappable ductile shear zone of white, phyllonitic, quartz-muscovite schist wherein schistosity parallels foliation in adjacent Henderson Gneiss (Fig. 2).

Henderson Gneiss of sheet I extends westward into the Brevard, NC, quadrangle, which is not mapped. The contact at the base of sheet I lies outside SM quadrangle, and its nature is open to question. By extrapolation of geologic patterns southwestward into Table Rock and Eastatoe Gap quadrangles (Garihan and Ranson, 2001a, 2001b) (Fig. 4), I infer that sheet I is bounded below by the easternmost fault in the regional Brevard fault zone (Hatcher, 2001).

Thrust sheet II Muscovite-biotite-feldspar-quartz gneiss (metasiltstone) Brevard-Poor Mountain transitional unit

Muscovite-biotite-feldspar-quartz gneiss of sheet II underlies a narrow, arcuate zone (0.1-0.8 km wide) striking N55˚-75˚E (Fig. 2). Sheet II is bound above and below by regional thrust faults (Fig. 5, section A-A'; note the thrust to the southeast is relatively steeper). Within this zone, resistant rocks form a ridge (200-500 ft relief) with a prominent north-facing escarpment (Fig. 6, A). The headquarters for the Holmes Educational Forest (Fig. 1) is situated at the base of this ridge. An extensive trail system crossing up and over the escarpment provides ready access to the geology. Impressive waterfalls occur along north-flowing tributaries of Crab Creek (at Shoal Creek and Dismal Creek, Fig. 1) where they cross perpendicular to the metasiltstone. Where state roads cross the gaps in the ridge produced by these tributaries, prominent roadcuts are available for study.

The rock of sheet II is a uniformly hard, dark, fine-crystalline, compositionally poorly layered, schistose, muscovite-biotite-feldspar-quartz gneiss. Shape-modified K-feldspar porphyroclasts (generally < 0.5-1 cm in long dimension, parallel to foliation) are rounded or strongly tapered by ductile deformation. Winged tails of myrmekite occur on K-feldspar margins. They are consistent with west or northwest transport. Coarser muscovite fish with finer biotite inclusions are visible on schistosity surfaces. Their monoclinic shape symmetry in thin section is useful as a

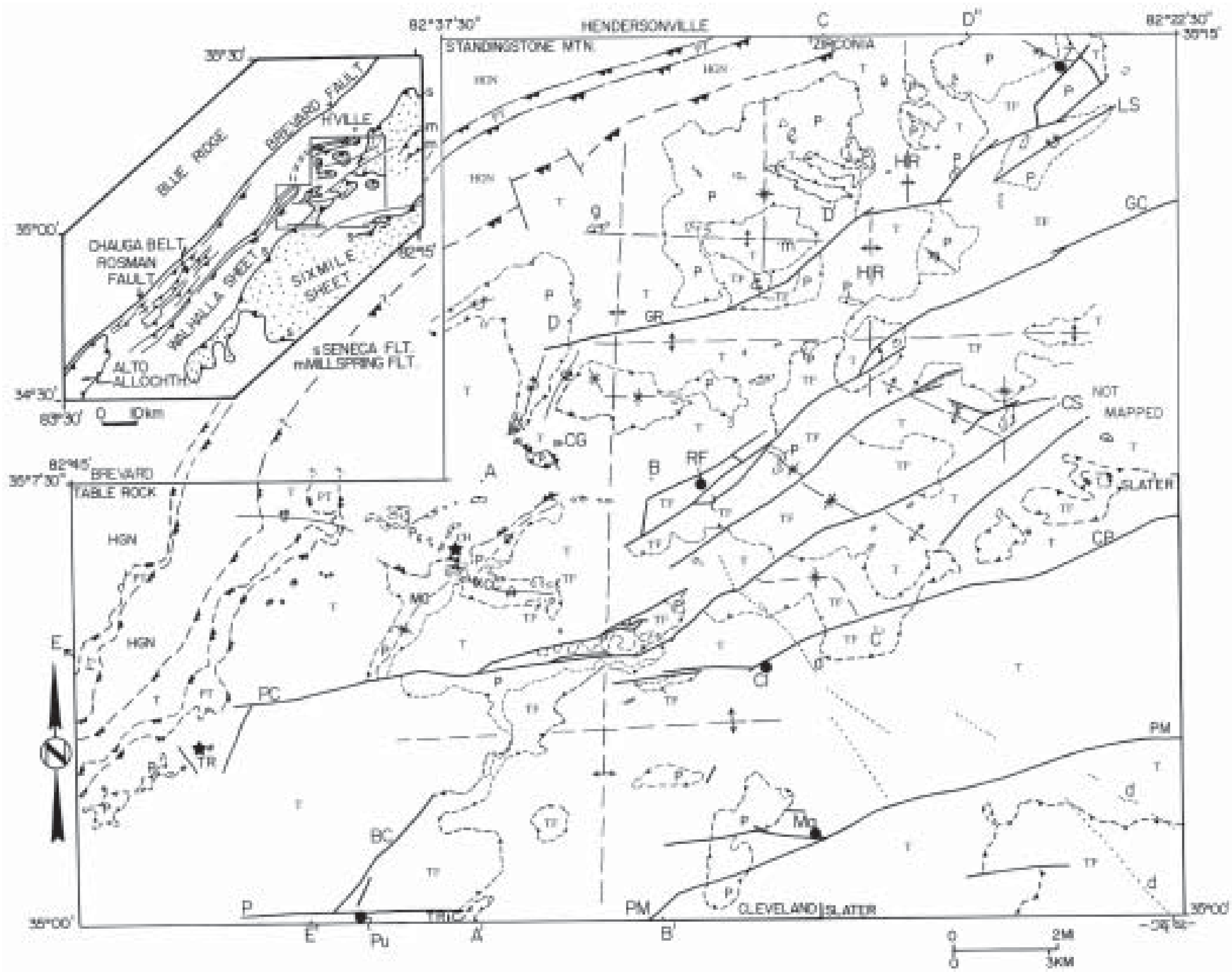

Figure 4. Generalized geologic and tectonic map of the western Inner Piedmont between Zirconia, NC, and Table Rock State Park, SC, area. Inset map shows location in the southern Appalachian Mountains. Revised after Garihan (1999, 2001). Rock units: d-diabase dike, PT-Brevard-Poor Mountain transitional member and Poor Mountain Formation, undivided, P-Poor Mountain Formation, TF-Tallulah Falls Formation, T-Table Rock gneiss, augen gneiss, HGn-Henderson Gneiss. Localities: M-Maybin Mountain, CG-Camp Greenville, g-Grassy Mountain, CH-Caesars Head, RF-River Falls, SC, Z-Zirconia, NC, Pu-Pumpkintown, SC, Ma-Marietta, SC, Cl-Cleveland, SC, TR-Table Rock State Park. Folds: LS-Lake Summit synform, MC-Matthews Creek synform, HR-Huckleberry Ridge antiform, CC-Caesars Head-Campbell Mountain synform. S-Seneca fault sawteeth on hanging wall; double sawteeth on hanging wall side of other thrust faults. Mesozoic faults: GR-Green River fault, GC-Gap Creek fault, CS-Cox Creek-Short Branch fault, PM-Pax Mountain fault, CP-Cross Plains fault, PC-Palmetto Cove fault, P-Pumpkintown fault, BC-Burgess Creek fault. The regional cross sections A-A', B-B', C-C', D-D'-D", E-E' are provided elsewhere (Garihan, 1999, Fig. 2; 2001, Fig. 2).

shear-sense indicator (references in Passchier and Trouw, 1998). At the mesoscopic scale, S-C structure is developed locally in schistose gneiss (Fig. 6, B), due to motion on small, cross-sheet faults.

Stereoplot analysis indicates foliation attitudes within sheet II (n=39) are oriented approximately N40˚E, 21˚SE. A few scarce, tight, overturned mesoscopic folds in this zone verge northwest. Elsewhere, anticlockwise-rotated boudins indicate a sinistral sense of shearing along the schistosity of these ductile rocks (Fig. 6, C).

Garnet is the highest grade index mineral found in these rocks. The lack of sillimanite or kyanite, for example, suggests the metamorphic grade of the rocks carried in sheet II may only be in the upper greenschist or lower amphibolite facies. Metasiltstone is a reasonable protolith for this lithology. The fine muscovite-biotite-feldspar-quartz gneiss likely is correlative with the Brevard-Poor Mountain transitional member (metasiltstone) of the Poor Mountain Formation described by Hatcher and Acker (1984) along strike to the southwest in the Salem quadrangle.

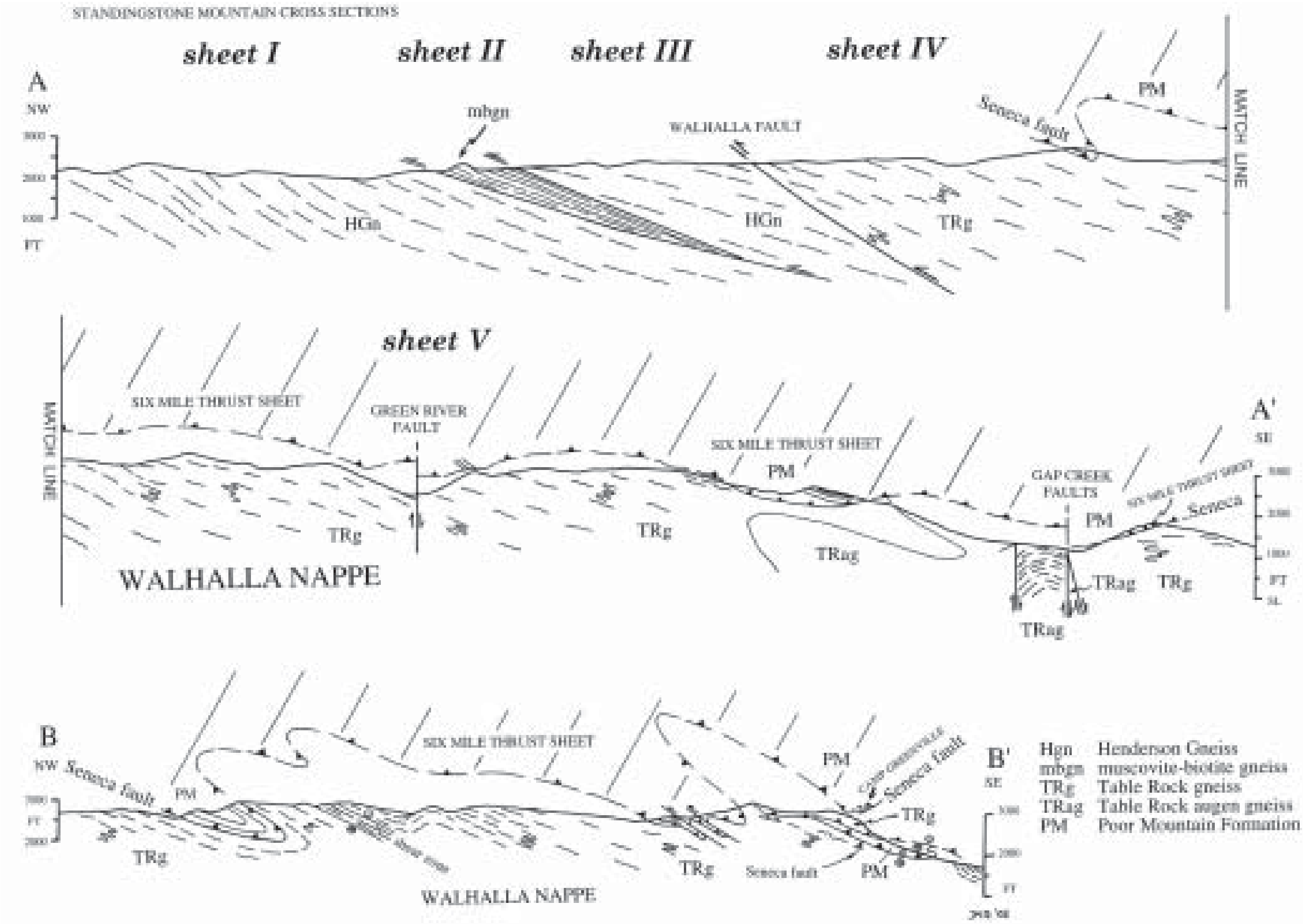

Figure 5. Cross sections through Standingstone Mountain quadrangle. Cross section locations are shown in Figure 2. Rock unit designations are the same as Figure 2. Short, wavy lines are apparent dips of foliation, projected into the cross sections.

Structural complexity at the mesoscopic scale is visible at a roadcut on NC State Road 1128, which follows the Dismal Creek drainage (Fig. 1). Here the thrust sheet is only 0.2 km wide. Muscovite-biotite-feldspar-quartz gneiss is interleaved with Henderson Gneiss along several small thrusts located within sheet II. The faults in outcrop are estimated visually to dip ~ 15˚ SE. The fault contact at the base of sheet II is a sharp break (Fig. 6, D).

Thrust sheet III Henderson Gneiss

Henderson Gneiss of sheet III underlies a zone 0.7-3 km wide (Fig. 2). The rock units are the same as in thrust sheet I. A rugged, north-facing ridge with ~1000 ft of relief winds across the area of sheet III. Impressive exposures of Henderson Gneiss occur at Triple Falls and High Falls along the Little River within Dupont State Forest (Fig. 1).

Stereoplot analysis indicates foliation attitudes within sheet III (n=60) are oriented approximately N32˚E, 13˚SE, essentially the same as Henderson Gneiss attitudes within sheet I (N37˚E, 19˚SE). In general, foliations in the gneiss in outcrop strike more northerly than the orientation of the N50˚-70˚E-striking zone itself. The foliations in Henderson Gneiss are truncated by the fault bounding the top of sheet III.

Thrust sheet IV (Walhalla Nappe) Table Rock gneiss

Regional geologic maps and compilations (Hatcher, 1999a, 1999b; Kalbas et al., 2001) and mapping in Table Rock, Cleveland, and SM quadrangles (Garihan, 2000, 2001, 2002; Garihan and Ranson, 2001b) indicate that sheet IV is correlative with Griffin's (1971, 1974) Walhalla nappe. The allochthon contains resistant Table Rock Plutonic Suite biotite gneiss and lesser biotite-feldspar augen gneiss, with interlayered Poor Mountain Amphibolite (?) and minor schist. Metaquartzite, metagabbro, and ultramafic schists found interlayered with biotite gneiss in the Walhalla nappe in Table Rock quadrangle to the southwest are absent in SM quadrangle.

Table Rock gneiss is the dominant lithology in sheet IV. The foliation attitudes (n=315) generally strike 1) northerly (variably northwest to northeast) and dip gently eastward; and 2) easterly and dip gently both north and south.

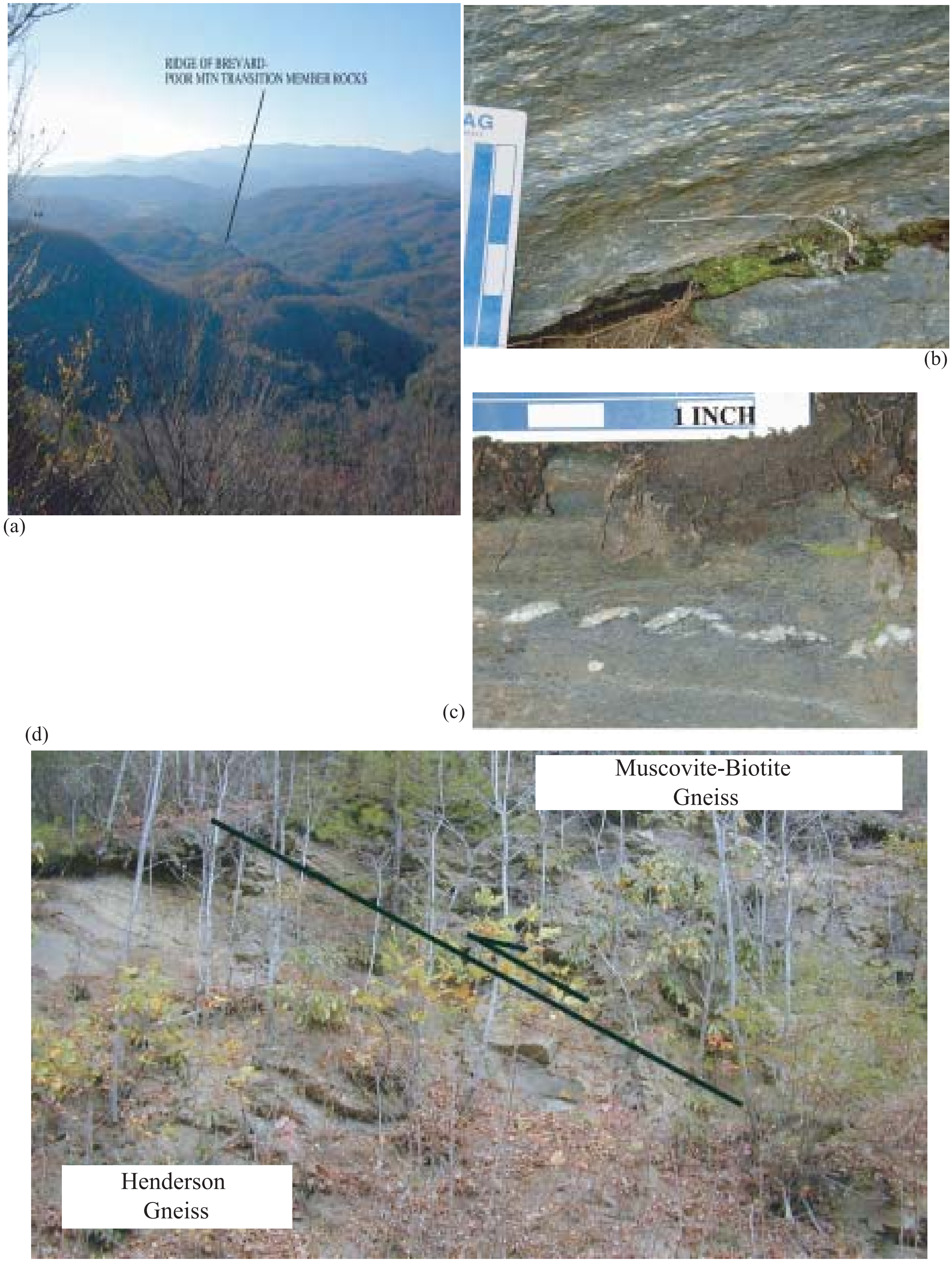

Figure 6. Photographs from Standingstone Mountain quadrangle. (a) View west-northwest from the summit of Stone Mountain. Continuous, resistant ridge in middle distance is underlain by muscovite-biotite-feldspar gneiss of sheet II. Henderson Gneiss flanks the ridge on both sides. (b) S-C structure in muscovite-biotite-feldspar gneiss, Shoal Creek area. C surfaces dipping moderately to the left (oriented ~N10˚E, 30˚SE) indicate normal sense motion, down to the southeast. The origin of S-C structure is probably the motion along a small fault near the exposure, which has caused minor offset of the belt of muscovite-biotite feldspar gneiss. (c) Anticlockwise-rotated boudins, due to sinistral shearing along schistosity in muscovite-biotite-feldspar-quartz gneiss, perhaps during emplacement of sheet II. (d) Henderson Gneiss (sheet I), muscovite-biotite-feldspar-quartz gneiss (sheet II) thrust fault contact, Dismal Creek area.

(e)

(f)

(g)

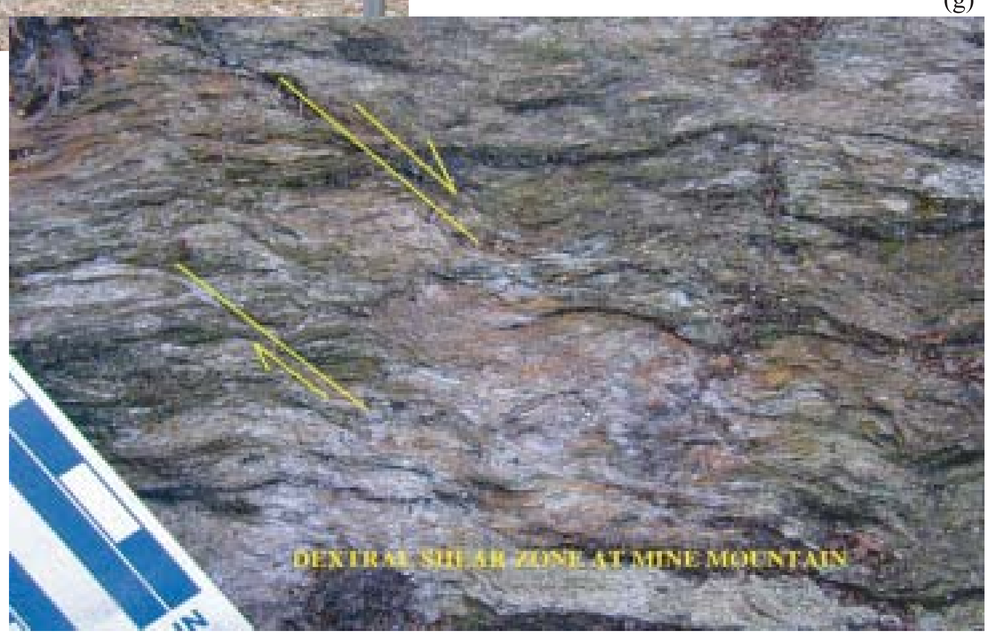

Figure 6. (continued) (e) Overturned chevron folds in Table Rock gneiss, Stone Mountain area. (f) Poor Mountain Amphibolite thrust over Table Rock gneiss along the Seneca fault, Camp Greenville. (g) Dextral shear zone in micaceous Table Rock gneiss, in core of overturned antiform, south of Bridal Veil Falls.

(h)

(i)

Figure 6. (continued) (h) Boudinaged epidote-rich layers in Poor Mountain Amphibolite, beneath overthrust Table Rock gneiss. South of Camp Greenville. (i) Composite image of sill-like body of Table Rock gneiss, forming balds above the Middle Saluda River. Powerline lies just east of Symmes Chapel at Camp Greenville.

On the macroscopic scale, these foliation attitudes probably reflect at least in part the geometry of northwest-vergent, overturned, chevron and isoclinal passive folds in Table Rock augen gneiss commonly seen at mesoscopic scale (Fig. 6, E). The outcrop-scale folds with this geometry generally plunge gently north or east. In southeastern SM quadrangle, large, west-vergent, overturned macroscopic folds are outlined by the contact between two lithologic varieties of Table Rock gneiss: biotite feldspar-augen gneiss and biotite gneiss (Fig. 2). Stereoplot analysis of foliation attitudes (n=26) indicates the folds plunge 9˚/N11˚W. A cross section through these folds is depicted in Fig. 5 (section A-A', right side).

Sill-like bodies of Table Rock biotite gneiss underlie Table Rock, Caesars Head, Stone Mountain, and The Pinnacle (Fig. 1). They continue northeast into North Carolina where they form large lenticular masses surrounded by Henderson Gneiss in Hendersonville, Bat Cave, and Fruitland quadrangles. The rock is designated as OSgg (Ordovician-Silurian) granitic gneiss by Lemmon and Dunn (1973) or as the "438 Ma granitoid" (see references in Davis, 1993). The nature of the contact between Henderson Gneiss (below) and Table Rock gneiss (above) is equivocal because the contact is not exposed. In the North Carolina Columbus Promontory, Davis (1993; pers. comm., 2002) noted an abrupt change over a short distance in the field from augen to non-augen gneiss. Intense deformation clearly has obscured the original relationships, but Davis favored an intrusive origin of Table Rock gneiss into Henderson Gneiss in the Hendersonville, Bat Cave, and Fruitland quadrangles (Lemmon, 1973). Based on its abrupt, dipping trace across topography in SM and Table Rock quadrangles, however, we interpret the contact to be the regional Walhalla fault, at the base of the Walhalla nappe (Fig. 5, section A-A'). In SM quadrangle, the trace of the Walhalla fault between sheets III and IV is broken by small faults of north-northwest strike (local offsets of 0.5-1 km, Fig. 2).

Thrust sheet V (Six Mile) Poor Mountain and Tallulah Falls Formations

Rocks of the Poor Mountain and Tallulah Falls formations lie at the higher elevations (2200-3600 ft) of the quadrangle. They comprise discontinuous klippes of the Six Mile thrust sheet, with the Seneca fault at the base. The geologic arguments to used correlate the Sugarloaf Mountain fault of the Columbus Promontory (Davis, 1993; Garihan, 1999) to the Seneca fault in northwestern South Carolina are summarized elsewhere (Garihan, 2001). The irregular trace of the Seneca fault in central and south SM quadrangle is due to a combination of factors: 1) a shallow regional southeastward dip; 2) the rugged relief in the region, prompted by Cenozoic tectonic activity and erosion; and 3) the complex geometry of the fault surface. The latter is produced by at least two phases of folding, plus a still younger episode of thrust faulting. Imbricate structure interleaving Table Rock gneiss and Poor Mountain Amphibolite along the Seneca fault is visible at an accessible exposure at Camp Greenville (Fig. 6, F) in SM quadrangle (Garihan, 2001).

Rocks of the Poor Mountain Formation in the Six Mile sheet include abundant amphibolite, garnet-mica schist, biotite-muscovite gneiss, and metaquartzite. Rocks of the Tallulah Falls Formation include muscovite-biotite-sillimanite gneiss, muscovite-biotite-sillimanite schist, biotite-porphyroblastic feldspar gneiss, biotite gneiss, minor amphibolite, and calc-silicate gneiss (Fig. 3). The units are migmatitic; commonly they contain quartz-feldspar (granitoid) layers and lenses, which serve to substantially thicken the metamorphic sequence.

Polyphase folding relationships within the Six Mile sheet are complex, and only a part of the complex fold history is described here. The contact between Tallulah Falls and Poor Mountain Formation units within sheet V outlines several west-vergent, south plunging isoclinal folds on the geologic map (Fig. 2). These early fold patterns are truncated by the Seneca fault and thus are believed to predate final emplacement of the Six Mile allochthon. Subsequent to final Seneca fault emplacement, 1) northeast to northerly striking and later 2) northwest to westerly striking, overturned folds deformed the Seneca fault surface (Fig. 4). Hanging wall and footwall metamorphic units were affected as well by these fold sets. Several windows at the culmination positions of earlier northeast- and later northwest-striking, superposed folds expose Table Rock gneiss beneath a large klippe (6 km by 7 km) of Six Mile rocks in eastern SM and western Zirconia quadrangles (Fig. 2). The southwest margin of each window involves the overturned part of a thrust that has been antiformally folded. The folded character of the Seneca fault surface is depicted in sections A-A' and B-B' (Fig. 5).

A dextral shear zone with pronounced S-C structure occurs in micaceous Table Rock gneiss (Fig. 6, G) in the core of a northwest-vergent fold in southwest SM quadrangle (Fig. 2). Partitioning of ductile deformation into a relatively narrow zone has produced coarse, recrystallized muscovite fish. The shear zone may be the product of intense deformation of gneiss producing a room problem in the core region of a developing antiform. This antiform also deforms the Seneca fault surface and hanging wall rocks of the Six Mile sheet along a northeast axis.

Post-Seneca fault thrusting

An exceptional exposure at Mulligan's View (Fig. 1) reveals several younger thrust faults that clearly displace the older Seneca fault surface. Overturned folds have been produced during displacement of the younger thrusts. They warp the Seneca fault and hanging wall and footwall units (Garihan, 2001, see Fig. 5). Along the younger faults, the Table Rock gneiss in the hanging wall has overridden Poor Mountain Amphibolite of the Six Mile thrust sheet. This outcrop scale observation mimics relationships on the map scale. South of Camp Greenville, the regional Seneca fault is overridden by one of the younger thrusts. It carries Table Rock gneiss southwestward over Poor Mountain Formation rocks (Fig. 5, right side of section B-B'). Immediately below the younger thrust, one can see impressive boudins of epidote-rich layers within Poor Mountain Amphibolite (Fig. 6, H). Intense flattening and layer-parallel stretching is presumably the effect of the overriding sheet of Table Rock gneiss. Such boudinage is not common elsewhere in the Six Mile thrust sheet.

Mineralization

In southwest SM quadrangle, several prospect pits have been dug near the trace of the Seneca fault (Fig. 2), on the upright limb of a southwest-vergent synform. Samples of mineralized Poor Mountain Amphibolite contain abundant sphalerite, chalcopyrite, and galena (K. A. Sargent, pers. comm., 2001). The property has never been commercially developed.

Brittle faults

The Marietta-Tryon graben is part of a regional system of discontinuous, siliceous cataclastic rocks and brittle faults in the Inner Piedmont of the Carolinas (Garihan and Ranson, 1992). Recent mapping demonstrates that previously unrecognized sets of brittle faults with both oblique sinistral and dextral movement are present, which postdate the silicified cataclastic rock bodies and commonly displace them significantly (Clendenin and Garihan, 2001).

Brittle faults form a complex pattern of horsts and grabens near the southwest termination of the Gap Creek fault (Fig. 4). These structures disrupt the Seneca fault and hanging wall rocks of the Six Mile allochthon in southeastern SM and Cleveland quadrangles (Fig. 5, section A-A', where the Seneca fault is dropped down ~500 ft on the south side of Gap Creek fault). Regional analysis of slickenlines from rocks at or near the Gap Creek fault indicates dominant left normal-oblique motion. The Seneca fault is dropped down 500 to 600 ft on the south side of the Green River fault, (Fig. 5, section A-A'); in map view, the Seneca fault is right separated about 1.3 km across the Green River fault. Analysis of slickenlines from rocks at or near the Green River fault in central SM quadrangle indicates both right and left normal-oblique motions (Garihan et al., 1990).

DISCUSSION

SM quadrangle provides an opportunity to view, via geologic cross sections, a transect through a stack of five regionally continuous Paleozoic thrust sheets in the Inner Piedmont (Fig. 5). At the structurally lowest position, Henderson Gneiss of sheet I lies immediately southeast of the Brevard fault zone (Hatcher, 2001; Kalbas et al., 2001 map compilation). Statistically similar attitudes of Henderson Gneiss foliation in sheet I and III suggest they were initially part of one continuous thrust sheet, rather than sequentially emplaced sheets of Henderson Gneiss. A narrow thrust wedge (sheet II) of muscovite-biotite-feldspar-quartz gneiss (Brevard-Poor Mountain transitional member metasiltstone) cuts across the belt of Henderson Gneiss. Resistant, quartzose Table Rock gneiss of the Walhalla nappe (sheet IV) was emplaced over less resistant, feldspathic Henderson Gneiss along the Walhalla fault. The Six Mile sheet (sheet V), involving rocks of the Poor Mountain and Tallulah Falls Formations, lies structurally highest in the thrust stack. Extensive erosion at the higher elevations of the quadrangle has reduced a continuous Six Mile sheet to an area of numerous klippes. Current outcrop is roughly half the areal dimensions of the allochthon in the quadrangle. Hence Table Rock gneiss exposures in the footwall beneath the Seneca fault are widespread in SM quadrangle. Intense ductile shearing developed locally within Henderson Gneiss and Table Rock gneiss. A five-mile stretch of cleared powerline between Symmes Chapel and Bridal Veil Falls to the northwest is accessible for a geological traverse up and over the Front, crossing numerous balds developed on Table Rock gneiss (Fig. 1; Fig. 6, I) and a klippe of the Six Mile allochthon.

The lateral continuity of the thrust faults bounding the margins of sheet II is not known with certainty to the west and southwest of SM quadrangle in unmapped Brevard quadrangle. Fault relationships in Table Rock and Eastatoe Gap quadrangles (Fig. 4) (Garihan and Ranson, 1999, 2001a, 2001b), however, provide some insight. The muscovite-biotite-feldspar-quartz gneiss (Brevard-Poor Mountain transitional member metasiltstone) of sheet II found in northern SM quadrangle probably is correlative with the more western of two separate thrust packages (~3 km apart) farther southwest in Table Rock and Eastatoe Gap quadrangles. Both of these separate thrust packages carry variable amounts of Brevard – Poor Mountain transitional member metasiltstone, as well as Poor Mountain Amphibolite and garnet-mica schist. Conjectured structures within Brevard quadrangle may be comparable to structures of the complex Stumphouse Mountain nappe mapped some 70 km to the southwest in the Chauga belt by Hatcher (1999a, see Fig. 2, B-B'). Hatcher and Acker (1984, see their Plate

I, cross section B-B') in Salem quadrangle mapped corresponding contacts between Henderson Gneiss (above) and the Brevard-Poor Mountain transitional member metasiltstone (below) as part of a single, folded thrust. In their Salem cross section, northwest-vergent anticlinal isoclines fold the thrust, thereby producing narrow, continuous belts of metasiltstone within wider Henderson Gneiss belts.

One alternative, a fault-bound wedge interpretation, is shown in Fig. 5 (section A-A'). It is consistent with the attitudes of fault contacts in SM and Table Rock quadrangles that "V" in relation to topography, viz. a shallower fault on the northwestern margin of sheet II and a steeper fault on the southeast margin. The faulted wedge interpretation for sheet II rocks suggests the imbrication and interleaving of footwall muscovite-biotite-feldspar-quartz gneiss and hanging wall units during regional transport of Henderson Gneiss (originally a continuous sheet, now sheets I and III) over metasiltstone.

A second alternative, clearly speculative, is the correlation of the two separate thrust packages of Brevard – Poor Mountain transitional member metasiltstone and Poor Mountain Amphibolite and garnet-mica schist in Table Rock quadrangle (Fig. 4) with Poor Mountain rock exposures of the Six Mile allochthon in southwest SM quadrangle. In this interpretation the two thrust packages are laterally continuous, northwest-vergent synformal belts affecting the Seneca fault and hanging wall rocks. Duplication of the belt then is due to thrusting along the Walhalla fault. Therefore, by this interpretation, in the Table Rock quadrangle portion of Figure 4, belts labeled PT are tight downfolds affecting the Six Mile thrust sheet. An alternate explanation is shown in Figure 7.

Multiple folding events developed subsequent to emplacement of the Six Mile allochthon along the Seneca fault. Hanging wall and footwall rocks of that thrust, of course, must also be affected by these deformations. Earlier folds are northeast to northerly striking, and later ones are northwest to westerly striking. The result is the current complex configuration of the Six Mile sheet in southern SM and Cleveland quadrangles. This fold superposition in SM quadrangle is consistent with an interpretation of the regional distribution of mineral stretching lineations in the Inner Piedmont (Davis, 1993; Hatcher, 1999a, 2001): northwest- and west-directed thrust sheets were deflected southwestward, the result of their interaction with an active Brevard fault zone, during a Neoacadian (360-350 Ma) deformational event.

Several types of important structures developed in association with the later (post-Seneca fault) phase of southwest vergent, intense folding: 1) local thrusts of Table Rock gneiss were emplaced southward over the Six Mile sheet; and 2) west striking, ductile shear zones developed within Table Rock gneiss, producing abundant fish of recrystallized muscovite.

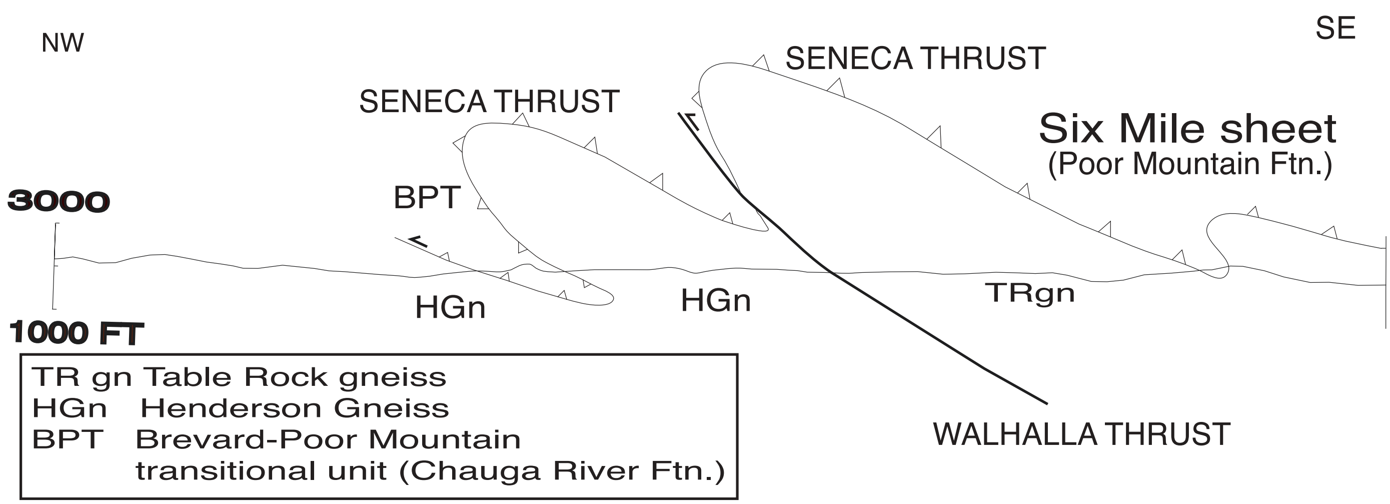

Figure 7. Alternate cross section. Speculative correlation of sheet of sheet II and sheet IV.

ACKNOWLEDGMENTS

My thanks go to C. W. Clendenin of the South Carolina Geological Survey and cartographer Malynn D. Fields, for their help in the preparation of the illustrations. R. D. Hatcher, Jr. provided beneficial comments in a critical review of the manuscript. Furman University provided logistical support for fieldwork. My colleague William A. Ranson has participated with me in the mapping of several Inner Piedmont quadrangles.

REFERENCES CITED

Citron, G. P., and Brown, L. D., 1979, Recent vertical crustal movements from precise leveling surveys in the Blue Ridge and Piedmont provinces, North Carolina and Georgia: Tectonophysics, v. 52, p. 223-238.

Clark, G. M., 1993, Quaternary geology and geomorphology of part of the Inner Piedmont of the southern Appalachians in the Columbus Promontory upland area, southwestern North Carolina and northwestern South Carolina, *in* Hatcher, R. D., Jr., and Davis, T. L., eds., Studies of Inner Piedmont geology with a focus on the Columbus Promontory: Carolina Geological Society annual field trip guidebook, North Carolina Geological Survey, p. 67 - 84.

Clendenin, C. W., and Garihan, J. M., 2001, Timing of brittle faulting on Pax Mountain: A chicken or the egg question applicable to Piedmont mapping: Geological Society of America Abstracts with Programs, v. 33, no. 2, p. A-18.

Davis, T. L., 1993, Geology of the Columbus Promontory, western Inner Piedmont, North Carolina, southern Appalachians, *in* Hatcher, R. D., Jr., and Davis, T. L., eds., Studies of Inner Piedmont geology with a focus on the Columbus Promontory: Carolina Geological Society annual field trip guidebook, North Carolina Geological Survey, p. 17-43.

Gable, D. J., and Hatton, T., 1983, Maps of vertical crustal movements in the conterminous United States over the last 10 million years: U. S. Geological Survey, Map 1-1315, 1:5,000,000-1:10,000,000 scale.

Garihan, J. M., 1999, The Sugarloaf Mountain thrust in the western Inner Piedmont between Zirconia, North Carolina and Pumpkintown, South Carolina, *in* A compendium of selected field guides, Geological Society of America, Southeast Section Meeting, The University of Georgia, p. 34-42.

Garihan, J. M., 2000, Geologic map of the Cleveland 7.5-minute quadrangle, Greenville and Pickens Counties, South Carolina: SC Dept. of Natural Resources, Geological Survey, Open-file report 130 (2000), 1:24,000 scale.

Garihan, J. M., 2001, Observations of the Seneca fault and their implications for thrust sheet emplacement in the Inner Piedmont of the Carolinas: South Carolina Geology, v. 43, p. 1-13.

Garihan, J. M., 2002, Geology of the Standingstone Mountain 7.5-minute quadrangle, Inner Piedmont, SC-NC: Geological Society of America Abstracts with Programs, v. 34, no. 2, p. A-11.

Garihan, J. M., and Ranson, W. A., 1992, Structure of the Mesozoic Marietta-Tryon graben, South Carolina and adjacent North Carolina, *in* Bartholomew, M. J., Hyndman, D. W., Mogk, D. W., and Mason, R., eds., Basement tectonics 8: Characterization and comparison of ancient and Mesozoic continental margins: Proceedings of the Eighth International Conference on Basement Tectonics, Kluwer Academic Publishers, Dordrecht, p. 539-555.

Garihan, J. M., and Ranson, W. A., 1999, Roadlog and descriptions of stops in parts of the Table Rock, Cleveland, and Standingstone Mountain quadrangles, SC-NC, *in* A Compendium of Selected Field Guides, Geological Society of America, Southeastern Section Meeting, The University of Georgia p. 43-51.

Garihan, J. M., and Ranson, W. A., 2001a, Geologic map of the Table Rock 7.5-minute quadrangle, Greenville and Pickens Counties, South Carolina: SC Dept. of Natural Resources, Geological Survey, Open-file report 141, 1:24,000 scale.

Garihan, J. M., and Ranson, W. A., 2001b, Geologic transect across the Table Rock and Eastatoe Gap 7.5-minute quadrangles, western Inner Piedmont, Greenville and Pickens Counties, SC-NC: Geological Society of America Abstracts with Programs, v. 33, no. 2, p. A-3.

Garihan, J., Ranson, W., Vaughan, C., Perry, E., Hicks, S., and Palmer, J., 1997, Structural control of erosional topography across the Blue Ridge Front in the Zirconia 7 1/2 minute quadrangle, Inner Piedmont, SC-NC: Geological Society of America Abstracts with Programs, v. 29, no. 3, p. 18.

Griffin, V. S., Jr., 1971, The Inner Piedmont belt of the southern crystalline Appalachians: Geological Society of America Bulletin, v. 82, p. 1885-1898.

Griffin, V. S., Jr., 1974, Analysis of the Piedmont in northwest South Carolina: Geological Society of America Bulletin, v. 85, p. 1123-1138.

Hatcher, R. D., Jr., 1999a, Geotraverse across part of the Acadian orogen in the southern Appalachians, *in* A compendium of selected field guides, Geological Society of America, Southeastern Section Meeting, The University of Georgia, p. 12-33.

Hatcher, R. D., Jr., 1999b, Digital geologic maps of the eastern Blue Ridge, and part of the Inner Piedmont in northeastern Georgia, northwestern South Carolina, and southwestern North Carolina: map compilation from various sources. 1:140,800 scale.

Hatcher, R. D., Jr., 2001, Rheological partitioning during multiple reactivation of the Palaeozoic Brevard fault zone, southern Appalachians, *in* Holdsworth, R. E., Strachan, R. A., Magloughlin, J. F., and Knipe, R. J., eds., The nature and tectonic significance of fault zone weakening: Geological Society of London, Special Publication 186, p. 257-271.

Hatcher, R. D., Jr., and Acker, L. L., 1984, Geology of the Salem quadrangle, South Carolina: South Carolina Geological Survey, MS-26, 23 p., 1:24,000 scale.

Haselton, G. M., 1974, Some reconnaissance geomorphological observations in northwestern South Carolina and adjacent North Carolina: South Carolina Geological Survey/South Carolina State Development Board, Geologic Notes, v. 18, no. 4, p. 60-74.

Kalbas, J. L., Bream, B. R., and Bier, S. E., 2001, Geologic map of the Brushy and South Mountains, central and western Inner Piedmont, North Carolina: University of Tennessee, Structural Geology and Tectonics Research Group, 100,000 scale.

Lemmon, R. E., 1973, Geology of the Bat Cave and Fruitland quadrangles and the origin of the Henderson Gneiss, western North Carolina [Ph. D. dissertation]: Chapel Hill, University of North Carolina, 145 p.

Lemmon, R. E., and Dunn, D. E., 1973, Geologic map and mineral resources of the Bat Cave quadrangle, North Carolina:

North Carolina Department of Natural Resources and Community Development Map GM-202 NW, 1:24,000 scale.

Nelson, A. E., Horton, J. W., Jr., and Clarke, J. W., 1986, Stacked thrust sheets of the Piedmont and Blue Ridge Provinces, northeast Georgia and western South Carolina: Geological Society of America, Abstracts with Programs, v. 17, p. 674.

Nelson, A. E., Horton, J. W., Jr., and Clarke, J. W., 1987, Generalized tectonic map of the Greenville 1˚ x 2˚ quadrangle, Georgia, South Carolina, and North Carolina: U. S. Geological Survey Map MF-1898, scale 1:250,000.

Nelson, A. E., Horton, J. W., Jr., and Clarke, J. W., 1998, Geologic map of the Greenville 1˚ x 2˚ quadrangle, Georgia, South Carolina, and North Carolina: U. S. Geological Survey Map I-2175, scale 1:250,000.

Passchier, C. W., and Trouw, R. A. J., 1998, Microtectonics: Springer, Berlin, 289 p.

Ranson, W. A., and Garihan, J. M., 2001, Geology of the Inner Piedmont in the Caesars Head and Table Rock State Parks area, northwestern South Carolina: 2001 Carolina Geological Society Field Trip: South Carolina Geology, v. 43, p. 73-86.

Carolina Geological Society
Annual Field Trip
October 19-20, 2002

The Walker Top Granite: Acadian granitoid or eastern Inner Piedmont basement?

Scott D. Giorgis[1, a]
Russell W. Mapes[2, b]
Brendan R. Bream[1]

[1]Department of Geological Sciences
University of Tennessee–Knoxville
306 Geological Sciences Building
Knoxville, TN 37996-1410

[2]Department of Geology
Vanderbilt University
5717 Stevenson Center
Nashville, TN 37235-1805

present addresses:
[a]Department of Geology and Geophysics, University of Wisconsin–Madison, Madison WI 53706, scott@geology.wisc.edu
[b]Department of Geological Sciences, University of North Carolina–Chapel Hill, Chapel Hill, NC 27599

ABSTRACT

Geologic mapping in the central Inner Piedmont has delineated a feldspar megacrystic biotite gneiss unit (herein named the Walker Top Granite) that outcrops in the hanging wall of the Brindle Creek fault near Morganton, North Carolina. This lithology has an igneous origin with a granitic to granodioritic composition. Contacts of the Walker Top Granite with the enclosing rocks are concordant but do not reveal evidence of crosscutting relationships. These observations initially suggest that the Walker Top Granite was a depositional basement for the enclosing schist and paragneiss. Geochronologic data place the crystallization age of the Walker Top Granite at 366 ± 3 Ma. There are no detrital zircons of this age in the enclosing rocks. Based on these data, we conclude that the Walker Top Granite is a Late Devonian pluton that was most likely intruded during the Acadian orogeny. The presence of the Walker Top Granite solely in the hanging wall of the Brindle Creek fault suggests that movement occurred after emplacement; the Brindle Creek fault, therefore, is a syn- to post-Acadian feature. While textural, mineralogical, and geochemical similarities suggest that the Walker Top Granite and the Henderson Gneiss are genetically related, differences in crystallization age (Late Devonian vs. Early Ordovician) indicate that this is not the case.

INTRODUCTION

The Tugaloo terrane, bounded to the west by the Hayesville fault and to the east by the Central Piedmont suture, is separated by the Brevard fault into the eastern Blue Ridge and the Inner Piedmont (Hatcher, this guidebook). Three Grenvillian internal basement massifs occur in the eastern Blue Ridge, one exposed around Trimont Ridge, one with-

Giorgis, S.D., Mapes, R.W., and Bream, B.R., 2002, The Walker Top Granite: Acadian granitoid or eastern Inner Piedmont basement?, *in* Hatcher, R.D., Jr., and Bream, B.R., eds., Inner Piedmont geology in the South Mountains-Blue Ridge Foothills and the southwestern Brushy Mountains, central-western North Carolina: North Carolina Geological Survey, Carolina Geological Society annual field trip guidebook, p. 33-43.

in the Tallulah Falls dome, and one within the Toxaway dome (Hatcher *et al*., in review). Grenville basement units in the Inner Piedmont are less clearly recognizable. The best candidate for basement in the Inner Piedmont is the Forbush Gneiss, which is exposed on the southwestern flank of the Sauratown Mountains window (Heyn, 1985; Carrigan et al., in press). The origin of the Inner Piedmont is a critical question in southern Appalachian tectonics, although a key difficulty in determining its crustal affinity is the absence of clearly identifiable basement units. Using detrital zircon geochronology, igneous zircon geochronology, and trace element and Nd isotope geochemistry Bream (this guidebook) concludes that the western Inner Piedmont has a Laurentian origin.

Based on contact relationships and field evidence, Giorgis and Hatcher (1999) proposed the Walker Top Granite is Inner Piedmont basement. The Walker Top Granite, located east of the Brindle Creek fault in the eastern Inner Piedmont, was originally recognized by Goldsmith *et al.* (1988) in the Charlotte 1˚ x 2˚ geologic map. Using textural evidence, Goldsmith *et al.* (1988) hypothesized that the Walker Top Granite represents less deformed Henderson Gneiss. Recognition of basement in the eastern Inner Piedmont could provide important clues about crustal relationships between the eastern and western Inner Piedmont. Alternatively, demonstrating a connection between the Henderson Gneiss and the Walker Top Granite could provide constraints on the plutonic and deformation histories of the eastern and western Inner Piedmont.

This study combines petrologic, geochemical, geochronologic, and field data to summarize our current knowledge of the Walker Top Granite. Our objectives are to: 1) test the hypothesis that Walker Top Granite is eastern Inner Piedmont basement; 2) determine what regional constraints the Walker Top Granite can place on the tectonic evolution of the Inner Piedmont and southern Appalachians; and 3) weigh any possible relationships between Henderson Gneiss and Walker Top Granite.

GEOLOGIC SETTING

The Inner Piedmont is bordered on the west by the Brevard fault zone and to the east by the central Piedmont suture and Carolina terrane (Fig. 1). The western and eastern flanks of the Inner Piedmont locally contain lower-grade rocks (Hatcher, 1972), while the interior contains progressively higher-grade rocks. The 1:250,000-scale map by Goldsmith *et al.* (1988) delineated a series of rock units consisting of biotite gneiss, sillimanite schist, amphibolite, and a feldspar megacrystic biotite in the central Inner Piedmont. Additional mapping (e.g., Davis, 1993) subdivided the western Inner Piedmont units into packages of biotite gneiss, amphibolite, granitic gneiss, pelitic schist, and quartzite. The paragneiss sequence in the western Inner

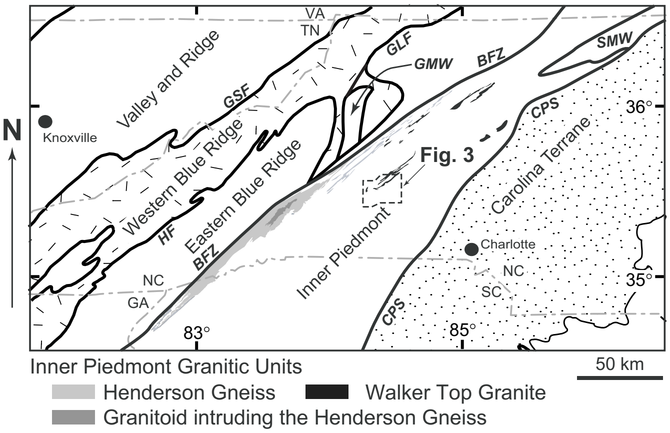

Figure 1. Generalized tectonic map of the southern Appalachians. GSF - Great Smoky fault, HF - Hayesville fault, GLF - Gossan Lead fault, BFZ- Brevard fault zone, CPS - Central Piedmont suture (modified from Hatcher *et al.*, 1990).

Piedmont can be subdivided into three members: a lower metagraywacke-schist-amphibolite member, separated by an aluminous schist member from the upper graywacke-schist member, which locally contains amphibolite. The similarity between marker units and lithologies of this portion of the sequence and assemblages present in the easternmost Blue Ridge and flanking the southwestern end of the Sauratown Mountains window has led previous workers (e.g., Hatcher, 1975, 1989; Heyn, 1984; Davis, 1993; Hill, 1999; Bream, 1999) to conclude that these rocks are eastern equivalents of the Tallulah Falls/Ashe Formation.

All of the standard subdivisions of the Tallulah Falls Formation of Hatcher (1971) are mappable in the Marion, North Carolina, area in the western Inner Piedmont (Bream, 1999; Hill, 1999). In the hanging wall of the Brindle Creek thrust sheet, however, this hierarchy is less clear. Sillimanite schist thickens eastward and directly overlies Walker Top Granite, while in other places the schist is separated from it by a thin metagraywacke, schist, and amphibolite unit (Fig. 2). The sillimanite schist is in turn overlain by metagraywacke and biotite-muscovite schist. Because of the uncertainty in correlating these units east across the Brindle Creek fault, and the implications of new U-Pb detrital zircon geochronologic data (Bream, this guidebook), we have abandoned the Tallulah Falls Formation stratigraphic hierarchy employed by Giorgis (1999), Willliams (2000), and Bier (2001) for the Brindle Creek thrust sheet.

Unconformably overlying the Tallulah Falls Formation in the western Inner Piedmont is the Poor Mountain Formation (Hatcher, this guidebook), which was originally recognized in South Carolina (Shufflebarger, 1961; Hatcher, 1969). In the immediate footwall of the Brindle Creek thrust the Poor Mountain Formation is intensely migmatitic and consists of laminated amphibolite, hornblende gneiss, and quartz-feldspar metaquartzite/metatuff (Giorgis, 1999; Wil-

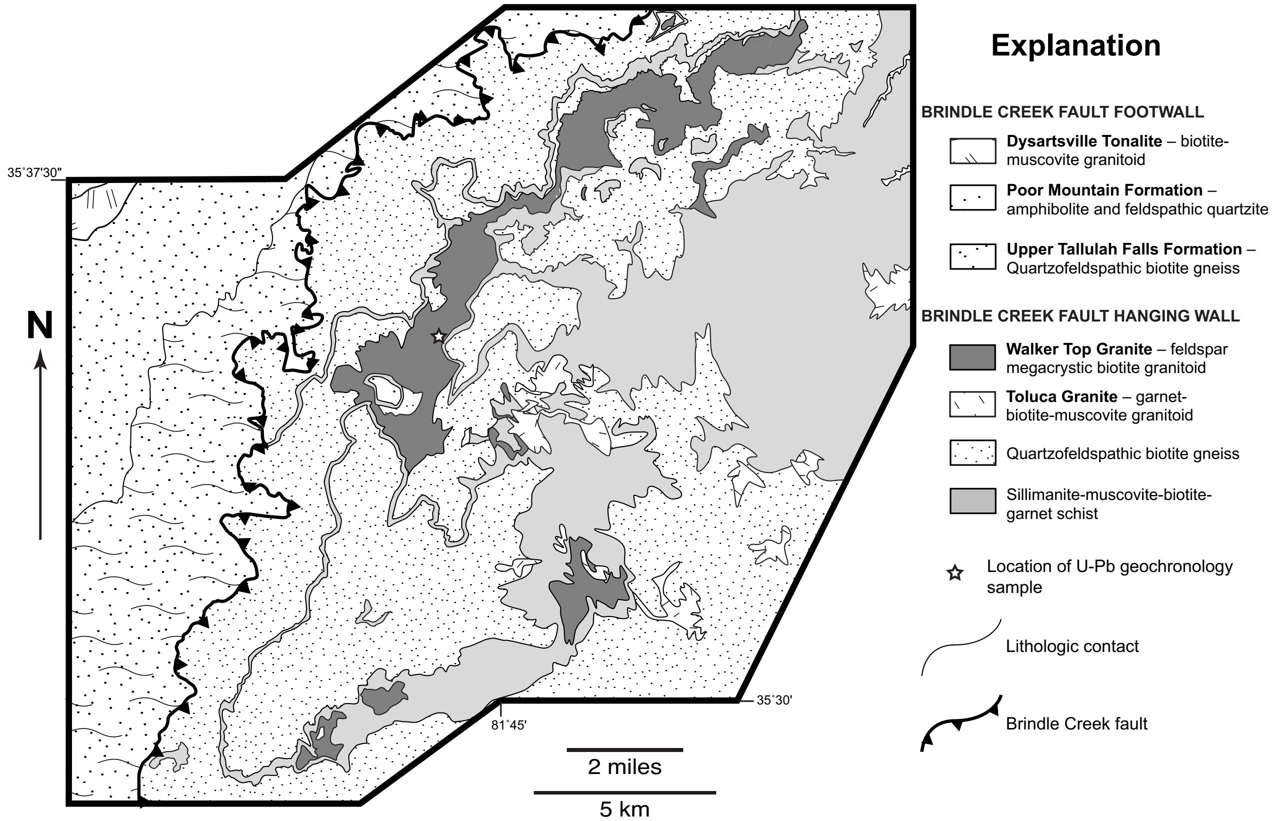

Figure 2. Simplified bedrock geologic map of the South Mountains area. Mapping by Giorgis (1999), Williams (2000), Bier (2001), and Jeffrey Riedel (unpublished).

liams, 2000). The Poor Mountain Formation is less migmatitic to the northwest where it is preserved in synclines in the footwalls of several thrust sheets at slightly lower metamorphic grade (Bream, 1999; Hill, 1999).

A series of plutons intruded the Inner Piedmont from the Middle Ordovician to the Early Silurian (Vinson, 1999; Carrigan *et al*., 2001a; Mapes *et al*., 2002). In addition to the Henderson Gneiss (~490 Ma, Vinson, 1999; Carrigan *et al.,* 2001), Goldsmith *et al.* (1988) mapped several plutons, including the Dysartsville pluton and the Toluca Granite. The Dysartsville pluton has a Middle Ordovician age (~465 Ma; Bream, unpublished data) and consists of a medium- to coarse-grained, weakly banded biotite granitoid (Bream, 1999). The Toluca Granite (~375 Ma; Mapes *et al*., 2002) is also is a fine- to medium-grained and is commonly garnetiferous. The Toluca Granite and Walker Top Granite outcrop solely in the hanging wall of the Brindle Creek fault (Fig. 2), suggesting that movement on the Brindle Creek fault occurred after emplacement of these granitoids (see Hatcher, this guidebook, and Bream, this guidebook for more details on the nature and significance of the Brindle Creek fault).

THE WALKER TOP GRANITE

The Walker Top Granite and equivalent bodies were first mapped by Goldsmith *et al*. (1988) as porphyritic Henderson Gneiss, describing it as locally containing rapakivi texture and enclosing small charnockite bodies. They showed that this unit is widely distributed in the central Inner Piedmont on the Charlotte 1° x 2° sheet (Fig. 1). Kish and Odom (1999) obtained a ~430 Ma conventional U-Pb zircon age on charnockite at Cat Square, North Carolina.

In outcrop and hand sample, the Walker Top Granite is characterized by 1 cm to 8 cm-long blocky potassium feldspar megacrysts with myrmekitic rims and aspect ratios of 1:2 to 1:8 (Fig. 3a). Feldspar megacrysts tend to be randomly oriented and foliation is mostly weak and confined to the matrix. Local strongly foliated zones wherein mega-

(a)

(b)

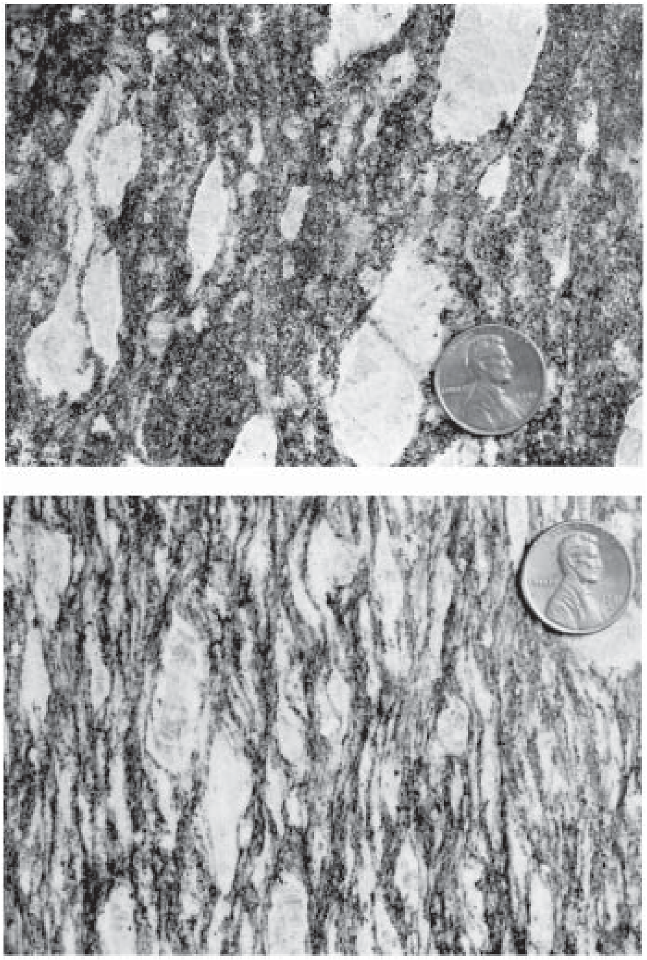

Figure 3. (a) Polished slab of Walker Top Granite from the South Mountains. (b) Polished slab of Henderson Gneiss from the Vulcan Materials Company quarry at Hendersonville, North Carolina.

crysts are deformed from otherwise euhedral to subhedral crystals with Carlsbad twinning to flattened tailed porphyroclasts are interpreted here as ductile shear zones. Goldsmith *et al.* (1988) interpreted the blocky euhedral feldspars as less deformed versions of characteristic potassium feldspar augen in the Henderson Gneiss (Fig. 3b), thus suggesting the Walker Top Granite could be the Henderson Gneiss protolith.

A medium-grained granitoid is associated with the Walker Top Granite, often present along the contact with the enclosing metasedimentary units. This lithology contains biotite as the mafic phase and is characterized by the presence of garnet. A mappable unit of a medium-grained altered gabbro has also been found within the Walker Top Granite (Giorgis, 1999). This rock unit consists predominantly of plagioclase (An_{70-80}), orthopyroxene, orthopyroxene altered to hornblende, and biotite.

Type Area

The type area of the Walker Top Granite is located in the southwestern quarter of the Morganton South 7.5-minute quadrangle, North Carolina (Fig. 4). Walker Top Granite is well exposed along Burkemont Mountain Road in the vicinity of Walker Top Mountain. Outcrops range from pavement exposures to moderate size cliffs to roadcuts. The best outcrops occur as small cliffs on the steep, northwest-facing slopes of Walker Top and Burkemont Mountains below the ridge crest (Fig. 4).

Mineralogy

The Walker Top Granite consists predominantly of plagioclase, potassium feldspar, quartz, biotite, and muscovite (Table 1). Lesser amounts of myrmekite, garnet, and opaque minerals are present with trace amounts of sphene, zircon, and apatite. Myrmekite occurs most commonly as an overgrowth on K-feldspar megacrysts but can also be found in the matrix. The matrix consists of medium-grained (<4 mm) quartz, biotite, muscovite, and two feldspars. Modal data indicate that this unit is granite to granodiorite in the IUGS modal classification (Fig. 5a; Streckeisen, 1976). The Henderson Gneiss also plots as granite or granodiorite. Classification of these units using normative mineralogy (Table 2) determined from chemical analysis of whole-rock powders yields similar results (Fig. 5b).

Geochemistry

The bulk chemistry of eight Walker Top Granite samples was determined using energy dispersive X-ray fluorescence (XRF; Table 3) with an automated protocol prepared for igneous rocks at the instrument at the University of Tennessee. Most samples were prepared using a tungsten carbide mill. Two samples, one each of the Henderson Gneiss and the Walker Top Granite, were prepared in an alumina ceramic mill and analyzed professionally (XRAL and ACTLABS, respectively) using a combination of XRF and inductively coupled plasma mass spectrometry. The XRAL and ACTLABS results were comparable to our XRF data.

In highly metamorphosed rocks, such as the rocks examined in this study, it is critical to take into account alteration of the original bulk chemical concentrations. Alteration due to weathering processes can be eliminated through sample selection. Metamorphic alteration cannot be eliminated; therefore, elements used for comparison should be selected based on their immobility during metamorphism. It is generally accepted (e.g., Pearce and Cann, 1973; Wilson, 1989) that cations with high charge to radius ratios and small ionic radii are the most immobile.

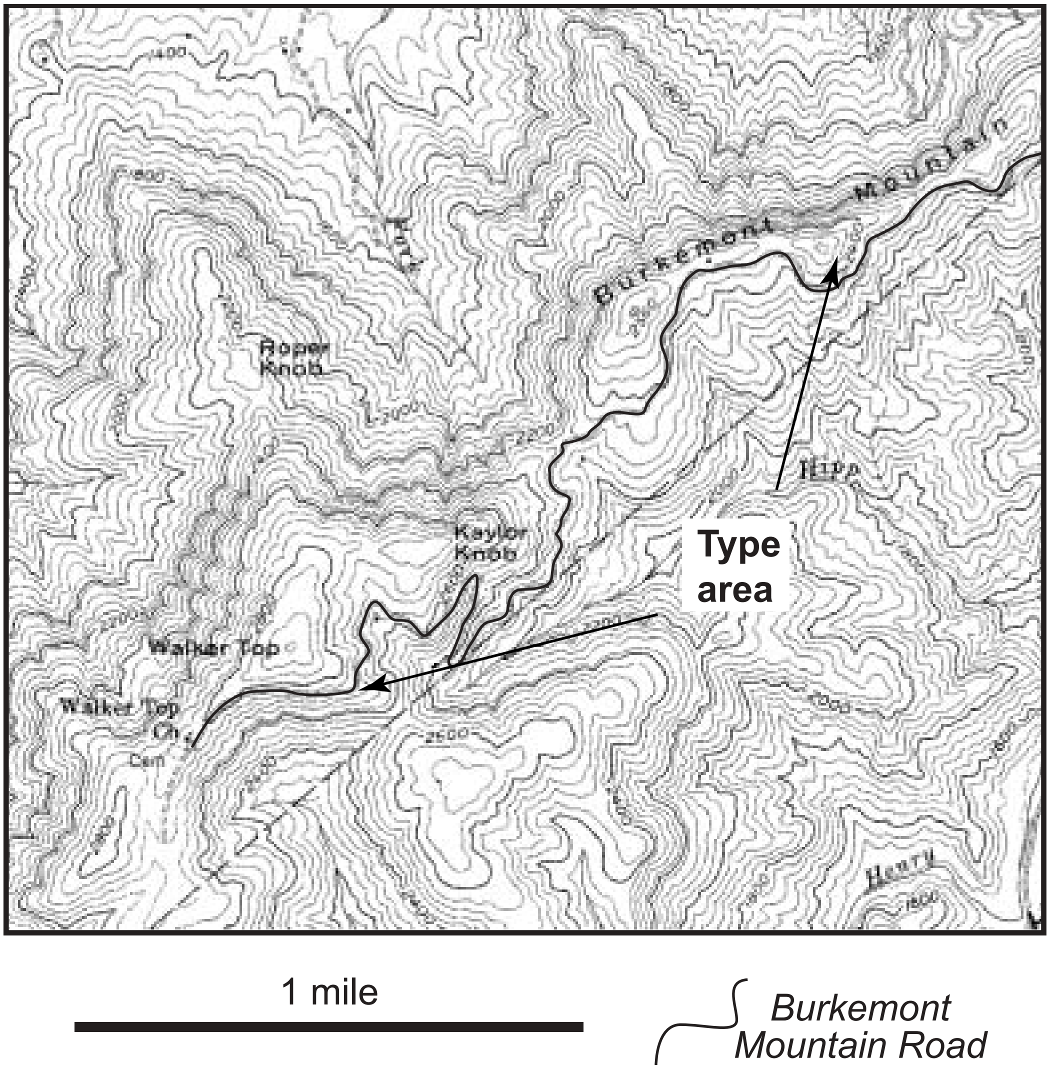

Figure 4. The type area of the Walker Top Granite, located in the southwestern quarter of the Morganton South 7.5-minute quadrangle. Good outcrops of the Walker Top Granite occur on the northwest-facing slope of Walker Top and Burkemont Mountains.

Table 1. Modal mineralogy of Walker Top Granite and Henderson Gneiss samples.

	Qtz	P	Kspr	Bio	Ms	Ch	E	Gt	My	Sp	Ap	Zir	All	Op	Pts
Walker Top Granite															
MS53	21.6	35.2	10.3	26.5	5.0	—	—	tr	1.0	—	—	tr	—	tr	1014
D341	27.8	35.3	8.8	26.0	0.5	—	—	tr	0.9	—	—	tr	—	tr	1022
BK111	20.5	34.3	17.9	19.0	7.0	—	tr	—	1.2	—	—	—	—	—	1024
D708	30.7	24.0	12.5	27.5	3.8	—	—	—	1.2	—	tr	tr	—	tr	1019
MS26	38.1	21.1	16.6	15.4	5.8	—	—	1.2	1.6	—	—	tr	—	—	1023
Henderson Gneiss															
G681	18.5	32.3	21.3	19.8	2.0	—	2.4	—	—	2.8	—	—	tr	0.9	1058
SH75	24.2	40.2	16.6	12.8	3.8	—	1.0	—	—	0.9	—	—	tr	0.5	1019
SH137	27.3	29.4	25.9	13.0	1.2	—	1.4	—	—	0.9	—	—	0.3	0.9	1086
SH301	23.5	30.0	20.0	20.7	0.5	tr	2.5	—	—	2.9	—	—	tr	—	1026

Note: Qtz - quartz, P - plagioclase, Kspr - microcline, Bio - biotite, Ms - muscovite, Ch - chlorite, E - epidote, Gt - garnet, My - myrmekite, Sp - sphene, Ap - apatite, Zir - zircon, All - allanite, Op - opaques, Pts - total points counted, tr - mineral occurs in trace amounts (<0.5%)

Rubidium (Rb), yttrium (Y), and niobium (Nb) are immobile elements that show a systematic variation in granitoids based on their tectonic origin (Pearce *et al*., 1984). A plot of Nb vs. Y yields a tight clustering of both Walker Top Granite and Henderson Gneiss data (Fig. 7a). A Rb vs. Nb+Y ratio yields a similar result (Fig. 7b). The significant overlap between these two data sets suggests that these granitoids originated in an identical tectonic setting, despite the almost 100 m.y. difference in their crystallization ages (see below).

Orthogneiss vs. Paragneiss

Texture, zircon morphology, and bulk chemistry can be used as criteria for determining if a metamorphic rock has an igneous origin (orthogneiss) or a sedimentary (paragneiss) origin. The characteristic tabular, subhedral to euhedral feldspar megacrysts (Fig. 3a) do not readily suggest sedimentary origin for the Walker Top Granite. Vinson (1999) examined the morphology of zircons in the Walker Top Granite and determined that, in general, the zircons

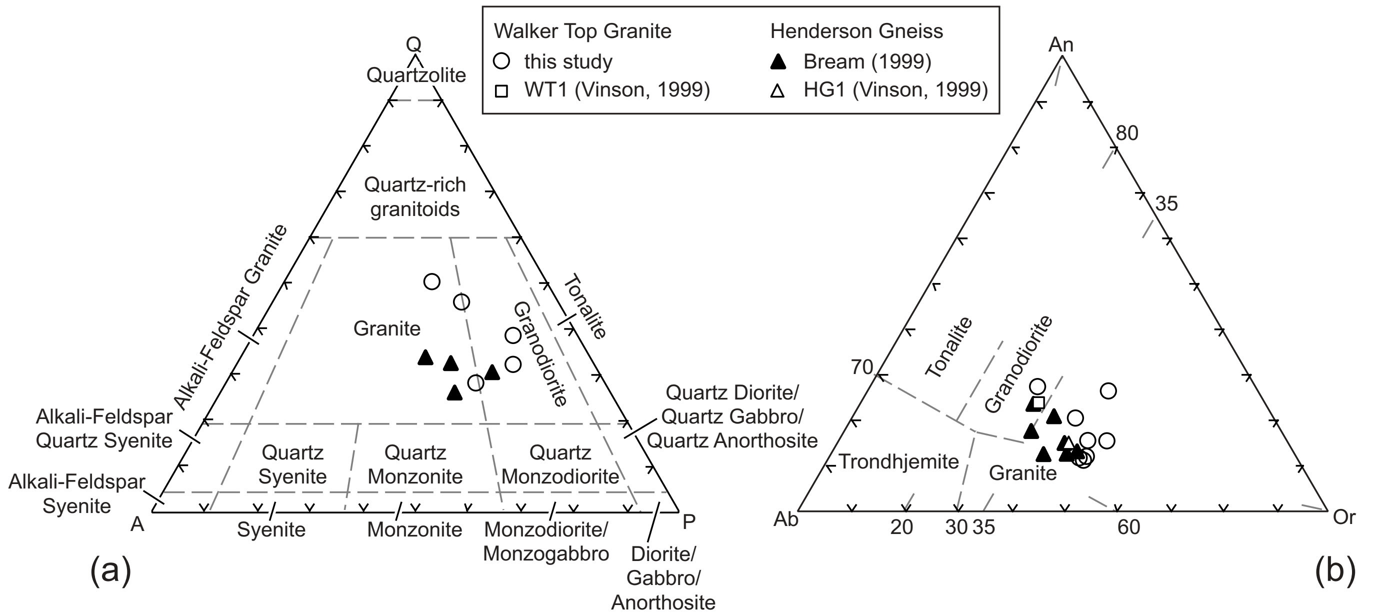

Figure 5. (a) IUGS classification of granitoids using modal mineralogy (Streckeisen, 1976). Walker Top Granite: n = 5, Henderson Gneiss: n = 4. (b) Classification of granitoids using normative mineralogy after Barker (1979). Walker Top Granite: n = 8, Henderson Gneiss: n = 8. Note that samples HG1 and WT1 are only on the normative mineralogy plot.

Table 2. Normative mineralogy of the Walker Top Granite and the Henderson Gneiss.

Walker Top Granite

	Qtz	Cor	Or	Ab	An	Hy	Mt	Il	Ap
BK111	19.9	3.40	28.6	23.1	10.0	10.6	0.67	1.24	0.24
D341	24.0	3.69	27.9	19.2	9.17	11.0	0.71	1.60	0.50
D740	13.5	2.75	31.4	27.6	8.80	11.2	0.76	1.58	0.68
MS26	15.3	1.44	34.3	28.4	9.13	6.86	0.45	0.78	0.41
MS53	15.6	3.12	29.3	25.0	7.72	7.57	0.48	0.89	0.31
D733	11.4	3.43	25.7	23.2	13.2	14.9	0.93	2.23	0.87
D708	23.1	3.09	17.0	22.5	15.6	12.8	0.81	1.86	0.61
WT1[#]	20.1	3.76	20.2	27.6	14.1	13.4	0.93	2.05	1.07

Henderson Gneiss

	Qtz	Cor	Or	Ab	An	Hy	Mt	Il	Ap
SH301	14.8	1.89	23.4	26.0	13.8	13.2	0.92	2.13	0.70
SH137	20.7	1.60	27.3	27.4	10.4	9.66	0.62	1.35	0.33
SH088	18.6	3.58	29.2	26.3	9.05	9.31	0.61	1.48	1.11
BG681	2.48	0.43	27.6	38.0	14.9	11.2	0.83	1.88	0.46
HQR[†]	16.7	0.70	31.4	31.0	9.92	8.02	0.51	0.95	0.35
BG662	17.4	2.71	19.9	27.1	15.2	12.8	0.79	1.50	0.46
SH075	12.8	1.51	28.5	34.2	9.9	9.6	0.67	1.45	0.33
HG1[#]	20.8	0.06	29.5	29.5	10.30	7.06	0.54	1.24	0.48

Qtz - quartz, Cor - corundum, Or - orthoclase, Ab - albite, An - anorthite, Hy - hypersthene, Mt - magnetite, Il - ilmenite, Ap - apatite.
[†] Sample from the Vulcan Materials Company quarry in Hendersonville, NC.
[#] From Vinson (1999).

are corroded, but crystal faces can still be identified. Detrital zircons are commonly rounded to the point that crystal faces cannot be recognized (Passchier *et al.*, 1990); consequently, zircon morphology favors an igneous origin for the Walker Top Granite. Werner (1987) proposed a P_2O_5/TiO_2 to MgO/CaO ratio to discriminate between metamorphic rocks of magmatic origin and those of sedimentary origin. Bulk chemical analyses (Table 1) plot almost en-

Table 3. XRF bulk chemical analyses of the Walker Top Granite and the Henderson Gneiss.

Walker Top Granite

	Oxides (Weight %)										Trace Elements (ppm)								
	SiO2	TiO2	Al2O3	Fe2O3*	MnO	MgO	CaO	Na2O	K2O	P2O5	Cr	Nb	Ni	Rb	Sr	V	Y	Zr	**Total**
BK111	64.1	0.65	16.8	4.61	0.08	1.73	2.16	2.73	4.85	0.11	43	17.3	nd	170	161	54.6	39.9	262	97.89
D341	64.9	0.84	15.9	4.92	0.09	1.82	2.15	2.27	4.73	0.23	22	17.4	nd	180	156	62.6	32.8	311	97.94
D740	62.3	0.83	17.1	5.25	0.04	1.73	2.18	3.26	5.32	0.31	nd	15.4	nd	177	200	65.6	29.7	311	98.48
MS26	64.5	0.41	16.6	3.09	0.03	1.06	2.09	3.36	5.81	0.19	nd	13.9	nd	258	148	12.8	24.9	231	97.19
MS53	59.0	0.47	16.2	3.29	0.07	1.23	1.74	2.96	4.97	0.14	nd	14.5	nd	216	1320	14.4	31.2	269	100.1
D733	57.4	1.17	17.5	6.41	0.08	2.66	3.19	2.74	4.36	0.40	86	22.9	41.5	167	215	115	32.5	348	96.06
D708	62.9	0.98	16.3	5.58	0.10	2.20	3.51	2.66	2.88	0.28	nd	18.8	8.8	122	201	91	41.4	343	97.63
WT1**	61.5	1.08	18.0	6.37	0.08	2.03	3.48	3.27	3.42	0.49	nd	26.0	20.0	156	186	88.0	51.0	436	100.6

Henderson Gneiss

	Oxides (Weight %)										Trace Elements (ppm)								
	SiO2	TiO2	Al2O3	Fe2O3*	MnO	MgO	CaO	Na2O	K2O	P2O5	Cr	Nb	Ni	Rb	Sr	V	Y	Zr	**Total**
SH301	60.5	1.12	16.29	6.36	0.11	1.97	3.20	3.07	3.97	0.32	nd	25.8	nd	78.9	276	116	47.3	449	97.01
SH137	66.6	0.71	15.75	4.28	0.10	1.58	2.29	3.24	4.63	0.15	nd	23.3	nd	106	214	49.4	42.7	298	99.44
SH088	64.3	0.78	17.37	4.19	0.08	1.56	2.49	3.11	4.95	0.51	nd	26.0	nd	132	226	67.4	39.0	428	99.41
BG681	58.5	0.99	18.34	5.68	0.11	1.49	3.28	4.49	4.68	0.21	98	32.8	nd	78.5	384	138	51.1	719	97.97
HQR#	66.7	0.50	16.13	3.53	0.08	1.27	2.21	3.67	5.32	0.16	nd	18.4	nd	138	194	28.0	38.2	325	99.64
BG662	62.2	0.79	17.21	5.46	0.10	2.17	3.34	3.21	3.37	0.21	nd	13.6	nd	106	386	78.8	22.5	292	98.10
SH075	63.9	0.76	17.02	4.62	0.10	1.36	2.20	4.04	4.83	0.15	nd	22.5	nd	149	201	71.1	35.4	355	99.07
HG1**	68.2	0.65	15.00	3.71	0.07	0.88	2.37	3.49	5.00	0.22	nd	26.0	5.0	128	164	46.0	36.0	418	100.0

Note: nd - not detected.
* Total Fe
† Sample from Vulcan Materials Company quarry at Hendersonville, NC.
** From Vinson (1999).

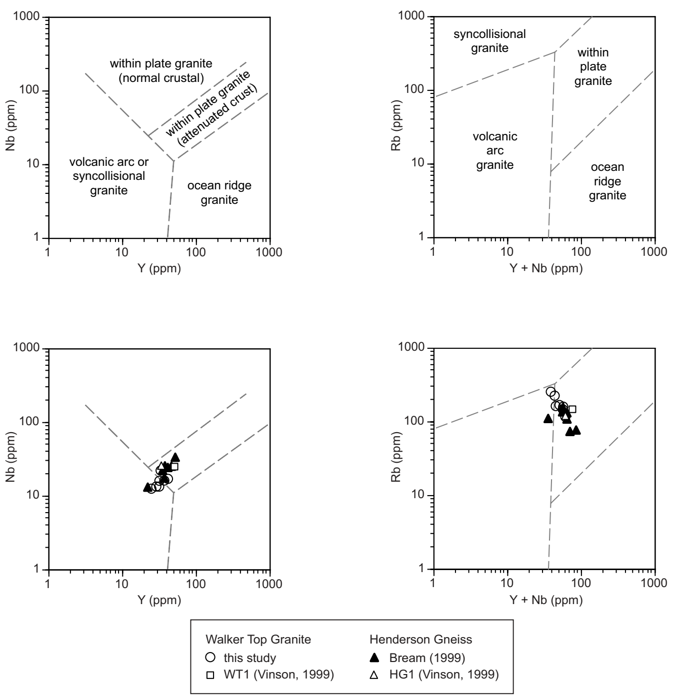

Figure 6. Plots of trace element chemistry for Walker Top Granite (n = 8) and Henderson Gneiss (n = 8).

tirely within the magmatic field (Fig. 7). The textural characteristics, zircon morphology, and bulk chemistry all agree and confirm that the Walker Top Granite is an orthogneiss.

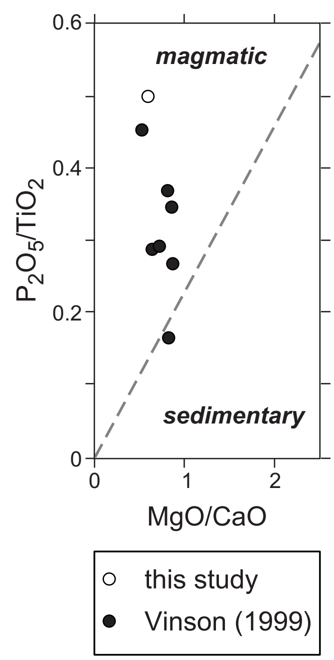

Figure 7. Magmatic vs. sedimentary protolith discriminant diagram (after Werner, 1987).

Contact Relationships

The Walker Top Granite-cover rocks contact could be interpreted as a fault, an intrusive contact, or a nonconformity. Several lines of evidence support a fault interpretation: 1) the contact cuts up-section from the lower metasandstone-schist-amphibolite unit into the sillimanite schist unit in places, truncating the lower unit (Fig. 2); 2) the contact is often at the base of the sillimanite schist unit, a weak mica-rich unit that a fault might exploit; and 3) the Henderson Gneiss has been interpreted to be emplaced by a combination of faulting (Liu, 1991; Hatcher, 1993) and sheath folding (Bream et al., 1998; Hatcher, this guidebook). The contact, however, does not remain in the weak sillimanite schist unit and cuts both up-section and down-section throughout the South Mountains (Fig. 2). These observations, coupled with a lack of fault rocks at the contact, suggest that a fault is not the best interpretation.

There are no dikes or sills of Walker Top Granite in the enclosing metasedimentary sequence. Within the Walker Top Granite there are only rare small xenoliths of metasedimentary rocks (mostly quartzite), no plutonic zoning has been observed, and no contact metamorphic aureole is present. These data indicate the Walker Top was not emplaced in the upper crust. The foliation within the Walker Top Granite is concordant with the foliation in the surrounding rock, a relationship consistent with either deformational transposition of foliation or intrusion of the Walker Top Granite as a mid-crustal pluton. Therefore, except for the xenoliths, there is no strong field evidence for an intrusive origin.

Relationships are similar between the Walker Top Granite-cover rocks contact, the Grenville basement-Tallulah Falls contact in the eastern Blue Ridge, and the Ordovician Whiteside Granite-Tallulah Falls contact. In the Tallulah Falls and Toxaway domes this contact has been interpreted as a nonconformity (Hatcher, 1971; Hatcher *et al.*, in review); the contact is irregular, with the metagraywacke-schist-amphibolite (lower Tallulah Falls) member interpreted as being deposited in topographic lows and the garnet aluminous schist member (sillimanite-mica-schist equivalent) being deposited subsequently over both the lower member and possible basement highs.

Similar relationships exist between the Walker Top Granite and the enclosing metasedimentary units in the South Mountains. The contact changes position within the stratigraphic sequence, remaining mostly in the lower two units, consistent with the topographic relief interpretation proposed by Hatcher (1971; 1977) for basement cover on the Tallulah Falls and Toxaway domes. No basal conglomerate, however, has been observed along the Walker Top Granite-enclosing rocks contact.

A fault contact for the Walker Top Granite-paragneiss contact is the least viable interpretation. The intrusive and nonconformity interpretations of this contact are consistent with map patterns and field relationships. A nonconformity interpretation, however, is more consistent with the previously recognized relationships between igneous units in the same position and the Tallulah Falls Formation. Additional geochronologic data, however, tilt the balance toward an intrusive origin for the Walker Top Granite.

Geochronology

High-resolution ion microprobe U-Pb analysis of zircons from Inner Piedmont paragneisses and granitoids have recently been made by several workers (e.g., Ranson *et al.*, 1999; Vinson, 1999; Bream *et al.*, 2001a; Mapes *et al.*, 2002). Near the study area in the North Carolina Inner Piedmont, granitoids fall into two age groups: Ordovician (Henderson Gneiss ~490 Ma, Vinson, 1999; Carrigan *et al.*, 2001; Dysartsville pluton ~465 Ma, Bream, unpublished data); and Devonian and Devono-Mississippian (Toluca Granite ~375 Ma, Cherryville granitoid, ~350 Ma; Mapes *et al.*, 2001). Ordovician granitoids are located along the length of the western Inner Piedmont between the Brevard fault zone and the Brindle Creek fault, and middle Paleozoic granitoids occur as small to medium size bodies throughout the eastern Inner Piedmont.

The Stanford University SHRIMP RG (sensitive high resolution ion microprobe reverse geometry) was used to obtain U-Pb zircon data for a sample of Walker Top Granite collected at an outcrop near the type area below Icy Knob (IK-WT; Fig. 2). Individual zircon grains were separated, mounted, polished, and imaged (cathodoluminescence and a combination of transmitted and reflected light) prior to analysis. These images were used to assess zoning, morphology, and structural integrity (i.e., presence or absence of fractures and inclusions) of each grain prior to ion microprobe analysis. The primary ion beam produced analytical spots in the zircon grains approximately 30 μm by 40 μm in diameter and roughly 1 μm deep. After the SHRIMP RG session, the grains were reimaged at the University of Tennessee using a Cameca SX-50 electron microprobe to confirm the placement and size of analytical spots.

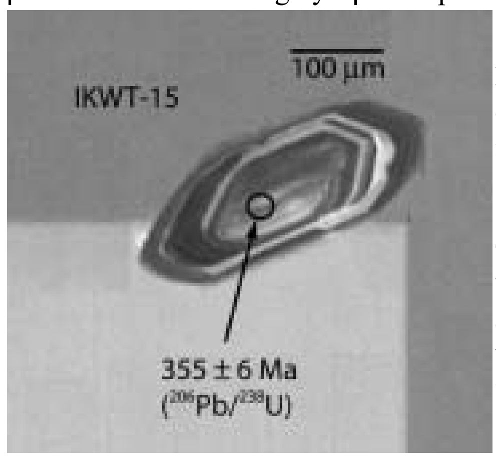

Figure 8. Cathodoluminescence image of a representative zircon from the Walker Top Granite (IK-WT) with the location and age of U-Pb geochronologic analysis.

Walker Top Granite zircons from the Icy Knob sample are mostly acicular, doubly terminated euhedral grains that appear magmatic. They have widths that vary from 65 to 210 μm, lengths between 200 and 550 μm, and aspect ratios between 2.1 and 6.1. Some grains contain rounded zones that appear to have been dissolved and reprecipitated after formation of the original zircon grain. Internal zoning is normally concentric euhedral or modified (Fig. 8). With the exception of one analysis, which we interpret to have lost Pb, all Icy Knob data points have $^{206}Pb/^{238}U$ ages within the range 344-388 Ma (Fig. 9a). A weighted mean age for the data is 366 ± 3 Ma (MSWD = 1.30, 2 sigma error). This age is consistent with the peak in a cumulative probability plot for the same data (Fig. 9b); we interpret this to be the magmatic age for intrusion of the Walker Top Granite.

DISCUSSION

Based on texture, zircon morphology, and bulk chemistry, the Walker Top Granite has an igneous origin. Modal and normative mineralogy suggest a granitic to granodioritic protolith. Contact relationships and field observations

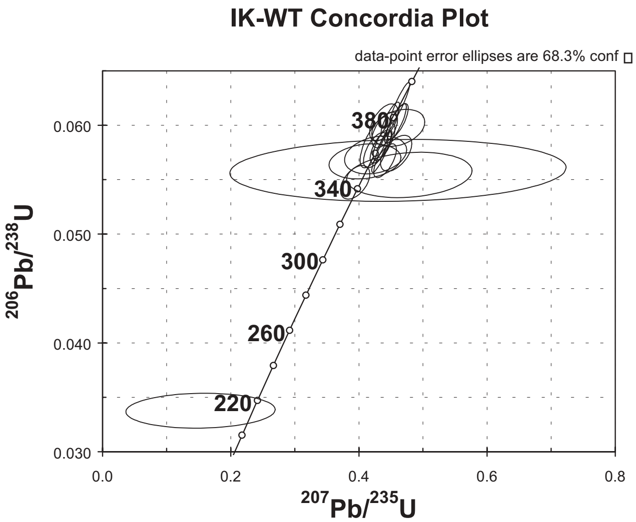

(a)

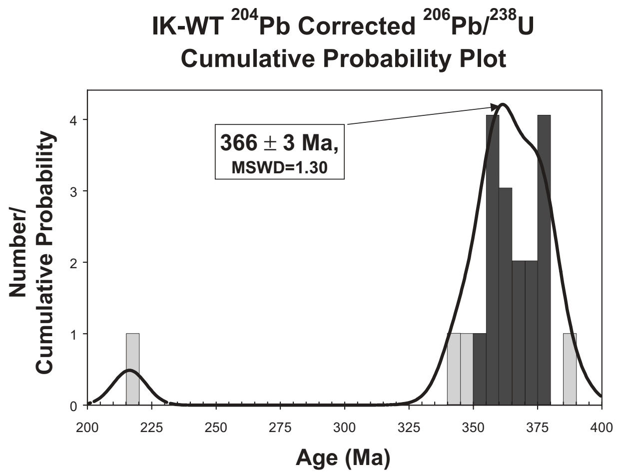

(b)

Figure 9. Walker Top (IK-WT) data. (a) Concordia diagram and (b) cumulative probability plot/histogram.

are consistent with basement or intrusive interpretations for the Walker Top Granite. Geochronological analysis of detrital zircons from the Inner Piedmont of North Carolina reveals no primary age components younger than Silurian (Bream *et al.,* 2001a, 2001b; Bream, this guidebook). Therefore, detrital contributions from a Walker Top Granite source (Late Devonian) have not been identified. The lack of Devonian age detrital zircons in the enclosing rocks suggests that the Walker Top Granite is not basement for the enclosing sequence.

Zircon rims on grains from western Inner Piedmont granitoids, Tallulah Falls Formation rocks in the western Inner Piedmont and eastern Blue Ridge, and eastern inner Piedmont metasedimentary and igneous rocks have been dated at ~350 Ma in the western and central Inner Piedmont (Carrigan *et al*., 2001). This age is consistent with a 360 Ma monazite growth event dated by Dennis and Wright (1997) in the Inner Piedmont. These growth events have been interpreted to be related to Neoacadian-early Alleghanian metamorphism. The Walker Top Granite crystallized at ~366 Ma and the Inner Piedmont was regionally metamorphosed at ~350 Ma. The basement interpretation for the Walker Top Granite requires uplift from mid-crustal emplacement depth, deposition of the entire covert paragneiss sequence, then burial to depths where sillimanite grade metamorphism occurs in <16 Ma (366 to 350 Ma). Rates of uplift and burial required by this scenario are geologically incompatible, which argues strongly against the basement hypothesis. Thus we conclude that the Walker Top Granite is a deformed Late Devonian pluton that intruded the paragneiss sequence. The data brought to bear here, unfortunately, yield no direct information about the crustal affinity of the eastern Inner Piedmont. The Walker Top Granite, however, was most likely the product of melting of eastern Inner Piedmont crust, and therefore may contain geochemical clues of the crustal affinity of this tectonic block. Additionally, Walker Top Granite outcrops only in the hanging wall of the Brindle Creek fault, which suggests that it was emplaced prior to movement on the fault. Thus movement on the Brindle Creek fault occurred after 366 ± 3 Ma. These age data constrain deformation on the Brindle Creek fault to syn- to post-Neoacadian.

While the strong correlation between the texture, mineralogy, and trace element chemistry of the Walker Top Granite and the Henderson Gneiss suggests a common igneous origin, the geochronologic data prohibit that interpretation. The age data presented here indicate that Walker Top Granite (366 ± 3 Ma) and Henderson Gneiss (~490 Ma; Vinson, 1999; Carrigan *et al.*, 2001) were never parts of the same pluton that subsequently went through different deformational histories. Textural, mineralogical, and chemical similarities, however, are most likely related to similarity in igneous process rather than a coeval origin.

CONCLUSIONS

The Walker Top Granite consists of a several 366 ± 3 Ma granitic to granodioritic plutons that are not genetically related to the Henderson Gneiss. Based on field relationships an intrusive contact or a nonconformity interpretation is viable. Geochronologic, petrographic, and geochemical data, however, strongly favor an intrusive origin for the Walker Top Granite. A Late Devonian age for the Walker Top Granite indicates that it was most likely emplaced during the Neoacadian orogeny, along with the Toluca Granite and related granitoids in the eastern Inner Piedmont. The position of the Walker Top Granite in the hanging wall of the Brindle Creek fault suggests that the Brindle Creek fault is a syn- to post-Neoacadian structure.

ACKNOWLEDGMENTS

This work was funded by EDMAP Grants 1434-HQ-97-AG-01720, 99HQAG2026, 99HGAG0026 to R.D. Hatcher, Jr., National Science Foundation grants EAR-9814800 to R.D. Hatcher, Jr. and EAR-9814801 to C.F. Miller, and the University of Tennessee Science Alliance Center for Excellence. Calvin Miller (Vanderbilt University) is gratefully acknowledged for assistance with collection and interpretation of the geochronologic data and Joe Wooden (USGS) is acknowledged for operational assistance with the Stanford University SHRIMP RG. Scott Williams, Sara Bier, and Jeffrey Riedel also collected geologic map data in the South Mountains.

REFERENCES CITED

Barker, F., 1979, Trondhjemite: Definition, environment and hypotheses of origin, *in* Barker, F., ed., Trondhjemites, dacites, and related rocks: New York, Elsevier Scientific Publishing Company, p. 1-12.

Bier, S. E., 2001, Geology of the southeastern South Mountains, North Carolina [M.S. thesis]: Knoxville, University of Tennessee, 162 p.

Bream, B. R., 1999, Structure and stratigraphic relationships of ortho- and paragneisses southwest of Marion, North Carolina [M.S. thesis]: Knoxville, University of Tennessee, 155 p.

Bream, B. R., Hatcher, R. D., Jr., and Hill, J. C., 1998, The Henderson augen gneiss of the western Inner Piedmont, North Carolina and South Carolina: Geological Society of America Abstracts with Programs (Annual Meeting), v. 30, p. A125.

Bream, B. R., Hatcher, R. D., Jr., Miller, C. F., and Fullagar, P. D., 2001, Geochemistry and provenance of Inner Piedmont paragneisses, North Carolina and South Carolina: Evidence for an internal terrane boundary?: Geological Society of America Abstracts with Programs (Southeastern Section) v. 33, p. A65.

Bream, B. R., Hatcher, R. D., Jr., Miller, C. F, Carrigan, C. W., and Fullagar, P. D., 2001, Provenance and geochemistry of Late Proterozoic southern Appalachian crystalline core paragneisses, North Carolina-South Carolina-Georgia-Tennessee: Geological Society of America Abstracts with Programs (Annual Meeting), v. 33, p. A29.

Carrigan, C. W., Bream, B. R., Miller, C. F., and Hatcher, R. D., Jr., 2001, Ion microprobe analyses of zircon rims from the eastern Blue Ridge and Inner Piedmont, North Carolina-South Carolina-Georgia: Implications for the timing of Paleozoic metamorphism in the southern Appalachians: Geological Society of America Abstracts with Programs (Southeastern Section), v. 33, p. A7.

Carrigan, C. W., Miller, C. F., Fullagar, P. D., Bream, B. R., Hatcher, R. D., Jr., and Coath, C. D., in press, Ion microprobe age and geochemisry of southern Appalachian basement, with implications for Proterozoic and Paleozoic reconstructions: Precambrian Research.

Davis, T. L., 1993, Lithostratigraphy, structure, and metamorphism of a crystalline thrust terrane, western Inner Piedmont, North Carolina [unpublished Ph.D. dissertation]: Knoxville, University of Tennessee, 245 p.

Dennis, A. J., and Wright, J. E., 1997, Middle and late Paleozoic monazite U-Pb ages, Inner Piedmont, South Carolina: Geological Society of America Abstracts with Programs (Southeastern Section), v. 29, p. A12.

Giorgis, S. D., 1999, Geology of the South Mountains near Morganton, North Carolina [unpublished M..S. thesis]: Knoxville, University of Tennessee, 183 p.

Goldsmith, R., Milton, D. J., and Horton, J. W., Jr., 1988, Geology of the Charlotte 1˚ x 2˚ quadrangle, North Carolina and South Carolina: U.S. Geological Survey Map I-1251-E, scale 1:250,000.

Hatcher, R. D., Jr., 1969, Stratigraphy, petrology, and structure of the low rank belt and part of the Blue Ridge of northwesternmost South Carolina: South Carolina Division of Geology, Geologic Notes, v. 13, p. 105-141.

Hatcher, R. D., Jr., 1971, The geology of Rabun and Habersham Counties, Georgia: A reconnaissance study: Geological Survey of Georgia, Department of Mines, Mining, and Geology Bulletin 83, 48 p.

Hatcher, R. D., Jr., 1972, Developmental model for the southern Appalachians: Geological Society of America Bulletin, v. 83, p. 2735-2760.

Hatcher, R. D., Jr., 1975, The second Penrose field conference: The Brevard zone: Geology, v. 3, p. 149-152.

Hatcher, R. D., Jr., 1977, Macroscopic polyphase folding illustrated by the Toxaway dome, South Carolina-North Carolina: Geological Society of America Bulletin, v. 88, p. 1678-1688.

Hatcher, R. D., Jr., 1989, Tectonic synthesis of the U.S. Appalachians, Chapter 14, *in* Hatcher, R. D., Jr., Thomas, W. A., and Viele, G. W., eds., The Appalachian-Ouachita orogen in the United States: Boulder, Colorado, Geological Society of America, The geology of North America, v. F-2, p. 511-535.

Hatcher, R. D., Jr., 1993, Perspective on the tectonics of the Inner Piedmont, southern Appalachians, *in* Hatcher, R. D., Jr., and Davis, T. L., eds., Studies of Inner Piedmont geology with a focus on the Columbus Promontory: Carolina Geological Society annual field trip guidebook, p. 1-16.

Hatcher, R. D., Jr., and Hopson, J. L., 1989, Geologic map of the eastern Blue Ridge, northeastern Georgia and the adjacent Carolinas, *in* Fritz, W. J., Hatcher, R. D., Jr., and Hopson, J. L., eds., Geology of the eastern Blue Ridge of northeast Georgia and the adjacent Carolinas: Georgia Geological Society Guidebooks, v. 9, scale 1:100,000.

Hatcher, R. D., Jr., Osberg, P. H., Robinson, P., and Thomas, W. A., 1990, Tectonic map of the U.S. Appalachians: Geological Society of America, The Geology of North America, v. F–2, Plate 1, scale 1/2,000,000.

Hatcher, R. D., Jr., Bream, B. R., Miller, C. L., Eckert, J. O., Jr., Fullagar, P. D., and Carrigan, C. W., in review, Paleozoic structure of southern Appalachian Blue Ridge Grenvillian internal basement massifs, in Tollo, R.P., Corriveau, L., McLelland, J., and Bartholomew, M.J., eds., Proterozoic evolution of the Grenville orogen in North America: Boulder, Colorado, Geological Society of America Special Paper.

Heyn, T., 1984, Stratigraphic and structural relationships along the southwestern flank of the Sauratown Mountains anticlinorium [unpublished M.S. thesis]: Columbia, University of South Carolina, 192 p.

Hill, J. C., 1999, Geology of the Marion East quadrangle, North Carolina, and the stratigraphy of the Tallulah Falls Formation in the Chauga belt [M.S. thesis]: Knoxville, University of Tennessee, 188 p.

Kish, S. A., 1983, A geochronological study of deformation and metamorphism in the Blue Ridge and Piedmont of the Carolinas [unpublished Ph.D. thesis]: Chapel Hill, University of North Carolina. 220 p.

Kish, S. A., and Odom, A. L., 1999, In search of Precambrian basement in the Piedmont of the southern Appalachians — All that is granulite is not Grenville: Geological Society of America Abstracts with Programs (Southeastern Section), v. 31, p. A26.

Liu, A., 1991, Structural geology and deformation history of the Brevard fault zone, Chauga belt, and Inner Piedmont, northwestern South Carolina and adjacent areas [unpublished Ph.D. dissertation]: Knoxville, University of Tennessee, 200 p.

Mapes, R. W., Miller, C. F., Fullagar, P. D., and Bream, B. R., 2001, Nature and origin of Acadian plutonism, Piedmont terrane, North Carolina and Georgia.: Geological Society of America Abstracts with Programs (Annual Meeting), v. 33, p. A304.

Mapes, R. W., Maybin, A. H., Miller, C. F., Fullagar, P. D., and Bream, B. R., 2002, Geochronology and geochemistry of mid-Paleozoic granitic magmatism, central and eastern Inner Piedmont, North Carolina and South Carolina: Geological Society of America Abstracts with Programs (Southeastern Section), v. 34, p. A92.

Passchier, C. W., Myers, J. S., and Kroner, A., 1990, Field geology of high-grade gneiss terrains: New York, Springer-Verlag, 150 p.

Pearce, J. A., and Cann, J. P., 1973, Tectonic setting of basic volcanic rocks determined using trace element analysis: Earth and Planetary Science Letters, v. 19, p. 209-300.

Pearce, J. A., Harris, N. B. W., and Tindle, A. G., 1984, Trace element discrimination diagrams for the tectonic interpretation of granitic rocks: Journal of Petrology, v. 25, p. 956-983.

Ranson, W. A., Williams, I. S., and Garihan, J. M., 1999, SHRIMP zircon U-Pb ages of granitoids from the Inner Piedmont of South Carolina: Evidence for Ordovician magmatism involving Mid to Late Protereozoic crust: Geological Society of America Abstracts with Programs (Annual Meeting), v. 31, p. A167.

Shufflebarger, T. E., 1961, Notes on relationships of Piedmont sedimentary rocks with emphasis on the Poor Mountain-Chauga River area, Oconee County, South Carolina: South Carolina Division of Geology, Geologic Notes, v. 5, p. 31-38.

Streckeisen, A. L., 1976, To each plutonic rock its proper name: Earth Science Reviews, v. 12, p. 1-33.

Vinson, S., 1999, Ion probe geochronology of granitoid gneisses of the Inner Piedmont, North Carolina and South Carolina [unpublished M.S. thesis]: Nashville, Tennessee, Vanderbilt University, 84 p.

Werner, C. D., 1987, Saxonian granulites - igneous or lithogenous? A contribution to the geochemical diagnosis of the original rocks in high-metamorphic complexes, *in* Gerstenberger, H., ed., Contributions to the geology of the Saxonian granulite massif: Sachsisches Granulitegebirge, Zfl-Mitteilungen Nr. v. 133, p. 221-250.

Williams, S. T., 2000, Structure, stratigraphy, and migmatization in the southwestern South Mountains, North Carolina [M.S. thesis]: Knoxville, University of Tennessee, 111 p.

Wilson, M., 1989, Igneous petrogenesis: London, Unwin-Hyman, 466 p.

Carolina Geological Society
Annual Field Trip
October 19-20, 2002

The southern Appalachian Inner Piedmont: New perspectives based on recent detailed geologic mapping, Nd isotopic evidence, and zircon geochronology

Brendan R. Bream
Department of Geological Sciences
University of Tennessee–Knoxville
306 Geological Sciences Building
Knoxville, TN 37996-1410
bbream@utk.edu

INTRODUCTION

The objectives of this paper are to summarize geochemical and geochronologic data from the southern Appalachian crystalline core, to integrate and examine recent detailed mapping along strike from the Columbus Promontory, and to present several new or revised ideas and interpretations concerning the evolution of the southern Appalachian Inner Piedmont. Numerous contributions to our understanding of the Inner Piedmont have been made over the last ten years since the last University of Tennessee-affiliated CGS field trip. Because of the ongoing nature and volume of new Inner Piedmont research, any attempt to integrate and present this work is admittedly limited. Therefore, for the purpose of this guidebook and from a practical standpoint, this synthesis emphasizes new work in the North Carolina Inner Piedmont and highlights recent and/or pertinent work from other areas of the southern Appalachians where appropriate. This overview contains some information from UTK M.S. theses (Bream, 1999; Giorgis, 1999; Hill; 1999; Williams, 2000; Bier, 2001; Kalbas, in preparation; Merschat, in preparation), Vanderbilt M.S. theses (Vinson, 1999; Carrigan, 2000; Thomas, 2001; Mapes, 2002), and the work of several undergraduate students at both universities.

The traditional geologic and tectonic divisions of the southern Appalachians include the Cumberland-Allegheny Plateau, Valley and Ridge, western Blue Ridge, eastern Blue Ridge, Inner Piedmont, and Carolina composite terrane (Fig. 1). Together, the Blue Ridge (exclusive of the frontal thrust sheet), Inner Piedmont, and portions of the Carolina composite terrane comprise the crystalline core of the southern Appalachians. Most of the Inner Piedmont has not been studied in detail partially due to the common misconception that this region lacks exposure and a recognizable stratigraphy. For these reasons, a large portion (~75 %) of Inner Piedmont remains unmapped; recent detailed mapping, however, has delineated coherent and extensive lithotectonic packages throughout much of the Inner Piedmont. As in most high-grade gneiss terranes, the rocks of the Inner Piedmont are varied, intensely deformed, and partially to intensely migmatitic. The dominant rock types of the Inner Piedmont include quartzofeldspathic gneiss, amphibolite, quartzite and pelitic schist with lesser amounts of amphibole gneiss, calc-silicate, and ultramafic rocks.

Current thinking regarding the Inner Piedmont is an extension of several pioneering researchers, namely Griffin (1967; 1969a; 1969b; 1971a; 1971b; 1974a; 1974b), Hatcher (1969; 1970; 1978), Bentley and Neathery (1970), and contributions included in the 1993 Carolina Geological Society Guidebook (Hatcher, 1993; Davis, 1993a; Yanagihara, 1993; Garihan et al., 1993; Clark, 1993; Hibbard, 1993; Grimes et al., 1993; Goldberg and Fullagar, 1993). Hatcher (1993), in particular, provided a more detailed summary of significant contributions prior to 1993. Many of the original ideas and concepts, or slightly modified versions, presented by these workers are the foundation on which nearly all subsequent Inner Piedmont work is built.

Bream, B.R., 2002, The southern Appalachian Inner Piedmont: New perspectives based on recent detailed geologic mapping, Nd isotopic evidence, and zircon geochronology, *in* Hatcher, R.D., Jr., and Bream, B.R., eds., Inner Piedmont geology in the South Mountains-Blue Ridge Foothills and the southwestern Brushy Mountains, central-western North Carolina: North Carolina Geological Survey, Carolina Geological Society annual field trip guidebook, p. 45–63.

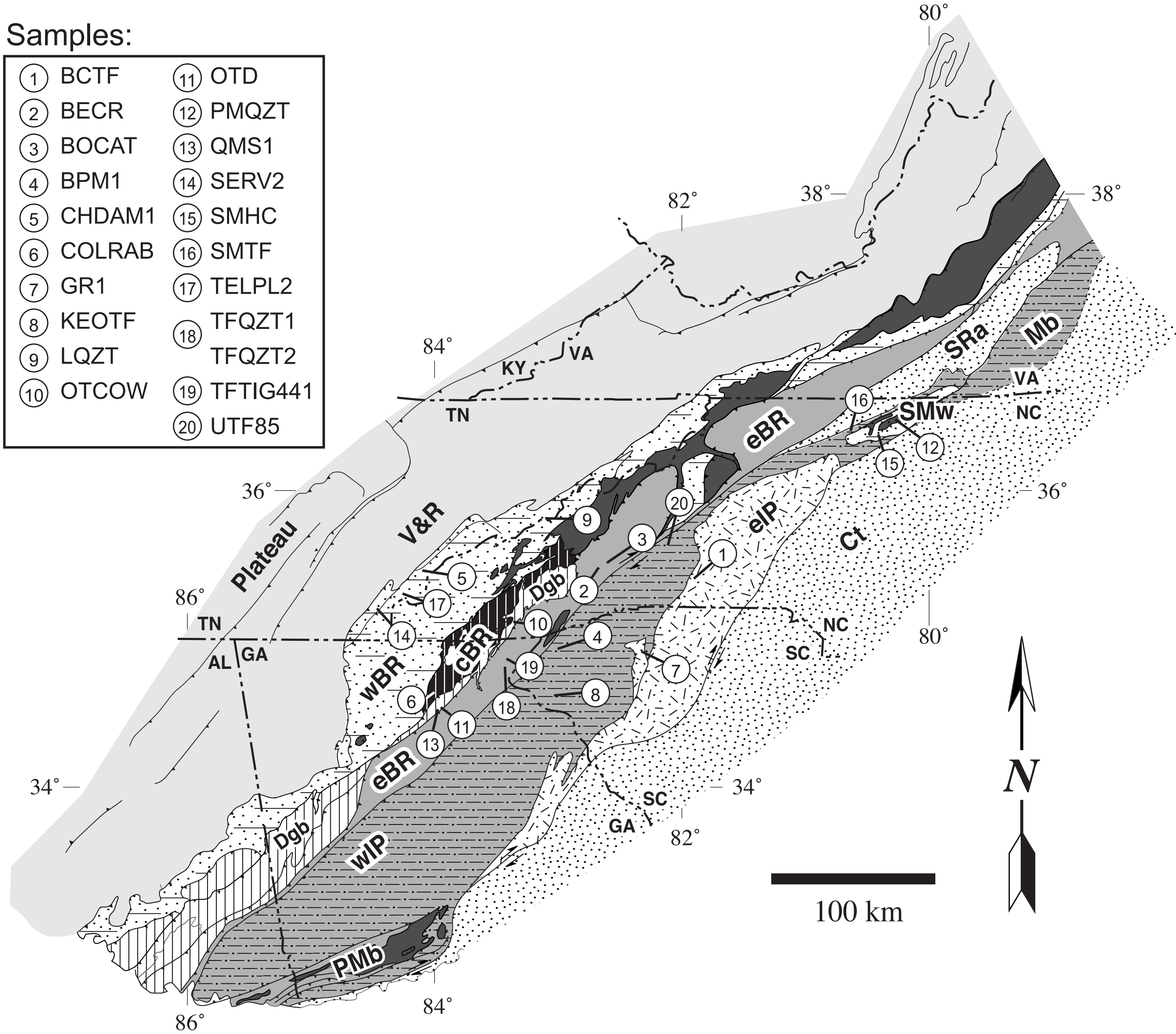

Figure 1. Tectonic map of the southern Appalachians modified from Hatcher et al. (1990) and Bream et al. (in review). cBR-central Blue Ridge; Ct-Carolina terrane; Dgb-Dahlonega gold belt; eBR-eastern Blue Ridge; eIP-central and eastern Inner Piedmont; Mb-Milton belt; PMb-Pine Mountain block; SMw-Sauratown Mountains window; SRa-Smith River allochthon; V&R-Valley and Ridge; wBR-western Blue Ridge; wIP-western Inner Piedmont. Sample locations and associated formations are provided in Table 1.

Tectonostratigraphic terranes within the crystalline core are based on the crustal affinity and tectonic history of the rocks present. The terrane boundaries within and bounding the crystalline core are variably interpreted and defined (e.g., Williams and Hatcher, 1983; Horton et al., 1989; Hibbard and Samson, 1995). The Inner Piedmont is often grouped with the adjacent Blue Ridge in tectonic maps and has been designated as the eastern part of the larger Piedmont terrane, Piedmont zone, or Tugaloo terrane (Williams and Hatcher, 1983; Hibbard and Samson, 1995; Hatcher et al., 1999; respectively). This grouping favors interpretations that correlate sedimentary packages, and likely crustal affinity, across the Brevard fault zone. Other tectonic affinity interpretations for the North Carolina Inner Piedmont are varied: mélange complex (Goldsmith et al., 1988; Horton et al., 1989); accretionary wedge (Abbot and Raymond, 1984; Hatcher, 1987; Rankin, 1988); probable accreted exotic terrane (Dennis, 1991; Rankin et al., 1989; Rankin, 1994; Dennis and Wright, 1997). Incomplete detailed mapping and the paucity of geochemical and geochronologic data have exacerbated attempts to subdivide or correlate lithotectonic packages thus further obscuring relationships within the southern Appalachians and between the southern and northern Appalachians.

Table 1. Sample locations with formations keyed to Figure 1.

Sample	Figure 1 Location	Formation	7.5-minute quadrangle	County (State)
western Blue Ridge				
CHDAM1	5	Walden Creek Group (Ocoee Supergroup)	Tallassee	Blount (TN)
LQZT	9	Snowbird Group (Ocoee Supergroup)	Waterville	Cocke (TN)
SERV2	14	Walden Creek Group (Ocoee Supergroup)	McFarland	Polk (TN)
TELPL2	17	Great Smoky Group (Ocoee Supergroup)	Tellico Plains	Monroe (TN)
central Blue Ridge				
COLRAB	6	Coleman River Formation	Hightower Bald	Rabun (GA)
Dahlonega gold belt				
OTCOW	10	Otto Formation	Prentiss	Macon (NC)
OTD	11	Otto Formation	Campbell Mountain	Lumpkin (GA)
QMS1	13	Otto Formation	Campbell Mountain	Lumpkin (GA)
eastern Blue Ridge				
BECR	2	Tallulah Falls Formation-Ashe Formation (metagraywacke member)	Dunsmore Mountain	Buncombe (NC)
BOCAT	3	Tallulah Falls Formation-Ashe Formation (metagraywacke member)	Asheville	Buncombe (NC)
TFQZT1	18	Tallulah Falls Formation (quartzite member)	Tiger	Rabun (GA)
TFQZT2*	18	Tallulah Falls Formation (quartzite member)	Tallulah Falls	Rabun (GA)
TFTIG441	19	Tallulah Falls Formation-Ashe Formation (metagraywacke member)	Tiger	Rabun (GA)
Sauratown Mountains window				
SMHC	15	Hogan Creek Formation	Siloam	Surry (NC)
PMQZT	12	Pilot Mountain Quartzite	Pinnacle	Surry (NC)
western Inner Piedmont				
BPM1	4	Chauga River Formation (Brevard-Poor Mountain Transitional member)	Salem	Oconee (SC)
KEOTF	8	Tallulah Falls Formation-Ashe Formation (metagraywacke member)	Seneca	Oconee (SC)
SMTF	16	Tallulah Falls Formation-Ashe Formation (metagraywacke member)	Copeland	Surry (NC)
UTF85	20	Tallulah Falls Formation-Ashe Formation (metagraywacke member)	Marion East	McDowell (NC)
eastern Inner Piedmont				
BCTF	1	metagraywacke not presently assigned to a formation	Benn Knob	Rutherford (NC)
GR1	7	metagraywacke not presently assigned to a formation	Greer	Spartanburg (SC)

*Nd and Sr isotopic analysis only.

GEOLOGIC SETTING AND PREVIOUS WORK

Despite the highly enigmatic nature of the Inner Piedmont, several general observations can be made regarding its complex history; and are divided here into four broad categories: stratigraphic, metamorphic, magmatic, and tectonic. The following sections focus on background information for the North Carolina Inner Piedmont and establishes the framework from which a revised perspective can be drawn based on new detailed geologic mapping, geochemistry, and geochronology.

Stratigraphic

The opening of the Iapetus ocean is temporally constrained by rift-related magmatism and deposition that suggests: (1) rifting separated west Gondwana cratons from Laurentia around 570 Ma, (2) the Iapetus ocean was developed before 550 Ma, and (3) this Early Cambrian rifting could have propagated along zones already weakened by earlier Neoproterozoic failed rifting ~760-700 Ma (e.g., Su et al., 1994; Aleinikoff et al., 1995; Cawood et al., 2001). Paragneisses within the Appalachian crystalline core are commonly interpreted as post-Grenvillian rift fill, possibly time-transgressive from west to east, from Late Proterozoic in the western Blue Ridge to as young as Silurian in the eastern Inner Piedmont (e.g., Bream et al., 2001a). Portions of the same lithologic packages, on the other hand, have been interpreted as large Ordovician accretionary wedges (Abbott and Raymond, 1984), Devonian transtensional basins (Unrug et al., 2000), and Grenville basement (Espenshade et al., 1975; Gillon, pers.comm., 2000).

A recognizable stratigraphy, traceable along strike into Georgia and across strike in several thrust sheets, has been identified throughout the North Carolina western Inner Piedmont. This stratigraphy consists of the following dominant rock types (from bottom to top): metagraywacke and amphibolite; aluminous schist; metagraywacke with minor amphibolite; metasiltstone and pelitic schist with minor carbonate; finely laminated amphibolite; quartzite, marble, feldspathic quartzite, and calcareous quartzite. Lithologies similar to the lower part of the sequence are present in the eastern Inner Piedmont, in the hanging wall of the Brindle Creek thrust, but show a considerable increase in the amount of metapelite relative to metagraywacke. Correlation of western Inner Piedmont stratigraphy with the eastern Inner Piedmont lithologies is not made now because of new geochronologic data discussed later in this paper.

Tallulah Falls-Ashe Formation. The lowest part of the stratigraphic sequence, below the Poor Mountain amphibolite, is correlative with Davis' (1993a, 1993b) Mill Spring complex that includes the thick biotite gneiss unit recognized by Lemmon (1973) below his Sugarloaf Mountain group. The knotted biotite gneiss of Whisnant (1975, 1979) in the Sugar Hill 7.5-minute quadrangle is roughly correlative with the upper biotite gneiss unit in the stratigraphy whereas his porphyroclastic schist and gneiss unit contains portions of the upper and lower biotite gneiss units recognized in recent mapping (Bream, 1999; Hill, 1999). The Tryon formation and Mill Spring group of Conley and Drummond (unpublished) also contain a similar sequence of rock units. Within the Sugarloaf Mountain thrust sheet, this formation occurs discontinuously from at least the northeast edge of the Marion East quadrangle into South Carolina where Garihan (1999) has mapped it. Due to the remarkable similarity of the western Inner Piedmont stratigraphy to the Tallulah Falls and Ashe Formations of the eastern Blue Ridge, Hatcher (1978, 1987, 1989, this volume), Heyn (1984), Hopson and Hatcher (1988), Davis (1993b), and Hill (1999) have correlated the western Inner Piedmont psammitic-pelitic sequence with the Tallulah Falls-Ashe Formation. The name Tallulah Falls Formation is used here, therefore, to refer to the biotite paragneiss and aluminous schist units of the western Inner Piedmont and eastern Blue Ridge, or the Tugaloo terrane of Hatcher (this guidebook).

Poor Mountain Formation. The upper portion of the western Inner Piedmont stratigraphy can be correlated with the Poor Mountain sequence first described by Sloan (1907) northwest of Walhalla, South Carolina. Shufflebarger (1961) first subdivided the Poor Mountain sequence and Hatcher (1969, 1970) subsequently correlated the Poor Mountain rocks with the Chauga River Formation in South Carolina. Hatcher (1969, 1970) also defined the Poor Mountain sequence as a formation and attributed lithologic differences between the Chauga River and Poor Mountain Formation to facies changes. Additionally, Hatcher (1969, 1970) defined the Brevard-Poor Mountain transitional member as the lowest part of the Poor Mountain Formation. The transitional unit is recognized from the Chauga belt in South Carolina along strike to as far north as the Columbus Promontory of North Carolina.

Metamorphic

Originally defined by King (1955) as a high-grade gneiss terrane, the Inner Piedmont is now widely regarded as the southern Appalachian Acadian metamorphic core (e.g., Osberg et al., 1989; Hatcher, 1993; Hatcher et al., 1999). Regional studies in the southern Appalachian crystalline core (e.g., Griffin, 1974a; Osberg et al., 1989; Butler, 1991; Hatcher and Goldberg, 1991) identify the southeast dipping kyanite-sillimanite isograd that places more migmatitic sillimanite grade assemblages over less migmatitic kyanite and lower grade assemblages in the western Inner Piedmont (Fig. 2). The internal Inner Piedmont is dominated by sillimanite-grade rocks almost entirely encompassed by relatively thin flanks of kyanite and/or kyanite + staurolite-grade (lower in South Carolina) rocks near its southeastern and northwestern boundaries.

The Inner Piedmont contains abundant evidence of polyphase deformation at or near middle- to upper-amphibolite facies conditions later superposed by brittle event(s). The presence of migmatite at all scales throughout most of the Inner Piedmont demonstrates that these rocks were at or near minimum melt conditions during prograde metamorphism. Based on textural and mapping evidence in the South Carolina Cashiers, Tamassee, and Satolah 7.5-minute quadrangles, Roper and Dunn (1973) defined two metamorphic events; an earlier amphibolite facies Taconic (?) event and a later greenschist facies Acadian (?) event that retrogressed some of the earlier prograde mineral assem-

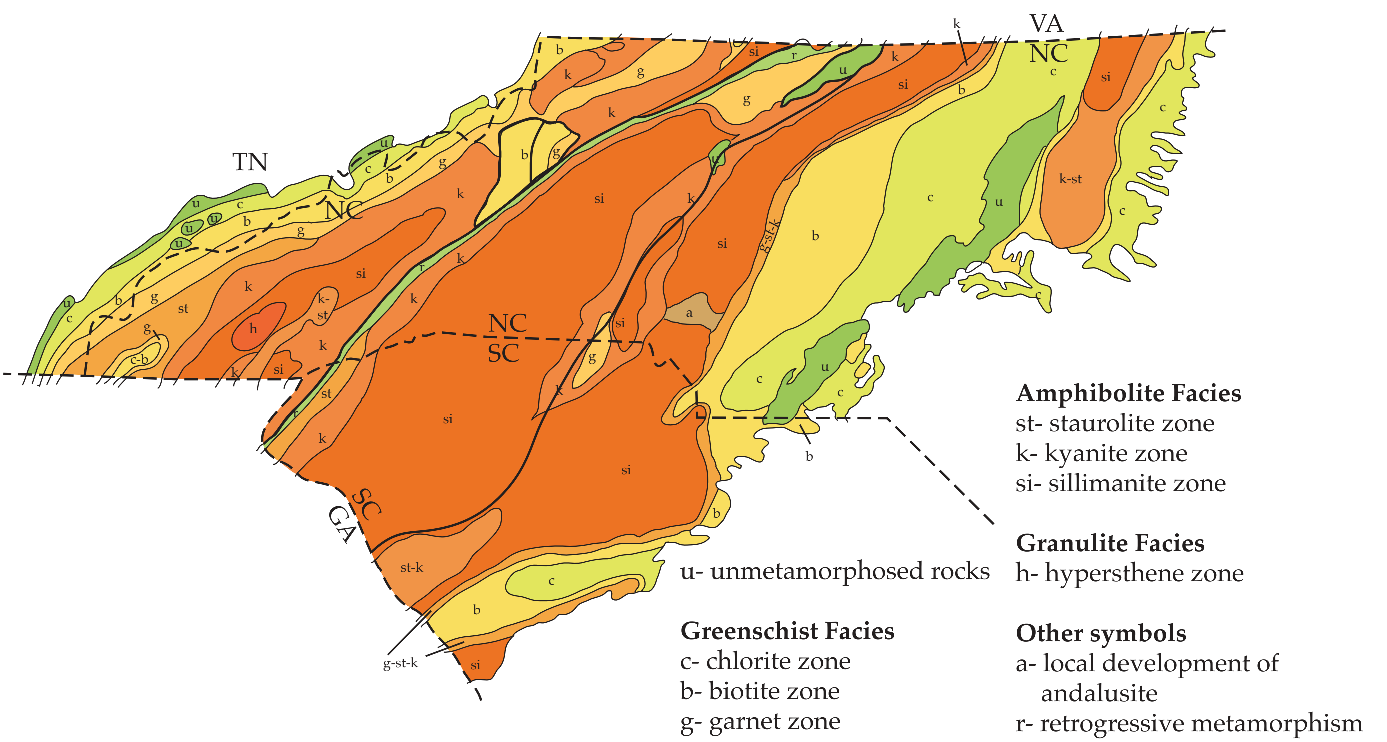

Figure 2. Metamorphic isograd map of North Carolina, South Carolina, and part of east Tennessee. Modified from Butler (1991) and Hatcher and Goldberg. (1991). Modified from a figure drafted by Scott D. Giorgis.

blages. Lemmon (1973) proposed two prograde metamorphic events (possibly Taconic and Acadian equivalents) for the North Carolina Inner Piedmont, whereas Davis (1993a, 1993b) indicated only a single prograde Acadian metamorphic event occurred here.

Magmatic

The Inner Piedmont contains abundant outcrop- and map-scale granitoid bodies with small mafic and ultramafic bodies (with the notable exception of the Poor Mountain Amphibolite) (Hatcher, this guidebook, his Fig. 1). Sinha et al. (1989) suggested several magmatic phases affected the central and southern Appalachian Blue Ridge, Inner Piedmont, and Carolina terrane: a 520-490 Ma magmatic arc along the cratonic margin; 460-440 Ma high pressure magmas resulting from arc collapse followed by thrusting; Siluro-Devonian decompressional melting following the Taconic orogeny in the Blue Ridge and Inner Piedmont; and extensive 330-270 Ma subduction related magma generation largely restricted to the Inner Piedmont and Carolina terrane. McSween et al., (1991) defined four distinct age groups for plutonic rocks: 1197-1005 Ma intrusions into Precambrian basement of the Blue Ridge and Sauratown Mountains window; 734-495 Ma for basaltic and peralkaline granitic magmas in the Blue Ridge and plutons of the slate belt; 436-375 Ma for the Blue Ridge Spruce Pine Plutonic Suite and western Inner Piedmont granitoids; and 340-385 Ma for granitoid-gabbro plutons of the central and eastern Piedmont. The nature and timing of granitoid genesis within the Inner Piedmont is now better constrained but regional perspectives are largely lacking and the distribution of many bodies are poorly delineated and several are likely unidentified. Harper and Fullagar (1981), Drake et al. (1989), Osberg et al. (1989), Horton and McConnell (1991), McSween et al. (1991), and Fullagar et al. (1997) provided more detailed regional accounts and interpretations of the igneous rocks in the southern Appalachians. The presentation here focuses on magmatic Inner Piedmont rocks that have been more thoroughly studied since the 1993 CGS field trip.

Henderson Gneiss. The Henderson Gneiss is one of the most areally extensive granitoids of the Appalachian orogen and is by far the largest (~5000 km^2) granitoid of the North and South Carolina Inner Piedmont. Spectacular Henderson Gneiss outcrops occur primarily in locations where the across-strike outcrop width of the main body is greatest (e.g., North Carolina Columbus Promontory). Keith (1905, 1907) first described the Henderson Gneiss and defined the type locality in Henderson County, North Carolina. Reed (1964) and Bryant and Reed (1970) restricted the Henderson Gneiss to a belt southeast of the Brevard fault zone. Citing the complex map pattern and compositional variability of the Henderson Gneiss in South Carolina, Hatcher (1970) proposed that the Henderson Gneiss and Poor Mountain Formation have sedimentary protoliths and are Late Proterozoic to Early Cambrian. Lemmon (1973) concluded that the Henderson Gneiss has an igneous protolith based on zircon morphology. Numerous Rb-Sr whole-rock ages have been determined for the Henderson Gneiss: 509 Ma (Sinha et al., 1989) using a revised decay constant for Odom and Fullagar (1973) data; 460 ± 9 Ma (Harper and Fullagar, 1981) for lithologies initially mapped as Henderson Gneiss in Wilkes County, NC (Rankin et al., 1972); 438 ± 22 Ma for the large intrusive granitoid within the Henderson Gneiss (Odom and Russell, 1975); 356 and 387 Ma for mylonitic Henderson Gneiss in the Brevard fault zone (Odom and Fullagar, 1973; Bond and Fullagar, 1974, respectively). Using conventional U-Pb data from Henderson Gneiss zircon fractions, Sinha and Glover (1978) proposed a 593 Ma intrusive age for the protolith, 456 Ma age for Taconic metamorphism, and a 360-390(?) Ma age range for Acadian metamorphism.

Caesars Head Granite. The Caesars Head Granite, originally named the Caesars head Quartz Monzonite by Hadley and Nelson (1970), was renamed by Horton and McConnell (1991) and grouped with several smaller Inner Piedmont granitoids into the Table Rock Plutonic Suite. Geochronology for the Caesars Head Granite includes a 435 Ma $^{207}Pb/^{206}Pb$ zircon age (J.W. Horton and T.W. Stern, unpublished data) and a 409 Ma Rb-Sr whole-rock age (P.D. Fullagar, unpublished data). The Caesars Head Granite, as depicted on the Greenville 1° x 2° sheet (Nelson et al., 1998) and the preliminary South Carolina Blue Ridge and Piedmont map (Horton and Dicken, 2001), crosscuts at least two Paleozoic faults, implying that movement on these faults pre-dates intrusion.

Smaller Inner Piedmont Granitoids. Numerous smaller granitoids (relative to the Henderson Gneiss and Caesars Head Granite) are present in the Inner Piedmont. Several of these granitoids were included in the Table Rock Plutonic Suite of Horton and McConnell (1991), which "consists mainly of gneissic biotite granitoids and granitoid gneisses of probably Late Ordovician to Early Silurian age." Granitoids that were included in the Table Rock Plutonic Suite include the Brooks Crossroads, NC (Harper and Fullagar, 1981), Dysartsville, NC (Goldsmith et al., 1988), Reedy River, SC (Wagener, 1977), and Toluca, NC (see Overstreet et al., 1963b) granitoids. Other Inner Piedmont granitoids, most fitting the criteria for the Table Rock Plutonic Suite, which will be mentioned here include the Anderson's Mill, SC (Curl, 1998); Call, NC (Rankin et al., 1972); Pelham, SC (Maybin, 1997); Sugarloaf Mountain, NC (Lemmon, 1973); Toccoa, GA (R.D. Hatcher Jr., unpublished mapping); and Walker Top, NC (possible less sheared shallow-level Henderson Gneiss of Goldsmith et al., 1988) granitoids. Granitoids that Horton and McConnell (1991) designated as Devonian and Early Carboniferous include the Cherryville, NC (Griffitts and Overstreet, 1952) and Gray Court, SC (Wagener, 1977). Several other granitoids have been recognized in the Inner Piedmont for which no new data exist. In North Carolina these include the Sandy Mush granite, less foliated (relative to the Henderson Gneiss) megacrystic granitoid southeast of the Brindle Creek fault, and unnamed granitoid and migmatitic granitoid gneisses (all delineated by Goldsmith et al., 1988). Based on new geochronologic, isotopic, and geochemical data, and as proposed by Mapes et al. (2002), division of the Inner Piedmont into eastern and western magmatic belts is appropriate.

Western Inner Piedmont magmatic belt. Goldsmith et al. (1988) mapped the Dysartsville Tonalite as granitoid gneiss (termed the Dysartsville pluton on the tectonic inset) and indicated that the unit continues northeastward along strike from near Dysartsville, NC. Bream (1999), Giorgis (1999), Hill (1999), and Williams (2000) remapped the Dysartsville Tonalite southeast of Marion, North Carolina; and Yanagihara (1994) noted that the Mill Spring complex (Tallulah Falls Formation equivalent) contains significant amounts of granitoid that are likely correlative with the main Dysartsville Tonalite body. Several mafic and ultramafic bodies are present within the Dysartsville Tonalite in the Glenwood 7.5-minute quadrangle. Data for other western Inner Piedmont smaller granitoids is largely limited to a whole-rock Rb-Sr age, 427 ± 9 Ma, for the Brooks Crossroads pluton (Harper and Fullagar, 1981), originally mapped as Inner Piedmont granitic rock (Espenshade et al., 1975), and a whole-rock Rb-Sr age of 460 ± 9 Ma for granitoids originally mapped as Henderson Gneiss (Rankin et al., 1972) near Call, North Carolina.

Eastern Inner Piedmont magmatic belt. Several mappable megacrystic K-feldspar granitoids (first recognized by Goldsmith et al., 1988) are present in the South Mountains (Giorgis, 1999; Bier, 2001) and along strike in the Brushy Mountains (Merschat and Kalbas, this guidebook). They occur as discontinuous linear elongate bodies in the immediate hanging wall of the Brindle Creek thrust, and have been formally named the Walker Top Granite (Giorgis et al., this guidebook). A similar megacrystic K-feldspar augen gneiss was recognized by Curl (1998) near Spartanburg, South Carolina, and was informally named the Anderson's Mill gneiss. The Toluca Granite, named by Griffitts and Overstreet (1952) and first mapped in detail near Shelby (Griffitts and Overstreet, 1962; Griffitts et al., 1962; Yates and Overstreet, 1962; Yates, 1963; Overstreet et al., 1963a; compiled by Overstreet et al., 1963b), occurs as small- to moderate-sized bodies that parallel regional fabrics from at least the Brushy Mountains in North Carolina southwestward into northern Cherokee County, SC (Goldsmith et al., 1988). Davis et al. (1962) proposed that the Toluca Granite has a minimum age of 400 Ma and noted that zircon morphology favors a sedimentary origin.

The Cherryville granite is located along the Central Piedmont suture at the southeastern boundary of the Inner Piedmont. Griffitts and Overstreet (1952) also named this unit, which was subsequently included in work by Davis et al. (1962) and Kish (1983). Kish (1983) determined younger Rb-Sr whole-rock isochron (351 Ma), Rb-Sr muscovite (311 Ma), and Rb-Sr biotite (277 Ma) ages than the Rb-Sr biotite (375 Ma) age determined by Davis et al. (1962).

Mafic and ultramafic rocks. Small (relative to the Poor Mountain Amphibolite) bodies of amphibolite and amphibole gneiss are present throughout the Inner Piedmont but have received little attention. This is partially due to the fact that many occur as boudins or small outcrops, which are not mappable at most scales; however, Goldsmith et al. (1988) delineated several large (up to 10 km length) amphibolite bodies near the southeastern edge of the North Carolina Inner Piedmont in the Charlotte 1:250,000-scale map. Most detailed accounts of mafic and ultramafic occurrences have focused on ultramafic or altered ultramafic outcrops (e.g., Misra and Keller, 1978; Misra and McSween, 1984; Butler 1989; Mittwede, 1989; Warner et al., 1989).

Tectonic

Fault relationships in the Inner Piedmont have been ascribed to tectonic slides (Griffin, 1974a), metamorphic gradients (Hatcher and Acker, 1984), fold-related Type-F thrusts (Hatcher and Hooper, 1992), and crustal-scale shear zones (Davis, 1993a, 1993b). Because detailed mapping in the Inner Piedmont is incomplete, regional correlations of thrust stacks, faults, structural trends, etc. remain somewhat speculative (see Hatcher this guidebook, his Fig. 1). As a result, major compilation efforts are unavoidably oversimplified and often support improper correlation of lithologies and tectonic features in the crystalline core.

The Inner Piedmont stack of crystalline thrust sheets represents the metamorphic core of middle Paleozoic orogenic events in the southern Appalachians (Davis, 1993a, 1993b; Hatcher, 1998). Penetrative deformation in the Inner Piedmont is attributed to these events and was coeval with peak upper-amphibolite facies metamorphism. In the western Inner Piedmont, Type-F thrust sheets originated by shearing the common limb of ductile antiform-synform pairs and evolved as they cooled into more coherent Type-C thrust sheets (Hatcher and Hooper, 1992). Most transport indicators are parallel or sub-parallel to a strong mineral lineation and show a gradual change from NW-directed transport in the core of the Inner Piedmont to SW-directed transport at the western flank (Davis, 1993a; Hatcher, 2001). Previous workers (Griffin, 1974a; Goldsmith, 1981) noted the mineral lineation trend but did not attribute it to regional flow or transport direction. Davis (1993a, 1993b) used this pattern and the partially mylonitic character of the dominant foliation to conclude that regionally extensive shear occurred parallel and oblique to the penetrative foliation surface, and that the entire western Inner Piedmont is a crustal-scale shear zone. This regional orogen-parallel and orogen-oblique heterogeneous simple shear produced the majority of near-metamorphic peak structures.

NEW PERSPECTIVES ON OLD PROBLEMS

Detailed geologic maps remain the fundamental reference frame, albeit incomplete, from which Inner Piedmont work is evaluated. Isotopic and geochronologic data greatly complement mapping and provide important temporal and chemical constraints not offered by geologic mapping alone. We now have more of the Inner Piedmont mapped in detail (most also within reasonable regional context) than ever before and, given the renewed interest and resurgence of isotopic and geochronologic work, can offer a new and improved conceptual framework for the evolution of the Inner Piedmont.

Stratigraphic

A significant amount of Nd and Sr isotopic data now exist for crystalline rocks (mainly granitoids) of the Blue Ridge, Inner Piedmont, and Carolina terrane. Nd isotopic data for metasedimentary rocks can provide an independent measure of crustal affinity not afforded by U-Pb zircon data alone due to the robust nature of Sm/Nd ratios in sediments during sedimention (e.g., McCulloch and Wasserburg, 1978), the relative immobility of REE (e.g., Bernard-Griffiths et al., 1985), and similar behavior of Sm and Nd during metamorphism. Nd isotopic data from the metasedimentary rocks of the Blue Ridge and Inner Piedmont clearly overlap with the Grenville basement data of Carrigan et al. (in press) and to a lesser degree with data from the Mars Hill terrane (Ownby et al., in review), Chopawamsic (Wortman et al., 1996; Coler et al., 2000) (Fig. 3). Based on these data, it is possible that the sediments were derived from a combination of more isotopically evolved (relative to the Grenville basement) source(s) and less evolved more juvenile crustal source(s); or, more likely, directly derived from rocks similar in age and isotopic maturity to Blue Ridge and Sauratown Mountains window Grenville basement (Bream et al., in review).

The variety of proposed tectonic settings and crustal affinities (sometimes inferred) of the areally extensive metasedimentary packages within and surrounding the Inner Piedmont are undoubtedly related to our incomplete understanding of tectonic evolution in the southern Appalachian crystalline core. This is due to the intense deformation and metamorphism that obscure most primary relationships, a general lack of detailed mapping, and paucity of studies that integrate available geochronologic and geochemical constraints with existing or proposed tectonic models. With the exception of a few focused studies (mostly on granitoids), little analytical data (specifically U-Pb zircon data) are available for the Inner Piedmont; therefore, it is difficult to critically delimit tectonic models and the crustal affinity of most lithotectonic packages, which are dominated by metasedimentary rocks.

High-resolution ion microprobe analyses of detrital zircon separates can determine multiple source ages in sedimentary and metasedimentary rocks. For the southern Appalachian crystalline core paragneisses, this data (albeit preliminary) places important new constraints on the tectonic evolution of the entire orogen Composite probability age plots for southern Appalachian quartzofeldspathic and quartzite paragneiss samples presented by the traditional tectonic divisions of western Blue Ridge, eastern Blue Ridge, Dahlonega gold belt, western Inner Piedmont, and eastern Inner Piedmont reveal a significant Grenville component in each of the divisions and subtle differences (Fig. 4). For comparison, composite probability plots of detrital zircon ages can also be constructed for the Blue Ridge, Dahlonega gold belt, and the proposed crystalline core subdivisions of Hatcher (this volume): Cartoogechaye, Tugaloo, and Cat Square (Fig. 5). The summed probabilities should be viewed as "relative" abundances due to differences in number and types of samples; number of individual analyses for each division; separation and analytical bias; and the consolidation of samples in potentially artificial divisions. These plots illustrate the predominance of Grenville magmatic (~1000-1250 Ma) and metamorphic (~850-1000 Ma) ages in detrital zircons for most and suggest that the proposed crystalline core divisions of Hatcher (this volume) contain lithostratigraphic packages of similar crustal provenance.

The detrital zircon ages reveal a pre-Grenvillian component for most of the divisions, except for the eastern Blue Ridge and Sauratown Mountains window, which based on four and six samples respectively, contain only Grenvillian detrital zircons. Non-Grenvillian grains are broadly categorized as Middle Proterozoic (1.25-1.6 Ga), Early Proterozoic (1.6-2.1 Ga), and Late Archean (2.7-2.9 Ga). Exclusive of the eastern Blue Ridge and Sauratown Mountains window, Early Proterozoic peaks are discernable and the western and central Blue Ridge, Dahlonega gold belt, and eastern Inner Piedmont contain Late Archean zircons. Post-Grenvillian detrital zircons are also present in many of the samples. These ages are Late Proterozoic (570-850 Ma) and early Paleozoic (440-500 Ma) for detrital components with "Neoacadian" zircon rim age peaks. Overall,

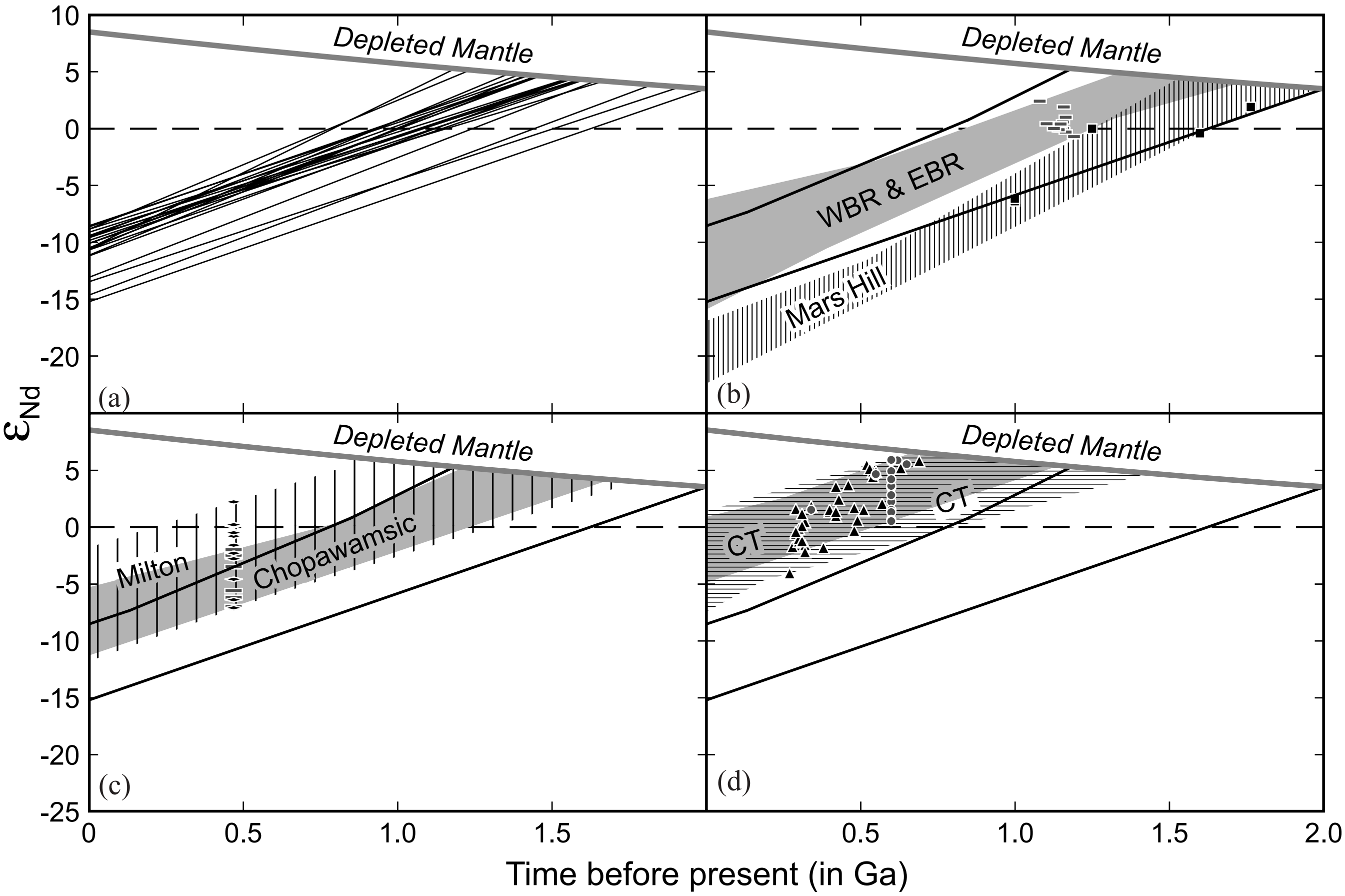

Figure 3. Epsilon Nd evolution over time for metasedimentary samples compared with data from Blue Ridge basement (Carrigan et al., in press; Ownby et al., in review), Carolina terrane (Samson et al., 1995; Fullagar et al., 1997), and Chopawamsic-Milton terranes (Wortman et al., 1996; Coler et al., 2000). (a) Metasedimentary sample data presented here showing evolution from present to intersection with the depleted mantle. (b) Metasedimentary data with fields defined for western and eastern Blue Ridge Grenvillian basement (WBR & EBR; gray field) and Mars Hill terrane (vertical lines). (c) Metasedimentary data with Chopawamsic (gray) and Milton belt (vertical lines) data. (d) Metasedimentary data with Carolina terrane data (CT; gray field defined by data of Samson et al., 1995; horizontal line field defined by data of Fullagar et al., 1997). Note evolution lines in (b-d) are defined by upper and lower boundaries of data in (a), symbols represent values at the estimated time of crystallization and/or deposition for the reference fields, and depleted mantle curve defined by DePaolo (1981). Figure modified from Bream et al., in review.

the data define several important age ranges and suggest that the Dahlonega gold belt, and possibly central Blue Ridge, contains a greater proportion of sediment derived from Late Archean crust than the other divisions.

Grenvillian detrital zircons are clearly the dominant component for southern Appalachian paragneisses. These ages, however, have limited use for establishing distinct source(s) because of the numerous Grenvillian belts on the margins of pre-Grenvillian cratons that were near or adjacent to the Laurentian margin during the Rodinian break-up (e.g., Hoffman, 1991). Consequently, the ages that provide the best constraints on the provenance of the paragneisses have pre- and post-Grenvillian ages. Based on the presence of 2.2-2.4 and ~1.35 Ga detrital zircons in the Pine Mountain window of Alabama, Heatherington et al. (1997) and Steltenpohl et al. (2002) suggested that the Hollis Quartzite could have been derived from the Gondwanan Rio de la Plata, Kalahari, or Congo cratons and that the mixture of Laurentian (or South American Rondonian province) and probable Gondwanan detrital zircons favor deposition of the Hollis Quartzite roughly coeval with the separation of the Pine Mountain window from Gondwana. Miller et al. (2000) cited the lack of Early Proterozoic and presence of Late Archean inherited zircons in eastern Blue Ridge mid-Ordovician and mid-Devonian plutons, as evidence for one of the following scenarios: the presence of an unrecognized Archean component within southern Appalachian basement; southern Appalachian paragneisses contain detrital zircons derived from the Superior Province of Canada; or that the eastern Blue Ridge is exotic and contains detrital zircons from a non-Laurentian source (probably Gondwanan). As noted by Miller et al. (2000), a substantial amount of published ages for Archean detrital and inherited zircons within and to the east of the Appalachians are considered to be derived from Gondwanan or peri-Gondwanan crustal fragments. The data shown in Figures 5 and 6 do not preclude any of the aforementioned scenarios given that the age ranges reported by Miller et al. (2000), Heath-

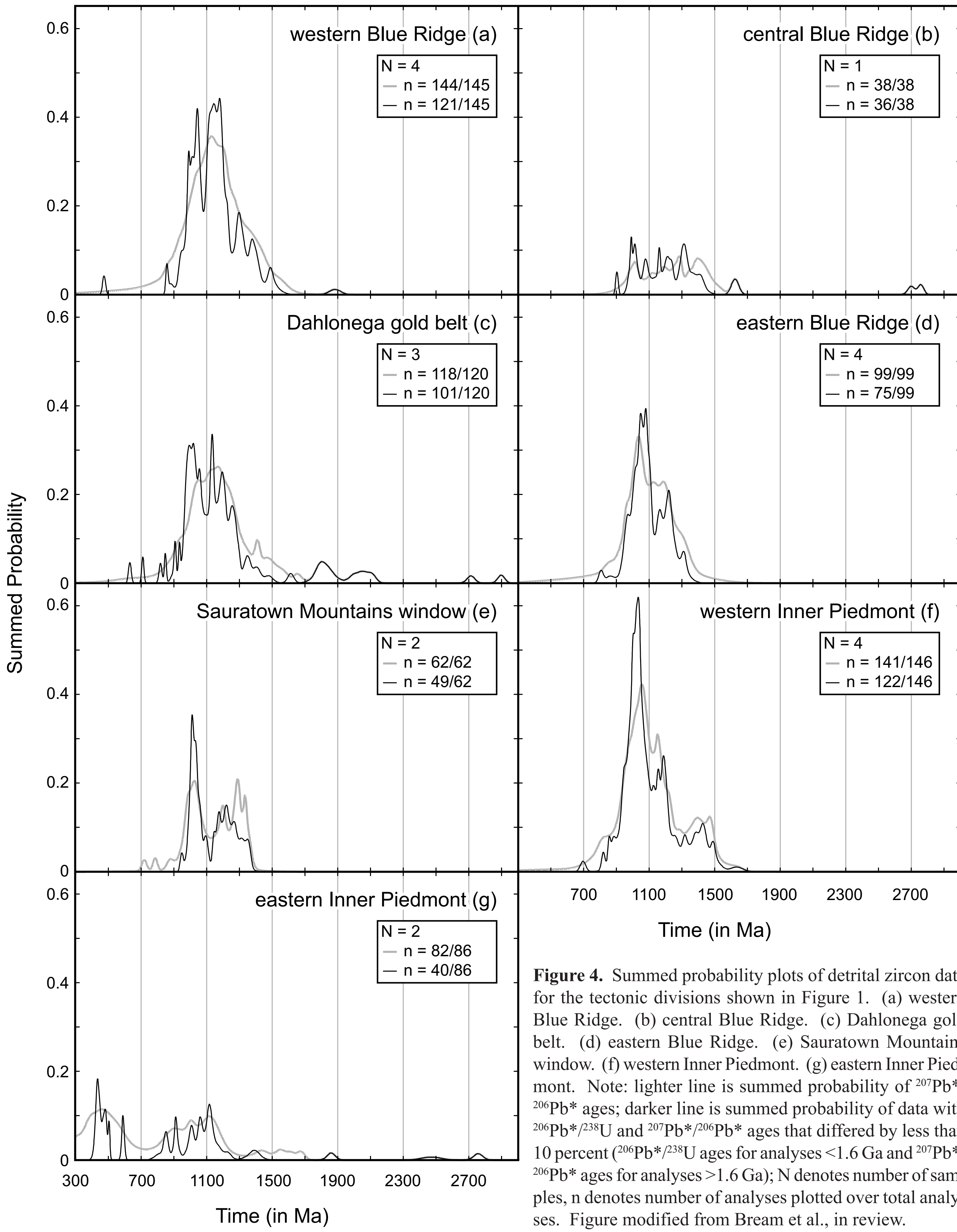

Figure 4. Summed probability plots of detrital zircon data for the tectonic divisions shown in Figure 1. (a) western Blue Ridge. (b) central Blue Ridge. (c) Dahlonega gold belt. (d) eastern Blue Ridge. (e) Sauratown Mountains window. (f) western Inner Piedmont. (g) eastern Inner Piedmont. Note: lighter line is summed probability of $^{207}Pb^*/^{206}Pb^*$ ages; darker line is summed probability of data with $^{206}Pb^*/^{238}U$ and $^{207}Pb^*/^{206}Pb^*$ ages that differed by less than 10 percent ($^{206}Pb^*/^{238}U$ ages for analyses <1.6 Ga and $^{207}Pb^*/^{206}Pb^*$ ages for analyses >1.6 Ga); N denotes number of samples, n denotes number of analyses plotted over total analyses. Figure modified from Bream et al., in review.

erington et al. (1997), and Steltenpohl et al. (2002), except for the 2.2-2.4 Ga range, are also present. The data differ from each, however, in that there is a minor Early Proterozoic component in most divisions. Based solely on the pre-Grenvillian detrital zircon ages, this allows for the possibility that the paragneisses of the southern Appalachian crys-

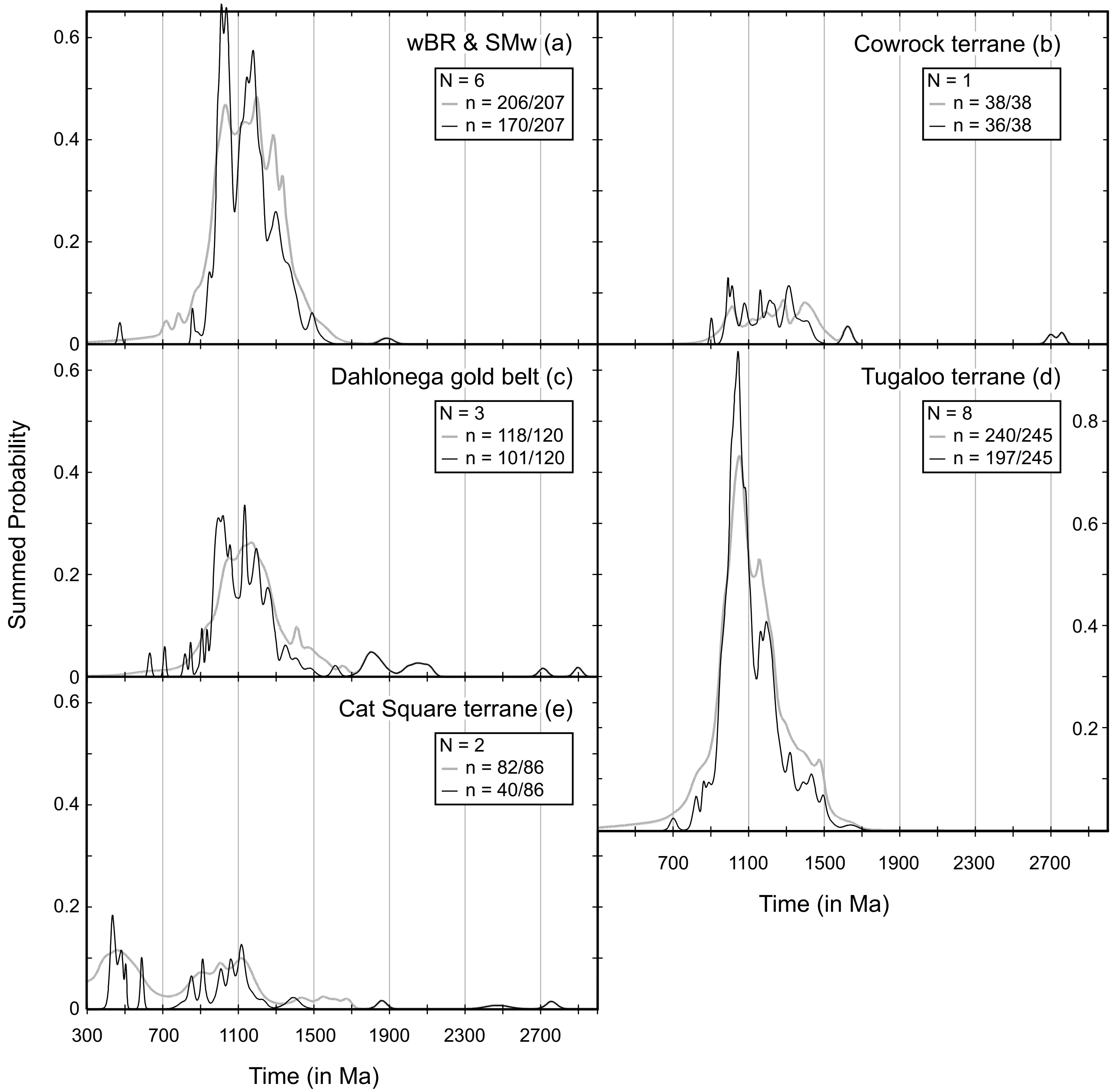

Figure 5. Summed probability plots of detrital zircon data for the tectonic divisions shown in Figure 1 and proposed divisions of Hatcher (this guidebook) for divisions southeast of the Hayesville fault. (a) western Blue Ridge (wBR) and Sauratown Mountains window (SMw). (b) Cowrock terrane (central Blue Ridge). (c) Dahlonega gold belt. (d) Tugaloo terrane (eastern Blue Ridge and western Inner Piedmont. (e) Cat Square terrane (eastern Inner Piedmont). Ages used and abbreviations same as Figure 4.

talline core (exclusive of the Cat Square terrane): (1) are entirely derived from Laurentian sources Hatcher (this guidebook); (2) are exotic to Laurentia and contain sediments derived from the Kalahari, Congo, and/or Amazonian cratons; or (3) contain a mixture of (1) and (2) as proposed by Heatherington et al. (1997) and Steltenpohl et al. (2002). The post-Grenvillian detrital zircon ages could represent sediment input from one or more of the following: pan-African crustal fragments (e.g., Carolina terrane), late Neoproterozoic rift-related igneous rocks (e.g., Crossnore pluton or Catoctin Formation equivalent?), or Ordovician magmatic rocks (eastern Inner Piedmont only).

A Laurentian crustal affinity for the paragneisses is favored here for all tectonic divisions, except the eastern Inner Piedmont (Cat Square terrane) based on the presence of similar North American cratonic ages and the lack of distinctly Gondwanan (2.2-2.4 Ga) detrital zircons. Samples from the eastern Inner Piedmont contain a unique suite of detrital zircons relative to the other tectonic subdivisions (Figs. 5 and 6). Most notably, a significant number of Ordovician and a smaller component of Neoproterozoic grains are present. Using the youngest detrital zircon age (~430 Ma) and the oldest zircon rim age (~400 Ma) we can establish a 30 Ma time interval in which the sediments of the eastern Inner Piedmont were deposited and metamorphosed to sillimanite grade. It is most likely that the Neoproterozoic grains from the eastern Inner Piedmont samples were shed from the approaching Carolina terrane as the Iapetus ocean closed. Ordovician detrital zircons most likely were eroded from exposed volcanic rocks in the immense magmatic belt in the eastern Tugaloo terrane. Based on these ages the eastern Inner Piedmont is distinct from the adjacent western Inner Piedmont and, as proposed by Bream et al. (2001b), the Brindle Creek fault is the boundary. In addition, Bream et al. (2001a) and Hatcher (this guidebook) proposed that the entire sequence from the western Blue Ridge to the western Inner Piedmont could represent a time-transgressive sequence that reflects the opening of the Iapetus ocean and the younging of oceanic crust (and deposition) to the east. The Cat Square terrane is thus composed of an even more distal sequence that was still being deposited *after* Ordovician plutonism and volcanism in the Tugaloo terrane.

Metamorphic

Several southern Appalachian crystalline core workers have produced a significant amount of new evidence that supports the presence of one or more widespread thermal events between 360 and 320 Ma (e.g., Dennis and Wright, 1997; Bream et al., 2000; Mirante and Patino-Douce, 2000; Carrigan et al., 2001; Mirante, 2001; Kohn, 2001; Kalbas et al., 2002). This age range and lack of evidence for earlier metamorphism supports the single prograde Neoacadian event proposed by Davis (1993a, 1993b). Consequently, Inner Piedmont migmatization, upper amphibolite grade mineral assemblages, and penetrative deformation are likely related to Neoacadian and early Alleghanian orogenesis. These ages, interpreted to represent growth or recrystallization of monazite and zircon during peak metamorphic conditions, are similar to the 333-322 Ma hornblende cooling ages of Dallmeyer (1988) for the eastern Blue Ridge, Chauga belt, Walhalla thrust sheet, and the Six Mile thrust sheet. Other reported U-Pb zircon ages include conventional data of T.W. Stern (USGS) for the Chauga belt-Walhalla thrust assemblage and the eastern Six Mile thrust sheet, which, according to Nelson et al. (1998), record ~385 Ma and 391 to 365 Ma thermal events, respectively.

The ~350 Ma peak reported for southern Appalachian metamorphism does not correspond to ages for the northern Appalachian Acadian peak 384-402 Ma (e.g., Eusden and Barreiro, 1988) and ending by 355 Ma (Eusden et al., 2000). The Valley and Ridge foreland basin contains evidence of the Taconic orogenic events, but only minor evidence of Neoacadian orogenesis. As proposed by Rogers (1967), Acadian deformation may have migrated southwestward over time, which favors oblique convergence, possibly providing an explanation for the younger southern Appalachian metamorphic ages. The 470 Ma metamorphic age reported by Moecher and Miller (2000) in the central Blue Ridge delimits the timing of granulite facies metamorphism there; this event, however, is either not present or not recorded by zircon and monazite in the eastern Blue Ridge and Inner Piedmont.

Evidence previously cited of the similarity and exact correlation of sequences on both sides of the Brevard fault is complicated by geochronologic data from granitoids of the eastern Blue Ridge and Inner Piedmont. Most notably, Paleozoic granitoids of the Inner Piedmont contain few Grenville and younger inherited zircon cores (e.g., Ranson et al., 1999; Mapes et al., 2002; Vinson, 1999) whereas similar age granitoids of the eastern Blue Ridge contain abundant Grenville and older inherited zircon cores (Miller et al., 2000). Additionally, the lack of Grenvillian basement in the Inner Piedmont represents another contrast across the Brevard fault zone. Although deposition of Inner Piedmont paragneisses on oceanic crust could explain the lack of Grenville basement in the Inner Piedmont and presence of small Grenville massifs within the adjacent eastern Blue Ridge, this basement distribution remains a major contrast across the Brevard fault zone. The peak at ~1.4 Ga for detrital zircons from the western Inner Piedmont and absence of pre-Grenvillian detrital zircons in the eastern Blue Ridge suggests a difference across the Brevard fault zone that could be real or related to sampling and/or statistical issues. Regardless, 1.4 Ga detrital zircons are also present in the western Blue Ridge so Laurentian derivation is not precluded.

Magmatic

Given the complex history of the southern Appalachian crystalline core, it is not surprising that whole-rock Rb-Sr and conventional U-Pb zircon ages are difficult to interpret. New ion microprobe U-Pb zircon data for several western Inner Piedmont granitoids document a sizeable Middle Ordovician (dominantly between 460 and 470 Ma) magmatic complex (Ranson et al., 1999; Vinson, 1999) and several Late Silurian to Late Carboniferous (most are Late Devonian to Early Carboniferous, 375 to 325 Ma) granitoids (Mapes, 2002) in the eastern Inner Piedmont. Recent detailed mapping has further documented the occurrence of mafic and ultramafic rocks (many of which are associated with granitoids) in the western Inner Piedmont. Whole-rock geochemical data have also been collected from the South Carolina crystalline core (Maybin and Niewendorp, 1997); however, the petrogenesis and regional context of these mostly mafic rocks remain largely unexplored.

Vinson (1999) reported a range of U-Pb zircon ages from 350 to 490 Ma with clusters at 420, 445, 471, and 492 Ma for a Henderson Gneiss sample from the Vulcan Materials Company Hendersonville, NC, quarry. Unpublished data (Miller and Meschter McDowell) of another sample from the Moffitt Hill quadrangle revealed a similar age range with a single distinct Middle Ordovician grouping, interpreted to represent the magmatic age for the Henderson Gneiss. Recent U-Pb zircon ion microprobe data for augen and banded gneisses from near Caesars Head State Park yield Ordovician magmatic ages (Late Ordovician according to Ranson et al., 1999, their Table Rock gneiss; Middle Ordovician according to Vinson, 1999, his Caesars Head gneiss) with Mid to Late Proterozoic inheritance. Other recently dated Ordovician granitoids of the western Inner Piedmont include: 440-490 Ma Brooks Crossroads, NC (Vinson, 1999); ~465 Ma Dysartsville, NC (Bream, unpublished data); ~490 Ma Sugarloaf Mountain gneiss (Vinson, 1999); and ~460 Ma Toccoa, GA (Bream, unpublished data). Zircon separates from a sample of Poor Mountain Quartzite yielded a single Middle Ordovician age of ~460 Ma (Bream, unpublished data; Kalbas et al., 2002). This age is interpreted as a magmatic age, favoring the interpretation that the Poor Mountain Quartzite had a volcanic or immature volcaniclastic protolith. If this is a metatuff, components of the Poor Mountain Formation might represent the volcanic equivalent of the large magmatic belt in the western Inner Piedmont. Tectonic discriminant diagrams indicate that the overlying and interlayered Poor Mountain Amphibolite has a probable oceanic affinity (Davis, 1993b; Yanigihara, 1994; Bream, 1999; Kalbas, in progress) suggesting a complex depositional and magmatic setting for the western Inner Piedmont during the Middle Ordovician. Recently dated eastern Inner Piedmont granitoids, ranging in age from Late Silurian to Pennsylvanian, include: ~415 Ma Anderson's Mill, SC (Mapes, 2002); ~357 Ma Gray Court, SC (Mapes, 2002); ~364 Ma Pelham, SC (Mapes, 2002); ~325 Ma Reedy River, SC (Mapes, 2002); ~380 Ma Toluca, NC (Mapes, 2002), and ~366 Ma Walker Top, NC (Vinson, 1999; Mapes, 2002). Based on these new granitoid crystallization ages and the clear distinction across the Brindle Creek fault as noted by Mapes et al., (2002), I propose that the name Table Rock Plutonic Suite (Horton and McConnell, 1991) either be restricted to western Inner Piedmont granitoids or dropped.

As noted by Vinson (1999), the chemistry of most western Inner Piedmont granitoids is likely the product of collisional or postcollisional crustal thickening, not the subduction related magmatic arc or continental margin arc as depicted in many tectonic models (e.g., Harper and Fullagar, 1981; Sinha et al., 1989; Hatcher, 1989; Hibbard, 2000). It has been proposed that a small ocean basin like the one between Kamchatka and the Okhotsk Sea (Hatcher, 1978) or the Gulf of California (Thomas et al., 2001) with an apex in what is now North Carolina could have developed or that the arc-related rocks are either eroded or deeply buried (Thomas et al., 2001). Fullagar et al. (1997) concluded that Inner Piedmont granitoids are isotopically intermediate between western Blue Ridge and Carolina terrane granitoids, perhaps reflecting the mixing of evolved Laurentian margin material with less evolved Pan-African material. Based on geochronology, isotopic evidence, and trace element concentrations, Mapes et al. (2002) proposed that the magmatic histories of the western and eastern Inner Piedmont are distinct from one another both temporally and petrogenetically. Regional structural relationships support this conclusion (Hatcher, this guidebook, his Fig. 1b).

Despite a plethora of new mapping and geochemical work in the western Inner Piedmont, the relationships between the Henderson Gneiss and Table Rock Plutonic Suite remain somewhat enigmatic near the North and South Carolina border. For example, mapping in the Zirconia (Davis, 1993b; Garihan, 1999) and Standingstone Mountain (Garihan, 1999; Garihan, this volume) quadrangles reveals that both units occur in the footwall of the Sugarloaf Mountain thrust sheet as undifferentiated granitoids. Previous mapping in the Hendersonville (Lemmon, 1973), Bat Cave (Lemmon and Dunn, 1973a), and Fruitland (Lemmon and Dunn, 1973b) quadrangles however, did not delineate mappable granitoids fitting the Table Rock Plutonic Suite criteria in the footwall of the Sugarloaf Mountain thrust beyond the extent of the OSgg granitoid, which is completely enclosed in Henderson Gneiss. As discussed previously, similarity of zircon U-Pb ages (470-490 Ma) for the Henderson Gneiss and Caesars Head-Table Rock gneiss suggests these granitoids were emplaced during the same magmatic event. The true extent and nature of the contacts between each lithology remain problematic, and the tectonic setting for this major Ordovician magmatic event remains poorly constrained. Difficulties related to these suites are further complicated by the numerous unnamed or informally named granitoids that are not mapped in detail, incompletely portrayed, or loosely catalogued on regional compilations.

Tectonic

Recent detailed mapping by geologists from the University of Tennessee to the northeast and Furman University to the southwest of previous mapping in the Columbus Promontory permits correlation of several thrust stacks across the North and South Carolina border. The regional tectonic model of Davis (1993a, 1993b) remains unrefuted; new conclusions addressing the extent, nature, and displacement of several major Inner Piedmont faults can now be considered (Fig. 7). The major faults of the central and southern North Carolina Inner Piedmont are discussed below in ascending order, from the Brevard fault zone southeastward.

While the correlation of major Inner Piedmont faults through the Carolinas allows us to ask questions concerning the nature, continuity, timing, and correlation of fault and lithologic units, it also brings into question some of the conclusions that previous workers have drawn for portions of these faults and lithotectonic packages. Correlation of the Mill Spring fault across a reconnaissance-mapped area to the Brushy Mountains of North Carolina and correlation of the Seneca (Six Mile) and Sugarloaf Mountain faults represents over 100 km of continuous faults. Although the Seneca fault represents a major lithologic break in South Carolina, displacement on the North Carolina equivalent (Sugarloaf Mountain fault) decreases to zero near Marion, North Carolina, and has possibly transferred motion up the thrust stack to the Mill Spring thrust (Merschat and Kalbas, this guidebook). The mapped truncations of major Paleozoic faults in the western Inner Piedmont by Ordovician granitoids (Nelson et al., 1998) could be incorrect but, if correct, suggest that faulting occurred prior to magma intrusion, penetrative deformation, and peak metamorphism in contrast to the new geochronologic and field data (Hatcher and Acker, 1984; Davis, 1993a, 1993b; Hatcher, in preparation) that strongly indicate faulting was post-Ordovician. Additional detailed mapping in North and South Carolina should better resolve the extent of Inner Piedmont faults.

Marion thrust sheet. The Marion thrust sheet, defined herein and by Merschat and Kalbas (this guidebook), is the structurally lowest thrust sheet in the North Carolina Inner Piedmont. The Marion thrust sheet includes the lithotectonic packages from the Brevard fault zone southeastward to the Mill Spring thrust in North Carolina. Correlation of this nappe in South Carolina is presently uncertain; however, it occurs in the same structural position as the South Carolina Chauga belt, but the Chauga belt contains several additional thrust sheets (see Hatcher, this guidebook, his Fig. 3). Along the northwestern boundary of the Marion thrust sheet, western Inner Piedmont metasedimentary packages are juxtaposed with similar eastern Blue Ridge packages. Folded Tallulah Falls metasedimentary units of the Marion thrust sheet are truncated by the main Henderson Gneiss body and by numerous small elongate bodies. This contact is either intrusive or fault-defined (Tumblebug Creek fault of Davis 1993a, 1993b).

Tumblebug Creek thrust. The Tumblebug Creek thrust fault placed Henderson Gneiss over Tallulah Falls Formation in North Carolina (Davis, 1993a; 1993b). Fault emplacement for the Henderson Gneiss is favored over intrusive or unconformable relationships based on the truncation of footwall folds and the size reduction of K-feldspar augen in the Henderson Gneiss near the contact. Truncated contacts in the footwall of the Tumblebug Creek fault indicate that fault emplacement occurred subsequent to a folding event; however, the folded nature of the Tumblebug Creek fault and observations of mesoscopic isoclinal reclined folds and other fabric elements in the Henderson Gneiss (Bream, 1999) suggest that the Henderson Gneiss and Tallulah Falls Formation rocks of the Marion thrust sheet were juxtaposed prior to penetrative deformation.

Sugarloaf Mountain-Seneca thrust. Garihan (2001) has correlated the Seneca fault, renamed by Horton and McConnell (1991) from Griffin's (1969) Six Mile thrust, at the base of the Six Mile thrust sheet with the Sugarloaf Mountain fault of Davis (1993b). Thus, the Sugarloaf Mountain-Seneca fault placed Tallulah Falls and Poor Mountain Formation rocks over migmatitic Tallulah Falls Formation, metagrabbro amphibolite, ultramafic schist, and granitoids (various biotite gneisses and augen gneisses including the Caesars Head Granite) of the Walhalla nappe in South Carolina and thrusts Tallulah Falls and Poor Mountain Formations over the Henderson Gneiss in North Carolina. Within the Sugar Hill 7.5-minute quadrangle, Bream (1999) noted that the Sugarloaf Mountain fault tips out and that the outcrop pattern of the Henderson Gneiss with the overlying Tallulah Falls Formation is related to reclined to recumbent isoclinal folding. As previously noted, Nelson et al., (1998) depicted the truncation of Paleozoic faults (including the Six Mile fault) in South Carolina by the Caesars Head Granite, suggesting that movement of this fault occurred before the Middle Ordovician. Klippes of Poor Mountain Formation rocks on Henderson Gneiss, windows of Henderson Gneiss to the southeast of the main body, and small linear elliptical bodies of Henderson Gneiss to the northeast suggest low-angle Type-F thrusting.

Mill Spring thrust. The Mill Spring thrust fault emplaced mid- to upper-Tallulah Falls Formation, migmatitic Poor Mountain Formation, and granitoids over Poor Mountain and upper Tallulah Falls Formations. The Mill Spring thrust was originally defined by work of Tabor (unpublished mapping) in the Mill Spring 7.5-minute quadrangle and subsequently delineated in the Cliffield Mountain 7.5-minute quadrangle by Davis (1993b). Because the Pea Ridge and Fingerville West 7.5-minute quadrangles remain unmapped, correlation of the fault into the Sugar Hill 7.5-minute quadrangle is based on Davis' (1993a, 1993b) thrust stack model (Yanagihara, 1994). Map relationships in the Brushy Mountains suggest that the Mill Spring fault is also likely present along strike from detailed work near Marion, NC (Bream, 1999; Hill, 1999). Although the Mill Spring fault is mapped to the North Carolina-South Carolina border, the recent report of its absence and the presence of Henderson

Gneiss in the southern part of the Saluda quadrangle (Warlick et al., 2001) precludes correlation of this fault into South Carolina.

Brindle Creek thrust. The Brindle Creek thrust fault, first recognized and named by Giorgis (1999) in the Dysartsville quadrangle, thrusts a paragneiss sequence dominated by aluminous schist with Walker Top Granite over intensely migmatitic Tallulah Falls (?) and Poor Mountain Formations. This fault separates older Ordovician granitoids in the footwall from younger mainly Devonian granitoids in the hanging wall; the fault has not been mapped in detail along strike beyond, or between, the Brushy and South Mountains but, it can be extrapolated using the maps of Reed (1964), Rankin et al. (1972), Espenshade et al. (1975), and Goldsmith et al. (1988) (see Hatcher, this guidebook). Additionally, this fault may be present in South Carolina, but lack of detailed mapping near the border of both states permits only speculative extrapolation (Hatcher, this guidebook, his Fig. 1b). This fault juxtaposes paragneisses with distinct detrital zircon age ranges, represents a major crustal-scale boundary within the Inner Piedmont (Kalbas et al., 2002), and is possibly a terrane boundary as proposed by Bream et al. (2001b) and Bream and Hatcher (2002).

ACKNOWLEGMENTS

This paper summarizes a portion of the author's Ph.D. dissertation at the University of Tennessee–Knoxville, under the direction of Robert D. Hatcher Jr. and Calvin F. Miller (Vanderbilt University). Paul D. Fullagar collected the Nd isotopic data presented in this paper and is acknowledged for interpretive assistance. Calvin Miller, Joe Wooden, Anders Meibom, Chris Coath, and Mark Harrison are gratefully acknowledged for assistance with the Stanford and UCLA ion microprobes. Much of this work has benefited from numerous conversations with members of the North Carolina Geological Survey (Leonard Wiener, Carl Merschat, and Mark Carter), South Carolina Geological Survey (Butch Maybin), faculty at Furman University (Jack Garihan and Bill Ranson), UTK Inner Piedmont mappers (Joe Hill, Scott Giorgis, Scott Williams, Sara Bier, Jeff Riedel, Jay Kalbas, and Arthur Merschat) and Vanderbilt University students (Sam Vinson, Charles Carrigan, Susanne Meschter McDowell, Russ Mapes); however, any errors remain my responsibility. Detailed geologic mapping was funded by EDMAP grants 1434HQ97AG01720, 98HQAG2026, 99HQAG0026, 00HQAG0035, and 01HQAG0176 to R.D. Hatcher, Jr. from the National Cooperative Geologic Mapping Program (administered by U.S.G.S.). Ion microprobe work was funded by NSF grant EAR-9814800 to R.D. Hatcher, Jr. and NSF EAR-9814801 to C.F. Miller. Additional funding was provided by the UTK Science Alliance Center of Excellence.

REFERENCES CITED

Abbott, R.N., and Raymond, L.A., 1984, The Ashe metamorphic suite, northwest North Carolina: Metamorphism and observations on geologic history: American Journal of Science, v. 284, p. 350-375.

Aleinikoff, J.N., Zartman, R.E., Walter, M., Rankin, D.W., Lyttle, P.T., and Burton, W.C., 1995, U-Pb ages of metarhyolites of the Catoctin and Mount Rogers formations, central and southern Appalachians: Evidence for two phases of Iapetian rifting: American Journal of Science, v. 295, p. 428-454.

Bernard-Griffiths, J., Peucat, J.-J., Cornichet, J., Iglesias Ponce de Léon, M., and Gil Ibarguchi, J.I., 1985, U-Pb, Nd isotope and REE geochemistry in eclogites from the Cabo Ortegal Complex, Galicia, Spain: An example of REE immobility conserving MORB-like patterns during high-grade metamorphism, *in* Smith, D.C., and Vidal, Ph., eds., Isotope geochemistry and geochronology of eclogites: Chemical Geology, v. 52, p. 217-225.

Bond, P.A., and Fullagar, P.D., 1974, Origin and age of the Henderson augen gneiss and associated cataclastic rocks in southwestern North Carolina: Geological Society of America Abstracts with Programs, v. 6, no. 4, p. 336.

Bentley, R.D., and Neathery, T.N., 1970, Geology of the Brevard zone and related rocks of the Inner Piedmont of Alabama: Alabama Geological Society, Eighth annual field trip guidebook, 119 p.

Bier, S.E., 2001, Geology of the southeastern South Mountains, North Carolina [unpublished M.S. thesis]: Knoxville, University of Tennessee, 162 p.

Bream, B.R., 1999, Structural and stratigraphic relationships of ortho- and paragneisses southwest of Marion, North Carolina [M.S. thesis]: Knoxville, Tennessee, University of Tennessee, 155 p.

Bream, B.R., and Hatcher, R.D., Jr., 2002, Southern Appalachian terranes amended: timing of accretion and delimiting provenance from new detrital zircon and Nd isotopic data: Geological Society of America Abstracts with Programs.

Bream, B.R., Hatcher, R.D., Jr., Miller, C.F., and Fullagar, P.D., 2000, Paragneiss geochemistry and preliminary ion microprobe geochronology of detrital zircons from the southern Appalachian crystalline core: Geological Society of America Abstracts with Programs, v. 32, p. 31.

Bream, B.R., Hatcher, R.D., Jr., Miller, C.F., Carrigan, C.W., and Fullagar, P.D., 2001a, Provenance and geochemistry of Late Proterozoic southern Appalachian crystalline core paragneisses, NC-SC-GA-TN: Geological Society of America Abstracts with Programs, v. 33, p. 29.

Bream, B.R., Hatcher, R.D., Jr., Miller, C.F., and Fullagar, P.D., 2001b, Geochemistry and provenance of Inner Piedmont paragneisses, NC and SC: Evidence for an internal terrane boundary?: Geological Society of America Abstracts with Programs, v. 33, p. 65.

Bream, B.R., Hatcher, R.D., Jr., Miller, C.F., and Fullagar, P.D., in review, Detrital zircon ages and Nd isotopic data from the southern Appalachian crystalline core, GA-SC-NC-TN: New provenance constraints for Laurentian margin paragneisses, *in* Tollo, R.P., Corriveau, L., McLelland, J., and Bartholomew, M.J., eds., Proterozoic evolution of the Grenville orogen in North America: Boulder, Colorado, Geological Society of America Special Paper.

Bryant, B., and Reed, J.C., Jr., 1970, Geology of the Grandfather Mountain window and vicinity, North Carolina and Tennessee: U.S. Geological Survey Professional Paper 614, 189 p.

Butler, J.R., 1989, Review and classification of ultramafic bodies in the Piedmont of the Carolinas, *in* Mittwede, S.K., and Stoddard, E.F., eds., Ultramafic rocks of the Appalachian Piedmont: Boulder, Colorado, Geological Society of America Special Paper 231, p. 19-31.

Butler, J.R., 1991, Metamorphism, *in* Horton, J.W., Jr., and Zullo, V.A., eds., The Geology of the Carolinas: Knoxville, Tennessee, The University of Tennessee Press, p.127-141.

Carrigan, C.W., 2000, Ion microprobe geochronology of Grenville and older basement in the southern Appalachians [M.S. thesis]: Nashville, Tennessee, Vanderbilt University, 101 p.

Carrigan, C.W., Bream, B.R., Miller, C.F., and Hatcher, R.D., Jr., 2001, Ion microprobe analyses of zircon rims from the eastern Blue Ridge and Inner Piedmont, NC-SC-GA: Implications for the timing of Paleozoic metamorphism in the southern Appalachians: Geological Society of America Abstracts with Programs, v. 33, p. 7.

Carrigan, C.W., Miller, C.F., Fullagar, P.D., Hatcher, R.D., Jr., Bream, B.R., and Coath, C.D., in press, Ion microprobe age and geochemistry of southern Appalachian basement, with implications for Proterozoic and Paleozoic reconstructions: Precambrian Research.

Cawood, P.A., and Nemchin, A.A., 2001, Paleogeographic development of the east Laurentian margin: constraints from U-Pb dating of detrital zircons in the Newfoundland Appalachians: Geological Society of America Bulletin, v. 113, p. 1234-1246.

Cawood, P.A., McCausland, P.J.A., and Dunning, G.R., 2001, Opening Iapetus: Constraints from the Laurentian margin in Newfoundland: Geological Society of America Bulletin, v. 113, p. 443-453.

Clark, G.M., 1993, Quaternary geology and geomorphology of part of the Inner Piedmont of the southern Appalachians in the Columbus Promontory upland area, southwestern North Carolina and northwestern South Carolina, *in* Hatcher, R.D., Jr., and Davis, T.L., eds., Studies of Inner Piedmont geology with a focus on the Columbus Promontory: Carolina Geological Society annual field trip guidebook, p. 67-84.

Coler, D.G., Wortman, G.L., Samson, S.D., Hibbard, J.P., and Stern, R., 2000, U-Pb geochronologic, Nd isotopic, and geochemical evidence for the correlation of the Chopawamsic and Milton terranes, Piedmont Zone, southern Appalachian orogen: Journal of Geology, v. 108, p. 363-380.

Curl, D.C., 1998, Stratigraphy and structure of Wellford and Reidville quadrangles in part of the eastern Inner Piedmont, near Spartanburg South Carolina [M.S. thesis]: Knoxville, Tennessee, University of Tennessee, 129 p.

Dallmeyer, R.D., 1988, Late Paleozoic tectonothermal evolution of the western Piedmont and eastern Blue Ridge, Georgia: Controls on the chronology of terrane accretion and transport in the southern Appalachian orogen: Geological Society of America Bulletin, v. 100, p. 702-713.

Dalziel, I.W.D., 1997, Neoproterozoic-Paleozoic geography and tectonics: Review, hypothesis, environmental speculation: Geological Society of America Bulletin, v. 109, p. 16-42.

Dalziel, I.W.D., Mosher, S., and Gahagan, L.M., 1998, Laurentia-Kalahari collision and the assembly of Rodinia: Journal of Geology, v. 108, p. 499-513.

Davis, G.L., Tilton, G.R., and Wetherill, G.W., 1962, Mineral ages from the Appalachian province in North Carolina and Tennessee: Journal of Geophysical Research, v. 67, p. 1987-1996.

Davis, T.L., 1993a, Geology of the Columbus Promontory, western Piedmont, North Carolina, southern Appalachians, *in* Hatcher, R.D., Jr., and Davis, T.L., eds., Studies of Inner Piedmont geology with a focus on the Columbus Promontory: Carolina Geological Society annual field trip guidebook, p. 17-43.

Davis, T.L., 1993b, Lithostratigraphy, structure, and metamorphism of a crystalline thrust terrane, western Inner Piedmont, North Carolina [Ph.D. dissertation]: Knoxville, Tennessee, University of Tennessee, 245 p.

Dennis, A.J., 1991, Is the central Piedmont suture a low-angle normal fault?: Geology, v. 19, p. 1081-1084.

Dennis, A.J., and Wright, J.E., 1997, Middle and late Paleozoic monazite U-Pb ages, Inner Piedmont, South Carolina: Geological Society of America Abstracts with Programs, v. 29, p. 12.

DePaolo, D., 1981, Neodymium isotopes in the Colorado Front Range and crust-mantle evolution in the Proterozoic: Nature, v. 291, p. 193-196.

Drake, A.A., Jr., Sinha, A.K., Laird, J., and Guy, R.E., 1989, The Taconic orogen, *in* Hatcher, R.D., Jr., Thomas, W.A., and Viele, G.W., eds., The Appalachian-Ouachita orogen in the United States: Boulder, Colorado, Geological Society of America, The Geology of North America, v. F-2, p. 101-177.

Espenshade, G.H., Rankin, D.W., Shaw, K.W., and Neuman, R.B., 1975, Geologic map of the east half of the Winston-Salem quadrangle, North Carolina-Virginia: U.S. Geological Survey Miscellaneous Geologic Investigations Map I-709B, scale 1:250,000.

Eusden, J.K., Jr., Guzofski, C.A., Robinson, A.C., and Tucker, R.D., 2000, Timing of the Acadian orogeny in northern New Hampshire: Journal of Geology, v. 108, p. 219-232.

Eusden J.K., Jr., and Barreiro, B., 1988, The timing of peak high-grade metamorphism in central-eastern New England: Maritime Sediments and Atlantic Geology, v. 24, p. 241-255.

Fullagar, P.D., Goldberg, S.A., and Butler, J.R., 1997, Nd and Sr isotopic characterization of crystalline rocks from the southern Appalachian Piedmont and Blue Ridge, North and South Carolina, *in* Sinha, A.K., Whalen, J.B., and Hogan, J.P., eds., The nature of magmatism in the Appalachian orogen: Boulder, Colorado, Geological Society of America Memoir 191, p. 165-179.

Garihan, J.E., 1999, The Sugarloaf Mountain thrust in the western Inner Piedmont between Zirconia, North Carolina, and

Pumpkintown, South Carolina, *in* Hatcher, R.D., Jr., ed., Geotraverse across part of the Acadian orogen in the southern Appalachians: Southeastern Section Geological Society of America Field Trip Guidebook, p. 23-40.

Garihan, J.E., 2001, Observations of the Seneca fault and their implications for thrust sheet emplacement in the Inner Piedmont of the Carolinas: South Carolina Geology, v. 43, p. 1-13.

Garihan, J.M., Preddy, M.S., and Ranson, W.A., 1993, Summary of mid-Mesozoic brittle faulting in the Inner Piedmont and nearby Charlotte Belt of the Carolinas, *in* Hatcher, R.D., Jr., and Davis, T.L., eds., Studies of Inner Piedmont geology with a focus on the Columbus Promontory: Carolina Geological Society annual field trip guidebook, p. 55-65.

Giorgis, S.D., 1999, Geology of the northwestern South Mountains near Morganton, North Carolina [M.S. thesis]: Knoxville, Tennessee, University of Tennessee, 186 p.

Goldberg, S.A., and Fullagar, P.D., 1993, Alleghanian Rb-Sr mineral ages from the Inner Piedmont of southwestern North Carolina, *in* Hatcher, R.D., Jr., and Davis, T.L., eds., Studies of Inner Piedmont Geology with a focus on the Columbus Promontory: Carolina Geological Society annual field trip guidebook, p. 105-107.

Goldsmith, R., 1981, Structural patterns in the Inner Piedmont of the Charlotte and Winston-Salem 2-degree quadrangles, North Carolina and South Carolina, *in* Horton, J.W., Jr., Butler, J.R., and Milton, D.M., eds., Geological investigations of the Kings Mountain belt and adjacent areas in the Carolinas: Carolina Geological Society Guidebook annual field trip guidebook, p. 19-27.

Goldsmith, R., Milton, D.J., and Horton, J.W., Jr., 1988, Geology of the Charlotte 1˚ X 2˚ quadrangle, North Carolina and South Carolina: U.S. Geological Survey Map I-1251-E, scale 1:250,000.

Gray, M.B., and Zeitler, P.K., 1997, Comparison of clastic wedge provenance in the Appalachian foreland using U/Pb ages of detrital zircons: Tectonics, v. 16, p. 151-160.

Griffin, V.S., Jr., 1967, Geology of the Six Mile quadrangle, South Carolina: South Carolina Division of Geology MS-14, scale 1:24,000.

Griffin, V.S., Jr., 1969a, Inner Piedmont tectonics in the vicinity of Walhalla, South Carolina: South Carolina Division of Geology, Geologic Notes, v. 14, p. 15-28.

Griffin, V.S., Jr., 1969b, Migmatitic Inner Piedmont belt of northwestern South Carolina: South Carolina Division of Geology, Geologic Notes, v. 13, p. 87-104.

Griffin, V.S., Jr., 1971a, The Inner Piedmont belt of the southern crystalline Appalachians: Geological Society of America Bulletin, v. 82, p. 1885-1898.

Griffin, V.S., Jr., 1971b, Stockwork tectonics in the Appalachian Piedmont of South Carolina: Geologische Rundschau, v. 60, p. 868-886.

Griffin, V.S., Jr., 1974a, Analysis of the Piedmont in northwest South Carolina: Geological Society of America Bulletin, v. 85, p. 1123-1138.

Griffin, V.S., Jr., 1974b, Geology of the Walhalla quadrangle, South Carolina: South Carolina Division of Geology MS-19, scale 1:24,000.

Griffin, V.S. Jr., 1974c, Progress report on a geologic study in Anderson County, South Carolina: South Carolina Division of Geology, Geologic Notes, v. 18, p. 13-23.

Griffitts, W.R., and Overstreet, W.C., 1952, Granitic rocks of the western Carolina Piedmont: American Journal of Science, v. 250, p. 777-789.

Griffitts, W.R., and Overstreet, W.C., 1962, Preliminary geologic map of the southeast quarter of the Shelby quadrangle, Cleveland County, North Carolina: U.S. Geological Survey Field Studies Map MF 250, scale 1:24,000.

Griffitts, W.R., Yates, R.G., and Overstreet, W.C., 1962, Preliminary geologic map of the southwest quarter of the Shelby quadrangle, Cleveland and Rutherford counties, North Carolina: U.S. Geological Survey Field Studies Map MF-252, scale 1:24,000.

Grimes, J.E., Steltenpohl, M.G., Cook, R.B., and Keefer, W.D., 1993, Geology of the southernmost Brevard fault zone, Alabama, and its implications for southern Appalachian tectonostratigraphy, *in* Hatcher, R.D., Jr., and Davis, T.L., eds., Studies of Inner Piedmont geology with a focus on the Columbus Promontory: Carolina Geological Society annual field trip Guidebook, p. 91-103.

Hadley, J.B., and Nelson, A.E., 1970, Caesars Head Quartz Monzonite in the western Carolina Piedmont, *in* Cohee, G.V., Bates, R.G., and Wright, W.B., eds., Changes in stratigraphic nomenclature by the U.S. Geological Survey, 1969: U.S. Geological Survey Bulletin 1324-A, p. 23-24.

Harper, S.B., and Fullagar, P.D., 1981, Rb-Sr ages of granitic gneisses of the Inner Piedmont belt of northwestern North Carolina and southwestern South Carolina: Geological Society of America Bulletin, v. 92, p. 864-872.

Hatcher, R.D., Jr., 1969, Stratigraphy, petrology, and structure of the low rank belt and part of the Blue Ridge of northwesternmost South Carolina: South Carolina Division of Geology, Geologic Notes, v. 13, p. 105-141.

Hatcher, R.D., Jr., 1970, Stratigraphy of the Brevard zone and Poor Mountain area, northwestern South Carolina: Geological Society of America Bulletin, v. 81, p. 933-940.

Hatcher, R.D., Jr., 1978, Tectonics of the western Piedmont and Blue Ridge: Review and speculation: American Journal of Science, v. 278, p. 276-304.

Hatcher, R.D., Jr., 1987, Tectonics of the southern and central Appalachian internides: Annual Review of Earth and Planetary Science, v. 15, p. 337-362.

Hatcher, R.D., Jr., 1989, Tectonic synthesis of the U.S. Appalachians, *in* Hatcher, R.D., Jr., Thomas, W.A., and Viele, G.W., eds., The Appalachian-Ouachita orogen in the United States: Boulder, Colorado, Geological Society of America, The Geology of North America, v. F-2, p. 511-535.

Hatcher, R.D., Jr., 1993, Perspective of the tectonics of the Inner Piedmont, southern Appalachians, *in* Hatcher, R.D., Jr., and Davis, T.L., eds., Studies of Inner Piedmont geology with a focus on the Columbus Promontory: Carolina Geological Society annual field trip guidebook, p. 1-16.

Hatcher, R.D., Jr., 1998, Structure of the Appalachian Inner Piedmont: Geological Society of America Abstracts with Programs, v. 30, p. 17.

Hatcher, R.D., Jr., and Acker, L.L., 1984, Geology of the Salem quadrangle, South Carolina: South Carolina Geological Survey, MS-26, 23 p., scale 1:24,000.

Hatcher, R.D., Jr., and Goldberg, S.A., 1991, The Blue Ridge geologic province, *in* Horton, J.W., Jr., and Zullo, V.A., eds., The Geology of the Carolinas: Knoxville, Tennessee, The University of Tennessee Press, p. 11-35.

Hatcher, R.D., Jr., and Hooper, R.J., 1992, Evolution of crystalline thrust sheets in the internal parts of mountain chains, *in* McClay, K.R., ed., Thrust tectonics: London, Chapman and Hall, p. 217-234.

Hatcher, R.D., Jr., Osberg, P.H., Drake, A.A., Jr., Robinson, P., and Thomas, W.A., 1990, Tectonic map of the U.S. Appalachians, *in* Hatcher, R.D., Jr., Thomas, W.A., and Viele, G.W., eds., The Appalachian-Ouachita orogen in the United States: Boulder, Colorado, Geological Society of America, The Geology of North America, v. F-2, Plate 1.

Hatcher, R.D., Jr., Bream, B.R., Hill, J.C., Giorgis, S.D., and Williams, S.T., 1999, Transect through the Acadian orogen in the Carolinas and northeast Georgia: Geological Society of America Abstracts with Programs, v. 31, p. 19.

Hatcher, R.D., Jr., Bream, B.R., Miller, C.F., Eckert, J.O., Jr., Fullagar, P.D., and Carrigan, C.W., in review, Paleozoic structure of southern Appalachian Blue Ridge Grenvillian internal basement massifs, *in* Tollo, R.P., Corriveau, L., McLelland, J., and Bartholomew, M.J., eds., Proterozoic evolution of the Grenville orogen in North America: Boulder, Colorado, Geological Society of America Special Paper.

Heatherington, A.L., Steltenpohl, M.G., Yokel, L.S., and Mueller, P.A., 1997, Ages of detrital zircons from the Pine Mountain and Inner Piedmont terranes and the Valley and Ridge Province; implications for Neoproterozoic tectonics of the southern Laurentian margin: Geological Society of America Abstracts with Programs, v. 29, p. 432.

Hibbard, J., 1993, The Milton belt–Carolina slate belt boundary: the northern extension of the Central Piedmont suture?, *in* Hatcher, R.D., Jr., and Davis, T.L., eds., Studies of Inner Piedmont geology with a focus on the Columbus Promontory: Carolina Geological Society annual field trip guidebook, p. 85-89.

Hibbard, J., 2000, Docking Carolina: Mid-Paleozoic accretion in the southern Appalachians: Geology, v. 28, p. 127-130.

Hibbard, J.P., and Samson, S.D., 1995, Orogenesis exotic to the Iapetan cycle in the southern Appalachians, *in* Hibbard, J.P., van Staal, C.R., and Cawood, P.A., eds., Current Perspectives in the Appalachian-Caledonian orogen: Geological Association of Canada Special Paper 41, p. 191-205.

Hill, J.C., 1999, Stratigraphy, structure, and tectonics of the southern Appalachian Inner Piedmont, near Marion, North Carolina [M.S. thesis]: Knoxville, Tennessee, University of Tennessee, 188 p.

Hoffman, P.F., 1991, Did the breakout of Laurentia turn Gondwanaland inside-out?: Science, v. 252, p. 1409-1412.

Hopson, J.L., and Hatcher, R.D., Jr., 1988, Structural and stratigraphic setting of the Alto allochthon, northeast Georgia: Geological Society of America Bulletin, v. 100, p. 339-350.

Horton, J.W., Jr., and Dicken, C.L., 2001, Preliminary geologic map of the Appalachian Piedmont and Blue Ridge, South Carolina Segment: U.S. Geological Survey open-file report 01-298, scale 1:500,000.

Horton, J.W., Jr., and McConnell, K.I., 1991, The western Piedmont, *in* Horton, J.W., Jr., and Zullo, V.A., eds., The Geology of the Carolinas: Knoxville, Tennessee, The University of Tennessee Press, p. 36-58.

Horton, J.W., Jr., Drake, A.A., Jr., and Rankin, D.W., 1989, Tectonostratigraphic terranes and their Paleozoic boundaries in the central and southern Appalachians, *in* Dallmeyer, R.D., ed., Terranes in the circum-Atlantic Paleozoic orogens: Geological Society of America Special Paper 230, p. 213-245.

Kalbas, J.L., Bream, B.R., Hatcher, R.D., Jr., and Maybin, A.H., III, 2002, Evidence for mafic Ordovician magmatism and Acadian metamorphism in the Brushy Mountains, western Inner Piedmont, of North Carolina: Geological Society of America Abstracts with Programs, v. 34, p. 119.

Keith, A., 1905, Description of the Mount Mitchell quadrangle (North Carolina-Tennessee): U.S. Geological Survey Geologic Atlas, Folio 124, 10 p.

Keith, A., 1907, Description of the Pisgah quadrangle (North Carolina-Tennessee): U.S. Geological Survey Geologic Atlas, Folio 147, 8 p.

King, P.B., 1955, A geologic cross section across the southern Appalachians, an outline of the geology in the segment in Tennessee, North Carolina, and South Carolina, *in* Russell, R.J., ed., Guides to southeastern geology: Geological Society of America Annual Meeting, p. 332-373.

Kish, S.A., 1983, A geochronological study of deformation and metamorphism in the Blue Ridge and Piedmont of the Carolinas [Ph.D. dissertation]: Chapel Hill, University of North Carolina, 220 p.

Kohn, M.J., 2001, Timing of arc accretion in the southern Appalachians: Perspectives from the Laurentian margin: Geological Society of America Abstracts with Programs, v. 33, p. 262.

Lemmon, R.E., 1973, Geology of the Bat Cave and Fruitland quadrangles and the origin of the Henderson Gneiss, western North Carolina [Ph.D. dissertation]: Chapel Hill, University of North Carolina, 145 p.

Lemmon, R.E., and Dunn, D.E., 1973a, Geologic map and mineral resources of the Bat Cave quadrangle, North Carolina: North Carolina Department of Natural Resources and Community Development GM 202-NE, scale 1:24,000.

Lemmon, R.E., and Dunn, D.E., 1973b, Geologic map and mineral resources of the Fruitland quadrangle, North Carolina: North Carolina Deparment of Natural Resources and Community Development GM-202-NW, scale 1:24,000.

Mapes, R.W., Maybin, A.H., III, Miller, C.F., Fullagar, P.D., and Bream, B.R., 2002, Geochronology and geochemistry of mid Paleozoic granitic magmatism, central and eastern Inner Piedmont, NC & SC: Geological Society of America Abstracts with Programs, v. 34, p. 92.

Maybin, A.H., III, 1997, Bedrock geologic map of the Pelham 7.5-minute quadrangle, Greenville, Laurens and Spartanburg Counties South Carolina: South Carolina Department of Natural Resources, Geological Survey, Open-File Report 93, scale 1:24,000.

Maybin, A.H., III, and Niewendorp, C.A., 1997, Whole-rock geochemical analysis of samples from Abbeville, Greenville, Greenwood, Laurens, Newberry, Saluda, Spartanburg and Union Counties, South Carolina: South Carolina Geological Survey OFR-98, 16 p.

McCulloch, M.T., and Wasserburg, G.J., 1978, Sm-Nd and Rb-

Sr chronology of continental crust formation: Science, v. 200, p. 1003-1011.

McSween, H.Y., Speer, J.A., and Fullagar, P.D., 1991, Plutonic rocks, *in* Horton, J.W., Jr., and Zullo, V.A., eds., The Geology of the Carolinas: Knoxville, Tennessee, The University of Tennessee Press, p. 109-126.

Miller, C.F., Hatcher, R.D., Jr., Ayers, J.C., Coath, C.D., and Harrison, T.M., 2000, Age and zircon inheritence of eastern Blue Ridge plutons, southwestern North Carolina and northeastern Georgia, with implications for magma history and evolution of the southern Appalachian orogen: American Journal of Science, v. 300, p. 142-172.

Mirante, D.C., 2001, Monazite ages from the southern Appalachian Inner Piedmont – The Athens gneiss: Geological Society of America Abstracts with Programs, v. 33, p. 3.

Mirante, D.C., and Patino-Douce, A.E., 2000, Melting and migmatization in the southern Appalachian Inner Piedmont of northeast Georgia; The Athens gneiss: Geological Society of America Abstracts with Programs, v. 32, p. 297.

Misra, K.C., and Keller, F.B., 1978, Ultramafic bodies in the southern Appalachians: A review: American Journal of Science, v. 278, p. 389-418.

Misra, K.C., and McSween, H.Y., Jr., 1984, Mafic rocks of the southern Appalachians: A review: American Journal of Science, v. 284, p. 294-318.

Mittwede, S.K., 1989, The Hammett Grove Meta-igneous Suite; A possible ophiolite in the northwestern South Carolina Inner Piedmont, *in* Mittwede, S.K., and Stoddard, E.F., eds., Ultramafic rocks of the Appalachian Piedmont: Boulder, Colorado, Geological Society of America Special Paper 231, p. 45-62.

Moecher, D.P., and Miller, C.F., 2000, Precise age for peak granulite facies metamorphism and melting in the eastern Blue Ridge from SHRIMP U-Pb analysis of zircon: Geological Society of America Abstracts with Programs, v. 32, p. 63.

Nelson, A.E., Horton, J.W., Jr., and Clarke, J.W., 1998, Geologic map of the Greenville 1˚ X 2˚ quadrangle, Georgia, South Carolina, and North Carolina: U.S. Geological Survey Miscellaneous Investigations Series Map I-2175, scale 1:250,000, 2 sheets, 12 p. text.

Odom, A.L., and Fullagar, P.D., 1973, Geochronological and tectonic relationships between the Inner Piedmont, Brevard zone, and Blue Ridge belts, North Carolina: American Journal of Science, v. 273, p. 133-149.

Odom, A.L., and Russell, G.S., 1975, The time of regional metamorphism of the Inner Piedmont, North Carolina, and Smith River allochthon: Inference from whole-rock ages: Geological Society of America Abstracts with Programs, v. 7, p. 522-523.

Osberg, P.H., Tull, J.F., Robinson, P., Hon, R., and Butler, J.R., 1989, The Acadian orogen, *in* Hatcher, R.D., Jr., Thomas, W.A., and Viele, G.W., eds., The Appalachian-Ouachita orogen in the United States: Boulder, Colorado, Geological Society of America, The Geology of North America, v. F-2, p. 179-232.

Overstreet, W.C., Whitlow, J.W., White, A.W., and Griffitts, W.R., 1963a, Geologic map of the southern part of the Casar quadrangle, Cleveland, Lincoln, and Burke Counties, North Carolina: U.S. Geological Survey Field Studies Map MF-252, scale 1:24,000.

Overstreet, W.D., Yates, R.G., Griffitts, W.R., 1963b, Geologic map of the Shelby 15-minute quadrangle, North Carolina: U.S. Geological Survey Miscellaneous Geologic Investigations Map I-384, scale 1:62,500.

Ownby, S.E., Miller, C.F., Berquist, P.J., Carrigan, C.W., and Fullagar, P.D., in review, Geochemistry and U-Pb geochronology of a portion of the Mars Hill terrane, North Carolina-Tennessee: Constraints on origin, history, and tectonic assembly, *in* Tollo, R.P., Corriveau, L., McLelland, J., and Bartholomew, M.J., eds., Proterozoic evolution of the Grenville orogen in North America: Boulder, Colorado, Geological Society of America Special Paper.

Powell, C.M., Jones, D.L., Pisarevsky, S., and Wingate, M.T.D., 2001, Paleomagnetic constraints on the position of the Kalahari craton in Rodinia: Precambrian Research, v. 110, p. 33-46.

Rankin, D.W., 1988, The Jefferson terrane of the Blue Ridge tectonic province: An exotic accretionary prism: Geological Society of America Abstracts with Programs, v. 20, p. 310.

Rankin, D.W., 1994, Continental margin of the eastern United States: Past and present, *in* Speed, R.C., ed., Phanerozoic Evolution of North American continent-ocean transitions: Boulder, Colorado, Geological Society of America, DNAG continent-ocean transect volume, p. 129-218.

Rankin, D.W., Espenshade, G.H., and Neuman, R.B., 1972, Geologic map of the west half of the Winston-Salem quadrangle, North Carolina, Virginia, and Tennessee: U.S. Geological Survey Miscellaneous Geologic Investigations Map I-709A, scale 1:250,000.

Rankin, D.W., Chiarenzelli, J.R., Drake, A.A., Jr., Goldsmith, R., Hall, L.M., Hinze, W.J., Isachsen, Y.W., Lidiak, E.G., McLelland, J., Mosher, S., Ratcliffe, N.M., Secor, D.T., Jr., and Whitney, P.R., 1989, Proterozoic rocks east and southeast of the Grenville front, *in* Reed, J.C., Jr., Bickford, M.E., Houston, R.S., Link, P.K., Rankin, D.W., Sims, P.K., and Van Schmus, W.R., eds., Precambrian: Conterminous U.S.: Boulder, Colorado, Geological Society of America, The geology of North America, v. C-2, p. 335-461.

Ranson, W.A., Williams, I.S., and Garihan, J.M., 1999, SHRIMP zircon U-Pb ages of granitoids from the Inner Piedmont of South Carolina: evidence for Ordovician magmatism involving Mid to Late Protereozoic crust: Geological Society of America Abstracts with Programs, v. 31, p. 167.

Reed, J.C., Jr., 1964, Geology of the Linville Falls quadrangle North Carolina: U.S. Geological Survey Bulletin 1161-B, 53 p.

Rogers, J.J.W., 1967, Chronology of tectonic movements in the Appalachian region of eastern North America: American Journal of Science, v. 265, p. 408-427.

Roper, P.J., and Dunn, D.E., 1973, Superposed deformation and polymetamorphism, Brevard zone, South Carolina: Geological Society of America Bulletin, v. 84, p. 3373-3386.

Samson, S.D., Hibbard, J.P., and Wortman, G.L., 1995, Nd isotopic evidence for juvenile crust in the Carolina terrane, southern Appalachians: Contributions to Mineralogy and Petrology, v. 121, p. 171-184.

Shufflebarger, T.E., 1961, Notes on relationships of Piedmont sedimentary rocks with emphasis on the Poor Mountain-Chauga River area, Oconee County, South Carolina: South Carolina Division of Geology, Geologic Notes, v. 5, p. 31-38.

Sinha, A.K., and Glover, L., III, 1978, U/Pb systematics of zircons during dynamic metamorphism: Contributions to Mineralogy and Petrology, v. 66, p. 305-310.

Sinha, A.K., Hund, E.A., and Hogan, J.P., 1989, Paleozoic accretionary history of the North American plate margin (central and southern Appalachians): Constraints from the age, origin, and distribution of granitic rocks, *in* Hillhouse, J., ed., Deep structure and past kinematics of accreted terranes: American Geophysical Union Monograph Series, p. 219-238.

Sloan, E., 1907, Catalogue of the mineral localities of South Carolina: South Carolina Geological Survey Bulletin, v. 2, 4th series, 505 p.

Steltenpohl, M.G., Heatherington, A.L., Mueller, P.A., 2002, Our current understanding of the Grenville event in the southernmost Appalachians, Pine Mountain Window, Alabama: Geological Society of America Abstracts with Programs, v. 33, p. 29.

Su, Q., Goldberg, S.A., and Fullagar, P.D., 1994, Precise U-Pb zircon ages of Neoproterozoic plutons in the southern Appalachian Blue Ridge and their implications for the initial rifting of Laurentia: Precambrian Research, v. 68, p. 81-95.

Tabor, J.R., unpublished, Geologic map of the Mill Spring quadrangle [unpublished mapping]: Knoxville, University of Tennessee, scale 1:24,000.

Thomas, C.W., 2001, Origins of mafic-ultramafic complexes of the eastern Blue Ridge province, southern Appalachians: Geochronological and geochemical constraints [M.S. thesis]: Nashville, Tennessee, Vanderbilt University, 154 p.

Thomas, C.W., Miller ,C.F., Fullagar, P.D., Meschter McDowell, S.M., Vinson, S.B., and Bream, B.R., 2001, Where is the arc? Discontinuities in the Taconian arc magmatism in the southern Appalachians: Geological Society of America Abstracts with Programs, v. 33, p. 262.

Unrug, R., Ausich, W.I., Bednarczyk, J., Cuffey, R.J., Mamaet, B.L., Palmes, S.L., and Unrug, S., 2000, Paleozoic age of the Walden Creek Group, Ocoee Supergroup, in the western Blue Ridge, southern Appalachians: Implications for evolution of the Appalachian margin of Laurentia: Geological Society of America Bulletin, v. 112, p. 982-996.

Vinson, S., 1999, Ion probe geochronology of granitoid gneisses of the Inner Piedmont, North Carolina and South Carolina [M.S. thesis]: Nashville, Tennessee, Vanderbilt University, 84 p.

Wagener, H.D., 1977, The granitic stone resources of South Carolina: Columbia, South Carolina Geological Survey, Mineral Resources Series 5, 65 p.

Warlick, C.M., Clendenin, C.W., and Castle, J.W., 2001, Geology of The Cliffs at Glassy development, southern Saluda 7.5-minute quadrangle, Greenville County, South Carolina, *in* Garihan, J.M., Ranson, W.A., and Clendenin, C.W., eds., Geology of the Inner Piedmont in the Caesars head and Table Rock state parks area, northwestern South Carolina: Carolina Geological Society annual field trip guidebook, p. 37-56.

Warner, R.D., Griffin, V.S., Steiner, J.C., Schmitt, R.A., and Bryan, J.G., 1989, Ultramafic chlorite-tremolite-olivine schists; Three bodies from the Inner Piedmont belt, South Carolina, *in* Mittwede, S.K., and Stoddard, E.F., eds., Ultramafic rocks of the Appalachian Piedmont: Boulder, Colorado, Geological Society of America Special Paper 231, p. 63-74.

Whisnant, J.S., 1975, Geology of the southeastern quarter of the Marion 15-minute quadrangle, North Carolina [M.S. thesis]: Chapel Hill, University of North Carolina, 50 p.

Whisnant, J.S., 1979, Geologic map of the SE 1/4 of the Marion quadrangle, North Carolina: North Carolina Geological Survey and Tennessee Valley Authority GM 210-SE, scale 1:24,000.

Williams, S.T., 2000, Structure, stratigraphy, and migmatization in the southwestern South Mountains, North Carolina [M.S. thesis]: Knoxville, Tennessee, University of Tennessee, 111 p.

Williams, H., and Hatcher, R.D., Jr., 1983, Suspect terranes: a new look at the Appalachian orogen, *in* Hatcher, R.D., Jr., Williams, H., and Zietz, I., eds., Contributions to the tectonics and geophysics of mountain chains: Geological Society of America Memoir 158, p. 33-54.

Yanagihara, G.M., 1993, Evolution of folds associated with D_2 and D_3 deformation and their relationship with shearing in a part of the Columbus Promontory, North Carolina, *in* Hatcher, R.D., Jr., and Davis, T.L., eds., Studies of Inner Piedmont Geology with a focus on the Columbus Promontory: Carolina Geological Society annual field trip guidebook, p. 45-65.

Yanagihara, G.M., 1994, Structure, stratigraphy, and metamorphism of a part of the Columbus Promontory, western Inner Piedmont, North Carolina [M.S. Thesis]: Knoxville, Tennessee, University of Tennessee, 214 p.

Yates, R.G., 1963, Preliminary geologic map of the northwest quarter of the Shelby quadrangle, Cleveland and Rutherford Counties, North Carolina: U.S. Geological Studies Map MF-258, scale 1:24,000.

Yates, R.G., and Overstreet, W.C., 1962, Preliminary geologic map of the northeast quarter of the Shelby quadrangle, Cleveland County, North Carolina: U.S. Geological Survey Field Studies Map MF-249, scale 1:24,000.

Inner Piedmont stratigraphy, metamorphism, and deformation in the Marion-South Mountains area, North Carolina

Sara E. Bier[a]
Brendan R. Bream
Scott D. Giorgis[b]
Department of Geological Sciences
University of Tennessee–Knoxville
306 Geological Sciences Building
Knoxville, TN 37996-1410

present addresses:
[a]*Department of Geosciences, Pennsylvania State University, University Park, PA 16802*
sbier@geosc.psu.edu
[b]*Department of Geology and Geophysics, University of Wisconsin–Madison, Madison, WI 53706*

ABSTRACT

The western Inner Piedmont stratigraphy consists of Cambrian (?) metagraywacke, aluminous schist, and amphibolite of the Tallulah Falls Formation overlain by Middle Ordovician Poor Mountain Amphibolite and Poor Mountain Quartzite. This sequence is intruded by Middle Ordovician plutons (e.g., Dysartsville Tonalite) and is in thrust contact with Early Ordovician Henderson Gneiss. The eastern Inner Piedmont in the South Mountains contains mappable biotite gneiss and sillimanite schist units (Silurian to Early Devonian?) intruded by Devonian Walker Top and Toluca Granites. Pressure and temperature estimates with structural, geochronologic, and petrologic data for the North Carolina Inner Piedmont confirm the polydeformed nature of this terrane and delimit the timing and conditions of Paleozoic metamorphism. Peak metamorphic conditions are coeval with post-penetrative deformation and appear to postdate major displacement on the Mill Spring fault. Pressures of 5.1 and 5.3 (± 1) kbar were estimated for two samples from the kyanite + staurolite and sillimanite domains, respectively. Temperature estimates for six other samples, using these pressures, range from 520 to 670 ˚C. Deformational fabrics and temperature estimates do not appear to be offset by major Inner Piedmont faults. Map relationships demonstrate that major displacement on the Mill spring fault postdates the ~465 Ma crystallization age of the Dysartsville Tonalite and that this displacement is pre- to syn-metamorphic peak. Metamorphic zircon and monazite growth, deformation fabrics, and crosscutting relationships indicate a single high-T peak metamorphic prograde event during the Neoacadian orogeny in this part of the Inner Piedmont. A portion of the North Carolina Inner Piedmont from the Brevard fault zone to the eastern

Bier, S.E., Bream, B.R., and Giorgis, S.D., 2002, Inner Piedmont stratigraphy, metamorphism, and deformation in the Marion-South Mountains area, North Carolina, *in* Hatcher, R.D., Jr., and Bream, B.R., eds., Inner Piedmont geology in the South Mountains-Blue Ridge Foothills and the southwestern Brushy Mountains, central-western North Carolina: North Carolina Geological Survey, Carolina Geological Society annual field trip guidebook, p. 65–99.

Inner Piedmont is divisible into three fault-bounded domains and enables construction of a deformational framework that includes at least five episodes of deformation. The easternmost domain is further subdivided into five structurally homogeneous subdomains. Foliation (S_2) reflects a regional change in strike from NE-SW in the western flank to N-S in the eastern Inner Piedmont back to NE-SW in the southeastern part of the domains. Lineations are aligned NE-SW (orogen parallel) in the western Inner Piedmont and E-W in the eastern Inner Piedmont and probably indicate transport direction. Rare D_1 intrafolial folds and foliation are attributed to the Taconic orogeny. D_2 foliation, lineations, tight to isoclinal, recumbent to reclined folds, sheath folds and Type-F thrust faults represent penetrative Neoacadian deformation. D_3 folds and Type-C thrust faults probably constitute the latter portion of ductile Neoacadian deformation. D_4 broad open folds formed during the Alleghanian orogeny. D_5 fractures are a result of Mesozoic uplift and extension. The structural data and map patterns presented here are best explained by crustal flow during oblique collision.

INTRODUCTION

Rocks found in the internal portions of mountain chains reveal details about deep crustal processes. Despite decades of study, many important aspects of Paleozoic orogenesis in the central and southern Appalachians are unresolved. In particular, the nature and timing of metamorphism and deformation in the southern Appalachian crystalline core remain poorly understood. This paper outlines the stratigraphy of North Carolina Inner Piedmont in the Marion and South Mountains area, summarizes preliminary P-T estimates, and presents a deformational framework that addresses the relative timing of regional structures. Documenting the metamorphic history of this part of the Appalachians and its relationship to the deformational history of the Inner Piedmont is a fundamental key to understanding southern Appalachian tectonics, Appalachian terrane accretion, and the process of medium- to high-grade Barrovian metamorphism.

The southern Appalachians have been divided into several lithotectonic units (Fig. 1). The Piedmont and Carolina terranes were accreted to Laurentia during Paleozoic orogenesis (Williams and Hatcher, 1983) and together comprise the southern Appalachian crystalline core. The Inner Piedmont is located between the eastern Blue Ridge and the Carolina terrane and extends from northern North Carolina to the Coastal Plain in Alabama. Rock types here are varied, multiply deformed, strongly migmatitic, and bear similarities to other high-grade gneiss terranes (e.g., Shuswaps and Scottish Grampians). The Inner Piedmont is characterized by middle to upper amphibolite facies mineral assemblages and contains some of the most intensely deformed and metamorphosed rocks in the Appalachians. Regardless of the largely migmatitic and polydeformed nature of this terrane, the relationships between primary lithostratigraphic sequences, granitoids, and other rock types are only partially obscured. The Inner Piedmont has been interpreted as a mélange complex (Goldsmith et al., 1988; Horton et al., 1989), part of the larger Piedmont terrane (Williams and Hatcher 1983) or Tugaloo and Cartoogechaye terranes (Hatcher et al., 1999; Hatcher, 2001), and an accreted exotic terrane (Dennis, 1991; Rankin, 1994; Dennis and Wright, 1997). It has generally been accepted that accretion of the Tugaloo terrane to Laurentia occurred during Ordovician Taconian orogenesis (e.g., Hatcher, 1989; Horton et al., 1989). The timing of peak deformation and metamorphism within the Inner Piedmont, however, remains equivocal (e.g., Tull, 1980; Dallmeyer, 1988; Horton et al., 1989; Osberg et al., 1989; Hibbard, 2000). Only a small portion (~15%) of the Inner Piedmont has been mapped and studied in detail due to the complex nature of the terrane and the common misconception that this region lacks exposure and a recognizable stratigraphy. Our recent detailed mapping (1:12,000- and 1:24,000-scales) with accompanying structural analysis and geothermobarometric estimates define a mappable stratigraphy, key structures, and minimum peak metamorphic conditions for the study area.

GEOLOGIC SETTING

The Inner Piedmont consists of a stack of west- to southwest-vergent plastic thrust sheets rooted on the southeast flank of the belt. Transposition of earlier fabrics and map patterns reveal that penetrative deformation occurred at, or near, peak metamorphism with later superposition of brittle deformation and retrograde metamorphism. Mapping has identified the presence of a mostly orogen-parallel paragneiss sequence (Tallulah Falls/Ashe and Poor Mountain Formations) that is repeated in several thrust sheets across strike to the southeast. The area of recent detailed mapping is divisible into three fault-defined lithotectonic packages (Fig. 2). Each of the thrust sheets contains a portion of the western Inner Piedmont paragneiss stratigraphy

Figure 1. Tectonic map of the southern Appalachians modified from Hatcher et al. (1990) and Bream et al. (in review). cBR-central Blue Ridge; Ct-Carolina terrane; Dgb-Dahlonega gold belt; eBR-eastern Blue Ridge; eIP-central and eastern Inner Piedmont; Mb-Milton belt; PMb-Pine Mountain block; SMw-Sauratown Mountains window; SRa-Smith River Allochthon; V&R-Valley and Ridge; wBR-western Blue Ridge; wIP-western Inner Piedmont.

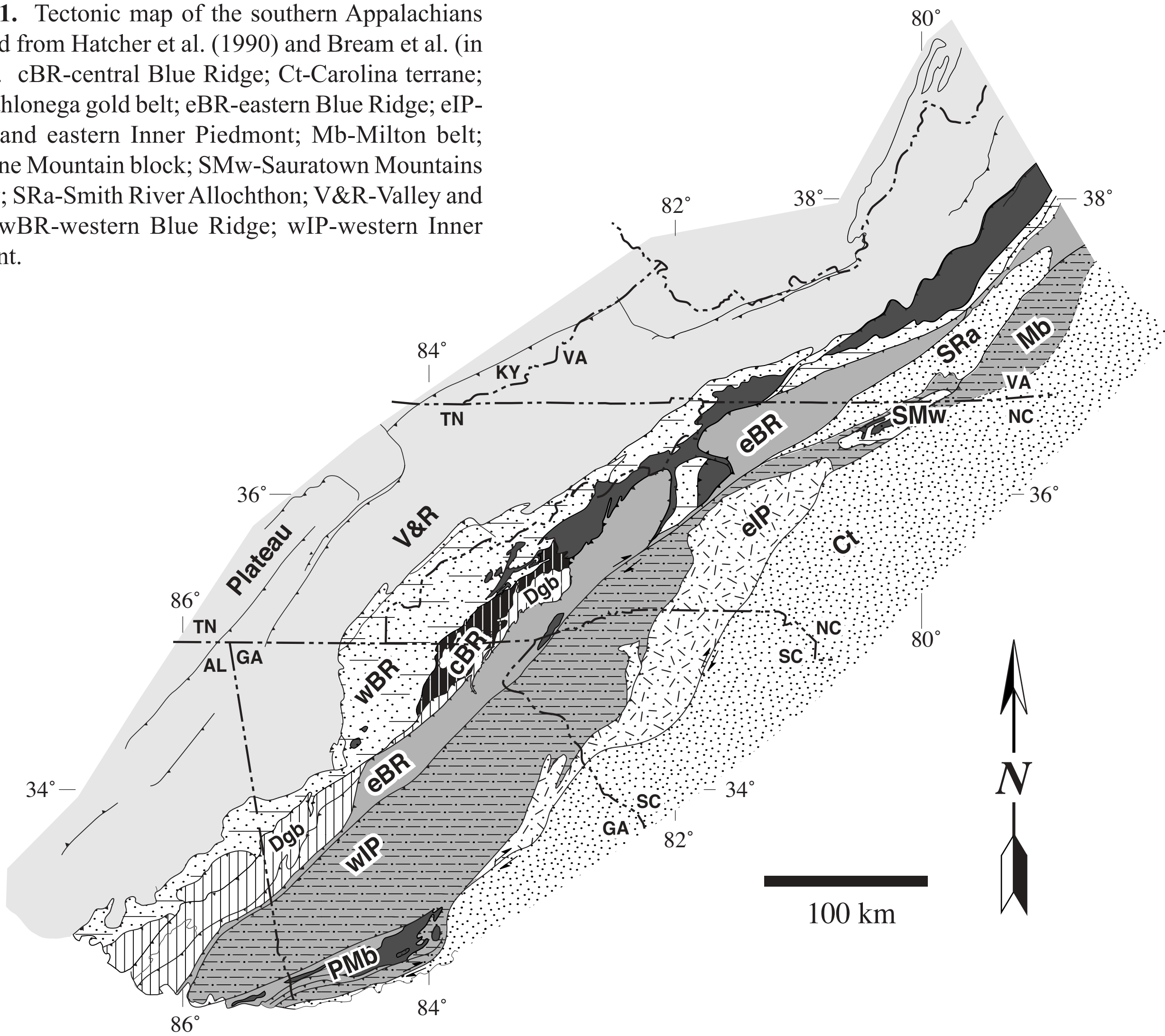

except for the Tumblebug Creek thrust sheet, which contains only the Henderson Gneiss, and the Brindle Creek thrust, which thrusts a younger paragneiss sequence over the western Inner Piedmont.

Metapsammite and metapelite paragneisses of the western Inner Piedmont are generally considered to have a Late Proterozoic to Cambrian age (Hatcher, 1969, 1987; Drake et al. 1989); the eastern Inner Piedmont paragneiss sequence which is dominated by metapelite with lesser metapsammite was likely deposited from the Silurian to Early Devonian (Bream et al., 2001, in review). Amphibole gneiss, amphibolite, quartzite, calc-silicate, and ultramafic rocks are also present. The quartzofeldspathic gneiss and aluminous schist portions of the western Inner Piedmont stratigraphy are interpreted to share a similar provenance to that of the eastern Blue Ridge Tallulah Falls/Ashe Formations over which they are thrust (Hatcher 1987). The finely laminated amphibolite and quartzite units are correlative with the South Carolina western Inner Piedmont Poor Mountain Formation of Hatcher (1969). Continuous portions of this stratigraphy occur parallel to and across strike from just southwest of the Sauratown Mountains window in North Carolina to Alabama. Numerous regional summaries (e.g., Griffin, 1974; Osberg et al., 1989; Butler, 1991; Hatcher and Goldberg, 1991) have identified the kyanite-sillimanite isograd that places migmatitic sillimanite-grade assemblages over kyanite-grade assemblages on the western flank of the Inner Piedmont. These prograde assemblages are overprinted within the Brevard fault zone by Alleghanian lower greenschist facies retrograde metamorphism (Reed and Bryant, 1964).

ROCK UNITS

Much of the Inner Piedmont has not been studied in detail partially because of a historical misconception that it contains an indecipherable high grade assemblage of gneiss, schist, migmatite, amphibolite, and granitoid (King, 1955), and a mappable stratigraphy is therefore not present. As in most high-grade gneiss terranes (Passchier et al., 1990), rocks of the Inner Piedmont *are* both lithologically and deformationally complex. A cursory look at this belt con-

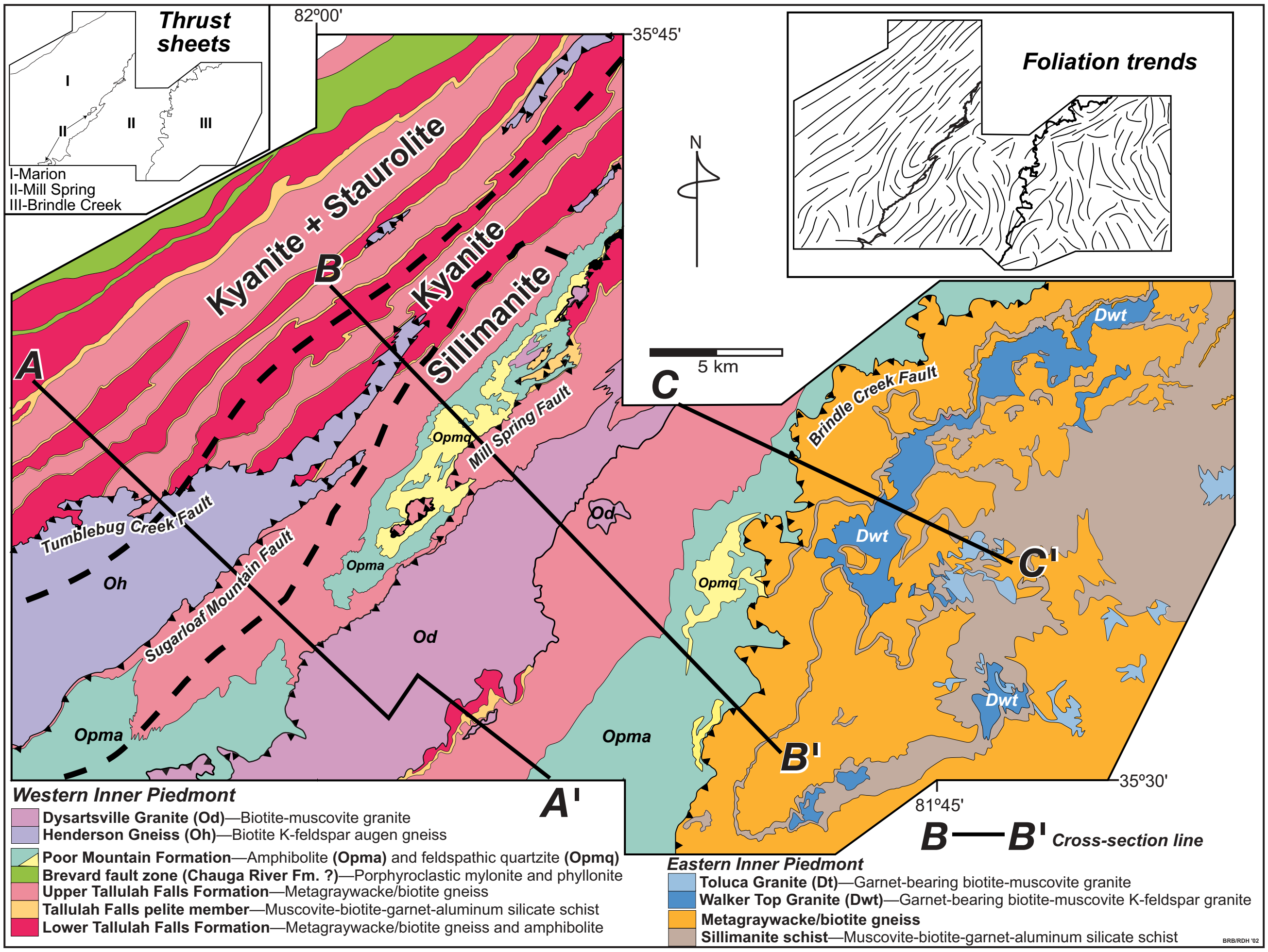

Figure 2. Geologic map of the Marion-South Mountains area. Compiled from detailed mapping of Whisnant (1975), Yanagihara (1994), Bream (1999), Giorgis (1999), Hill (1999), Williams (2000), and Bier (2001). Cross sections are in Figure 28.

firms the earlier misconception. Davis (1993), however, provided the first clues that the stratigraphic sequence in the Columbus Promontory of southwestern North Carolina is the same as that in the western Inner Piedmont and eastern Blue Ridge of South Carolina and northeastern Georgia (Hopson and Hatcher, 1988). New work by Hill (1999) and Bream (1999) reviewed during the 2002 CGS field trip has confirmed that the Tallulah Falls and Poor Mountain Formations stratigraphy does indeed exist between the Brindle Creek and pre-Alleghanian Brevard fault in the South Mountains and that it is readily mappable at the 1:12,000 and 1:24,000 scales employed for detailed mapping (Fig. 3).

Research by Giorgis (1999), Williams (2000), and Bier (2001) east of the Brindle Creek fault initially suggested Tallulah Falls Formation stratigraphy is present there as well but with large thickness changes in the aluminous schist member and the intervening metagraywacke. Detrital and igneous ion microprobe zircon studies (e.g., Mapes, 2002; Bream, this guidebook); however, indicate the paragneiss sequence east of the Brindle Creek fault may be as young as Early Devonian, whereas sequences west of the Brindle Creek fault are Middle Ordovician and older. Additionally, detailed and reconnaissance mapping (where available) has not delineated an eastern Inner Piedmont equivalent to the western Inner Piedmont Poor Mountain Formation. New stratigraphic and geochronologic data have thus resulted in delineation of a previously unrecognized terrane of younger rocks within the Inner Piedmont. The assemblage represented here may be analogous to the Siluro-Devonian sequence in the Merrimack synclinorium and Bronson Hill anticlinorium in the New England Appalachians.

Western Inner Piedmont

Rock types present in the western Inner Piedmont near Marion, North Carolina, include quartzofeldspathic biotite gneiss, amphibole gneiss, amphibolite, quartzite, metatuff, pelitic and aluminous schist, calc-silicate, and ultramafic rocks. Protoliths for this assemblage consist of immature quartzofeldspathic psammite and pelite overlain by metabasalt and feldspathic sandstone interlayered with felsic tuff(?).

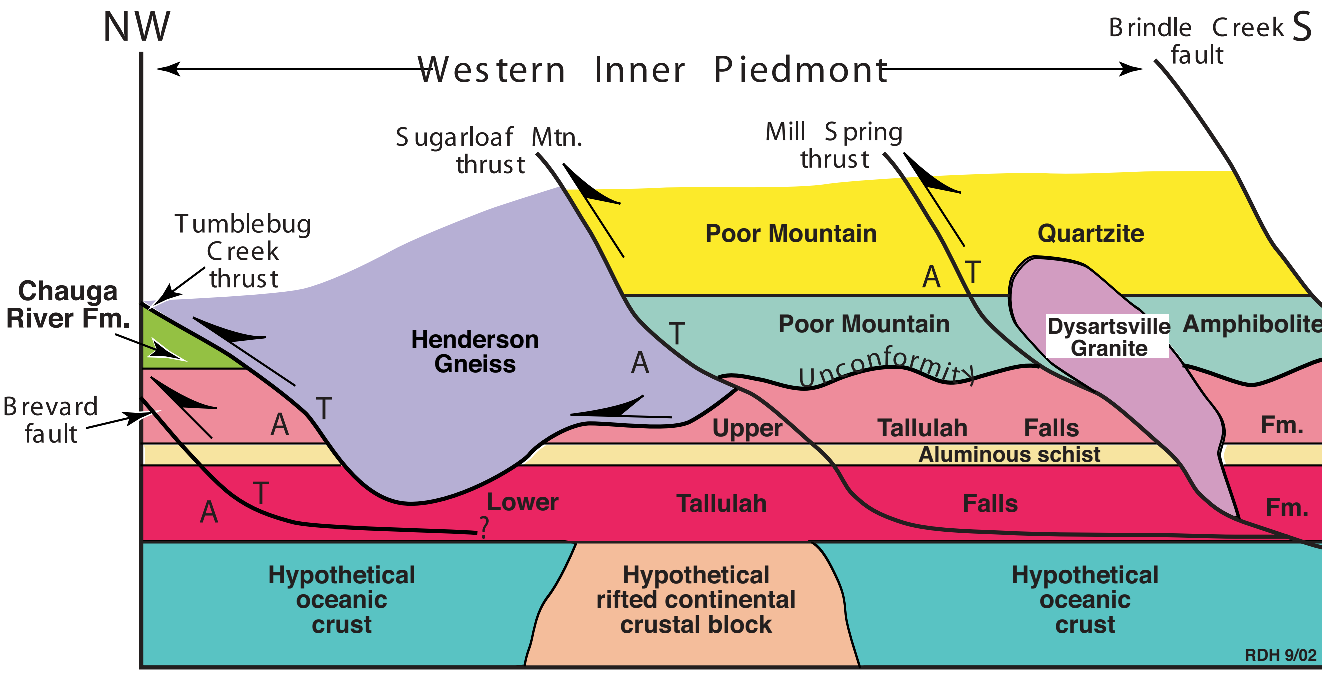

Figure 3. Western Inner Piedmont generalized stratigraphy with major faults. T-toward; A-away.

Granitic and mafic orthogneisses later intruded this assemblage. Hatcher (1978, 1987, 1989), Hopson and Hatcher (1988), Davis (1993), Bream (1999), and Hill (1999) correlated the western Inner Piedmont stratigraphy with the Tallulah Falls Formation in the eastern Blue Ridge. In this area, the main body of Henderson Gneiss truncates all units of the Tallulah Falls Formation, and the contact is faulted (see Hatcher, this guidebook, his Fig. 4). The amphibolite-quartzite-metatuff (?) units are correlative with the Poor Mountain Amphibolite and Quartzite. See Bream (this guidebook) for a more detailed discussion of correlative map units in the North and South Carolina western Inner Piedmont.

Tallulah Falls Formation. In the Marion area, Tallulah Falls Formation occurs in each thrust sheet west of the Brindle Creek fault, except for the Tumblebug Creek thrust sheet that carries only Henderson Gneiss. A thin aluminous schist unit divides the formation within the study area. Mapped subdivisions (Fig. 2) are the result of careful identification of the aluminous schist and relative abundance of amphibolite/amphibole gneiss in the metagraywacke-biotite gneisses of the upper and lower Tallulah Falls Formation. Tallulah Falls amphibolite and amphibole gneiss occur as pods, layers, and boudins within the lower and upper metagraywacke-biotite gneisses. Compositional layering is commonly parallel to the dominant foliation. It was also noted by Davis (1993), Yanagihara (1994), and Hill (1999) that the lower Tallulah Falls Formation is more migmatitic than the upper Tallulah Falls Formation. Bream (1999) noted, however, that both units are partially migmatitic and the metagraywacke-biotite gneiss of the upper Tallulah Falls appears more migmatitic than that of the lower Tallulah Falls. This is attributed mostly to the absence of the lower Tallulah Falls in the higher-grade thrust sheets above the Tumblebug Creek fault in the Marion area. Isoclinal folding in the lowest thrust sheet repeats the entire formation several times. The sillimanite isograd occurs at and immediately west of the Mill Spring thrust in the Marion area (Fig. 2).

Upper and lower Tallulah Falls metagraywacke-biotite gneiss and two-mica schist. The lower Tallulah Falls Formation is a light- to dark-gray metagraywacke-biotite gneiss and two-mica schist unit that contains more amphibolite and amphibole gneiss than the upper Tallulah Falls graywacke-biotite gneiss unit (Fig. 4). Where mica content is high, the lithology is coarser grained and schistose. Modal analyses reveal that metagraywacke-bioite gneiss contains: 26-46 percent quartz, 28-46 percent plagioclase (An_{25-35}), 15-30 percent biotite, and 1-7 percent muscovite. Minor constituents present include epidote, microcline, chlorite, and opaque minerals. Trace zircon and sphene are also present. Quartz commonly exhibits high-angle grain boundaries, indicating complete recrystallization. Brown biotite is variably replaced by green biotite in thin sections. Metagraywacke is frequently porphyroclastic with 0.5- to 3-cm composite quartz and white or milky microcline or plagioclase grains. Porphyroclastic texture is present in both metagraywacke units and does not appear to be gradational or limited to the lower unit, as suggested by Davis (1993). Foliation is defined by parallel alignment of quartzofeldspathic material and micas in the metagraywacke and by biotite and muscovite in schist. Modal compositions of

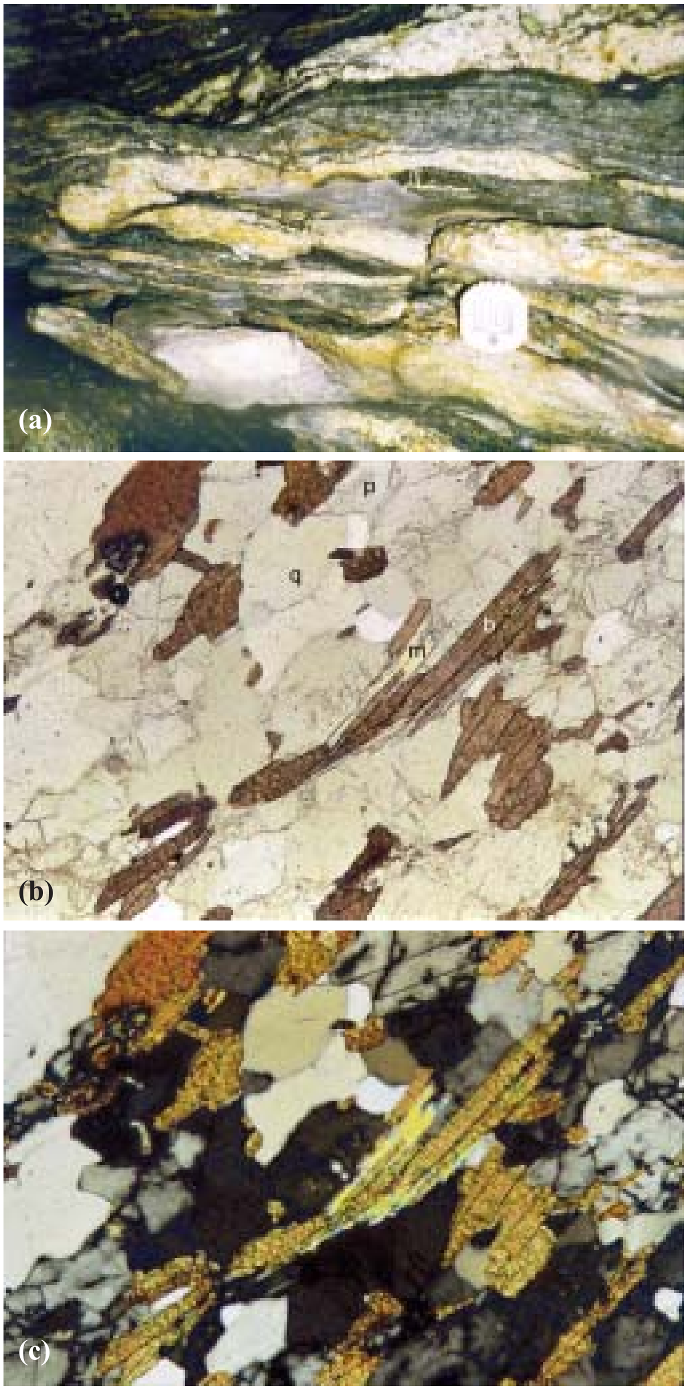

Figure 4. Photograph and photomicrographs of Tallulah Falls Formation. (a) photograph of upper Tallulah Falls Formation migmatitic bioite gneiss east of Pogue Mountain in the Glenwood 7.5-minute quadrangle. (b) Plane light photomicrograph of upper Tallulah Falls Formation from the Glenwood 7.5-minute quadrangle just south of Chestnut Mountain near the Tallulah Falls/Poor Mountain contact. Thin section was cut perpendicular to foliation and parallel to lineation. Abbreviations are as follows: q-quartz, p-plagioclase, b-biotite, m-muscovite. (c) Cross-polarized photomicrograph of same area in Figure 4b thin section. Width of field for (b) and (c) is 1.7 mm.

all metagraywackes plot as graywackes or arkoses using the modified Pettijohn (1949) sandstone classification (Fig. 6). Layer thicknesses vary from a few millimeters to several meters.

Tallulah Falls aluminous schist. The presence of kyanite or sillimanite in this unit is the principal characteristic used to separate it from the much thicker metagraywacke-biotite gneiss units that lie above and below it. Fresh aluminous schist is silver or light- to dark-gray whereas saprolite is tan or reddish-purple. Because of the garnetiferous nature of this unit, it is frequently mapped based on the abundance of garnet "gravel" especially along trails and dirt roads or in fields (Fig. 6). Aluminous schist modal analyses exhibit wide variation in dominant minerals: 7-40 percent quartz, 4-30 percent plagioclase, 3-46 percent muscovite, 0-22 percent biotite, and 8-16 percent garnet. Garnets range from less than 0.5 cm to over 2 cm in diameter, are subhedral, and contain numerous inclusions. Large subhedral and euhedral kyanite, up to one cm, is often present in the aluminous schist. Fibrolitic sillimanite makes up approximately 15 percent of a thin section of a sample collected above the Mill Spring thrust (Fig. 6). The aluminous schist is typically no more than 80 m thick, although thickness varies locally. The relative increase in outcrop width of the most northwesterly aluminous schist is probably related to the shallow dip produced by later folding. Individual schist layers can be traced from terminations against the main body of Henderson Gneiss through the Marion West and Marion East quadrangles and beyond (Bream, 1999; Hill, 1999) (Fig. 2).

Previous work in the Sugar Hill quadrangle by Whisnant (1975) and in the Marion West quadrangle by Conley and Drummond (1981) conservatively projected the aluminous schist unit as a series of disconnected lenses. This is partially related to the weathering characteristics of the aluminous schist that make it difficult to identify where dirt roads, undeveloped trails, or farmland are not present. Where the aluminous schist unit is identifiable, it can usually be followed or projected along strike to other outcrops. Tabor (1990), Davis (1993), and Yanagihara (1994) did not delineate the aluminous schist as a separate map unit in the Columbus Promontory, which allowed the Tallulah Falls Formation to be divided approximately only into upper (amphibolite-poor) and lower (amphibolite-rich) units. A single aluminous schist layer was noted by Whisnant (1975), who stated that the "lenses" are indistinguishable except where kyanite blades occur that are longer than 1 cm. We have been able to trace kyanite-bearing aluminous schist where size of kyanite is much smaller and sillimanite-bearing aluminous schist where sillimanite is identifiable only with a hand lens. The key to tracing this unit is first the location of abundant garnet accumulations on the surface or in saprolite, and then searching for the diagnostic aluminum silicate mineral.

Tallulah Falls-Poor Mountain Contact. Yanagihara (1994) noted that the contact between the upper Tallulah Falls Formation and Poor Mountain Amphibolite is sharp with lim-

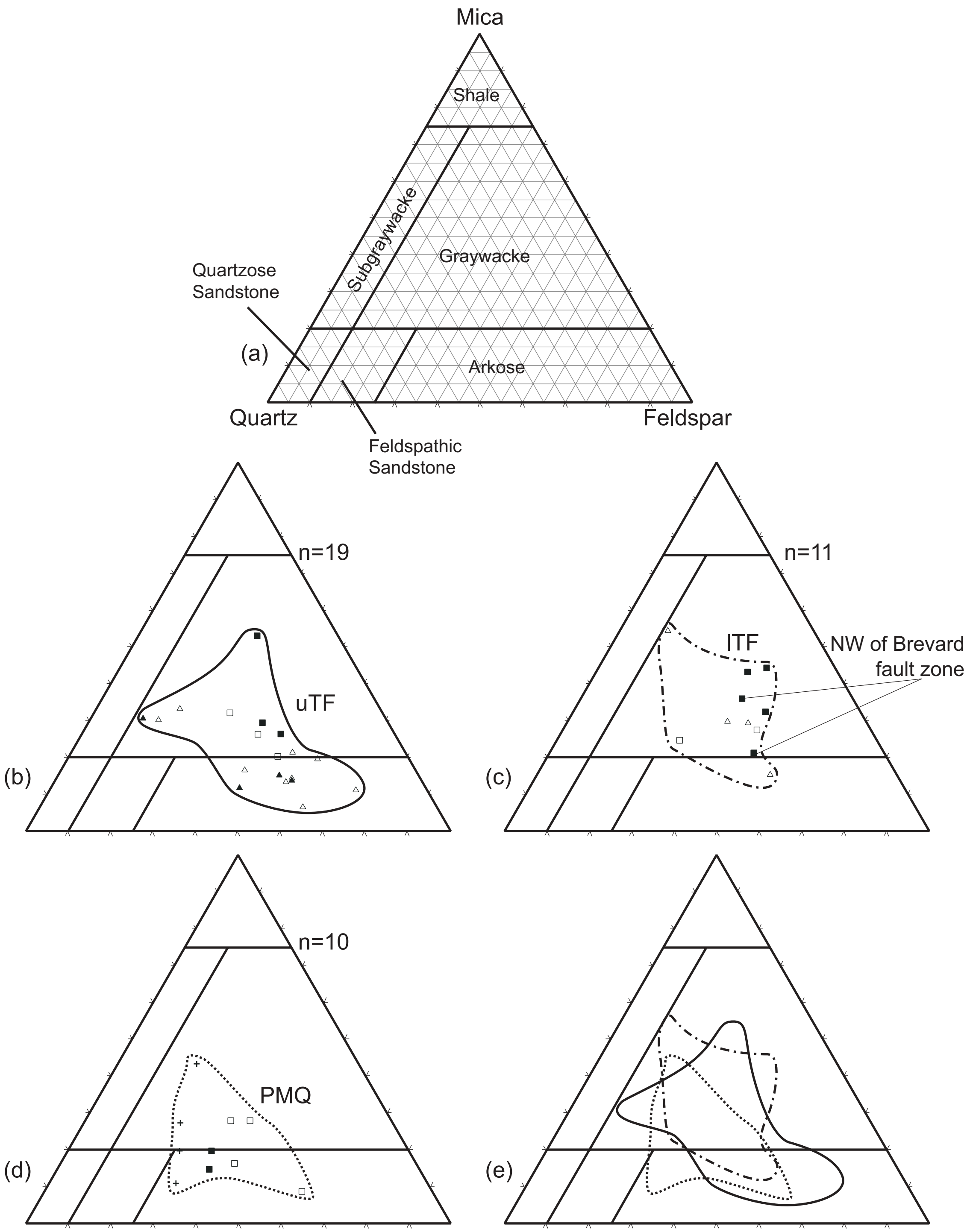

Figure 5. Quartz-feldspar-mica ternary diagram comparing the composition of the upper Tallulah Falls Formation, lower Tallulah Falls Formation, and Poor Mountain Quartzite. Filled triangles are data from Lemmon (1973), open triangles are data from Davis (1993), addition symbols are data from Yanagihara (1994), filled boxes are data from Hill (1999), and open boxes are from Bream (1999). (a) Modified sandstone classification from Pettijohn (1949). (b) uTF-upper Tallulah Falls Formation. (c) lTF-lower Tallulah Falls Formation. (d) PMQ-Poor Mountain Quartzite. (e) Composite field diagram of b, c, and d.

ited interlayering. This contact remains sharp and is well exposed on Second Broad River just south of Spooky Hollow Road immediately west of U.S. 221 in the Glenwood 7 1/2-minute quadrangle (STOP 4, this guidebook). Based on the Second Broad River exposure, distinct lithologic differences, lack of evidence for faulting, and limited interlaying, this contact is best explained as an unconformity.

Muscovite schist occurs along the exposed Tallulah Falls-Poor Mountain Formation contact in the Second Broad River. It is coarser grained than muscovite-rich Poor Mountain Quartzite. Figure 7 is a photomicrograph of the thin section made from the contact unit. There is limited exposure of this unit and its extent along strike is unknown. Some interlayers of this material are also present in the basal Poor

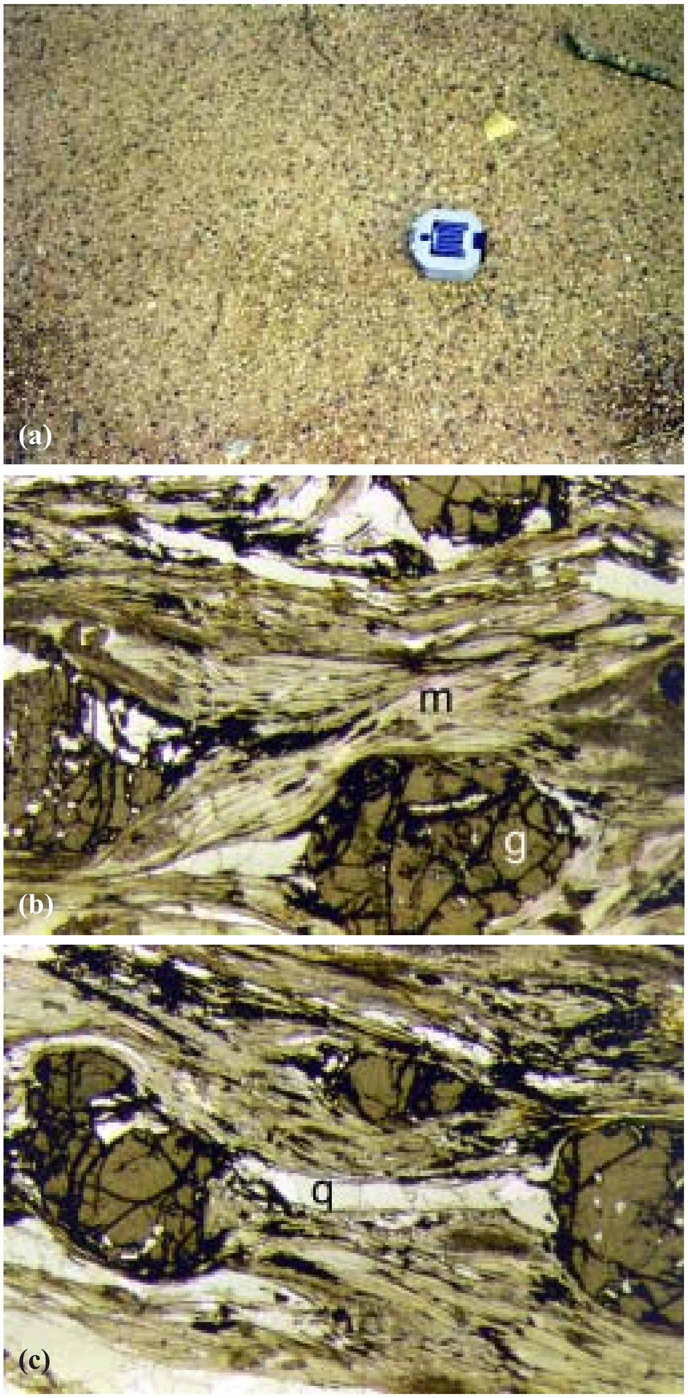

Figure 6. Photograph and photomicrographs of Tallulah Falls Formation garnet-mica schist. (a) Phtograph of garnet float near a recently developed housing site north of Goose Creek Road in the Marion West 7.5-minute quadrangle. (b) and (c) Plane light photomicrographs of a garnet-mica schist sample thin section. Abbreviations are as follows: m-muscovite, g-garnet, q-quartz. (d) and (e) Crossed polarized photomicrographs of the same sample. Width of field for all photomicrographs is 11.1 mm. The thin section sample is from the Sugar Hill 7.5-minute quadrangle south of Goose Creek Road and east of Lewis Mountain.

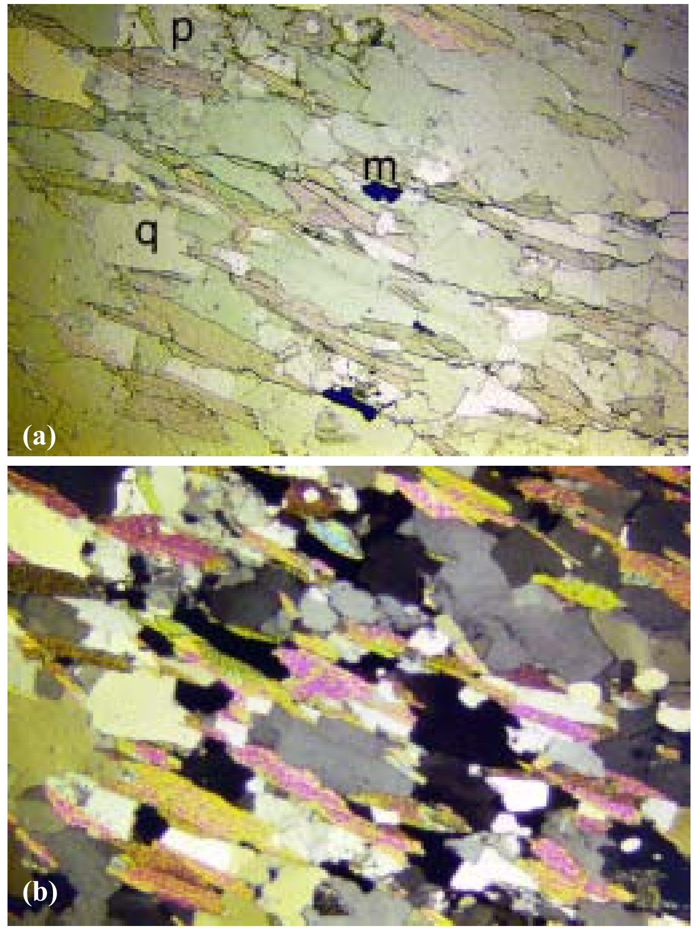

Figure 7. Photomicrographs of the unit at the contact between the upper Tallulah Falls Formation and the Poor Mountain Amphibolite. The sample is from the exposure in the Second Broad River south of Spooky Hollow Road in the Glenwood 7.5-minute quadrangle. (a) Plane light photomicrograph. Width of field is 4.25 mm. Abbreviations are as follows: p-plagioclase, m-muscovite, q-quartz. (b) Crossed polarized photomicrograph of same are as shown in (a).

Mountain Amphibolite that is also exposed just above the contact. The unit was sampled stratigraphically above and attached to porphyroclastic upper Tallulah Falls Formation. This unit is white to gray and weathers to light and dark tans. A modal analysis of the single thin section showed the following proportions: 38 percent plagioclase (An_{24}), 33 percent muscovite, and 24 percent quartz. Clinozoisite, sphene, and opaques are each present at less than 0.1 percent. Based on the mineralogy it is more likely that this unit represents the uppermost part of the Tallulah Falls Formation than the basal part of the Poor Mountain Formation or that it is a lens of Brevard-Poor Mountain transitional unit, which would further support the interpretation of this contact as an unconformity.

Poor Mountain Formation. The uppermost stratigraphic unit recognized to date in the western Inner Piedmont near Marion is correlative with the Poor Mountain sequence, first described by Sloan (1907) northwest of Walhalla, South Carolina. Shufflebarger (1961) first subdivided the Poor Mountain sequence into amphibolite and quartzite/marble units. Hatcher (1969, 1970) correlated the Poor Mountain rocks with the Chauga River Formation in northwestern

South Carolina, redefined the Poor Mountain sequence as a formation (adding the lower Brevard-Poor Mountain transitional member), and attributed lithologic differences between the Chauga River and Poor Mountain Formations to facies changes. The transitional member has been recognized with certainty only from the Chauga belt in South Carolina to the Columbus Promontory of North Carolina. New geochronologic data (Bream, this guidebook) indicate the Poor Mountain and Chauga River Formations are not correlative, as Hatcher previously indicated, and the Chauga River Formation is older than the Poor Mountain Formation but probably still younger than the Tallulah Falls Formation. See Hatcher (this guidebook, his Figs. 5, 6, and 7) for a revision of stratigraphic relationships based on a combination of Bream's geochronologic data and field relationships from the Marion, North Carolina, area to northeastern Georgia. Critical to this revision is Bream's (1999) recognition of the possible unconformable relationship between the Poor Mountain Formation and the rocks that occur beneath it at different places from northeast to southwest.

Lemmon (1973) observed that the amphibolite and hornblende gneiss on Chimney Rock in the Columbus Promontory is interlayered with feldspathic quartzite and muscovite schist. He also suggested that the amphibolite-hornblende gneiss unit thickens and undergoes a facies change southwestward from Chimney Rock in North Carolina. This relationship and a higher quartzofeldspathic granofels unit were described by Whisnant (1975) to the northeast in the Sugar Hill quadrangle. Based on relationships directly observed in the Glenwood quadrangle and the work of Yanagihara (1994) in the Sugar Hill quadrangle, the quartzofeldspathic granofels unit of Whisnant (1975) may actually be two units: Poor Mountain Quartzite and Dysartsville Tonalite. The contact between Dysartsville Tonalite and the Poor Mountain Formation rocks is interpreted as a fault most likely correlative with the Mill Spring fault of Davis (1993) and Yanagihara (1994). Whisnant (1975) also noted the presence of what appeared to be detrital garnets in his quartzofeldspathic granofels. Garnets with a detrital appearance were noted in the Poor Mountain Quartzite; only trace relict garnets, however, have been observed in Dysartsville Tonalite.

The Poor Mountain Formation is preserved in synclines in the eastern parts of the Sugarloaf Mountain and Mill Spring thrust sheets (Fig. 2). It comprises one of the most distinct rock units in the Marion area and consists of a basal amphibolite-rich (>70% amphibolite) unit that grades upward into a quartz-rich unit (>70% quartz + feldspar). The Poor Mountain Formation also contains layers of pelitic schist, metagraywacke, and granitoid gneiss (metatuff?). The Poor Mountain Formation in the Marion area lacks the basal garnet mica schist metasiltstone unit mapped by Lemmon (1973) and Davis (1993) and correlated with the Brevard-Poor Mountain transitional unit of Hatcher (1970). Poor Mountain Amphibolite here rests directly on upper Tallulah Falls Formation. In the Marion area, the Poor Mountain Formation is divisible into two mappable units, the basal amphibolite and amphibolite gneiss (Poor Mountain Amphibolite) that grades upward into feldspathic quartzite and metatuff (Poor Mountain Quartzite) (Bream, 1999; Hill, 1999).

Preliminary geochronologic data (Kalbas et al., 2002; Bream, unpublished data), based on ion microprobe analyses of zircons interpreted to have an igneous origin, reveal that a metatuff (?) component in the Poor Mountain Quartzite from the Glenwood 7 1/2-minute quadrangle has an age of ~460 Ma. A similar U-Pb age was obtained on zircon cores from an intensely migmatitic sample, interpreted by Kalbas (in preparation) to have a major protolith component of Poor Mountain Formation, from the Vulcan Materials Company Lenoir Quarry (STOP 12) (Kalbas et al., 2002; Bream, unpublished data). The Middle Ordovician age of the Poor Mountain Formation also favors interpretation of the contact with the underlying Tallulah Falls Formation rocks as an unconformity.

Poor Mountain Amphibolite. Nonmigmatitic Poor Mountain Amphibolite is predominantly fine-laminated amphibolite and lesser amounts of thin to thick bands of amphibole gneiss interlayered with feldspathic quartzite near the contact (Fig. 8). Mineral lineations of the Poor Mountain Amphibolite is defined by parallel alignment of elongate hornblende grains. Layering in the laminated amphibolite varies from a few mm to approximately 30 cm thick. The interlayering in the laminated amphibolite and feldspathic quartzite is interpreted as a primary sedimentary/volcanic feature of the Poor Mountain Formation, although transposition doubtlessly played a role here. Equivalents to this unit in the Columbus Promontory and in the Chauga belt of South Carolina are described as gray to black fine- to medium-grained amphibolite and amphibole gneiss interlayered with quartzite-marble-metatuff (?) (Hatcher, 1970; Davis, 1993; Yanagihara, 1994).

In the Marion area, the laminated amphibolite is mostly fine grained and rarely contains mesoscopic folding. This unit is dark- to medium-gray and weathers to an ochre-colored saprolite. Thin sections of laminated amphibolite from the Sugarloaf Mountain thrust sheet contain: 48-65 percent hornblende, 5-45 percent plagioclase (An_{25-32}), 0-28 percent epidote/clinozoisite, and 0-6 percent quartz. Trace and accessory minerals include biotite, sphene, zircon, and opaque minerals. Epidote and clinozoisite are found mostly in quartzofeldspathic layers, as products of either hydrous alteration or the prograde metamorphic reactions involving originally calcareous components with quartz. Recrystallized quartz occurs in the laminated amphibolite but is more common in the amphibole gneiss and quartzite

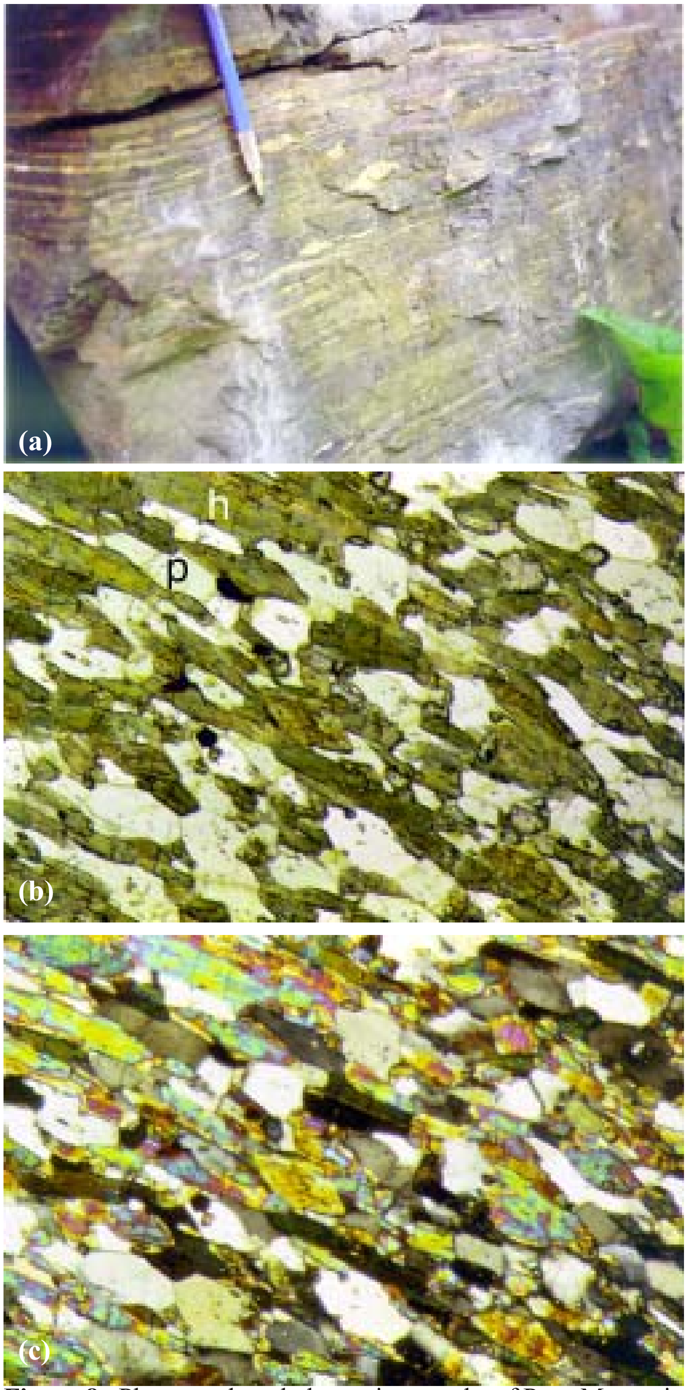

Figure 8. Photograph and photomicrographs of Poor Mountain Amphibolite. (a) Photograph of typical Poor Mountain Amphibolite outcrop along U.S. 221. (b) Plane light photomicrograph of a Poor Mountain Amphibolite sample from the Glenwood 7.5-minute quadrangle. Abbreviations are as follows: p-plagioclase, h-hornblende. (c) Crossed polarized photomicrograph of the same area in thin section as shown in (b). Width of field for (b) and (c) is 1.7 mm.

layers. The hornblende is prismatic and has strong green pleochroism. Nematoblastic and sometimes poikiloblastic textures are found in this unit.

Chemical analyses of nonmigmatitic Poor Mountain Amphibolite agree well with the geochemical results of Davis (1993) and Yanagihara (1994) who interpreted it as metamorphosed tholeiitic normal mid-oceanic basalt (N–MORB). Tectonic discriminant diagrams containing all of the available geochemical data for nonmigmatitic Poor Mountain Amphibolite are summarized by Hatcher (this guidebook, his Figs. 5, 6, and 7). Previous and current detailed geologic mapping, similarity and order of the stratigraphic sequence, and bulk chemical analyses confirm the occurrence of this unit throughout the western Inner Piedmont in the Carolinas and northeastern Georgia. The bulk chemistry and normative mineralogy of the Poor Mountain Amphibolite samples from this study show that the unit contains 45-52 percent SiO_2 and is mostly olivine-normative. The primary goal in the presentation of the chemical data is to show the strong agreement between samples collected as part of this study and those collected southwest of the study area. Amphibolites and amphibole gneisses of the Tallulah Falls Formation and Dysartsville Tonalite from the study area are plotted on all figures for comparison. Niggli *mg*-*c*-(*al-alk*) plots (Fig.9) of nonmigmatitic Poor Mountain Amphibolite samples define a trend that is at a high-angle to the proposed sedimentary trend of Leake (1964). This trend favors an igneous origin for the unit. The samples also indicate a tholeiitic source (Figs. 10 and 11) based on the fields of Irvine and Baragar (1971). The tectonomagmatic discriminant diagrams of Shervais (1982) and Meschede (1986) reconfirm the dominant mid-oceanic ridge basalt (MORB) chemistry of most samples. Based on this data set and plots on other tectonic discriminant diagrams (see Hatcher, this guidebook, his Figs. 5, 6, and 7) Poor Mountain Amphibolite most likely developed in an oceanic setting, possibly in an extensive deep-water basin along the Laurentian margin as suggested by Davis (1993). Presence of marble and clean quartzite farther southwest in South Carolina (Shufflebarger, 1961; Hatcher, 1969) remain difficult to explain if parts of the Poor Mountain Formation accumulated in deep water.

Migmatitic Poor Mountain Amphibolite (and Quartzite) occurs in synclines in the southeastern part of the exposed Mill Spring thrust sheet (immediate Brindle Creek footwall) in the South Mountains (Giorgis, 1999; Williams, 2000). Migmatization and metamorphic differentiation exploited the felsic layers in the amphibolite to enhance the layered character of the amphibolite, producing layered (stromatic) migmatite (STOP 9, this guidebook). Migmatization is sufficiently intense in places that layering is totally disrupted and only blocks of amphibolite remain in a more uniform matrix of totally homogenized granodioritic neosome-forming agmatite (Williams, 2000) (STOP 7, this guidebook). Similar relationships are present in the same structural position in the southwestern Brushy Mountains (Merschat and Kalbas, this guidebook).

Poor Mountain Quartzite. Poor Mountain Quartzite in the Marion area consists of massive to layered feldspathic micaceous quartzite and metatuff (Fig. 12) interlayered near

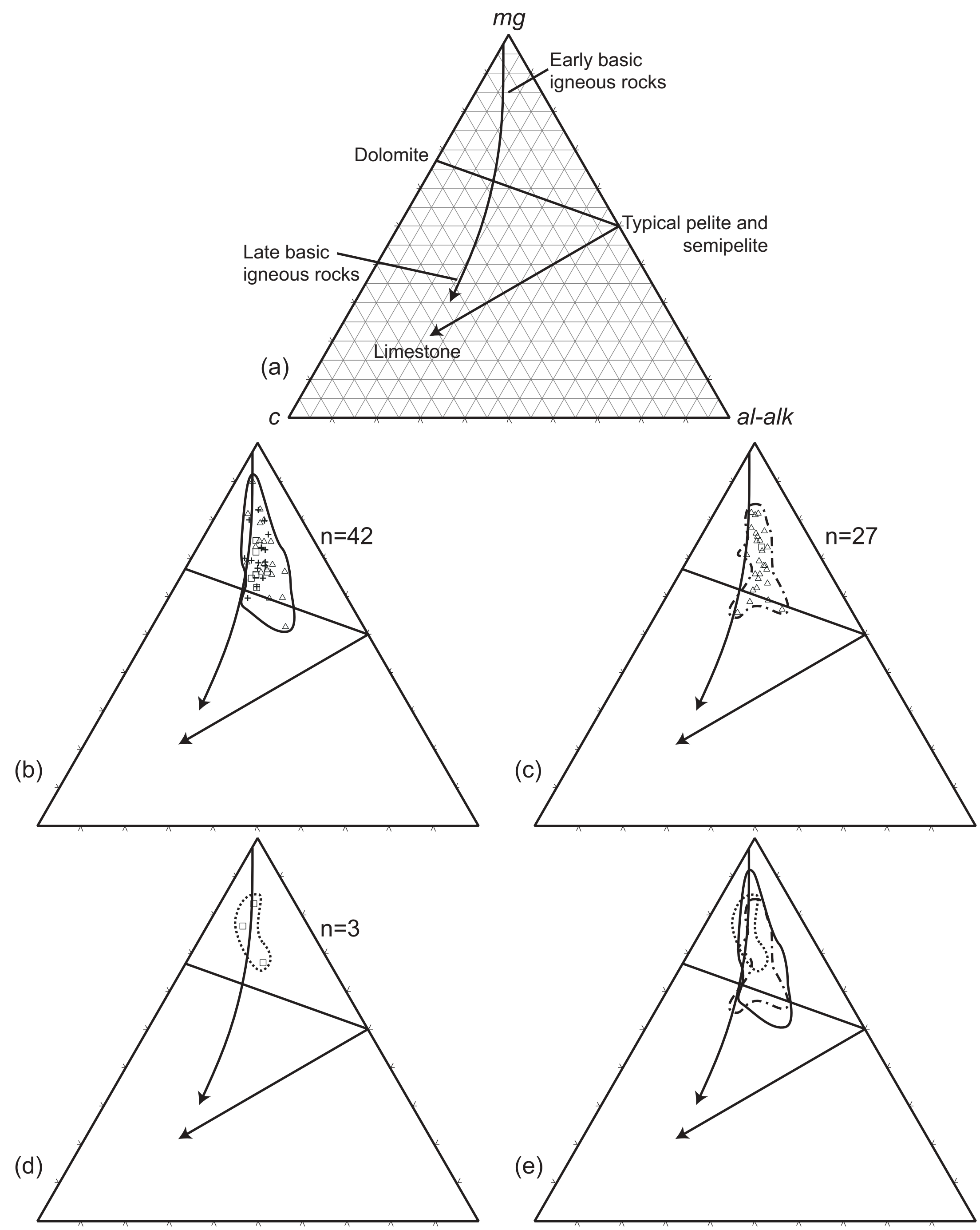

Figure 9. Ortho- and para-amphibolite discriminant diagram comparing amphibolites and amphibole gneisses of the Poor Mountain Formation, Tallulah Falls Formation, and Dysartsville Tonalite. Open triangles are data from Davis (1993), addition signs are data from Yanagihara (1994), and open boxes are data from Bream (1999). (a) *mg, c, al-alk* ternary diagram with igneous and sedimentary trends of Leake (1964). $mg = 100*(MgO/(FeO + MnO + 2Fe_2O_3))$; $c = CaO$; $al\text{-}alk = Al_2O_3\text{-}(K_2O + Na_2O)$, all in weight percent. Note that FeO and Fe_2O_3 were calculated assuming $Fe^{3+}/Fe^{2+} = 0.1$. (b) Poor Mountain Amphibolite. (c) Tallulah Falls Formation amphibolite and amphibole gneiss. (d) Dysartsville Tonalite amphibolite and amphibole gneiss. (e) composite field diagram of b, c, and d.

its base with laminated amphibolite. Layering in Poor Mountain Quartzite is considerably thicker (up to several m) than that in Poor Mountain Amphibolite. Parallel alignment of micas in Poor Mountain Quartzite defines a foliation and less commonly a lineation. Muscovite-rich outcrops of Poor Mountain Quartzite may be strongly schistose. Protolith of the quartzite component is graywacke or arkose (Fig. 5). The Poor Mountain Quartzite is white to light tan to light gray. Modal analyses of quartzite from the Marion area contain 30-60 percent plagioclase (An_{25-30}), 30-43 percent quartz, 0-20 percent biotite, 0-8 percent muscovite, 0-5 percent chlorite, and 0-2 percent microcline.

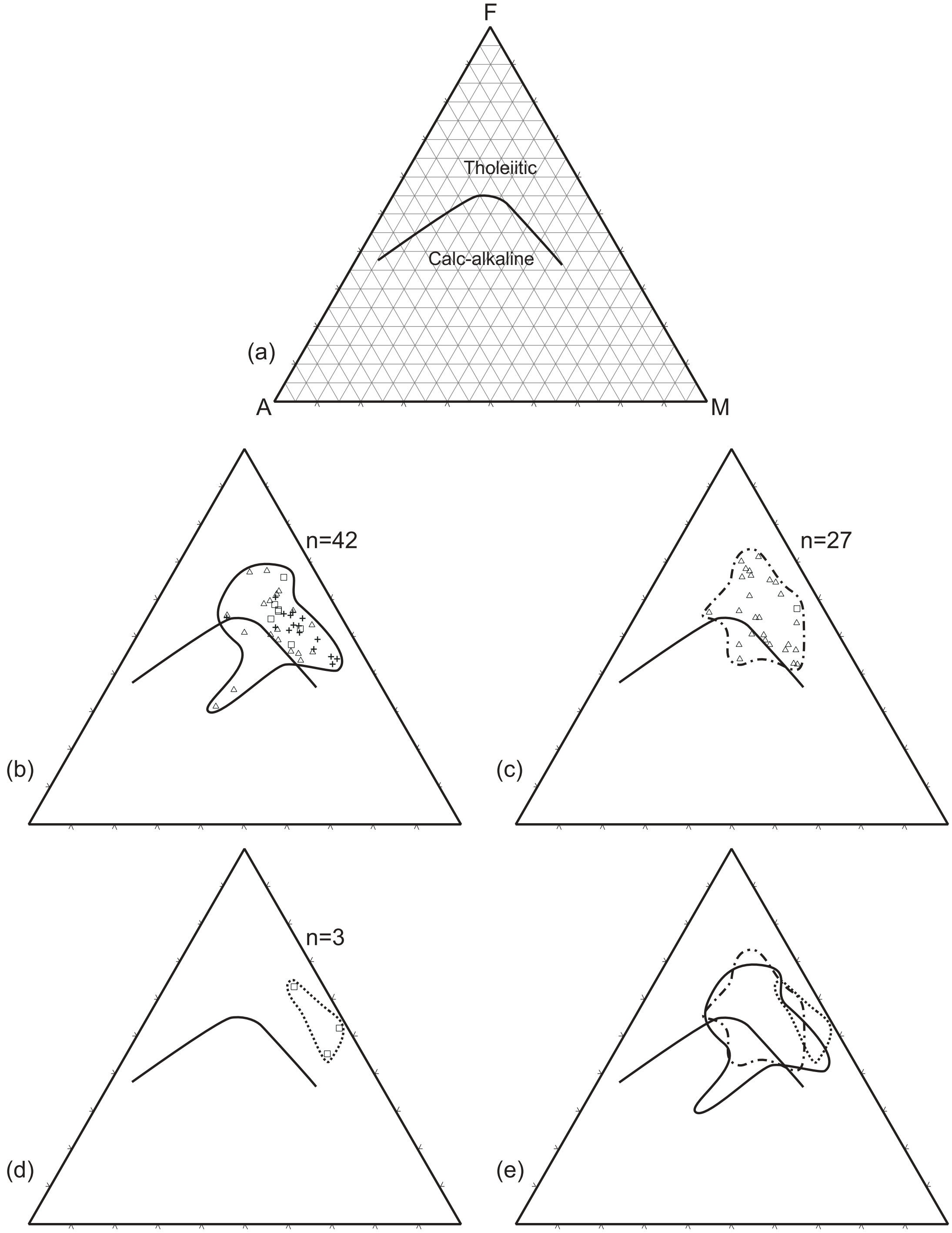

Figure 10. AFM diagram comparing amphibolites and amphibole gneisses of the Poor Mountain Formation, Tallulah Falls Formation, and Dysartsville Tonalite. Open triangles are data from Davis (1993), addition signs are data from Yanagihara (1994), and open boxes are data from Bream (1999). (a) AFM ternary diagram with the tholeiitic and calc-alkaline fields of Irvine and Baragar (1971). A = $Na_2O + K_2O$; F = $FeO + 0.8998\ Fe_2O_3$; M = MgO, all in weight percent. Note that FeO and Fe_2O_3 were calculated assuming $Fe^{3+}/Fe^{2+} = 0.1$. (b) Poor Mountain Amphibolite. (c) Tallulah Falls Formation amphibolite and amphibole gneiss. (d) Dysartsville Tonalite amphibolite and amphibole gneiss. (e) Composite field diagram of b, c, and d.

Accessory minerals include garnet, epidote/clinozoisite, and opaque minerals. As first noted by Yanagihara (1994), two generations of muscovite appear in thin section. The first is most likely synmetamorphic and the second is probably retrograde as indicated by the random orientation of the coarser-grained set.

Ordovician Granitoids. Two granitoids were mapped in the Marion area: the Dysartsville Tonalite and the Henderson Gneiss (Fig. 2). The structural relationship of the Henderson Gneiss to the Tallulah Falls Formation in the footwall of the Tumblebug Creek fault had previously not been mapped in the same detail or in the context provided by the

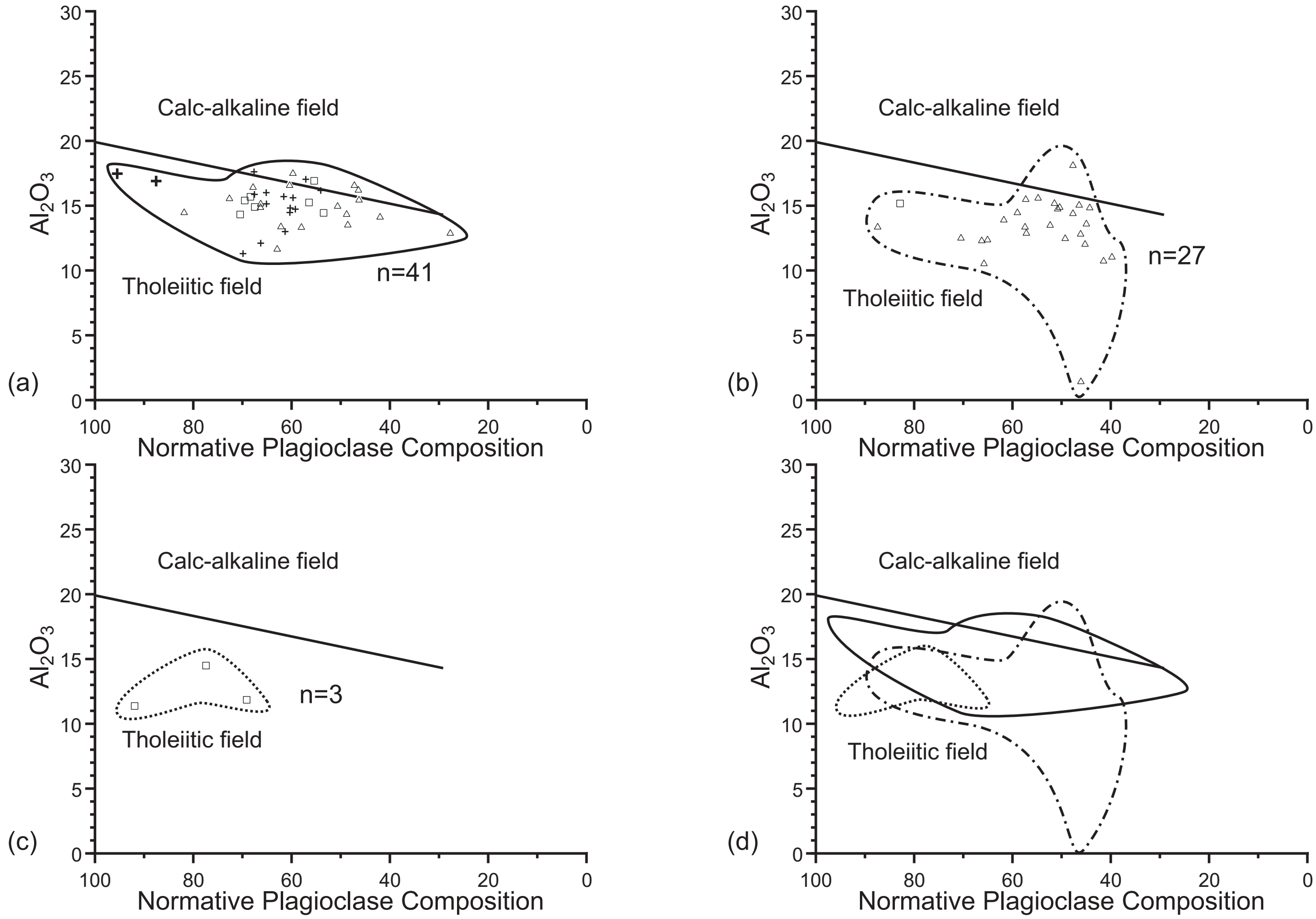

Figure 11. Plots of wt % Al_2O_3 versus normative plagioclase composition (P = 100*An/(An + Ab)) comparing amphibolites and amphibole gneisses of the Poor Mountain Formation, Tallulah Falls Formation, and Dysartsville Tonalite. The dividing line for the calc-alkaline and tholeiitic fields is from Irvine and Baragar (1971). All samples were plotted regardless of the MgO + CaO value. Open triangles are data from Davis (1993), addition symbols are data from Yanagihara (1994), and open boxes are data from Bream (1999). (a) Poor Mountain Amphbolite. (b) Tallulah Falls Formation amphibolite and amphibole gneiss. (c) Dysartsville Tonalite amphibolite and amphibole gneiss. (d) Composite field diagram of a, b, and c.

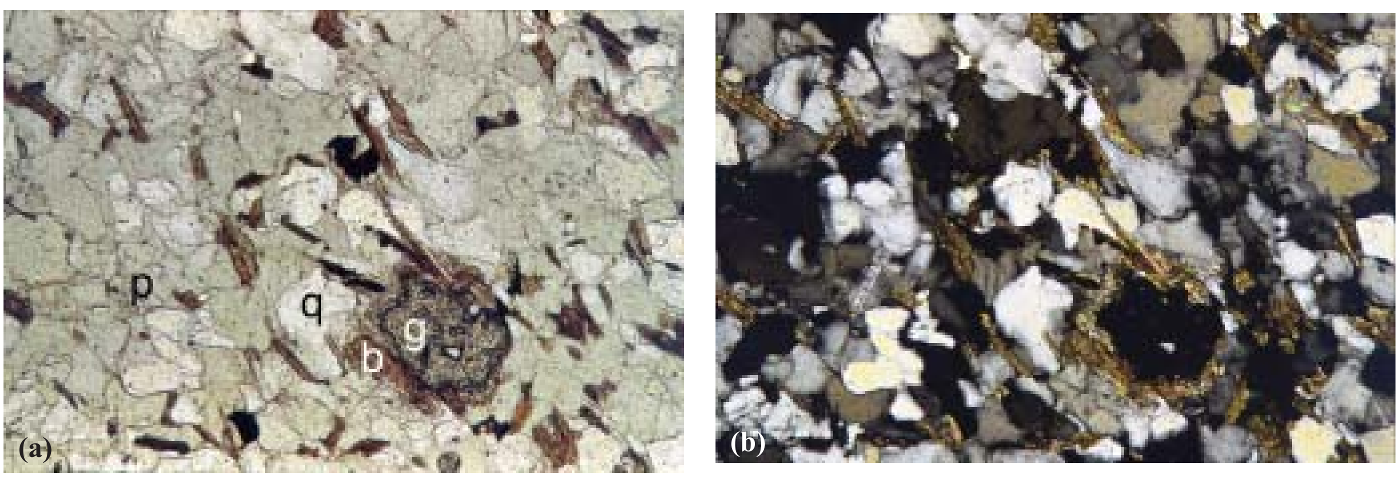

Figure 12. Photomicrograph of Poor Mountain Quartzite. The sample is from the Glenwood quadrangle in the Huntsville Branch of Stanfords Creek and is cut perpendicular to foliation and parallel to lineation. (a) Plane light photomicrograph. Note the rounded (detrital?) appearance of the garnet grain. Width of field is 1.7 mm. Abbreviations are as follows: g-garnet, q-quartz, p-plagioclase, b-biotite, m-muscovite. (b) Photomicrograph with polarizers crossed of the same area in thin section. Width of field is 1.7 mm.

western Inner Piedmont stratigraphy. Although not as extensive as the Henderson Gneiss, the Dysartsville Tonalite is significant both stratigraphically and structurally. Williams (2000) investigated the southeast contact of the Dysartsville Tonalite in the Glenwood 7 1/2-minute quadrangle. The contact of the Dysartsville Tonalite with the underlying Poor Mountain Amphibolite in the Sugar Hill quadrangle is the approximate contact between the "migmatitic" and "paragneiss and schist" units, respectively, of Hadley and Nelson (1971). Farther southwest in the Columbus Promontory the "migmatitic" unit of Hadley and Nelson (1971) also includes the lower part of the Tallulah Falls Formation. The two mappable granitoids are markedly dissimilar despite similar map patterns in the Marion area. The Henderson Gneiss is noted for its large feldspar augen, mostly microcline, and its unique augen texture. The Dysartsville Tonalite contains only trace amounts of microcline and is fine to medium grained.

Chemical analyses of the two units show that the Dysartsville Tonalite contains much less K_2O (0.65-1.71%) than other Inner Piedmont granitoids. Bulk chemical data from the Sugarloaf Mountain gneiss (Lemmon, 1973), the 438 Ma intrusive granitic gneiss (Lemmon, 1973), the Henderson Gneiss (Lemmon, 1973; Yanagihara, 1994; Bream, 1999), and the Devonian Walker Top Granite (Giorgis, this guidebook) have K_2O values ranging from 3.0 percent to 6.3 percent. Another difference found in the Dysartsville Tonalite is the much higher SiO_2 content (up to 82%). In addition to field observations during detailed mapping, the major element discriminant diagram of Werner (1987) further suggests that these units have igneous protoliths (Fig. 13). Sinha *et al.* (1989) divided southern and central Appalachian plutons into five age groups based primarily on geochronologic criteria: Late Proterozoic to Early Cambrian, Late Cambrian to Early Ordovician, Middle to Late Ordovician, Silurian-Devonian, and Permian-Carboniferous. The Henderson Gneiss was included in the Late Cambrian to Early Ordovician group based on a 509 Ma whole rock Rb-Sr age and despite older U-Pb ages (Sinha and Glover, 1978). Based on new ion microprobe U-Pb zircon analyses, the Henderson has an age of ~470 Ma (Vinson, 1999; Vinson and Miller, 1999). Modally and chemically the Dysartsville Tonalite is most similar to the granitoids in the Late Cambrian to Early Ordovician group or those in the Silurian-Devonian group. We now know, however, that the Dysartsville Tonalite has a Middle Ordovician ~465 Ma high resolution ion microprobe age (Bream, unpublished data).

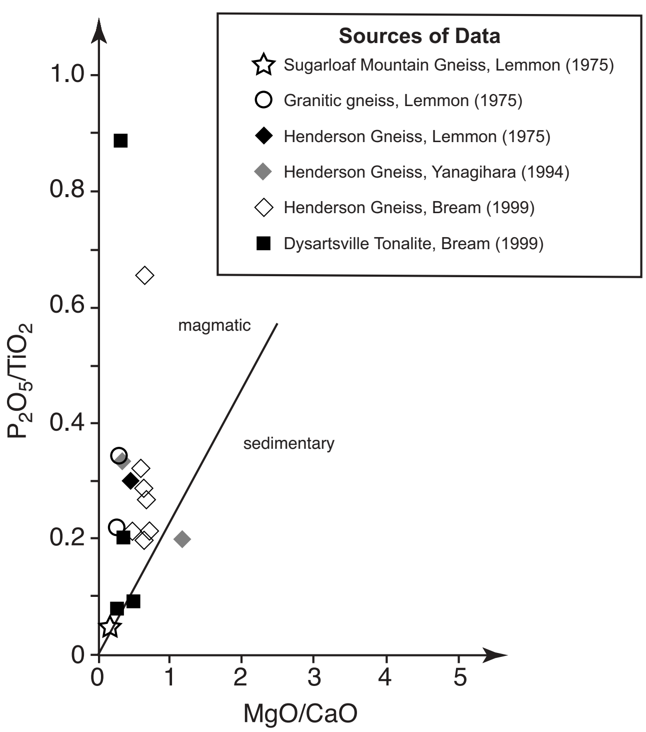

Figure 13. Major element discrimination diagram for distinguishing ortho- and paragneisses in metamorphic terranes. Plotted samples are from the western Inner Piedmont. Diagram after Werner (1987).

Dysartsville Tonalite. Structurally, this unit occurs within the highest thrust sheet of the Marion area and is in contact only with the Tallulah Falls Formation. The type area for the Dysartsville Tonalite is located in the Glenwood 7 1/2-minute quadrangle roughly parallel to Vein Mountain Road with excellent road exposures on U.S. 221 and in the CSX railroad cuts near and through Vein Mountain and Fero (all within the Glenwood 7 1/2-minute quadrangle). Goldsmith et al. (1988) mapped the Dysartsville Tonalite in the Charlotte 1° x 2° sheet as granitoid gneiss (termed the Dysartsville pluton on the tectonic map) and indicated the unit continues along strike to the northeast. Horton and McConnell (1991) compiled an exaggerated version of this unit and also used the Dysartsville pluton label. Adjacent to and southwest of the Marion area, Yanagihara (1994) noted that the upper Mill Spring complex contains abundant granitoid gneiss that is complexly folded with biotite gneiss, amphibolite, and minor pelitic schist and quartzite. Yanagihara (1994) mapped this as undifferentiated upper Mill Spring complex in the Sugar Hill and Shingle Hollow quadrangles southwest of Bream's (1999) mapping. The Dysartsville Tonalite mapped by Bream (1999) is probably related to Yanagihara's granitoid gneiss and is so depicted in our regional compilations. As previously noted, the quartzofeldspathic granofels unit of Whisnant (1975) in the Sugar Hill quadrangle has been separated into two units, one being Dysartsville Tonalite in the southeast corner of the quadrangle.

Dysartsville Tonalite is massive to foliated, fine to medium grained, and leucocratic (Fig. 14). Several amphibolite bodies, one containing an altered ultramafic body, have been mapped in the Dysartsville Tonalite (Bream, 1999; Williams, 2000). Smaller lenses and layers of amphibolite are also present but are not mappable. The Dysartsville Tonalite is locally called "blue granite." Limited gold production has been associated with veins and placer deposits in and near the body. Several small tourist gold panning camps and a larger failed gold mine are located in the Dysartsville Tonalite near Vein Mountain in the Glenwood quadrangle. The Dysartsville Tonalite plots as tona-

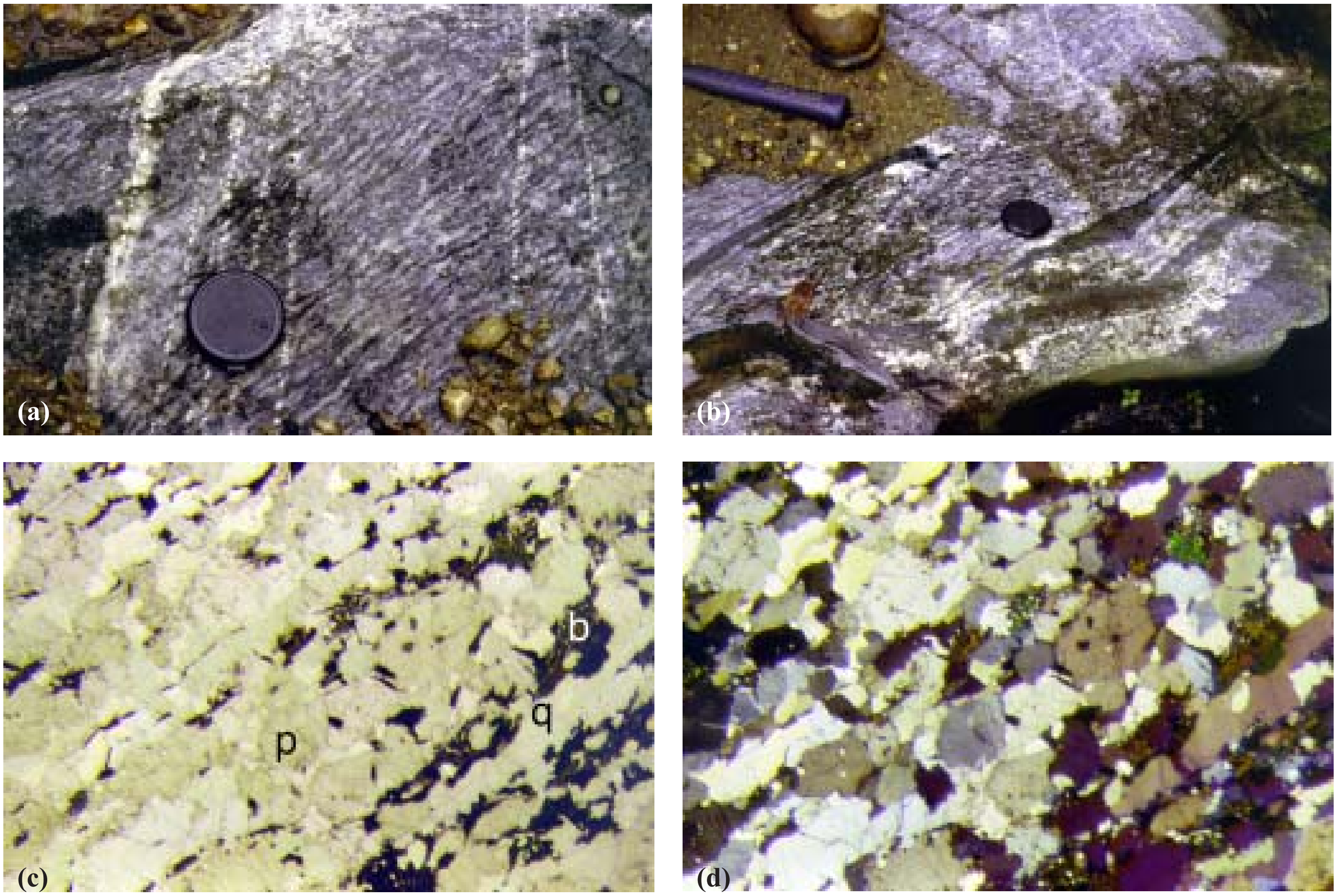

Figure 14. Photographs and photomicrographs of the Dysartsville Tonalite. (a) and (b) Typical outcrops of Dysartsville Tonalite. Photographs were taken north of Vein Mountain Road in South Muddy Creek. Note the amphibolite layers in (b). (c) Plane light photomicrograph of a Dysartsville Tonalite thin section. Abbreviations are as follows: b-biotite, p-plagioclase, q-quartz. Width of field is 11.1 mm. (d) Photomicrograph with polarizers crossed. Width of field is 11.1 mm. The sample is from the Glenwood quadrangle along U.S. 221 west of Wolf Mountain.

lite on the IUGS igneous classification of Streckeisen (1976) and mostly as a tonalite in the normative Ab-Or-An diagram (Fig. 15) of Barker (1979). Normative corundum for the Dysartsville Tonalite is high, from 1.14 to 3.15 percent, and the $K_2O/(K_2O + Na_2O)$ ratios are low, ranging from 0.16 to 0.30. The modal composition of Dysartsville Tonalite is: 40-55 percent plagioclase (An_{20-25}), 30-43 percent quartz, 4-15 percent biotite, and 0-10 percent muscovite. Muscovite, where it is abundant, is coarse-bladed and overgrown by biotite. Biotite is present as subhedral and euhedral pleochroic grains from 0.1 to 1 cm long that define the foliation. Epidote is colorless, commonly present as aggregates, and often forms bands with biotite and other accessory minerals along the foliation. Common accessory minerals are magnetite, pyrite, sphene, zircon, apatite, and allanite. Outcrops of this unit typically contain both granoblastic and lepidoblastic textures, often in the same outcrop.

Henderson Gneiss. The Henderson Gneiss has an outcrop area of ~5,000 km^2 in the North and South Carolina Inner Piedmont. Usually in locations where the Henderson Gneiss is widest in outcrop, it forms spectacular cliffs such as those in the Columbus Promontory at Chimney Rock. Henderson Gneiss underlies Hickorynut Mountain (elevation 976 m or 3,200 ft) in the Sugar Hill quadrangle, one of the highest points in the greater Marion area. Henderson Gneiss occurs only in the hanging wall of the Tumblebug Creek and Stumphouse Mountain faults. It is likely that the Henderson Gneiss was emplaced as a single large thrust sheet, consistent with the interpretations of Liu (1991) and Davis (1993). Explanation of the current distribution of Henderson Gneiss as a product of southwest-directed sheath folding was entertained by Bream (1999) and Hatcher (this guidebook). Goldsmith et al. (1988) identified several bodies to the east and southeast of the Marion area as a possible shallow-level, less sheared phase of Henderson Gneiss.

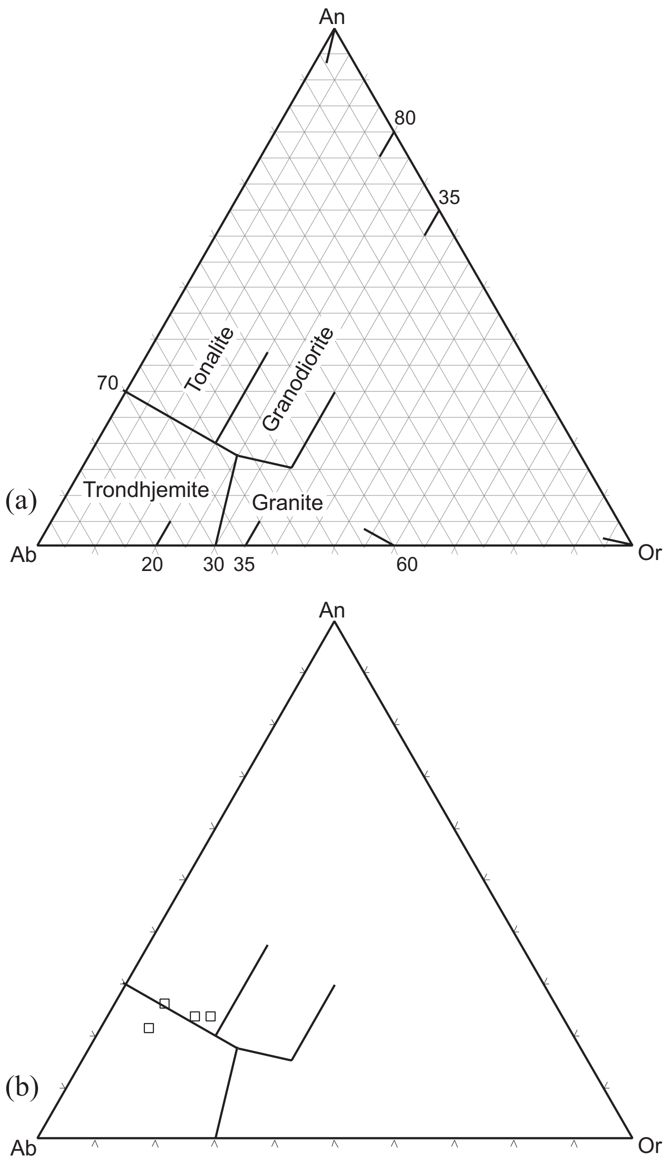

Figure 15. Anorthite (An)-Orthoclase (Or)-Albite (Ab) normative feldspar ternary diagram. Data are from Bream (1999). (a) Normative ternary diagram after Barker (1979). (b) Dysartsville Tonalite samples.

Giorgis (1999), Williams (2000), and Bier (2001) concluded this is a separate unit, now called Walker Top Granite (Giorgis et al., this guidebook). See Bream (this guidebook) for a review of Henderson Gneiss geochronology and interpretations.

Using the IUGS classification (Streckeisen, 1976), the Henderson Gneiss is mostly monzogranite, but a few samples plot in the granodiorite, tonalite, and quartz monzodiorite fields (Fig. 16). The distinctive 1- to 3-cm augen in the Henderson Gneiss (Fig. 17) are mostly individual crystals or clots of microcline and less frequently plagioclase. Myrmekite commonly comprises the rims of most of the augen. Based on textural evidence and the definitions provided by Shelley (1964), Lemmon (1973) concluded that the myrmekitic texture in the Henderson Gneiss is either syn- or post-tectonic. Lemmon (1973) also concluded that the groundmass quartz, microcline, and plagioclase surrounding the augen clearly prove that the augen are porphyroclasts. Henderson Gneiss thin sections contain 30-40 percent plagioclase (An_{15-22}), 18-28 percent quartz, 13-21 percent biotite, and 17-26 percent microcline. Accessory allanite and sphene occur in all samples.

Other Rock Units. Altered ultramafic bodies, small granitoids, pegmatite, vein quartz, and Quaternary deposits also occur in the western Inner Piedmont in the Marion area. Ultramafic bodies are small and often occur in or near the Dysartsville Tonalite. The small granitoid bodies are mostly unmappable. Whisnant (1975) delineated five granodiorite intrusions in the Sugar Hill quadrangle that are mineralogically similar to those in the Glenwood quadrangle. Pegmatites are present in most units and are likely related to a post-peak metamorphic intrusive event as suggested by Yanagihara (1994), but there is also an earlier deformed suite. Vein quartz is also present in most units but is especially abundant in both Henderson Gneiss and Dysartsville Tonalite. Quaternary alluvium is also present throughout the western (and eastern) Inner Piedmont. Other Quaternary units that are present but mostly not large enough to map include colluvium, stream terraces, debris flows, talus, and landslides.

Eastern Inner Piedmont—Brindle Creek Thrust Sheet

Lithologies present in the South Mountains include metagraywacke/biotite gneiss and aluminous schist. Goldsmith et al. (1988) mapped biotite gneiss and large amphibolite bodies to the east and northeast of the South Mountains. Walker Top and Toluca Granites occur as mappable plutons and disseminated pods throughout the hanging wall of the Brindle Creek thrust sheet.

Aluminous schist-Metagraywacke assemblage. The sedimentary sequence throughout the eastern Inner Piedmont is dominated by metapelite (aluminous schist) with a minor metapsammite (metagraywacke) component (~25%).

Metapelite. The aluminous schist unit thickens dramatically in the hanging wall of the Brindle Creek thrust (Giorgis, 1999; Bier, 2001). This thickness increase could be related to an original depositional thickness change or to complex folding. The aluminous schist unit contains sillimanite schist and sillimanite gneiss in the South Mountains. Fresh sillimanite schist and gneiss are gray to grayish-brown purple and weather to tan, yellow ochre, and purple-brown saprolite (Fig. 18). The well-developed foliation is defined by parallel alignment of micas—predominantly muscovite—sillimanite, and quartz. Sillimanite (up to 5 cm) occurs in foliation-concordant mats, rarely displaying a strong lineation. Modal analyses of aluminous

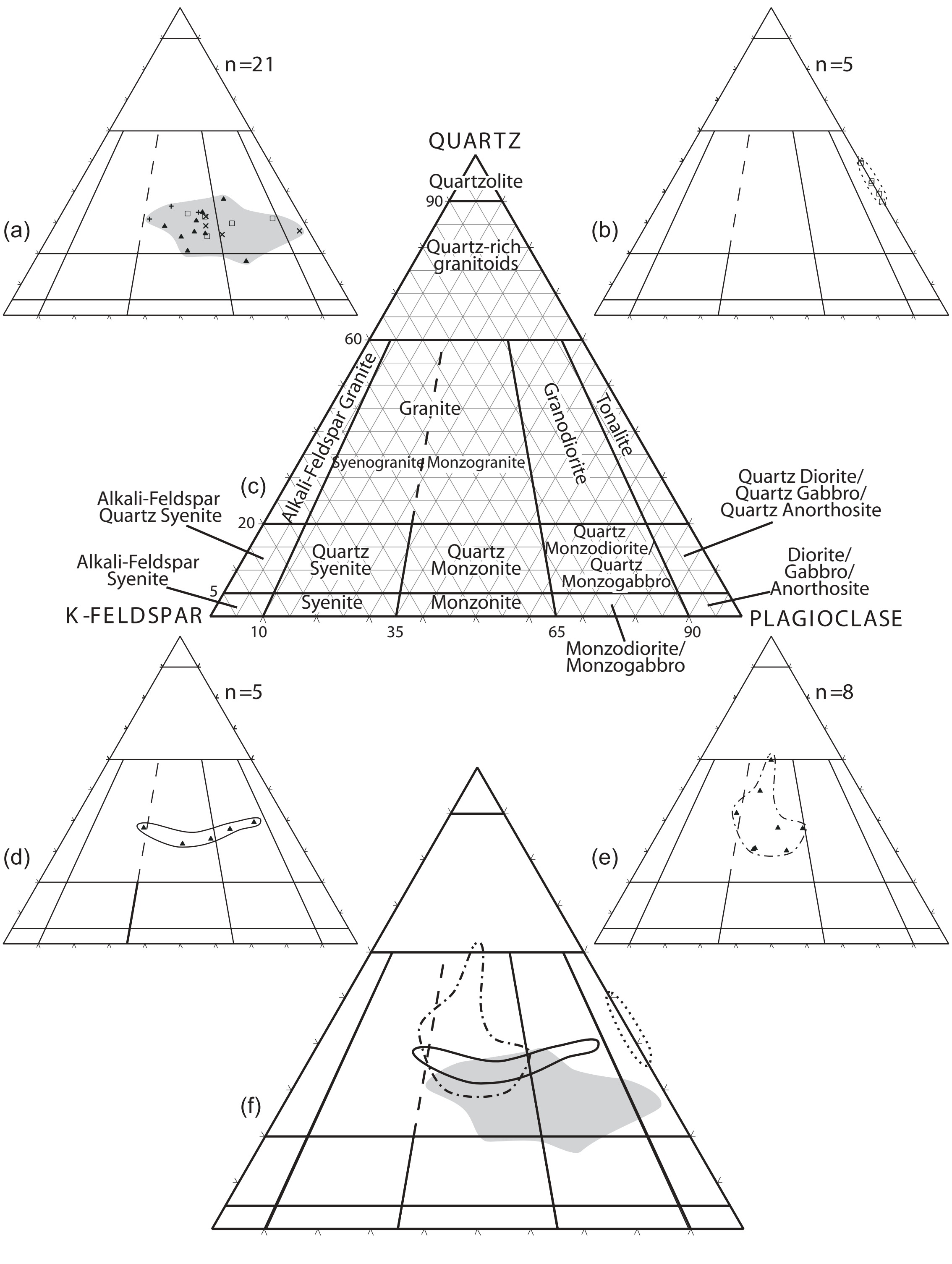

Figure 16. IUGS modal classification of granitoid units of the western Inner Piedmont. Triangles are data from Lemmon (1973), addition signs are data from Yanagihara (1994), crosses are data from Whisnant (1975) and open boxes are from Bream (1999). (a) Henderson Gneiss. (b) Dysartsville Tonalite. (c) IUGS igneous classification after Streckeisen (1979). (d) Granitic gneiss within Henderson Gneiss. (e) Sugarloaf Mountain Gneiss. (f) Composite field diagram of a, b, d, and e.

schist reveal a mineral assemblage of muscovite + quartz + plagioclase (An_{20-35}) + sillimanite + biotite + garnet ± tourmaline. Accessory chlorite and epidote occur as retrograde alterations of biotite and plagioclase, along with trace zircon, apatite, and opaque minerals. Muscovite occurs both as large grains (1-3 mm) and as fine-grained (0.2 mm) alterations within sillimanite mats. Both fibrolitic and prismatic sillimanite were recognized in thin sections. Fibrolite is commonly associated with muscovite layers, while prismatic sillimanite occurs throughout the sections.

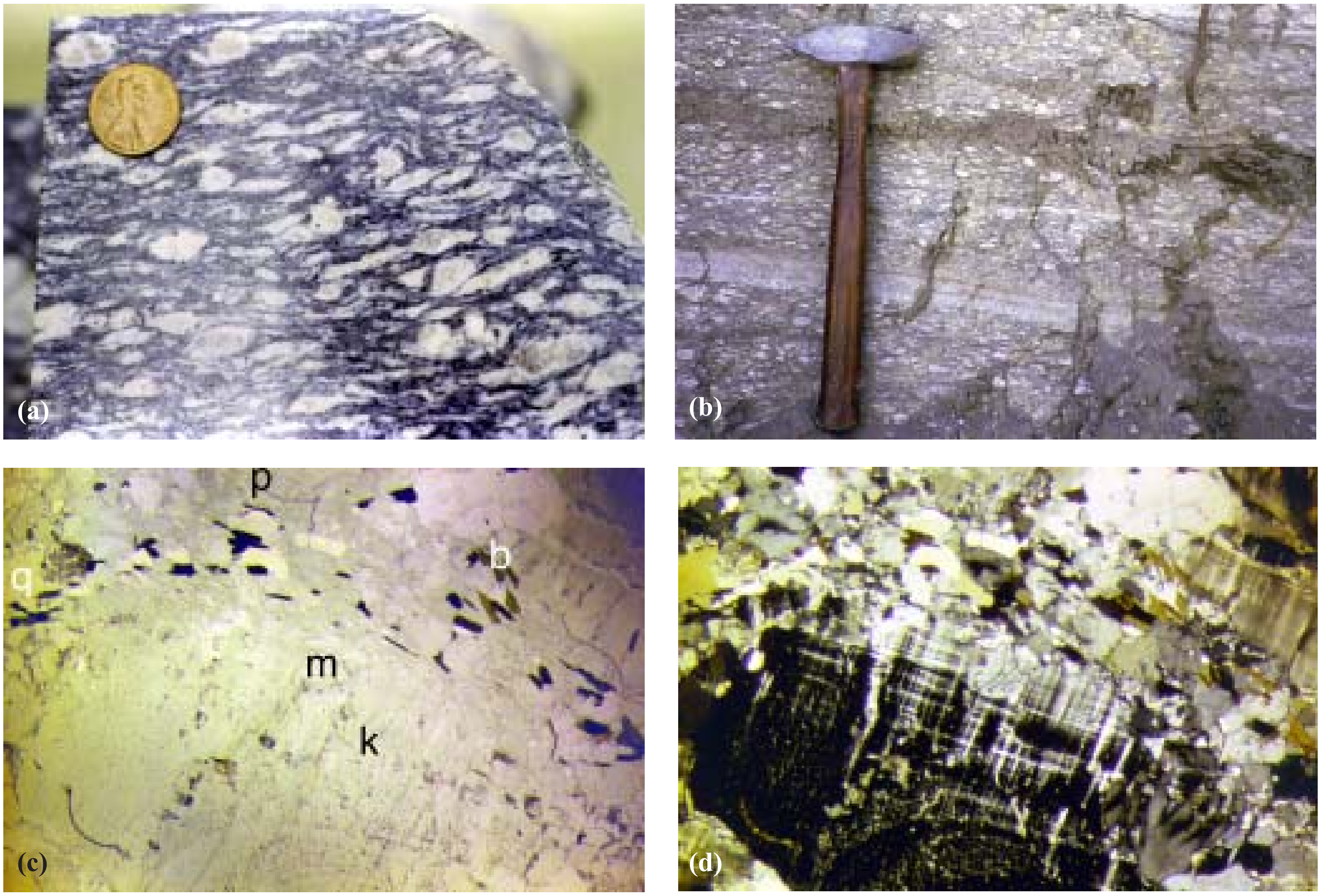

Figure 17. Photographs and photomicrographs of the Henderson Gneiss. (a) Polished hand sample from the Hendersonville quarry. (b) Typical saprolite outcrop of Henderson Gneiss near Heddrick Knob in the Sugar Hill 7.5-minute quadrangle. (c) Plane light photomicrograph. Abbreviations are as follows: b-biotite, k-K-feldspar, m-myrmekite, p-plagioclase, q-quartz. Width of field is 4.25 mm. (d) Photomicrograph with polarizers crossed. Width of field is 4.25 mm. The sample is from the Sugar Hill quadrangle on the ridge south of the Second Broad River and north of Mud Cut Road.

Metapsammite. In outcrop, the metagraywacke-biotite gneiss is gray; composed of quartz, plagioclase, and biotite; and contains migmatitic quartzofeldspathic leucosome. It is interlayered with biotite-muscovite schist (Fig. 19). Calc-silicate pods and layers are rare and were observed as float. The well-developed foliation is defined by the alignment of biotite, muscovite, and quartz. Alternating quartzofeldspathic and biotite-muscovite schist layers from one centimeter to several meters thick define compositional banding. Modal analyses of metagraywacke reveal a mineral assemblage of plagioclase ($An_{20\text{-}30}$) + quartz + biotite + muscovite ± sillimanite ± garnet. Zircon and chlorite occur as accessory or trace minerals. Biotite (0.5-3 mm) and muscovite (0.25-1.5 mm) define the foliation and are segregated into layers that alternate with quartz (0.1-2 mm) and plagioclase ($An_{20\text{-}30}$) layers 0.2 to 3 mm thick. Biotite frequently defines microscale structures.

Granitoids. Two granitoids are recognized in this part of the eastern Inner Piedmont: Toluca and Walker Top Granites.

Toluca Granite. Keith and Sterrett (1931) originally recognized the Toluca Granite (Goldsmith et al., 1988) and called it the Whiteside Granite. Griffitts and Overstreet (1952) subdivided the Whiteside Granite into the Toluca Quartz Monzonite and the Cherryville Quartz Monzonite. The Toluca Quartz Monzonite was renamed Toluca Granite by Goldsmith et al. (1988) to adhere to Streckeisen's (1976) IUGS classification (Fig. 20). Preliminary ion microprobe analyses yield zircon and monazite ages ranging from 370 to 385 Ma for the Toluca Granite (Mapes, 2002). Griffitts and Overstreet (1952) noted that individual Toluca Granite bodies range from cm to hundreds of meters thick, and from a few meters to kilometers long. The size of bodies mapped in the South Mountains is also widely variable, possibly indicating deformed sills rather than one large contiguous pluton. Toluca Granite is medium gray and weathers to light gray and tan saprolite. The unit is weakly to moderately foliated (Fig. 21), and, although bodies parallel the foliation of the enclosing aluminous schist and paragneiss, the foliation within the Toluca Granite does not always parallel the contacts. This may be the product

Figure 18. Photographs and photomicrograph of eastern Inner Piedmont sillimanite schist. (a) Sillimanite schist outcrop near Horse Ridge. (b) Sillimanite schist saprolite near Dogwood Stamp Mountain, Benn Knob 7.5-minute quadrangle. (c) Hand specimen from Benn Knob 7.5-minute quadrangle. Sillimanite pseudomorphs after kyanite. (d) Thin section from Huckleberry Mountain, Benn Knob quadrangle. Prismatic sillimanite (sil), kyanite (ky), and anhedral tourmaline (tur). Field of view is 1.7 mm.

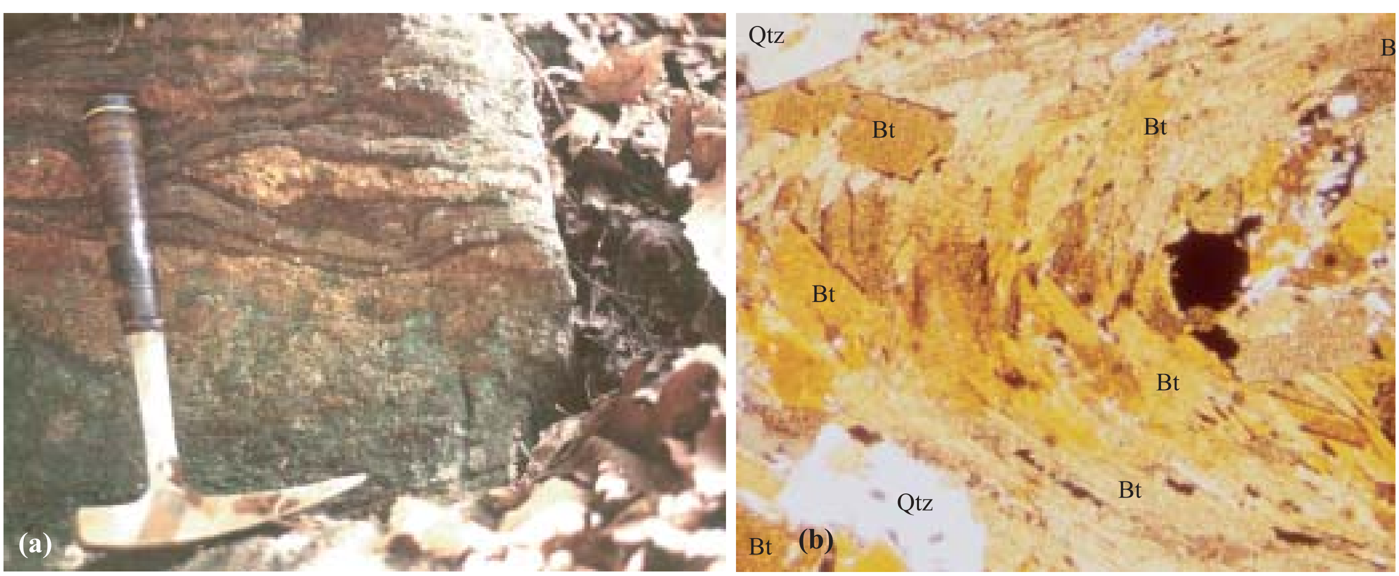

Figure 19. Photograph and photomicrograph of eastern Inner Piedmont metagraywacke. (a) Migmatitic metagraywacke near Gibbs Gap, Benn Knob 7.5-minute quadrangle. (b) Photomicrograph of a sample from Shinny Creek, Benn Knob 7.5-minute quadrangle. Microfold defined by biotite. Field of view is 4.25 mm. Qtz-quartz, Bt-biotite.

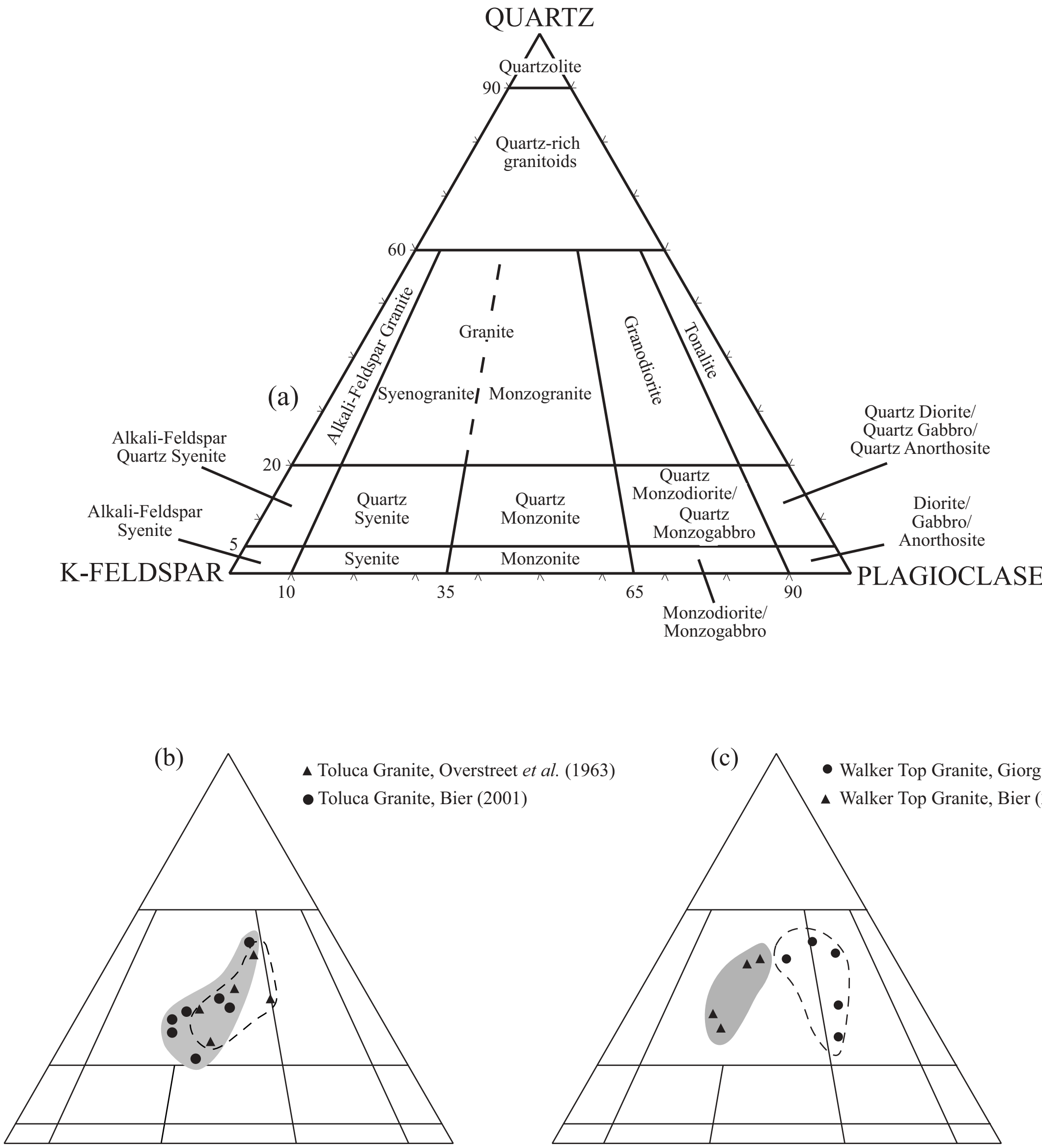

Figure 20. IUGS modal classification of Toluca Granite and Walker Top Granite. (a) IUGS igneous classification after Streckeisen (1976). (b) Toluca Granite. Dashed line encloses data from Overstreet et al. (1963b). (c) Walker Top Granite. Dashed line encloses data from Giorgis (1999). The difference in data sets is attributed to different point-counting techniques (Giorgis, 1999; Bier, 2001).

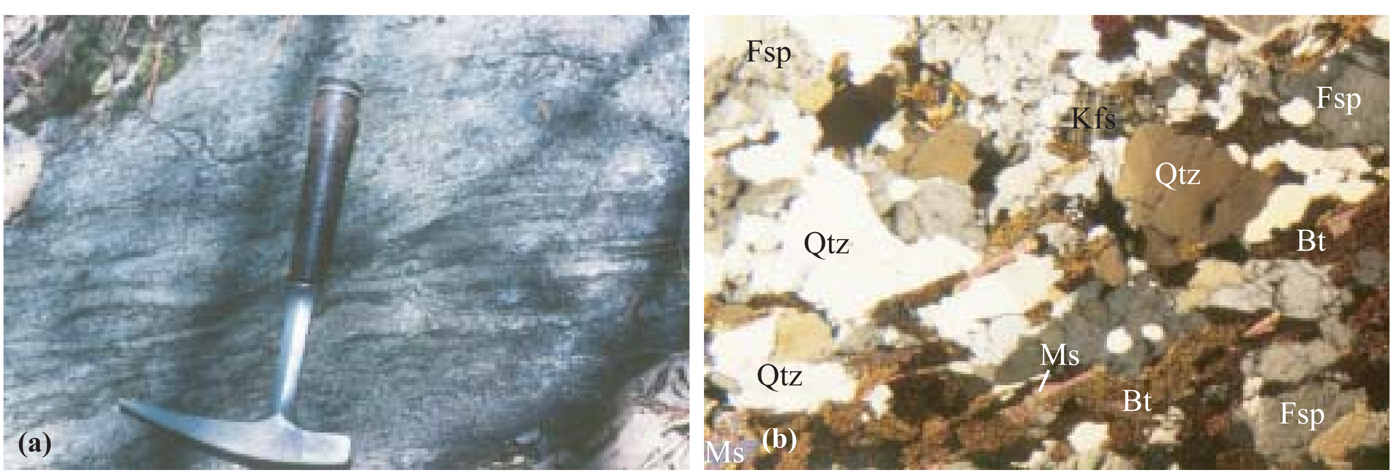

Figure 21. Photograph and photomicrograph of the Toluca Granite. (a) Toluca Granite near Black Mountain, Benn Knob 7.5-minute quadrangle. (b) Photomicrograph of a Toluca Granite sample thin section. Field of view is 1.7 mm. Fsp-feldspar (plagioclase), Kfs-Kfeldspar (microcline), Qtz-quartz, Ms-muscovite, Bt-biotite.

of folding, incomplete transposition, relict magmatic foliation, or rheological differences between granite and country rock. Foliation is defined by parallel alignment of muscovite, biotite, and quartz.

Modal analyses of Toluca Granite reveal a mineral assemblage plagioclase (An_{25-35}) + microcline + quartz + muscovite + biotite + garnet. Accessory or trace minerals include sillimanite, zircon, monazite, xenotime, apatite, and opaque minerals. The Toluca Granite is medium- to coarse-grained (1-4 mm) and usually equigranular but sometimes is porphyritic with megacrysts of either garnet or K-spar. Myrmekite forms rims around some microcline megacrysts. Bulk energy dispersive X-ray fluorescence analyses, with major elements plotted on Werner's (1987) tectonic discrimination diagram, supports the interpretation of Toluca Granite having an igneous protolith (Fig. 22).

Walker Top Granite. The Walker Top Granite was mapped by Goldsmith et al. (1988) as medium to dark gray, less foliated, less sheared, garnetiferous Henderson Gneiss. The Walker Top Granite and Henderson Gneiss both contain large dominantly microcline with some plagioclase (An_{20-30}) megacrysts surrounded by a coarse-grained equigranular groundmass of biotite, two feldspars, and quartz. Walker Top Granite was first recognized as a separate unit from Henderson Gneiss by spatial and textural differences. Feldspar megacrysts in the Henderson Gneiss are mostly lenticular (as part of an S-C fabric), whereas the feldspar megacrysts in Walker Top Granite are euhedral to subhedral (Fig. 23). Bulk chemical analyses suggest a strong genetic correlation between the Henderson Gneiss and the Walker Top Granite (Giorgis, 1999; Giorgis et al., this guidebook). A new high resolution ion microprobe $^{238}U/^{206}Pb$ age for Walker Top Granite is 366 ± 3 Ma (Mapes, 2002; Giorgis et al., this guidebook).

Megacrysts in Walker Top Granite are oriented parallel to the regional foliation (Merschat and Kalbas, this guidebook), but Goldsmith et al. (1988) concluded the foliation resembles a flow pattern rather than deformational foliation. The weak foliation in the groundmass is defined by parallel alignment of biotite (1-3 mm), muscovite (0.5-2 mm), quartz (0.5-3 mm), and plagioclase (0.5-2 mm). The mineral assemblage in Walker Top Granite is microcline +

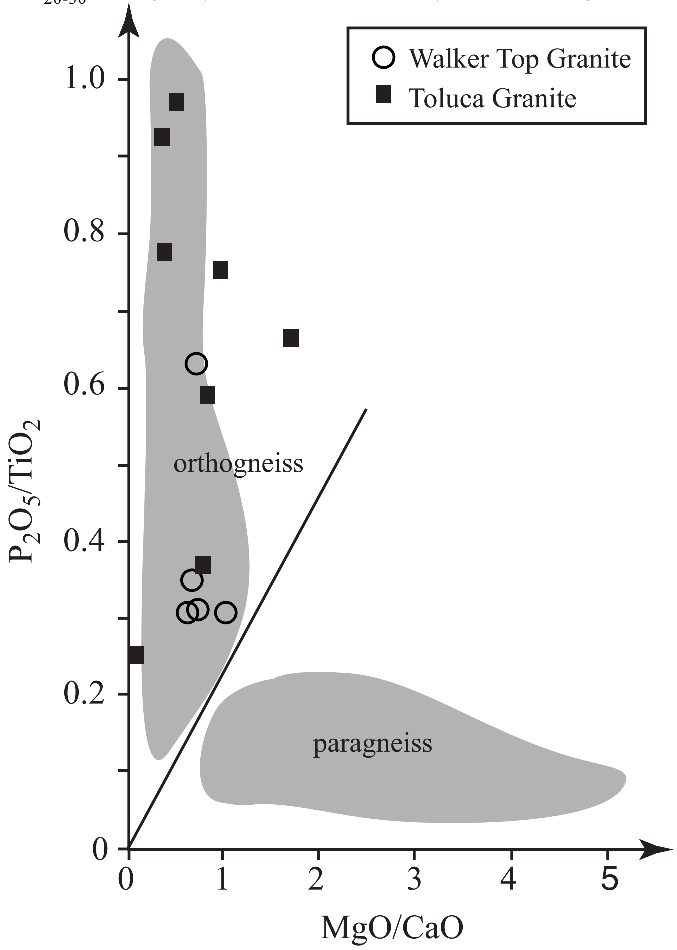

Figure 22. Major element discrimination diagram distinguishing ortho- and paragneisses in metamorphic terranes. Shaded areas are data from the Saxonian granulite massif used to construct the diagram. Diagram and fields from Werner (1987).

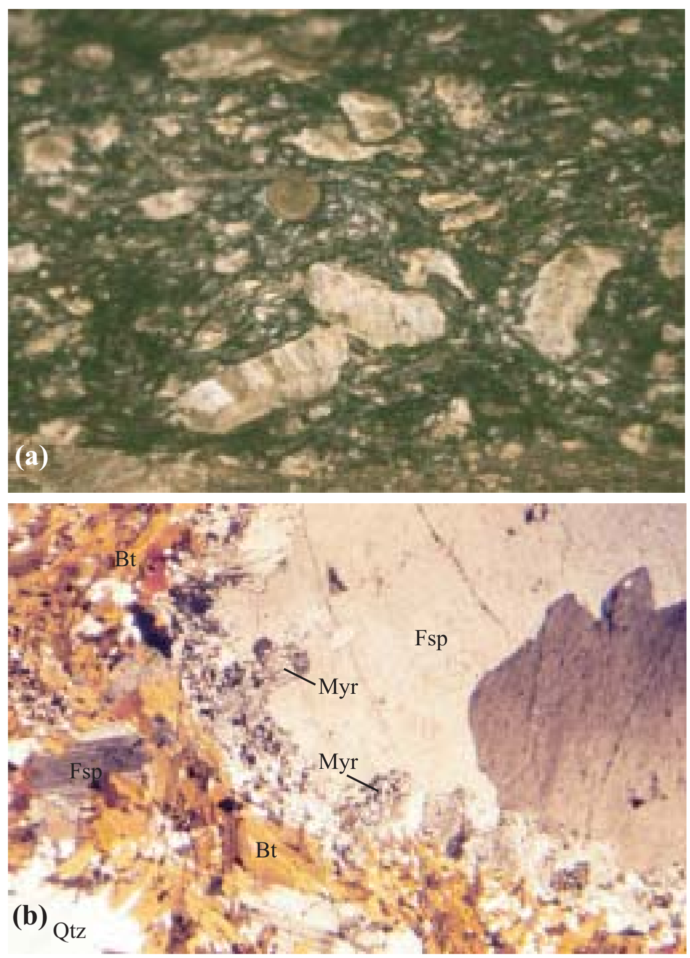

Figure 23. Photograph and photomicrograph of Walker Top Granite. (a) Walker Top Granite near Richland Mountain, Benn Knob 7.5-minute quadrangle. (b) Photomicrograph of a sample thin section obtained near Camp Knob, Benn Knob 7.5-minute quadrangle. Microcline megacryst with myrmekitic rim in a matrix of plagioclase (An_{20-30}), quartz, and biotite. Field of view is 11.1 mm. Bt-biotite, Fsp-feldspar, Myr-myrmekite, Qtz-quartz.

plagioclase (An_{20-30}) + quartz + biotite + muscovite, with trace zircon, apatite, epidote-clinozoisite, and opaque minerals. Microcline and plagioclase occur both as megacrysts and part of the coarse-grained groundmass. Microcline megacrysts (2-6 cm), which are much larger than plagioclase megacryts (1-4 cm), are rimmed by myrmekite. Modal analyses reveal that the Walker Top Granite ranges from granodiorite to granite (Fig. 21). Major elements from bulk X-ray fluorescence analyses of Walker Top Granite, when plotted on Werner's (1987) major element discrimination diagram (Fig. 23), support a magmatic origin for Walker Top Granite.

METAMORPHISM

Electron microprobe (EMP) analyses were performed on seven garnet-mica schist samples from the Marion and South Mountains area (Fig. 2). The metapelite and metapsammite samples chosen for EMP analysis are fine- to medium-grained (<0.25-1 mm), except for garnet (up to 2 cm diameter) and kyanite (up to 1 cm), and have a well-developed foliation. The following mineral assemblage is present: muscovite + biotite + garnet + quartz + plagioclase (An_{20}) + staurolite (NW of the ky-sill isograd only) + kyanite and/or sillimanite + ilmenite + magnetite. Garnets are dark red, mostly almandine (~80%), partially fractured, and contain minor chlorite alteration. Garnets occur as euhedral to subhedral porphyroblasts and commonly contain inclusions of biotite, ilmenite, magnetite, chlorite, and quartz. Accessory minerals include zircon, apatite, and allanite. Biotite and garnet chemistries are similar to analyses from other amphibolite-grade terranes. Samples containing sillimanite lack significant amounts of K-feldspar, placing the assemblage below the second sillimanite isograd of Chatterjee and Johannes (1974). Textural evidence suggests that staurolite was consumed, partially in rocks NW of our staurolite + kyanite-kyanite isograd and completely SE of this isograd, by terminal staurolite reactions (e.g., Pigage and Greenwood, 1982; Dutrow and Holdaway, 1989). The presence of mostly mesoscale migmatites above the middle kyanite zone demonstrates that much of this area was at or near minimum melt conditions. The presence of kyanite and sillimanite pseudomorphs after kyanite suggests that kyanite formed before sillimanite where both are present. The location of the staurolite + kyanite-kyanite isograd in the footwall of the Mill Spring fault is defined by the first appearance of prismatic kyanite, commonly at high angles to the dominant foliation.

The location of the kyanite-sillimanite isograd was determined by the first occurrence of fibrolitic sillimanite in aluminous schist. Where kyanite or sillimanite is the dominant prograde phase, growth does not reveal a preferred orientation with regard to the local structures; smaller and partially resorbed kyanite, however, is typically oriented parallel to regional foliation and lineation. Sillimanite is present in the Mill Spring fault hanging wall either as unoriented mats in proximity to the kyanite-sillimanite isograds or prismatic rhombs near the core of the Inner Piedmont. The lack of consistent orientation of sillimanite needles with respect to dominant mineral lineation, the presence of kyanite oriented at high angles to smaller partially resorbed kyanite grains, and the penetrative foliation suggest that growth of these minerals occurred toward the end of major penetrative deformation (D_2). Most garnets here are zoned and relatively inclusion-poor at the rims, whereas the cores commonly contain numerous small inclusions. Lemmon (1973) suggested that this textural relationship, in addition to the presence of small euhedral inclusion-poor garnets, indicates two prograde metamorphic events. Zoning profiles of garnet are relatively flat for the interiors with increasing almandine and spessartine content and decreasing grossular content toward the rims, suggesting a single event of diffusional growth and equilibrium (Spear, 1993) for garnets from both the staurolite-kyanite and sillimanite zones. Considering the zoning profiles, the textures and morphologies are more likely the result of decompressional post-thermal peak reequilibration, as noted by Spear et al. (1990) in southwest New Hampshire and suggested by Davis (1993) for metapelite samples from the Sugarloaf Mountain thrust sheet in the North Carolina Columbus Promontory area.

A single garnet-amphibolite from the Tallulah Falls Formation in the Mill Spring fault footwall was chosen for analysis. This lithology is not abundant in the study area and differs in mineral assembage from other amphibolites associated with the Tallulah Falls Formation. The mineral assemblage for this sample is hornblende + garnet + quartz + ilmenite + biotite + plagioclase (An_{25}) + magnetite. The foliation, defined by hornblende and quartz (both between 0.5 and 2 mm long), wraps subhedral to euhedral garnet porphyroblasts (3-5 mm in diameter). The garnets are dark red, mostly almandine (55-65%) with up to 30 percent grossular component, highly fractured, and inclusion-rich. Quartz, biotite, apatite, magnetite, and ilmenite inclusions are present within the garnets and are commonly oriented at high angles to the dominant foliation. Zoning in garnets of the garnet-amphibolite is characterized by an increase in the spessartine end-member toward the rims and suggests diffusional growth in response to net transfer reactions most likely with amphibole.

Analytical Methods

Detailed chemical analyses of garnet, biotite, hornblende, and plagioclase were performed using the four-spectrometer CAMECA SX-50 EMP at the University of Tennessee–Knoxville. An acceleration voltage of 15 kV and a beam current of 20 nA were used for all analyses. Beam size was varied depending on the mineral phase analyzed: a 5 μm beam was used for biotite, hornblende, and plagioclase; and a 2 μm beam was used for garnet. A peak counting time of 20 seconds was used for all analyses, except for Fe in plagioclase and Na in garnet where a counting time of 30 seconds was used. Some garnet cation totals indicated the presence of Fe^{3+}, but all iron was calculated as Fe^{2+} due to uncertainty in Fe^{3+} electron microprobe calculations (Sobolev et al., 1999). Analyses chosen for pressure and temperature estimates were obtained from 5-point line traverses across grain boundaries. The points were selected based on proximity to the rim boundaries, cation totals, and weight percent totals. In all cases, analyses were within 6 μm of the grain boundary and mineral pairs used for the PT estimates were no more than 10 μm apart.

Pressure and Temperature Estimates

The mineral assemblages present in the paragneisses delimit the pressure and temperature conditions to the stable staurolite, kyanite, and sillimanite fields of the aluminum silicate phase diagram (Holdaway, 1971) and KFMASH (SiO_2-Al_2O_3-MgO-FeO-K_2O-H_2O) system. To further constrain the fields for the footwall and hanging wall in the area, temperature estimates were calculated using EMP analyses of garnet and biotite pairs in the garnet-mica schist samples. Due to the presence of Mn and Ca, the Berman (1990) modification of the Ferry and Spear (1978) temperature estimate model was chosen for the paragneiss samples. Fe-Mg exchange between garnet and hornblende is also commonly used to estimate temperatures for mafic schists (e.g., Ghent et al., 1983; Labotka, 1987). Temperatures in the garnet-amphibolite were estimated using the model of Perchuk et al. (1985). The modified GASP pressure estimate of Koziol (1989) was used for two samples with garnet, plagioclase, and biotite in contact with one another. Equilibrium conditions of 520 ± 25˚C and 5.1 ± 1 kbar and 645 ± 25˚C and 5.3 ± 1 kbar were determined for samples ME658 and BK959, respectively (the intersection of the median temperature and pressure was used for ME658). These pressures fall within the mid- to upper ranges of estimates for the western Inner Piedmont: 3.5-5.2 kbar for metapelite from the Sugarloaf Mountain thrust sheet in North Carolina (Davis, 1993) and 4.5-5.7 kbar for Alto allochthon metapelite in Georgia (Schumann, 1988). The estimated pressure for ME658 was assumed for the garnet-amphibolite sample in the kyanite field and the estimated pressure for BK959 was assumed for the remaining samples in the sillimanite field lacking plagioclase in contact with the phases necessary to estimate pressures. Core temperature estimates obtained for biotite inclusions within garnet for the footwall metapelite are ~480˚C whereas rim temperature estimates for the same garnet are ~520˚C. This relationship indicates that the rim compositions reflect maximum prograde metamorphic conditions without complete retrograde or diffusional overprint. Mean temperature estimates for the samples range from 580 to 670 ˚C (Table 1). The variability in temperature estimates for individual samples is most likely a reflection of disequilibrium or net transfer between individual garnet-biotite and garnet-hornblende pairs rather than a temporal expression of metamorphic conditions or the pressures that were assumed for the footwall and hanging wall. If diffusion is a significant process at garnet rims, the kyanite zone temperature estimates from metapelite samples are underestimated, likely less varied than reported, and do not display a significant temperature gradient or necessitate a large amount of telescoping by post-metamorphic thrusting as suggested by Dallmeyer (1988) and Hopson and Hatcher (1988) for the Alto allochthon in Georgia.

Table 1. Pressure and temperature estimates from a garnet amphibolite sample and several pelitic schist samples from the Marion-South Mountains area.

Sample	Temperature in °C	n	Pressure in kbar	n
ME658-core	480 (14)*	5		
ME658-rim	517 (21)*	8	5.1 (0.1)§	4
SH340	610 (26)†	6		
D255	657 (41)*	4		
D537	583 (55)*	3		
GW1	669*	1		
GW230	599 (12)*	2		
DY36	669 (83)*	6		
BK959	645*	1	5.3§	1

*Temperatures calculated using the Berman (1990) for model and 5.1 kbar footwall samples and 5.3 kbar for hanging wall samples.
†Temperatures calculated using Perchuk et al. (1985).
§Pressures calculated using Koziol (1989).

Timing of Metamorphism and Deformation

The timing of deformation for the Inner Piedmont may be constrained using granitoid crystallization ages, monazite ages, zircon rim ages, and the crosscutting relationships of fabrics. The paucity of geochemical and geochronologic work in the North Carolina Inner Piedmont makes regional comparisons difficult; detailed work in the adjacent North Carolina eastern Blue Ridge, however, is abundant. Our timing and minimum metamorphic conditions correspond to the M3 event outlined by Abbott and Raymond (1984) for the Ashe metamorphic suite in northwest North Carolina. Based on our work, the peak Taconian event, M2 event of Abbott and Raymond (1984), is not preserved in garnet-biotite and garnet-amphibole rim compositions or zircon rim growth in North Carolina Inner Piedmont paragneisses. Minimum pressure and temperature estimates are best explained with a single prograde event synchronous with zircon rim and monazite growth in and nearby the study area at ~350 Ma (Neoacadian; Dennis and Wright, 1997; Bream et al., 2001; Carrigan et al., 2001).

Discussion

Temperature and pressure estimates for garnet-biotite and garnet-amphibole rims in the Marion and South Mountains areas do not reveal systematic northwest to southeast increases across the kyanite-sillimanite isograd, Mill Spring fault, or Brindle Creek fault. We suspect that additional geothermobarometric work will also reveal modest pressure and temperature differences across the kyanite-sillimanite isograd and other plastic faults in the Inner Piedmont. The faults do not offset the gradual change in fabric orientation from the core of the Inner Piedmont to the highly aligned zone along the western flank, indicating that movement on the Mill Spring fault either predates or is coeval with major penetrative deformation and metamorphism. The conditions at which major displacement occurred on both faults likely approach the minimum conditions estimated for peak metamorphism. The temperature estimates in the study area do not show appreciable telescoping by the Mill Spring fault, which implies that peak metamorphism also predates movement on the fault. The ~460 Ma crystallization age of the Dysartsville Tonalite (Bream, this guidebook) thus delimits the timing of metamorphism and displacement on the Mill Spring fault. The Dysartsville Tonalite is truncated by the Mill Spring fault and therefore must have crystallized prior to final movement on the fault. Taconian granulite facies metamorphism within the central Blue Ridge (Moecher and Miller, 2000) may not extend eastward into the Tugaloo terrane. The crystallization age of the Dysartsville Tonalite alone does not preclude Taconic deformation or metamorphism; however, recent geochronologic data (e.g., Dennis and Wright, 1997; Bream et al., 2001) indicate that there was significant thermal activity within the Tugaloo terrane during the Neoacadian.

STRUCTURAL GEOLOGY

Inner Piedmont rocks have been subjected to a complex deformational history, recording multiple episodes of folding and faulting. This section presents a deformational framework for the Inner Piedmont that addresses the relative timing of regional structures, using mesoscale and macroscale data. The analyzed area extends from the Brevard fault zone to the eastern Inner Piedmont and contains distinct changes in style, structural orientation, and displacement direction (Davis, 1993). Granitoid crystallization ages and U-Pb ages of monazite and zircon separates from the eastern Blue Ridge and Inner Piedmont help to delimit the timing of deformation. See Bream (this guidebook) for a summary of Inner Piedmont granitoid geochronology.

Structures parallel, normal, and oblique to the orogen have been recognized in the Inner Piedmont for decades (e.g., Reed and Bryant, 1964; Hatcher, 1972; Roper and Dunn, 1973; Griffin, 1974). Davis (1993) suggested that this structural pattern was a result of a "thrust-wrench partitioned deformation . . . and is a manifestation of an early oblique convergence within the southern Appalachians." The deformational framework outlined by Davis (1993) and subsequently modified by Yanagihara (1994), Bream (1999), Giorgis (1999), Hill (1999), and Williams (2000) identifies five deformational events. Compilation of recent detailed mapping from the above workers along with that of Overstreet et al. (1963a, 1963b) also supports five deformational events, although slightly modified (Table 2).

This compilation has been divided into three domains for structural analysis using thrust sheets as primary tectonic units (Fig. 24). The Brevard fault zone bounds Domain I to the northwest and the Mill Spring thrust forms the southeast boundary. The Mill Spring thrust to the west and the Brindle Creek thrust to the east form the boundary of Domain II. Domain III is composed of the Brindle Creek thrust sheet hanging wall. Due to the heterogeneity of structural fabrics and orientations, Domain III is additionally subdivided into 5 subdomains (IIIa, IIIb, IIIc, IIId, and IIIe). Structures will be discussed in chronological order of deformation events (D_1-D_5).

Deformation Events

D_1 Deformation. The D_1 deformation event occurred prior to the main phase of recrystallization (Davis, 1993) and because of later transposition, evidence of the D_1 is rare. Hopson and Hatcher (1988) recognized D_1 in the Alto allochthon, Georgia, represented by F_1 folds that produced the S_1 axial planar foliation. Hatcher (1995) recognized five or more deformations in the same rocks at Woodall Shoals (easternmost Blue Ridge) on the South Carolina-Georgia line in the Chattahoochee thrust sheet (still in the Tugaloo terrane). In the Columbus Promontory, Davis (1993) recognized compositional layering in the Poor Mountain Formation preserved in F_1 folds in a small window within the Tumblebug Creek thrust sheet.

As discussed earlier, truncated folds in the footwall of the Tumblebug Creek thrust provide macroscale evidence of D_1 (Bream, 1999). A regional recumbent antiform in the hanging wall of the Brindle Creek thrust also resulted from this early episode of deformation. Stratigraphic constraints necessitate the existence of this early folding episode. A regional scale F_1 antiform occurs in the eastern South Mountains. The antiform trends SW-NE, verges

Table 2. Deformational framework and related events for the Inner Piedmont, North Carolina.*

DEFORMATION EVENTS		STRUCTURES: FABRICS	STRUCTURES: FOLDS	STRUCTURES: FAULTS	OROGENIC EVENTS	
D_5		joints	———	———	Mesozoic Uplift and Extension	
D_4	b	joints	F_{4b} open, upright; trend NW	———	Alleghanian	
	a	joints	F_{4a} open, upright; trend N to NE	———		
D_3		S_3	F_3 tight reclined to upright trend N to NE	final movement of faults as Type-C thrusts	Neoacadian	
D_2	b	S_2 L_2	F_{2b} tight to isoclinal, reclined to recumbent; sheath folds	initial movement on the SMT, MST, and BCT as Type-F thrusts		prograde metamorphism
	a	S_2	F_{2a} upright folds	TCT		
D_1		S_1	F_1 intrafolial folds, map scale in TCT footwall and BCT hanging wall	———	Taconian(?) or Neoacadian	

*Modified from Davis (1993), Yanagihara (1994), Bream (1999), Giorgis (1999), and Williams, 2000). BCT-Brindle Creek thrust. MST-Mill Spring thrust; TCT-Tumblebug Creek thrust. SMT-Sugarloaf Mountain thrust.

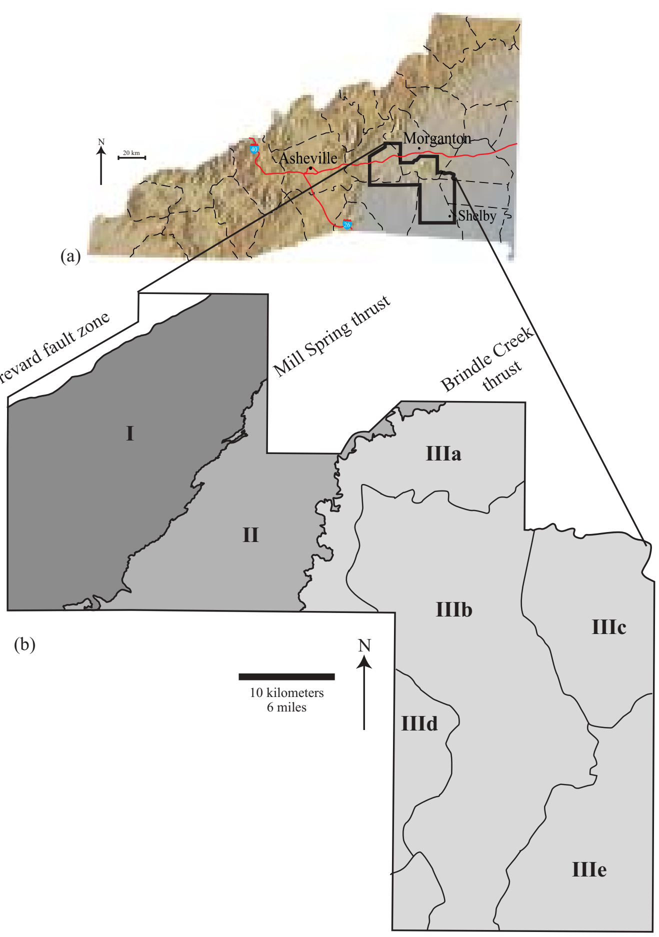

Figure 24. Domain map for a portion of the North Carolina Inner Piedmont. (a) Geographic location of the area. (b) Domains within the area. See text for details.

northwest, and comprises the hanging wall of the Brindle Creek thrust. Devonian Walker Top Granite may be localized in the core of the fold that abuts the Brindle Creek thrust. Mesoscale evidence of D_1 deformation in the Marion-South Mountains area (Domains I, II, and III) includes truncated folds and foliation within amphibolite boudins and rootless, intrafolial folds. These have been recognized as the most defining mesoscale criteria for D_1 deformation (Hopson and Hatcher, 1988; Davis, 1993; Yanagihara, 1994; Curl, 1998; Bream, 1999; Giorgis, 1999; Hill, 1999; Williams, 2000). Based on the younger depositional age of eastern Inner Piedmont sediments, it is unlikely that D_1 is preserved SE of the Brindle Creek fault.

D_2 Deformation. D_2 is the most pervasive deformation event in the Inner Piedmont, a penetrative polyphase event at or near peak metamorphism (e.g., Davis, 1993; Bream, 1999; Hill, 1999). This event formed the dominant foliation (S_2); the most prominent mineral lineation; reclined to recumbent, tight to isoclinal folds; sheath folds; and Type-F thrust faults. D_2 is interpreted to be "a progressive episode, in which heterogeneous and slightly diachronous deformation occurred as a continuum" (Hill, 1999). Equal-area fabric diagrams of over 10,000 foliations are presented in Figure 25. Southeast of the Brevard fault zone, S_2 strikes parallel to the fault zone and dips moderately (~40˚) to the southeast. S_2 in Domain I is roughly orogen-parallel and strikes N41E and dips 25˚ SE. The average foliation in the Mill Spring thrust sheet strikes N19E and dips 22˚ SE. In the Brindle Creek thrust sheet, the mean foliation in

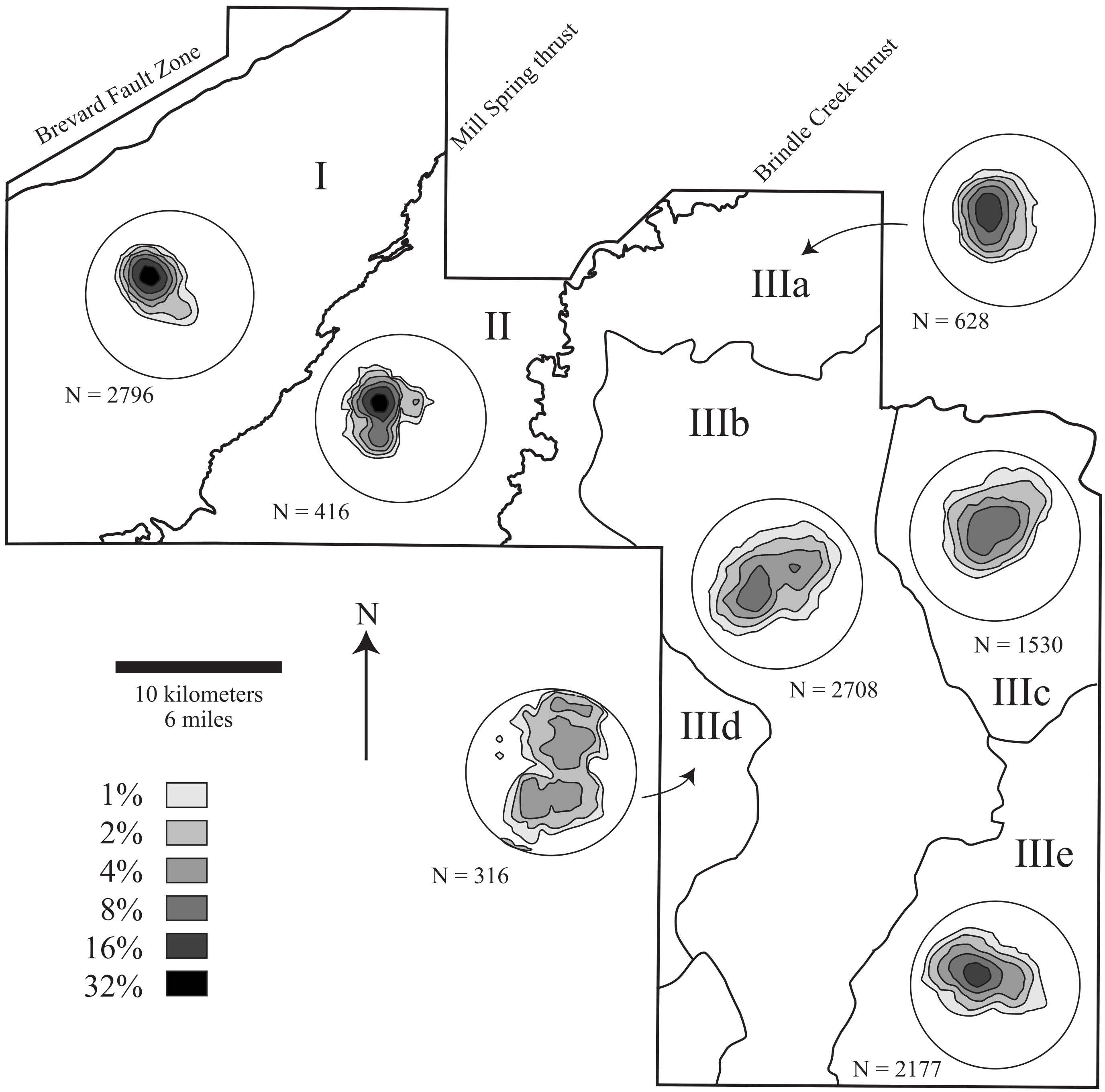

Figure 25. Lower hemisphere, equal-area contoured diagrams of poles to foliation for theMarion-South Mountains area.

Domain IIIa strikes N10E and dips 11˚ SE. Domains IIIb, IIIc, and IIId strike NE-SW and dip shallowly to the southeast. Domain IIId is dominated by a later (D_5) open fold in the eastern portions of the Polkville and Boiling Springs 7.5-minute quadrangles (Overstreet et al., 1963b). The foliations reflect a regional change in strike from NE-SW in the western flank to N-S in the eastern Inner Piedmont back to NE-SW in the southeastern part of the South Mountains.

In the western Inner Piedmont, mineral lineations were interpreted to be stretching lineations (e.g., Davis, 1993; Giorgis, 1999) based on the orientation of independent kinematic indicators (snowball garnets, asymmetric folds, winged porphyroclasts, boudinage, etc.) parallel to the lineation (Davis, 1993). L_2 lineations are defined by elongate and rodded quartz, micas, amphiboles, and feldspars in the western Inner Piedmont (Domains I and II) and by elongate micas, quartz rods, and sillimanite needles in the eastern Inner Piedmont. Lineations in Domain I and II trend NE-SW, roughly parallel to the trend of F_2 fold axes (Fig. 26). Whisnant (1975) observed the parallel nature of isoclinal fold axes and lineations in the western Inner Piedmont and interpreted isoclinal folding and lineation formation to be synchronous. An alternative explanation for the lineation trends in the Marion-South Mountains area in-

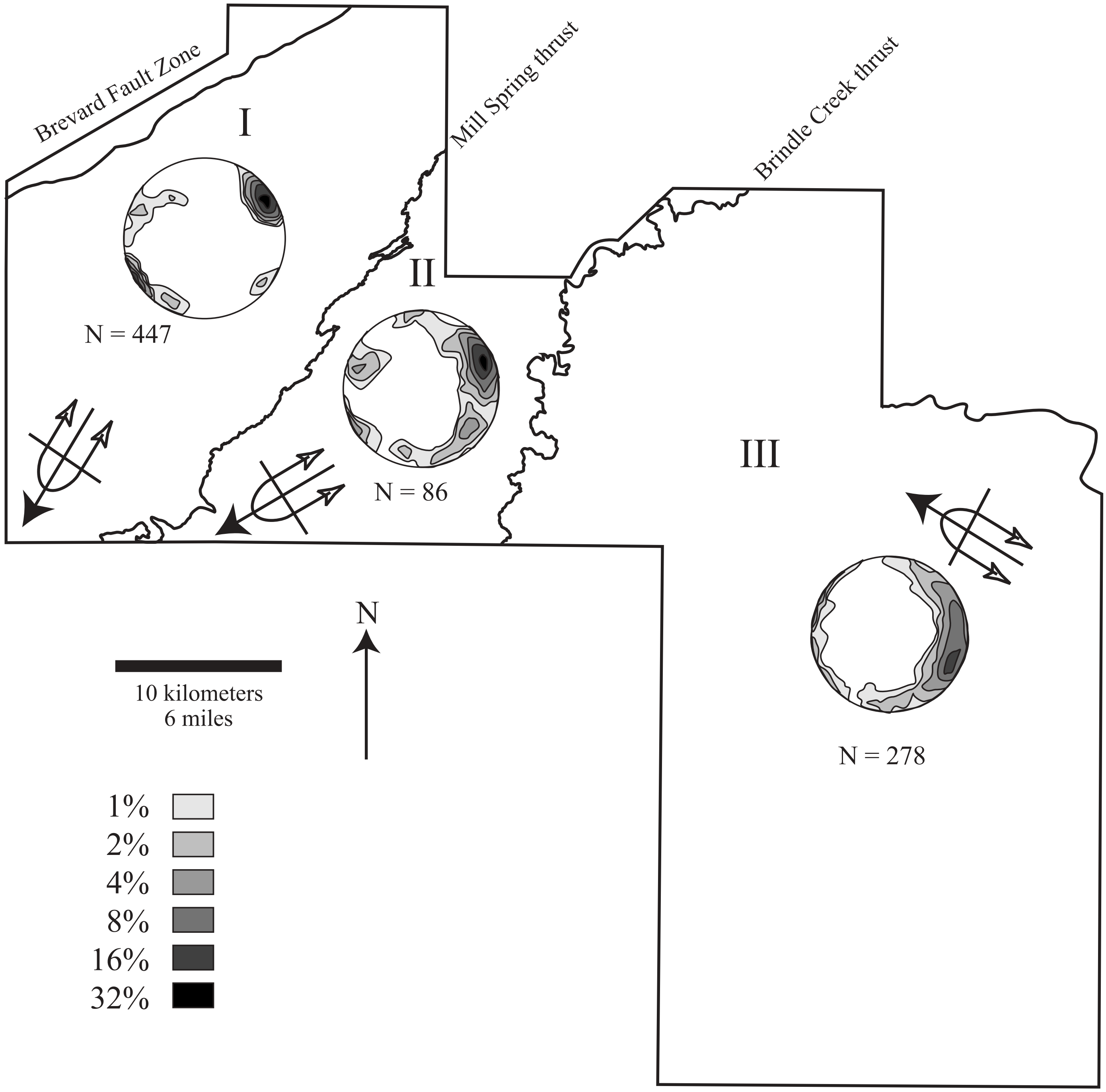

Figure 26. Lower hemisphere, equal-area contoured diagrams of lineations and directions of regional scale sheath fold axes in the Marion-South Mountains area.

volves transport parallel to axes of regional sheath folds (Bream, 1999). Structural data and map patterns here support a genetic association between mesoscopic sheath folds and lineations (Fig.26).

Davis (1993) was able to distinguish D_{2a} folds and D_{2b} folds based on truncated footwall structures, transposition of D_{2a} folds into S_2 and the abrupt structural and metamorphic relationships across D_{2b} folds. This division is supported by initial folding of the Tumblebug Creek thrust (a D_{2a} fault) in a Type-F thrust relationship that is then truncated by the Sugarloaf Mountain thrust, a D_{2b} fault (Bream, 1999). D_{2a} is characterized by upright isoclinal folds (Davis, 1993) and pre-peak metamorphism emplacement of the Henderson Gneiss by the Tumblebug Creek thrust. Timing of displacement on the Tumblebug Creek thrust (and later deformation) is constrained by the ~470 Ma age of the Henderson Gneiss (Vinson, 1999). Therefore, the most intense deformation and metamorphic conditions occurred after 470 Ma.

Mesoscopic and macroscopic sheath folds recognized throughout the South Mountains are attributed to D_{2b}. At the outcrop scale, these are identified by their characteristic eye or anvil shape (Davis, 1993). Bream (1999) recognized regional-scale sheath folding within the Henderson

Gneiss because of the map pattern at both southeast and northeast terminations of the main outcrop body. The outcrop pattern can be explained by northwest-directed thrusting on the Tumblebug Creek thrust prior to later southwest-directed sheath folding. Convincing structural evidence in support of large-scale sheath folds is the strong NE-SW-oriented mineral stretching lineation (Bream, 1999). Map-scale sheath folds are recognized in each of the thrust sheets in the Marion-South Mountains area. Hinges of these sheath folds are nearly parallel to the lineation trends in the respective domains. Map patterns and fabric diagrams support a transport direction that is NE-SW in the western Inner Piedmont that becomes more E-W in the central and eastern Inner Piedmont, which is consistent with the tectonic models proposed by Davis (1993) and Hill (1999). The spread in the lineations in Domains II and III may be related to later D_3 and D_4 folding. A conspicuous northwest-directed lineation in the study area may be the result of D_3 thrust emplacement.

Equal-area stereonets of fold axes (F_1-F_4) are presented in Figure 27. Due to the dominant D_2 deformation at both the meso- and macroscales, trends in the stereonets are primarily attributed to F_2. The most common folds indicative of D_{2b} deformation are tight to isoclinal, reclined to recumbent folds with west vergence. F_{2b} folds in Domain III show a wide variety of orientations. Regional map

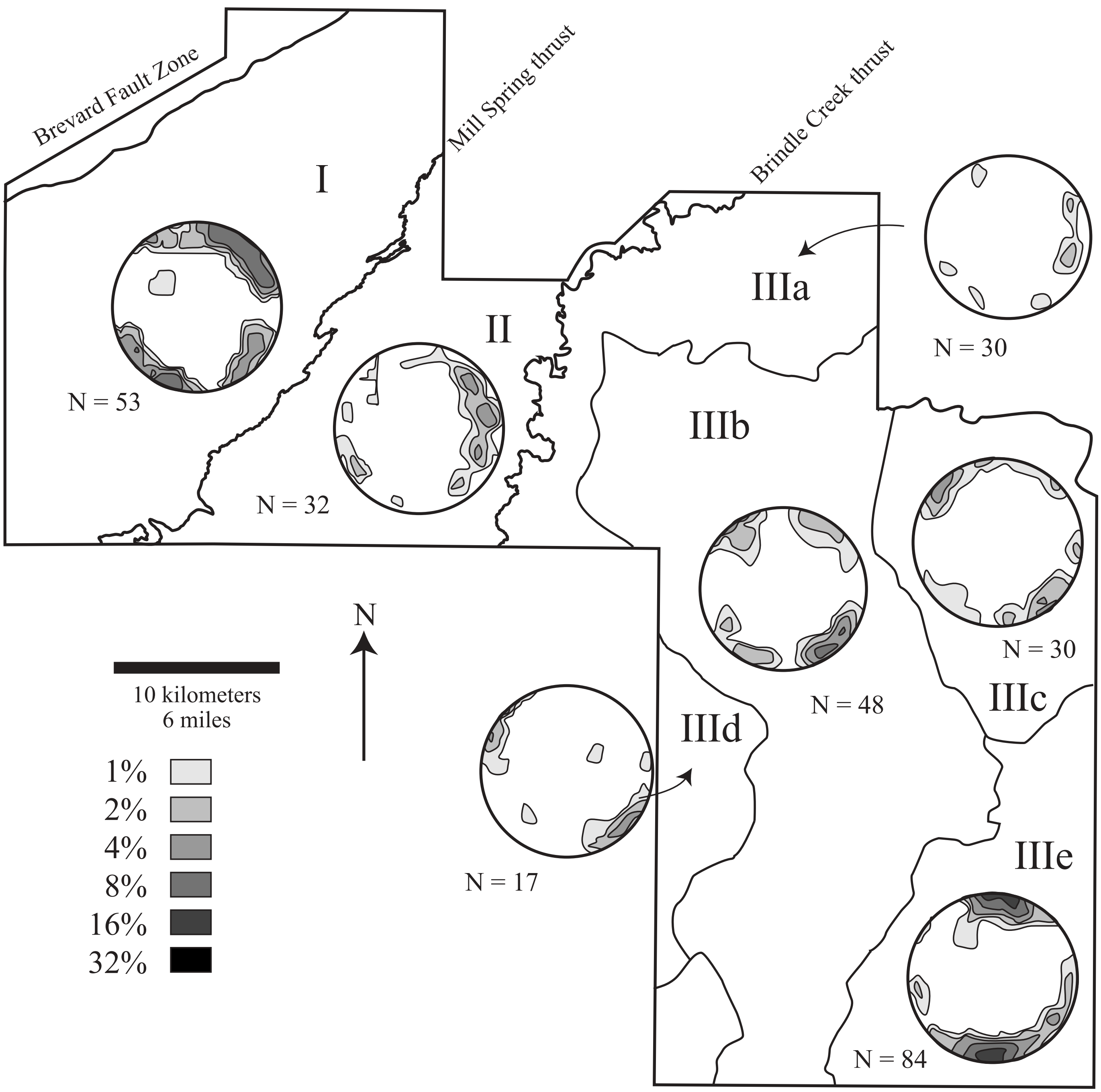

Figure 27. Lower hemisphere, equal-area contoured diagrams of fold axes in the area.

patterns reflect a strong N-NW trend of tight to isoclinal, reclined to recumbent F_{2b} folds. F_{2b} folds in the western portion of Domain III (IIIa) trend E-W, but become NW-SE in Domains IIIb, IIIc, IIId, and N-S in Domain IIIe. F_{2b} folds are tight to isoclinal, reclined to recumbent, and trend NE, parallel to the orogen. At the outcrop scale, F_{2b} folds have thickened hinges and attenuated limbs indicative of flexural flow to passive flow folding. The Mill Spring thrust, Sugarloaf Mountain thrust, and Brindle Creek thrust are examples of Type-F thrust faults that formed when the common limb of an F_{2b} antiform-synform pair is removed, and the fault then accommodates displacement. Initial movement on these faults is interpreted to have occurred late during D_{2b}.

D_3 Deformation. D_3 deformation occurred after peak metamorphism, but prior to complete cooling of the rocks (Hopson and Hatcher, 1988). D_3 structures are oriented parallel and subparallel to D_2 structures in Domains I and II. Davis (1993) noted that F_3 folds are common in the western Inner Piedmont but are not penetrative. These folds include outcrop-scale undulations that locally produce crenulation cleavage (Davis, 1993). Bream (1999) observed that F_3 folds have moderately inclined axial surfaces and maintain constant thickness in the limbs and hinges. F_3 folds are not conspicuous in Domain III, and may not be parallel to NW-SE- and W-E-oriented D_2 structures. Final emplacement of coherent thrust sheets took place during D_3. Earlier F_2 folds are truncated by each of these thrusts (Sugarloaf Mountain, Mill Spring, and Brindle Creek thrusts). D_3 deformation likely marks the end of the Neoacadian event or beginning of the Alleghanian.

D_4 Deformation. D_4 produced open, upright folds that overprinted earlier (F_1-F_3) folds resulting in map-scale folds and dome-and-basin interference patterns. F_{4a} folds trend NE and are orogen-parallel while F_{4b} folds trend NW, perpendicular to earlier structures. Bream (1999) suggested that D_{4a} may be the terminal event of D_3 probably as a result of the Alleghanian orogeny. The brittle nature and style of these open folds suggest they formed in the same deformational event. The perpendicular nature of these two fold sets can be explained by a spasmodic episode of deformation (Whitten, 1966). D_4 is coeval with or predates joint formation.

D_5 Deformation. Several major joint sets have been recognized in the Inner Piedmont. Unfilled fractures are typically planar with small apertures. Garihan et al. (1993) and Curl (1998) associated these fractures with later (Mesozoic) brittle faulting in the southern Appalachians. One joint set parallels to N50˚-N70˚ fault system that produced the Marietta-Tryon graben in South Carolina (Garihan et al., 1993).

Cross Sections

Locations of sections A-A', B-B', and C-C' (Fig. 2) were chosen for continuity with sections constructed earlier by Bream (1999), Giorgis (1999), and Williams (2000). Section D-D' was drawn perpendicular to major structures in the Shelby 15-minute quadrangle.

Section A-A'. Section A-A' is located in the Glenwood, Sugar Hill, and Dysartsville quadrangles and illustrates the subsurface geometry of the Tumblebug Creek, the Sugarloaf Mountain, and the Mill Spring thrusts (Fig 28). In this cross section, folds in the footwall of the Tumblebug Creek thrust represent the earliest episode of deformation (D_1). The Tumblebug Creek thrust emplaced the Henderson Gneiss over the Tallulah Falls Formation during D_{2a}. The Mill Spring thrust was active during D_{2b} as a Type-F (Hatcher and Hooper, 1992) thrust and then evolved into a Type-C thrust. The Sugarloaf Mountain thrust truncates the Tumblebug Creek thrust and is also attributed to D_{2b} deformation. The contact between Dysartsville Tonalite and Tallulah Falls Formation is interpreted as concordant because the contact at the surface mostly parallels foliation. The open folding of tight-to-isoclinal folds and faults in the section is a result of D_4 deformation.

Section B-B'. Section B-B', also located in the Sugar Hill, Glenwood, and Dysartsville quadrangles, depicts the subsurface geometry of the Tumblebug Creek, Mill Spring, and the Brindle Creek faults (Fig. 28). This section portrays the northeast termination of the Henderson Gneiss and bounding Tumblebug Creek thrust, possibly the distal end of a regional sheath fold. The Sugarloaf Mountain thrust dies out between section lines A-A' and B-B'. Erosion of the Mill Spring thrust formed a klippe (projected into the section) that is folded into an F_4 synform. Truncation of the main body of Middle Ordovician Dysartsville Tonalite by the Mill Spring thrust indicates emplacement prior to faulting. Like the Sugarloaf Mountain thrust, the Mill Spring thrust cuts up section to the southwest. The Brindle Creek thrust placed Siluro-Devonian bioite gneiss, sillimanite schist, and Devonian-Mississippian granitoids onto footwall Poor Mountain and Tallulah Falls Formation. Displacement on the Brindle Creek thrust was originally interpreted to be < 5 km (Giorgis, 1999), but because of stratigraphic and isotopic contrasts across the fault, displacement is probably much greater (Bream et al., 2001; Mershcat and Kalbas, this guidebook).

Section C-C'. Section C-C' is located in Dysartsville, Benn Knob, and Casar quadrangles and illustrates structural contrasts from the Brindle Creek hanging wall and footwall (Fig. 28). Isoclinal reclined folds (F_{2b}) in the footwall have been refolded by open, upright F_4 folds. Superposed and

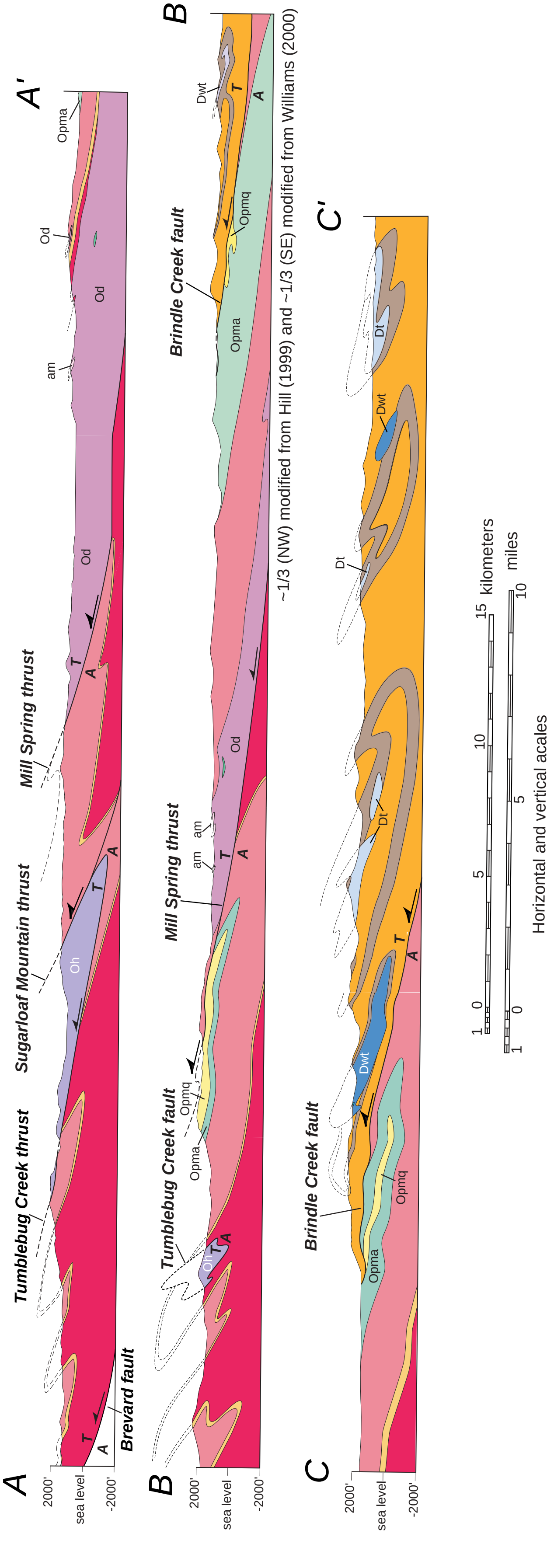

Figure 28. Cross sections. See Figure 2 for locations and explanation of symbols.

sheath folds complicate the structural geometry in the Brindle Creek hanging wall. F_2 macroscale boudinage segmented the F_1 regional antiform. The hook-shaped elliptical bodies of biotite gneiss and sillimanite schist represent sheath folds. The isolated occurrence of Walker Top Granite enclosed by the biotite gneiss and sillimanite schist may also represent parts of a sheath fold. Toluca and Walker Top Granites are consistently associated with the aluminous schist in the South Mountains. This relationship is less prevalent in the Brushy Mountains (Merschat and Kalbas, this guidebook).

Deformational synthesis and tectonic summary

Several tectonic models have been proposed for the Inner Piedmont and the crystalline southern Appalachians including regional scale nappes (Hatcher, 1972; Griffin, 1974), stockwork tectonics and tectonic slides (Griffin, 1971, 1974), and oblique convergence (Davis, 1993; Hill, 1999). Portions of each of these models are applicable to this portion of the North Carolina Inner Piedmont. In South Carolina, Griffin (1971) characterized the migmatitic Inner Piedmont as the infrastructure in his stockwork tectonics model. He initially recognized two major nappes (the Six Mile nappe and the Walhalla nappe) and a deep synformal structure (the nonmigmatitic belt, Hatcher's 1972 Chauga belt) in the South Carolina Inner Piedmont. Griffin (1974) recognized early plastic and late brittle folds in the Inner Piedmont, and attributed them to only two deformational events. The change in outcrop pattern and structural style between the nonmigmatitic belt (western Inner Piedmont) and the Walhalla and Six Mile nappes (eastern Inner Piedmont) was cited as evidence of a tectonic slide boundary (Griffin, 1974). In his model, the infrastructure is the Inner Piedmont, the Carolina slate belt (eastern Carolina terrane) is the suprastructure, and the nonmigmatitic Chauga belt represents an infolded *abscherung* or detachment zone, based on the concepts originally formulated by Wegmann (1935) and Haller (1956).

Hatcher (1972, 1978) recognized that nappes in the Inner Piedmont were formed during D_2. Hatcher (1978) stated that structures in the Inner Piedmont did not form in a single deformational episode as Griffin's (1971) stockwork-tectonics model suggests. The boundary between the Chauga belt and the Inner Piedmont was originally thought to be a fault (Hatcher, 1969; Griffin, 1971). Hatcher (1972) suggested that it is a metamorphic gradient across an antiform synform pair, rather than a tectonic boundary or detachment zone, but more recently realized that it is partly faulted, as indicated in the compilation by Nelson et al. (1998). In the Columbus Promontory, Davis (1993) recognized a change in displacement direction within the western Inner Piedmont from W-directed in the core of the Inner Piedmont to SW-directed in the western Inner Piedmont. The variations in structural orientation result from polyphase deformation, deformation partitioning during a single event, or ductile flow. The progressive change of orientation and similar metamorphic assemblages and textures across the western Inner Piedmont suggest that the structures formed from a single deformation event during amphibolite facies metamorphic conditions (Davis, 1993; Yanagihara, 1994). Davis (1993) argued that the E-W and NE-SW structures resulted from orogen-oblique to orogen-normal displacement of thrusts in the central Inner Piedmont that became orogen-parallel southeast of the Brevard fault zone. The pervasiveness of S_2 and its control of western Inner Piedmont D_2 and D_3 structures suggest that the western Inner Piedmont is a crustal-scale shear zone (Davis, 1993). "The S_2 mylonitic foliation was the common décollement that linked SW-directed transcurrent movement along the primordial Brevard fault zone with E-W contractional movement of Inner Piedmont thrust sheets" (Davis, 1993). Hatcher (1998) expanded on this crustal flow model by recognizing the NW-directed transport in the eastern Inner Piedmont in addition to W- and SW-directed transport in the western Inner Piedmont. Oblique collision and buttressing of ductile Inner Piedmont thrusts against the primordial Brevard fault zone caused this change in transport direction (Davis, 1993; Hatcher, 1998, 2001; Hill, 1999)

Hill (1999) proposed a two-stage oblique collision during the Acadian orogeny produced the map patterns and kinematic indicators in the North Carolina Inner Piedmont. Mineral stretching lineations and significant ductile extension subparallel to cylindrical and sheath fold axes and the orogen in the footwall are associated with first-phase structures, while the second phase starts with underthrusting towards the foreland (Ellis and Watkinson, 1987). "First-phase structures develop parallel to the orogen and later deformation in the hanging wall reflects isostatically driven emergence normal to the orogen" (Hill, 1999). First-phase structures (D_2 here) include mineral stretching lineations, sheath fold axes, and isoclinal folds. The stack of westward-vergent thrust sheets (D_{2b} and D_3) characteristic of both the South and North Carolina Inner Piedmont can be thought of as the imbricating blocks in the Ellis and Watkinson (1987) model. The map pattern in the eastern Inner Piedmont is complicated and disharmonic, indicative of progressively disharmonic deformation of the hanging wall during the second phase.

The detailed geologic map (Fig 27) illustrates map patterns that support portions of the above tectonic models. The Mill Spring and Brindle Creek thrust sheets resemble Griffin's (1974) Walhalla and Six Mile nappes in South Carolina, but Griffin (1974) failed to recognize multiple plastic deformation episodes. The lineation trends (NE-SW, E-W, and NW-SE) and sheath fold axes support Davis' (1993) and Hatcher's (1998) crustal flow model for the Inner Piedmont. Evidence of disharmonic deformation in the Brindle Creek hanging wall support Hill's (1999) two-stage oblique collisional model. Macroscopic evidence of a polyphase deformation includes the truncation of F_1 and F_2 folds by the Sugarloaf Mountain, Mill Spring, and Brindle Creek thrusts. Mineral stretching lineations and sheath fold axes support a crustal flow model (Davis, 1993; Hatcher, 1998), whereas map patterns provide additional support for Hill's (1999) two-stage oblique collisional model. Therefore, this portion of the Inner Piedmont experienced a polyphase deformational history that included crustal flow during oblique collision.

SUMMARY

The Inner Piedmont was influenced by a high-temperature event at ~350 Ma, which is coeval with penetrative deformation and postdates major faulting and crystallization of deformed Ordovician plutons in the southern Appalachian crystalline core. Within the South Mountains, these events are documented by penetrative fabrics, P-T estimates of prograde mineral assemblages, zircon rim ages, and deformed Henderson, Walker Top, Toluca, and Dysartsville granitoids. Based on existing geochronology, zircon zoning, observed mineral assemblages, garnet morphologies, and garnet zoning profiles, we conclude that the Inner Piedmont was affected by a single prograde Late Devonian-early Mississippian event.

Because of the rarity of D_1 evidence and the penetrative nature of later deformations, D_1 must have occurred early and may be either a vestige of the Taconic orogeny or the relicts of the earliest stages of the Neoacadian event. We interpret D_2 to represent the Neoacadian orogeny because it represents peak metamorphic conditions. D_3 structures resulted from either late Neocadian deformation or early Alleghanian. Because of its brittle overprinting nature, D_4 is likely a result of late Alleghanian deformation. D_5 structures resulted from Mesozoic and younger crustal extension.

ACKNOWLEDGMENTS

Mapping contributions of Jack Whisnant, Greg Yanagihara, Scott Williams, and Joseph Hill in the Marion area are also acknowledged. We thank Ted Labotka, Larry Taylor, and Allen Patchen for assistance with interpretation of the EMP data. Any errors in this paper remain the responsibility of the authors. Detailed geologic mapping was funded by contracts 1434HQ97AG01720 and 98HQAG2026, 99HQAG0026 and 00HQAG0035 from the National Cooperative Geologic Mapping Program EDMAP component (administered by the U.S. Geological Survey) to RDH. Electron microprobe work at UTK was funded by NSF grant EAR-9814800 (to RDH) and by the UTK Science Alliance Center of Excellence Distinguished Scientist Stipend.

REFERENCES CITED

Abbott, R. N., and Raymond, L. A., 1984, The Ashe metamorphic suite, northwest North Carolina: Metamorphism and observations on geologic history: American Journal of Science, v. 284, p. 350-375.

Barker, F., 1979, Trondhjemite: Definition, environment and hypotheses of origin, *in* Barker, F., ed., Trondhjemites, Dacites, and Related Rocks: New York, Elsevier Scientific Publishing Company, p. 1-12.

Berman, R. G., 1990, Mixing properties of Ca-Mg-Fe-Mn garnets: American Mineralogist, v. 75, p. 328-334.

Bier, S. E., 2001, Geology of the southeastern South Mountains, North Carolina [unpublished M.S. thesis]: Knoxville, University of Tennessee, 162 p.

Bream, B. R., 1999, Structural and stratigraphic relationships of ortho- and paragneisses southwest of Marion, North Carolina [unpublished M.S. thesis]: Knoxville, University of Tennessee, 155 p.

Bream, B. R., Hatcher, R. D., Jr., Miller, C. F., and Fullagar, P. D., 2001, Geochemistry and provenance of Inner Piedmont paragneisses, NC and SC: Evidence for an internal terrane boundary?: Geological Society of America Abstracts with Programs, v. 33, p. 65.

Bream, B. R., Hatcher, R. D., Jr., Miller, C. F., and Fullagar, P. D., in review, Detrital zircon ages and Nd isotopic data from the southern Appalachian crystalline core, GA-SC-NC-TN: New provenance constraints for Laurentian margin paragneisses, *in* Tollo, R. P., Corriveau, L., McLelland, J., and Bartholomew, M. J., eds., Proterozoic evolution of the Grenville Orogen in North America: Boulder, Colorado, Geological Society of America Special Paper.

Butler, J. R., 1991, Chapter 8, Metamorphism, *in* Horton, J. W., Jr., and Zullo, V. A., eds., The geology of the Carolinas, Carolina Geological Society Fiftieth Anniversary Volume: Knoxville, University of Tennessee Press, p. 127-142.

Carrigan, C. W., Bream, B. R., Miller, C. F., and Hatcher, R. D., Jr., 2001, Ion microprobe analyses of zircon rims from the eastern Blue Ridge and Inner Piedmont, NC-SC-GA: Implications for the timing of Paleozoic metamorphism in the southern Appalachians: Geological Society of America Abstracts with Programs, v. 33, p. 7.

Chatterjee, N. D., and Johannes, W., 1974, Thermal stability and standard thermodynamic properties of synthetic 2M1 muscovite, $KAl_2AlSi_3O_{10}(OH)_2$: Contributions to Mineralogy and Petrology, v. 48, p. 89-114.

Conley, J. F., and Drummond, K. M., 1981, Geologic map and mineral resources summary of the northeast 1/4 Marion quadrangle, North Carolina: North Carolina Department of Natural Resources and Community Development and Tennessee Valley Authority GM 210–NE, scale 1:24,000.

Curl, D. C., 1998, Stratigraphy and structure of Wellford and Reidville quadrangles in part of the eastern Inner Piedmont, near Spartanburg, South Carolina [unpublished M.S. thesis]: Knoxville, University of Tennessee, 129 p.

Dallmeyer, R. D., 1988, Late Paleozoic tectonothermal evolution of the western Piedmont and eastern Blue Ridge, Georgia: controls on the chronology of terrane accretion and transport in the southern Appalachian orogen: Geological Society of America Bulletin, v. 100, p. 702-713.

Davis, T. L., 1993, Lithostratigraphy, structure, and metamorphism of a crystalline thrust terrane, western Inner Piedmont, North Carolina [unpublished Ph.D. dissertation]: Knoxville, University of Tennessee, 245 p.

Dennis, A. J., 1991, Is the central Piedmont suture a low-angle normal fault?: Geology, v. 19, p. 1081-1084.

Dennis, A. J., and Wright, J. E., 1997, Middle and Late Proterozoic monazite U-Pb ages, Inner Piedmont, South Carolina: Geological Society of America Abstracts with Programs, v. 29, p. 12.

Drake, A. A., Jr., Sinha, A. K., Laird, J., and Guy, R. E., 1989, The Taconic orogen, *in* Hatcher, R. D., Jr., Thomas, W. A., and Viele, G. W., eds., The Appalachian–Ouachita orogen in the United States: Boulder, Colorado, Geological Society of America, The Geology of North America, v. F–2, p. 101-177.

Dutrow, B. L., and Holdaway, M. J., 1989, Experimental determination of the upper thermal stability of Fe-staurolite + quartz at medium pressures: Journal of Petrology, v. 30, p. 229-248.

Ellis, M., and Watkinson, A. J., 1987, Orogen-parallel extension and oblique tectonics: The relation between stretching lineations and relative plate motions: Geology, v. 15, p. 1022-1026.

Ferry, J. M., and Spear, F. S., 1978, Experimental calibration of the partitioning of Fe and Mg between biotite and garnet: Contributions to Mineralogy and Petrology, v. 66, p. 113-117.

Garihan, J. E., Preddy, M. S., and Ranson, W. A., 1993, Summary of Mid-Mesozoic brittle faulting in the Inner Piedmont and nearby Charlotte belt of the Carolinas, *in* Hatcher, R. D., Jr., and Davis, T. L., eds., Studies of the Inner Piedmont geology with a focus on the Columbus Promontory: Carolina Geological Society Guidebook, p. 55-65.

Ghent, E. D., Stout, M. V., and Raeside, R. P., 1983, Plagioclase-clinopyroxene-garnet-quartz equilibria and the geobarometry and geothermometry of garnet amphibolites from Mica Creek, British Columbia: Canadian Journal of Earth Science, v. 20, p. 699-706.

Giorgis, S. D., 1999, Geology of the northwestern South Mountains near Morganton, North Carolina [unpublished M.S. thesis]: Knoxville, University of Tennessee, 186 p.

Goldsmith, R., Milton, D. J., and Horton, J. W., Jr., 1988, Geology of the Charlotte 1° x 2° quadrangle, North Carolina and South Carolina: U.S. Geological Survey Map I–1251–E, scale 1:250,000.

Griffin, V. S., Jr., 1971, The Inner Piedmont belt of the southern crystalline Appalachians: Geological Society of America Bulletin, v. 82, p. 1885-1898.

Griffin, V. S., 1974, Analysis of the Piedmont in northwest South Carolina: Geological Society of America Bulletin, v. 85, p. 1123-1138.

Griffitts, W. C., and Overstreet, W. C., 1952, Granitic rocks of the western Carolina Piedmont: American Journal of Science, v. 250, p. 777-789.

Hadley, J. B., and Nelson, A. E., 1971, Geologic map of the Knoxville quadrangle, North Carolina, Tennessee, and South Carolina: U.S. Geological Survey Miscellaneous Geologic Investigations Map I-654, scale 1:250,000.

Haller, J., 1956, Problee der tiefentectonik: Bauformen in Migmatit-Stockwerk der ostgronlandischen Kaledoniden: Geologische Rundschau, v. 45, p. 159-167.

Hatcher, R. D., Jr., 1969, Stratigraphy, petrology, and structure of the low rank belt and part of the Blue Ridge of northwesternmost South Carolina: South Carolina Division of Geology, Geologic Notes, v. 13, p. 105-141.

Hatcher, R. D., Jr., 1970, Stratigraphy of the Brevard zone and Poor Mountain area, northwestern South Carolina: Geological Society of America Bulletin, v. 81, p. 933-940.

Hatcher, R. D., Jr., 1972, Developmental model for the southern Appalachians: Geological Society of America Bulletin, v. 83, p. 2735-2760.

Hatcher, R. D., Jr., 1978, Tectonics of the western Piedmont and Blue Ridge: Review and speculation: American Journal of Science, v. 278, p. 276-304.

Hatcher, R. D., Jr., 1987, Tectonics of the southern and central Appalachian internides: Annual Review of Earth and Planetary Science, v. 15, p. 337-362.

Hatcher, R. D., Jr., 1989, Tectonic synthesis of the U.S. Appalachians, *in* Hatcher, R. D., Jr., Thomas, W. A., and Viele, G. W., eds., The Appalachian-Ouachita orogen in the United States: Boulder, Colorado, Geological Society of America, The Geology of North America, v. F-2, p. 511-535.

Hatcher, R. D., Jr., Miller, C. F., and Lamb, D. D., 1995, Deformation processes related to emplacement of the Rabun Granite in the eastern Blue Ridge, Georgia and North Carolina, *in* Driese, S. G., ed., Guidebook for field trip excursions, Southeastern Section, GSA: Knoxville, Tennessee, University of Tennessee, Department of Geological Sciences, Studies in Geology 24, p. 39–56.

Hatcher, R. D., Jr., 1998, Structure of the Appalachian Inner Piedmont: Geological Society of America Abstracts with Programs, v. 30, p. 17.

Hatcher, R. D., Jr., 2001, Terranes and terrane accretion in the southern Appalachians: an evolved working hypothesis: Geological Society of America Abstracts with Programs, v. 33, p. 65.

Hatcher, R. D., Jr., and Goldberg, S. A., 1991, Blue Ridge Geologic Province, *in* Horton, J. W., Jr., and Zullo, V. A., eds., The geology of the Carolinas, Carolina Geological Society Fiftieth Anniversary Volume: Knoxville, University of Tennessee Press, p. 11-35.

Hatcher, R. D., Jr., and Hooper, R. J., 1992, Evolution of crystalline thrust sheets in the internal parts of mountain chains, *in* McClay, K. R., ed., Thrust tectonics: London, Chapman and Hall, p. 217-234.

Hatcher, R. D., Jr., Bream, B. R., Hill, J. C., Giorgis, S. D., and Williams, S. D., 1999, Transect through the Acadian orogen in the Carolinas and northeast Georgia: Geological Society of America Abstracts with Programs, v. 31, p. 19.

Hibbard, J., 2000, Docking Carolina: Mid-Paleozoic accretion in the southern Appalachians: Geology, v. 28, p.127-130.

Hill, J. C., 1999, Stratigraphy, structure, and tectonics of part of the southern Appalachian Inner Piedmont, near Marion, North Carolina [unpublished M.S. thesis]: Knoxville, University of Tennessee, 188 p.

Holdaway, M. J., 1971, Stability of andalusite and the aluminum silicate phase diagram: American Journal of Science, v. 271, p. 97-131.

Hopson, J. L., and Hatcher, R. D., Jr., 1988, Structural and stratigraphic setting of the Alto allochthon, northeast Georgia: Geological Society of America Bulletin, v. 100, p. 339-350.

Horton, J. W., Jr., and McConnell, K. I., 1991, The Western Piedmont, Chapter 3, *in* Horton, J. W., Jr., and Zullo, V. A., eds., The geology of the Carolinas, Carolina Geologic Society Fiftieth Anniversary Volume: Knoxville, Tennessee, The University of Tennessee Press, p. 36-58.

Horton, J. W., Jr., Drake, A., and Rankin, D., 1989, Tectonostratigraphic terranes and their Paleozoic boundaries in the central and southern Appalachians, *in* Dallmeyer, R. D., ed., Terranes in the circum-Atlantic Paleozoic orogens: Geological Society of America Special Paper 230, p. 213-245.

Irvine, T. N., and Baragar, W. R. A., 1971, A guide to the chemical classification of common rocks: Canadian Journal of Earth Science, v. 8, p. 523-548.

Kalbas, J. L., Bream, B. R., Hatcher, R. D., Jr., and Maybin, A. H., 2002, Evidence for mafic Ordovician magmatism in the Brushy Mountains, western Inner Piedmont of North Carolina: Geological Society of America Abstracts with Programs, v. 34, p. 119.

Keith, A., and Sterrett, D. B., 1931, Description of the Gaffney and Kings Mountain quadrangles, S. C.-N. C.: U. S. Geological Survey Folio 222, 18 p.

King, P. B., 1955, A geologic cross-section across the southern Appalachians, an outline of the geology in the segment in Tennessee, North Carolina, and South Carolina, *in* Russell, R. J., ed., Guides to southeastern geology: Geological Society of America Annual Meeting, p. 332-373.

Koziol, A. M., 1989, Recalibration of the garnet-plagioclase-Al_2SiO_5-quartz (GASP) geobarometer and applications for natural parageneses: EOS, v. 70, p. 493.

Labotka, T. C., 1987, The garnet + hornblende isograd in calcic schists from an andalusite-type regional metamorphic terrain, Panamint Mountains, California: Journal of Petrology, v. 28, p. 323-354.

Leake, B. E., 1964, The chemical distinction between ortho- and para-amphibolites: Journal of Petrology, v. 5, p. 238-254.

Lemmon, R. E., 1973, Geology of the Bat Cave and Fruitland quadrangles and the origin of the Henderson Gneiss, western North Carolina [unpublished Ph.D. dissertation]: Chapel Hill, University of North Carolina, 145 p.

Liu, A., 1991, Structural geology and deformation history of the Brevard fault zone, Chauga belt, and Inner Piedmont, northwestern South Carolina and adjacent areas [Ph.D. dissertation]: Knoxville, Tennessee, University of Tennessee, 200 p.

Mapes, R. W., 2002, Geochemistry and geochronology of mid-Paleozoic granitic plutonism in the southern Appalachian Piedmont terrane, North Carolina-South Carolina-Georgia [unpublished M.S. thesis]: Nashville, Vanderbilt University, 150 p.

Meschede, M., 1986, A method of discriminating between different types of mid-oceanic ridge basalts and continental tholeiites with the Nb-Zr-Y diagram: Chemical Geology, v. 56, p. 207-218.

Moecher, D. P., and Miller, C. F., 2000, Precise age for peak granulite facies metamorphism and melting in the eastern Blue

Ridge from SHRIMP U-Pb analysis of zircon: Geological Society of America Abstracts with Programs, v. 32, p. 63.

Nelson, A. E., Horton, J. W., Jr., and Clarke, J. W., 1998, Geologic map of the Greenville 1˚ x 2˚ quadrangle, Georgia, South Carolina, and North Carolina: U.S. Geological Survey Miscellaneous Investigations Series Map I–2175, scale 1:250,000.

Osberg, P. H., Tull, J. F., Robinson, P., Hon, R., and Butler, J. R., 1989, The Acadian orogen, Chapter 4, *in* Hatcher, R. D., Jr., Thomas, W. A., and Viele, G. W., eds., The Appalachian-Ouachita orogen in the United States: Boulder, Colorado, Geological Society of America, The Geology of North America, v. F-2, p. 179-232.

Overstreet, W. C., Whitlow, J.W., White, A. W., and Griffits, W. R., 1963a, Geologic map of the southern part of the Casar quadrangle, Cleveland, Lincoln, and Burke Counties, North Carolina: United States Geological Survey Field Studies Map MF-252, scale 1:24,000.

Overstreet, W. C., Yates, R. G., Griffits, W. R., 1963b, Geologic map of the Shelby 15-minute quadrangle, North Carolina: United States Geological Survey Miscellaneous Geologic Investigations Map 1-384, scale 1:62,500.

Passchier, C. W., Myers, J. S., and Kroner, A., 1990, Field geology of high-grade gneiss terrains: New York, Springer-Verlag, 150 p.

Perchuk, L. L., Aranovich, L. Y., Podlesskii, K. K., Lavrant'eva, I. V., Gerasimov, V. Y., Fed'kin, V. V., Kitsul, V. I., Karsakov, L. P., and Berdnikov, N. V., 1985, Precambrian granulites of the Aldan shield, eastern Siberia, USSR: Journal of Metamorphic Geology, v. 3, p. 265-310.

Pettijohn, F. J., 1949, Sedimentary rocks: New York, Harper and Brothers, 526 p.

Pigage, L. C. and Greenwood, H. J., 1982, Internally consistent estimates of pressure and temperature; the staurolite problem: American Journal of Science, v. 282, p. 943-969.

Rankin, D. W., 1994, Continental margin of the eastern United States: Past and present, *in* Speed, R. C., ed., Phanerozoic evolution of North American continent-ocean transitions: Boulder, Colorado, Geological Society of America, Decade of North American Geology Continent-Ocean Transect Volume, p. 129-218.

Reed, J. D., and Bryant, B., 1964, Evidence for strike-slip faulting along the Brevard zone in North Carolina: Geological Society of America Bulletin, v. 75, p. 1177-1196.

Roper, P. J., and Dunn, D. E., 1973, Superposed deformation and polymetamorphism, Brevard zone, South Carolina: Geological Society of America Bulletin, v. 84, p. 3373-3386.

Schumann, P. L., 1988, Metamorphic history of the Alto allochthon and petrology of the adjacent Chauga Belt, Ayersville Quadrangle, Georgia [unpublished M.S. thesis]: Knoxville, University of Tennessee, 95 p.

Shelley, D., 1964, On myrmekite: American Mineralogist, v. 49, p. 41-52.

Shervais, J. W., 1982, Ti-V plots and the petrogenesis of modern and ophiolitic lavas: Earth and Planetary Science Letters, v. 59, p. 101-118.

Shufflebarger, T. E., 1961, Notes on relationships of Piedmont sedimentary rocks with emphasis on the Poor Mountain-Chauga River area, Oconee County, South Carolina: South Carolina Division of Geology, Geologic Notes, v. 5, p. 31-38.

Sinha, A. K., and Glover, L., III, 1978, U/Pb systematics of zircons during dynamic metamorphism: Contributions to Mineralogy and Petrology, v. 66, p. 305-310.

Sinha, A. K., Hund, E. A., and Hogan, J. P., 1989, Paleozoic accretionary history of the North American plate margin (central and southern Appalachians): Constraints from the age, origin, and distribution of granitic rocks, *in* Hillhouse, J., ed., Deep structure and past kinematics of accreted terranes: American Geophysical Union Monograph Series, p. 219-238.

Sloan, E., 1907, Catalogue of the mineral localities of South Carolina: South Carolina Geological Survey Bulletin, v. 2, 4th series, 505 p.

Sobolev, V. N., McCammon, C. A., Taylor, L. A., Snyder, G. A., and Sobolev, N. V., 1999, Precise Mössbauer milliprobe determination of ferric iron in rock-forming minerals and limitations of electron microprobe analysis: American Mineralogist, v. 84, p. 78-85.

Spear, F. S., 1993, Metamorphic phase equilibria and pressure-temperature-time paths: Chelsea, Michigan, Book Crafters, Inc., 799 p.

Spear, F. S., Hickmott, D. D., and Selverstone, J., 1990, Metamorphic consequences of thrust emplacement, Fall Mountain, New Hampshire: Geological Society of America Bulletin, v. 102, p. 1344-1360.

Streckeisen, A. L., 1976, To each plutonic rock its proper name: Earth Science Reviews, v. 12, p. 1-33.

Tabor, J. R., 1990, Geologic map of the Mill Spring quadrangle [unpublished mapping]: Knoxville, University of Tennessee, scale 1:24,000.

Tull, J. F., 1980, Overview of the sequence and timing of deformational events in the southern Appalachians: evidence from the crystalline rocks, North Carolina to Alabama, *in* Wones, D. R., ed., The Caledonides in the U.S.A.: Virginia Polytechnic Institute Department of Geological Sciences Memoir, no. 2, p. 167-177.

Vinson, S. B., 1999, Ion probe geochronology of granitoid gneisses of the Inner Piedmont, North Carolina and South Carolina [unpublished M.S. thesis]: Nashville, Vanderbilt, 84 p.

Vinson, S. B, and Miller, C. F., 1999, Constraints on timing of Inner Piedmont plutonism, N.C.-S.C., from ion microprobe U-Pb zircon analysis: Geological Society of America Abstracts with Programs, v. 31, p. A77.

Wegmann, C. E., 1935, Zur Deutung der Migmatite: Geologische Rundschau, v. 26, p. 303-350.

Werner, C. D., 1987, Saxonian granulites—Igneous or lithogenous. A contribution to the geochemical diagnosis of the original rocks in high-metamorphic complexes, *in* Gerstenberger, H., ed., Contributions to the geology of the Saxonian granulite massif: Leipzig, Akademie der Wissenschaften der DDR Zentralinstitut für Isotopen- und Strahlenforschung, p. 221-250.

Whisnant, J. S., 1975, Geology of the southeastern quarter of the Marion 15-minute quadrangle, North Carolina [unpublished M.S. thesis]: Chapel Hill, University of North Carolina, 50 p.

Whitten, E. H. T., 1966, Structural geology of folded rocks: Chicago, Rand McNally and Company, 663 p.

Williams, H., and Hatcher, R. D., Jr., 1983, Appalachian suspect terranes, *in* Hatcher, R. D., Jr., Williams, H., and Zietz, I., eds., Contributions to the tectonics and geophysics of mountain chains: Geological Society of America Memoir 158, p. 33-53.

Williams, S. T., 2000, Geology, structure, and migmatization in the Inner Piedmont near Morganton, North Carolina [unpublished M.S. thesis]: Knoxville, University of Tennessee, 111 p.

Yanagihara, G. M., 1994, Structure, stratigraphy, and metamorphism of a part of the Columbus Promontory, western Inner Piedmont, North Carolina [unpublished M.S. thesis]: Knoxville, University of Tennessee, 214 p.

Carolina Geological Society
Annual Field Trip
October 19-20, 2002

Geology of the southwestern Brushy Mountains, North Carolina Inner Piedmont: A summary and synthesis of recent studies

Arthur J. Merschat

James L. Kalbas[a]

Department of Geological Sciences
University of Tennessee–Knoxville
306 Geological Sciences Building
Knoxville, TN 37996–1410
arthurmerschat@hotmail.com

present address:
[a]*Earth & Atmospheric Sciences, Purdue University, West Lafayette, IN 47907-1397*

ABSTRACT

Recent detailed work in a ~397 km² (~154 mi²) area at the southwestern termination of the Brushy Mountains in western North Carolina provides new insight into the geologic history of the Inner Piedmont. Three crystalline thrust sheets are recognized: the Marion, Mill Spring, and Brindle Creek thrust sheets. The Marion thrust sheet contains rocks of the Tallulah Falls/Ashe Formation, and the Henderson Gneiss. The Green Mountain fault may be the northern extension of the Mill Spring thrust and places muscovite schist and migmatitic mafic and intermediate metaigneous rocks of the Mill Spring thrust sheet over the Marion thrust sheet. The Brindle Creek thrust is the boundary between the western and eastern Inner Piedmont. The Brindle Creek thrust sheet contains a lithostratigraphy that is different from rocks immediately to its northwest, consisting of two sillimanite schist units separated by a metagraywacke unit. These metasedimentary units were intruded by the Devonian Walker Top and Toluca Granites.

The occurrence of sillimanite and K-feldspar and the absence of muscovite suggest that rocks locally attained second sillimanite grade metamorphic conditions. Second sillimanite grade rocks exist as lenses and pods within the assemblage of migmatitic, upper amphibolite facies rocks. P-T estimates from equilibrium garnet-biotite rim assemblages range from 585° C, 2.8 kbar to 710° C, 4.7 kbar. Estimates from garnet cores yield 450° C, 1.3 kbar, to 570° C, 2.5 kbar. Smooth zoning profiles, similar mineral phases preserved in garnet cores as in equilibrium with the garnet rims, and an increase in temperature from garnet cores to rims suggests continuous prograde metamorphism. These estimates define

Merschat, A. J., and Kalbas, J. L., 2002, Geology of the southwestern Brushy Mountains, North Carolina Inner Piedmont: A summary and synthesis of recent studies, *in* Hatcher, R.D., Jr., and Bream, B.R., eds., Inner Piedmont geology in the South Mountains-Blue Ridge Foothills and the southwestern Brushy Mountains, central-western North Carolina: North Carolina Geological Survey, Carolina Geological Society annual field trip guidebook, p. 101–126.

a counterclockwise P-T path for the rocks of the Brindle Creek thrust sheet/eastern Inner Piedmont that follows a trajectory indicative of Buchan metamorphism. Preliminary data suggest that rocks of the western Inner Piedmont followed an opposite path typical of Barrovian metamorphism. The contrasting P-T paths of the western and eastern Inner Piedmont suggest that the rocks of the Brindle Creek thrust sheet/eastern IP were emplaced hot onto cooler rocks of the western Inner Piedmont. Emplacement of a hot thrust sheet is a viable explanation of the zone of intense migmatization in the footwall of the Brindle Creek thrust sheet. Timing of metamorphism is ~350 Ma. These dates are constrained by U-Pb ages of zircon rims from the southwestern Brushy Mountains.

The study area is polydeformed; six deformational episodes are recognized. D_1, D_2 and D_3 are ductile deformations possibly related to one protracted Neoacadian to early Alleghanian tectonothermal event of which D_2 is responsible for the majority of the penetrative fabrics and major structures. Three later episodes were superposed on the earlier fabrics and structures at considerably lower temperatures and pressures. The NE-SW trends that dominate the southwestern Brushy Mountains are interpreted to be the result of buttressing NW-directed crystalline thrust sheets against the primordial Acadian Brevard fault zone. The primordial Brevard fault zone, ~ 15 km (9 mi) thick near the study area, is a crustal-scale shear zone that deflected the west-verging Inner Piedmont thrust sheets to the SW. In the southwestern Brushy Mountains, the Brindle Creek thrust may have a greater displacement and a greater strike-slip component than in other areas to the south.

INTRODUCTION

Orogenic cores contain the roots of mountain belts, exposing the complex internal workings of a mountain chain. These areas are crustal scale blending zones where primary sedimentary/volcanic structures are eradicated and existing stratigraphies are masked. Rocks of different affinities are juxtaposed and new rocks are created via anatexis. The complexity of orogenic cores often obscures their evolution, both spatially and temporally. Deciphering the history of these terranes yields important information about the crustal evolution.

This study examines a part of the Inner Piedmont (IP), the Acadian orogenic core of the southern Appalachians (Hatcher, 1987, 1989). The IP consists of a stack of west-verging crystalline thrust sheets containing dominantly high-grade metamorphic rocks (e.g., Griffin, 1969; Hatcher, 1969; Davis, 1993a, 1993b). The recent separation of two internal terranes, the western and eastern IP, resulted from integrating detailed geologic mapping, structural analysis, geochronology, and geochemistry (Bream et al., 2001; Mapes et al., 2002).

This paper summarizes the results of the first detailed 1:24,000-scale geologic mapping in the Brushy Mountains, western North Carolina. Rankin et al. (1972), Espenshade et al. (1975), and Goldsmith et al. (1988) conducted reconnaissance mapping in this area. Reed (1964a) also mapped the nearby Lenoir 15-minute quadrangle at 1/62,500-scale. These studies developed a geologic framework that is refined here. The study area covers ~397 km^2 (~154 mi^2) at the southwestern end of the Brushy Mountains, between Lenoir and Taylorsville, North Carolina. Our work, predominantly consisting of geologic mapping, was conducted in the Kings Creek, Ellendale, and southern third of the Boomer, North Carolina 7.5-minute quadrangles (Fig. 1). The study area uniquely straddles the boundary between the western and eastern IP. It is located northeast of previous studies in the Columbus Promontory and South Mountains, permitting along-strike correlations with these studies. At the present erosion level, the western IP narrows northward along strike, diminishing the outcrop width of the western IP. This provides a unique opportunity to examine a telescoped portion of the western IP and compare it with the deeper portions of the eastern IP. Detailed mapping, structural analysis, and petrologic and geothermobarometric data presented herein additionally characterize distinct patterns recognized by previous workers in other parts of the IP, principally by Overstreet et al. (1963) and Goldsmith et al. (1988). The purpose of this paper is to present new data and ideas about the evolution of the Acadian orogenic core in the southern Appalachians.

GEOLOGIC SETTING

The IP is one of the largest areas of sillimanite grade rocks in the world, extending from southwest of the Sauratown Mountains window in North Carolina to Alabama (Fig. 1; Hatcher, 1989). It is bounded to the west by the Brevard fault zone (BFZ) and to the east by a series of faults referred to as the Central Piedmont suture (Hatcher and Zietz, 1980; Horton and McConnell, 1991). It consists of a stack of crystalline thrust sheets containing an assemblage of intensely deformed para- and orthogneisses (Griffin, 1969; Hopson and Hatcher, 1988; Davis, 1993a, 1993b;

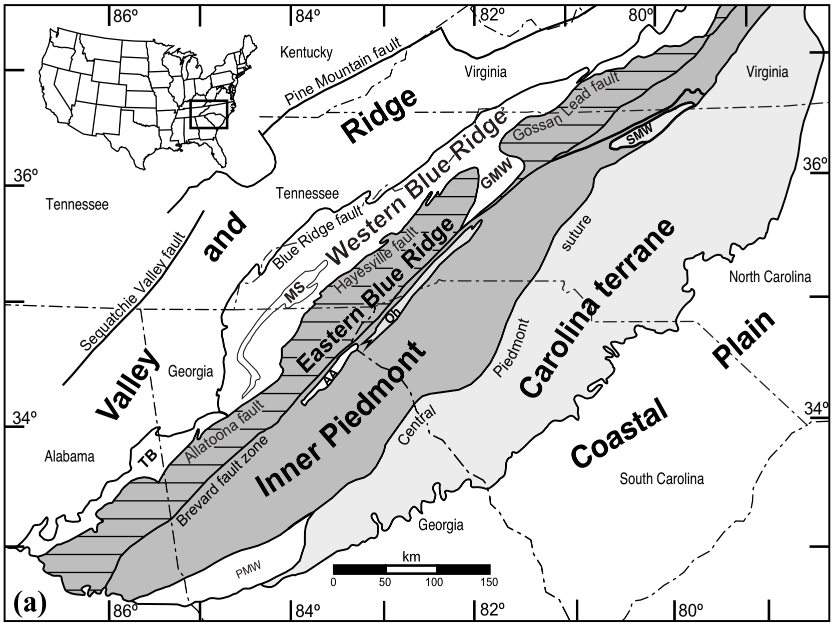

Figure 1. (a) Generalized geologic map of the southern Appalachian orogen. AA – Alto allochthon; GMW – Grandfather Mountain window; Oh – Henderson Gneiss; MS – Murphy syncline; PMW – Pine Mountain window; SMW – Sauratown Mountains window; TB – Talladega belt. Modified from Hatcher (1989). (b) Tectonic map of the North Carolina Inner Piedmont, showing the major thrust sheets, bounding faults and major plutons. SRA – Smith River Allochthon; SMW – Sauratown Mountains window; FF – Forbush fault; RsF – Rosman fault; MF – Marion fault; SMtF – Sugarloaf Mountain fault; MST – Mill Spring thrust; BCT – Brindle Creek thrust; bcr – Brooks Crossroads pluton; Od – Dysartsville tonalite; Oh – Henderson Gneiss; Dt – Toluca Granite; Mc – Cherryville Granite; sm – Sandy Mush Granite; rf – Rocky Face pluton; Hk – Hickory; Hv – Hendersonville; Sh – Shelby. Modified from Hatcher (this guidebook, his Fig. 1b).

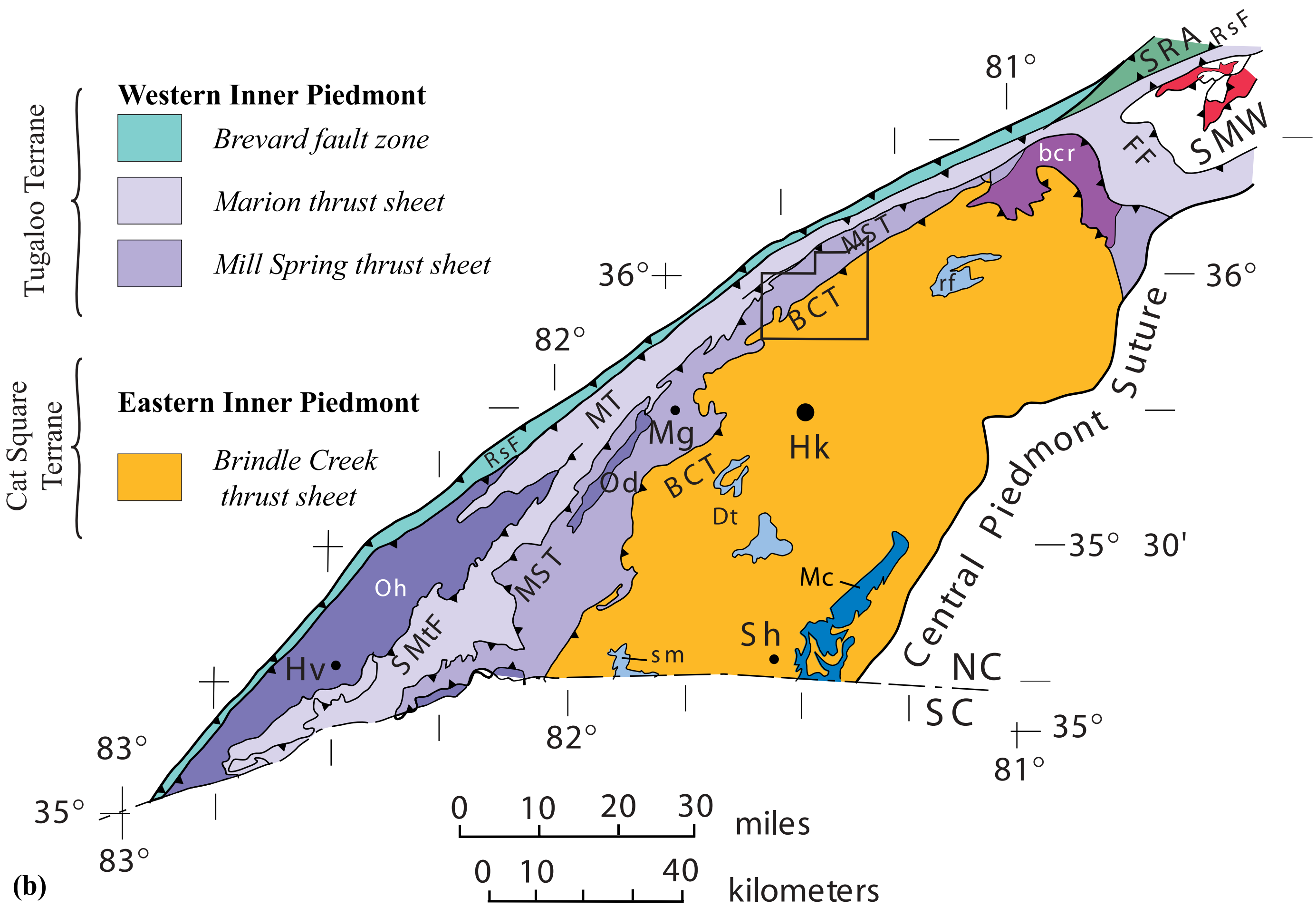

Garihan, 2001). Detailed geologic mapping, geochronologic, and geochemical data have revealed a lithostratigraphy and the separation of the IP into the western and eastern subdivisions (Bream et al., 2000; Bream, this guidebook).

Various workers have documented the geometry of IP crystalline thrust sheets. Griffin (1969, 1974a, 1974b) outlined the geometries and kinematics of the Walhalla, Six Mile, and Anderson nappes in South Carolina. Hatcher and Hooper (1992) related the evolution of these faults to Type-F faulting wherein, the common limb between a ductile antiform and synform is attenuated. Davis (1993a, 1993b) and Yanagihara (1993, 1994) described the geometries of the thrust sheets in the Columbus Promontory, North Carolina, and Davis developed a viable kinematic model for the IP, involving southwest deflection of west- and northwest-verging thrust sheets against the primordial (Acadian) BFZ (Davis, 1993a, 1993b). Finally, recent mapping near and within the South Mountains, North Carolina (Bream, 1999; Hill, 1999; Williams, 2000) recognized correlative thrusts with similar geometries described by previous workers, and defined at least one new fault, the Brindle Creek fault (Giorgis, 1999).

The Brindle Creek thrust, first defined and described as a low-angle Type-F thrust by Giorgis (1999), is now recognized as the boundary separating the western and eastern IP (Bream et al., 2001; Hatcher, this guidebook). Bream et al. (2001) proposed that it separates two internal terranes, the Tugaloo and Cat Square terranes of Hatcher (this guidebook). The subdivision is based principally on new detrital zircon age data that preclude correlation across the fault. An additional criterion for subdividing the IP is structural style and partitioning of an extensive belt of Ordovician plutons to the west from a group of Devonian-Mississippian plutons to the east (Mapes et al., 2002; Bream, this guidebook; Hatcher, this guidebook). The lateral continuity of map units in the Charlotte (Goldsmith et al., 1988) and Winston-Salem, North Carolina-Virginia-Tennessee

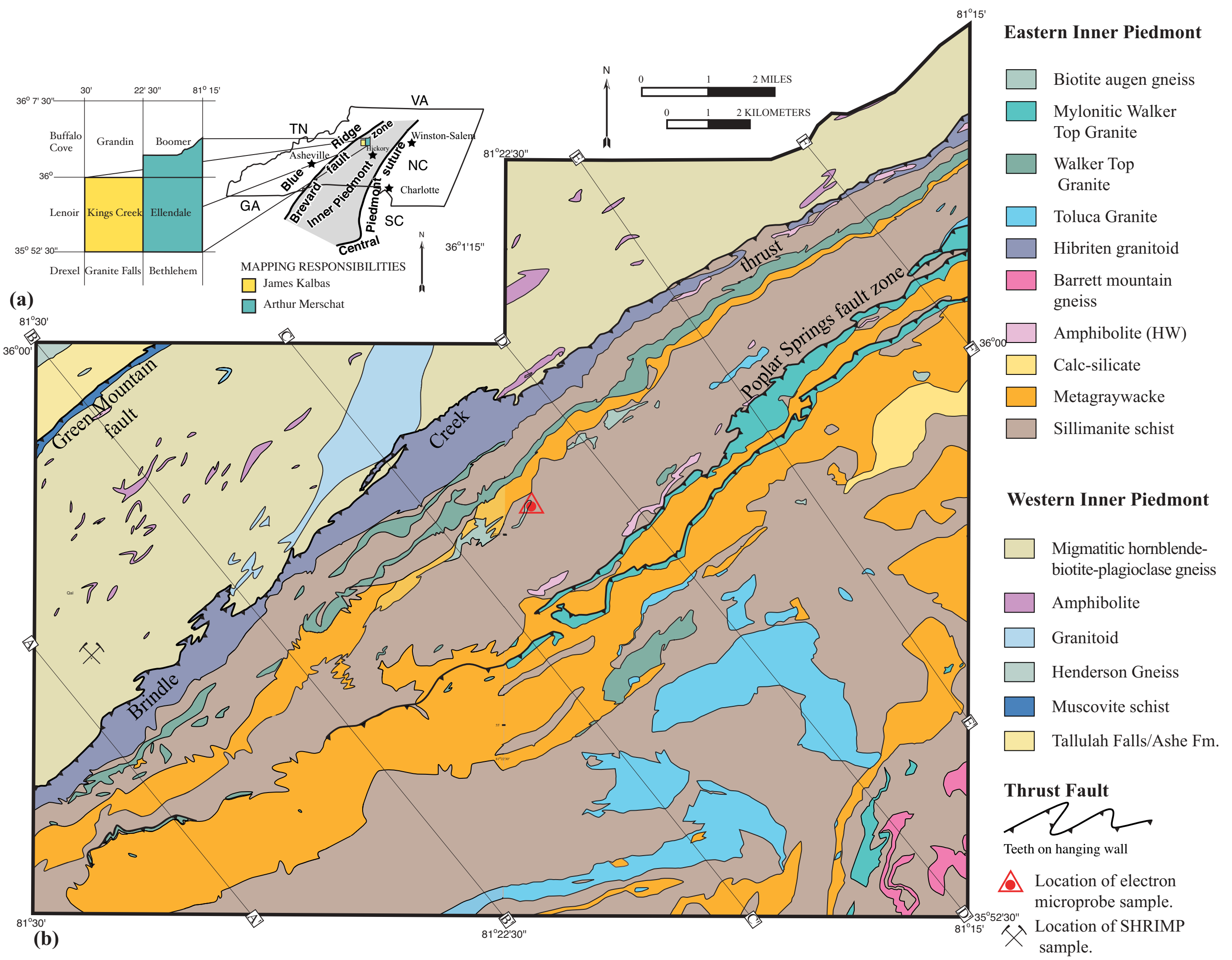

Figure 2. Geologic map and cross sections of the study area. (a) Index map showing location, 7.5-minute quadrangles, and mapping responsibilities. (b) Geologic map of the southwestern Brushy Mountains, NC. (c) Tectonic map (next page). (d) Metamorphic index map. (e) Cross sections. GMF – Green Mountain fault; BCT – Brindle Creek thrust; PSFZ – Poplar Springs fault zone.

(Rankin et al., 1972, Espenshade et al., 1975) 1°x 2° sheets suggests that the Brindle Creek thrust is a major structure that can be traced from near the southwest end of the Sauratown Mountains window in North Carolina and across South Carolina and possibly into Georgia (Hatcher, this guidebook, his Fig. 1b). Based on new detrital zircon age components in metasandstones, the Brindle Creek thrust juxtaposes rocks of the eastern IP as young as Silurian over older rocks of the western IP.

The western IP consists of early Paleozoic deep-water metasedimentary and metavolcanic rocks of the Tallulah Falls/Ashe Formation (Tallulah Falls) intruded by the Henderson Gneiss and overlain by the Middle Ordovician Poor Mountain Formation MORB volcanic rocks (Hatcher, 1969, 1972; Davis 1993b; Yanagihara, 1993; Kalbas et al., 2002; Bream, this guidebook; Hatcher, this guidebook). Detailed descriptions of the stratigraphy in the western IP were presented by Hatcher (1969, 1972, 1993), and Davis (1993a, 1993b). The western IP is characterized by; NE-SW trending units and structural features, a mappable stratigraphy dominated by metagraywacke with subordinate aluminous schist, amphibolite, and quartzite/metatuff, and Ordovician magmatism. Magmatic ages of plutons in the western IP cluster around 490 Ma and 465 Ma, and have similar chemistry (Mapes et al., 2001; Vinson, 2001; Kalbas et al., 2002; Mapes et al., 2002). The eastern IP is dominated by aluminous schist and subordinate metagraywacke that were deposited from the Silurian to the Early Devonian based on detrital zircons (Bream et al., 2001; Bream, this guidebook). A detailed lithostratigraphy has not been constructed for the eastern IP. Granitoids in the eastern IP have magmatic ages of 375-360 Ma (Vinson, 2001; Mapes et al., 2002) and intraplate tectonic affinity (Davis et al., 1962; Giorgis, 1999; Bier, 2001, Mapes et al., 2001; Vinson, 2001; Mapes et al., 2002).

Metamorphism is first sillimanite grade in most of the IP, but drops to staurolite-kyanite and garnet grade on the flanks (Butler, 1991). There are substantial data now to indicate that timing of metamorphism in the IP was Neoacadian. Dennis and Wright (1997) determined ages of ~360 and ~320 Ma from conventional U-Pb dating of monazite in the South Carolina IP. Bream (unpublished data) and

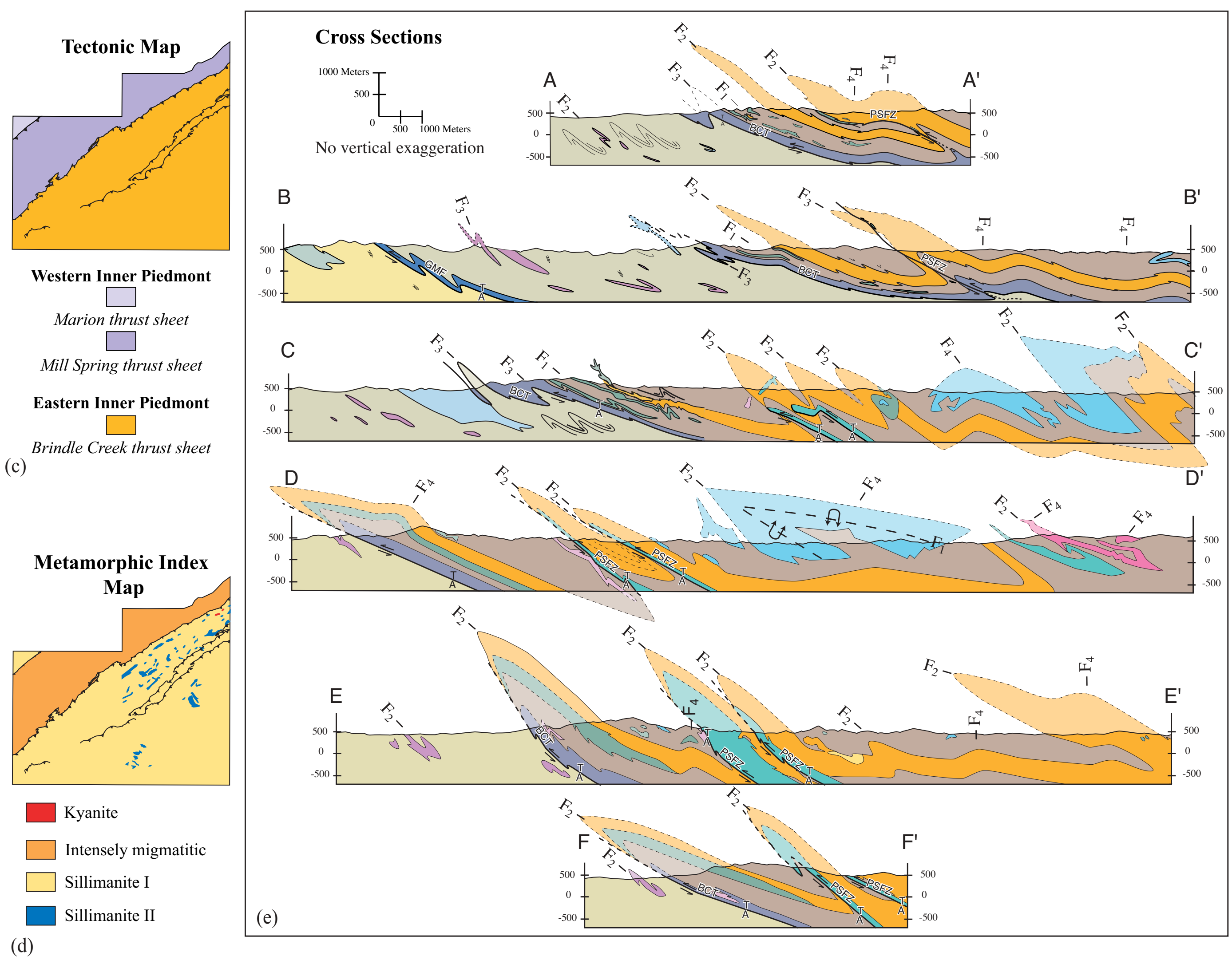

Figure 2. (continued)

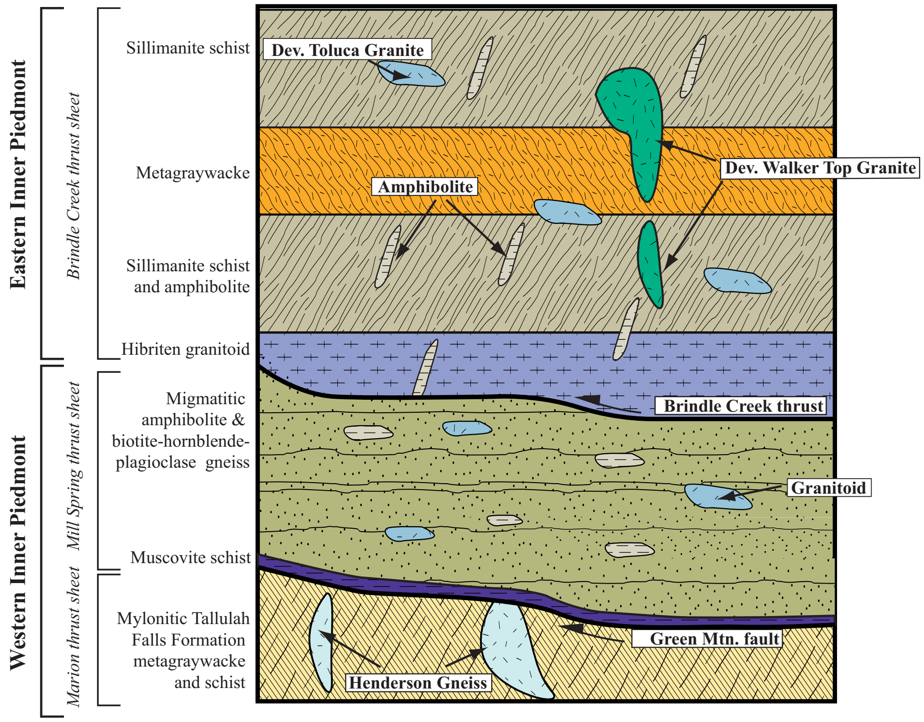

Figure 3. Generalized lithologic column for the study area.

Kalbas et al. (2002) determined ion probe U-Pb ages of ~350 Ma from metamorphic rims on zircons in the study area (Fig. 2). These ages are younger than traditional 380-360 Ma ages of the Acadian orogeny prompting Kohn (2001) and Hatcher (this guidebook) to employ the term Neoacadian.

LITHOSTRATIGRAPHY

Detailed geologic mapping in the Brushy Mountains has confirmed the general lithologic framework recognized during previous reconnaissance mapping (e.g., Rankin et al., 1972; Goldsmith et al., 1988), and has produced more precise surface map unit configurations and revealed significantly greater meso- and macroscale complexity (Fig. 2). Two faults, the Brindle Creek thrust and a second fault herein named the Green Mountain fault, separate the southwestern Brushy Mountains into three crystalline thrust sheets containing several lithologic units (Figs. 2 and 3). The lowest (northwesternmost) thrust sheet is referred to as the Marion thrust sheet, and is overlain by the Mill Spring thrust sheet. Finally, the Brindle Creek thrust sheet juxtaposes eastern IP rocks against western IP rocks. The Poplar Springs fault zone is an internal fault within the Brindle Creek thrust sheet.

The name Marion thrust sheet is proposed here to incorporate those rocks in the footwall of the Green Mountain fault. This thrust sheet terminates to the northwest outside of the study area, making this description incomplete. It is likely that Tallulah Falls rocks of the hanging wall of this thrust sheet rest against footwall rocks of the Chauga River Formation (Hatcher, 1969) to the northwest in the BFZ. In the study area, the rocks exposed in the footwall of the Green Mountain fault include mylonitic metagraywacke of the Tallulah Falls Formation and Henderson Gneiss. Reed (1964a, 1964b) and Bryant and Reed (1970) mapped muscovite schist, biotite gneiss/metagraywacke, ultramafic rocks, and Henderson Gneiss in the Marion thrust sheet to the west and southwest of the study area.

The Green Mountain fault hanging wall exposes migmatitic metagranodiorite, amphibolite, and muscovite schist over Tallulah Falls metagraywacke, and Henderson Gneiss of the Marion thrust sheet. The Sugarloaf Mountain thrust to the southwest terminates near Sugar Hill, North Carolina (Bream, 1999). The Mill Spring thrust is the remaining fault that juxtaposes Tallulah Falls Formation and Poor Mountain Formation rocks onto rocks of the Tallulah Falls Formation and Henderson Gneiss (Davis, 1993a, 1993b; Yanagihara, 1994; Hill, 1999). Based on similarity of lithostratigraphic units and structural position, the Green Mountain fault is the best candidate for the northern continuation of the Mill Spring thrust. Despite slight differences in the geometries of the Green Mountain fault and Mill Spring thrust (discussed below), this thrust sheet is referred to as the Mill Spring thrust sheet.

The Brindle Creek thrust juxtaposes Silurian to Devonian pelitic schist, metagraywacke, and Devonian metaigneous rocks against migmatite of the Mill Spring thrust sheet. Various workers (Overstreet et al., 1963; Goldsmith et al., 1988; Giorgis, 1999; Williams, 2000; Bier, 2001) have recognized a similar lithostratigraphy including sillimanite schist and metagraywacke intruded by Toluca Granite, and Walker Top Granite. The Poplar Springs fault zone repeats units within the Brindle Creek thrust sheet.

Marion Thrust Sheet

Henderson Gneiss. The Henderson Gneiss is the northwesternmost unit in the southwestern Brushy Mountains. Described first by Keith (1905, 1907) and later by Reed and Bryant (1964), the Henderson Gneiss is an easily recognizable monzogranitic, augen gneiss composed of microcline, oligoclase, quartz, biotite, and muscovite. Characteristic microcline augen commonly have metamorphic reaction rims of myrmekite and are typically 1 to 3 cm in diameter (Hatcher, 1993). The main body is traceable from near the South Carolina-Georgia border in South Carolina into central North Carolina (Lemmon, 1973; Lemmon and Dunn, 1975; Bream, 1999). It crops out entirely within the western IP in the footwalls of the Mill Spring and Sugarloaf Mountain thrusts and attains its greatest outcrop width in Henderson County near the type locality (Brown et al., 1985). Several workers, including Davis (1993a, 1993b) and Bream (1999) have enclosed the Henderson Gneiss in the Tumblebug Creek thrust. Northeast of Marion, North Carolina, the Henderson Gneiss occurs as a series of lenticular outliers that have been mapped with no surrounding faults (Reed, 1964a, 1964b). Hill (1999) reinterpreted some of these outliers near Marion, North Carolina to be fault bounded. The Brushy Mountains body crops out ~45 km northeast of and along strike with the main body. The emplacement of the Henderson Gneiss could not be accurately assessed in the study area. Less than 610 m (2,000 ft) of the Henderson Gneiss-Tallulah Falls Formation contact is exposed in the King Creek quadrangle. Moreover, our map (Fig. 2) does not include an entire body of the elliptical outliers shown by Reed (1964a, 1964b), Rankin et al., (1972) and Goldsmith et al., (1988), making it difficult to interpret the nature of the contact.

A variety of both Rb-Sr and conventional U-Pb ages are reported by several workers for the Henderson Gneiss (Odom and Fullagar, 1973; Odom and Russell, 1975; Sinha et al., 1989). The most recent and probably most reliable age is a $^{238}U/^{206}Pb$ ion microprobe age of ~490 Ma from zoned zircons (Carrigan et al., 2001).

Tallulah Falls Formation. The Henderson Gneiss dips beneath dark gray, mylonitic, fine- to coarse-grained, biotite-quartz-plagioclase gneiss/metagraywacke and biotite-muscovite schist. Reconnaissance mapping linked this mylonitic metagraywacke and schist with metasedimentary units of the Brindle Creek thrust sheet (Reed, 1964a, 1964b; Goldsmith et al., 1988); they are, however, restricted to the western IP (Fig. 2). The principal marker unit of the Tallulah Falls Formation, the garnet-aluminous schist member, does not crop out in the study area making it difficult to determine if the exposed metagraywacke belongs to the upper or lower member of the Tallulah Falls Formation. Based on the paucity of amphibolite observed in this unit, it is tentatively correlated to the graywacke-schist (upper) member of the Tallulah Falls Formation.

Tallulah Falls Formation rocks in the Kings Creek quadrangle are characterized by a mylonitic, inequigranular texture composed of subhedral and sheared composite quartz-plagioclase porphyroclasts in a fine- to medium-grained matrix. Representative matrix is composed of quartz (34-37%), biotite (23-30%), plagioclase (13-24%; An_{34-44}), muscovite (8-15%), and sillimanite (trace-3%). Accessory phases are K-feldspar, epidote, sericite, zircon, chlorite, and opaque minerals. Porphyroclasts are generally smaller than those in the Hibriten gneiss (~0.1 to <1.0 cm; discussed below), but produce a similar dimpled pattern on weathered surfaces. More intense weathering produces a reddish-brown schistose saprolite. The foliation in each sample is defined by parallel alignment of fine-grained quartz, biotite, muscovite, and less common plagioclase grains. In many cases, large (up to ~0.24 x 0.07 cm), deformed muscovite fish partially define a type II S-C mylonitic fabric.

Mill Spring thrust sheet

Muscovite Schist. Garnet-bearing, plagioclase-quartz-biotite-muscovite schist, quartz-muscovite-biotite schist, and quartz-rich schist are present in the immediate hanging wall of the Green Mountain fault. It is migmatitic and contains frequent lenses of medium- to coarse-grained quartzofeldspathic material in a sheared schistose fabric. Medium-grained, quartz, feldspar, biotite gneiss with a salt-and-pepper texture also occurs locally. Schist in the overlying migmatitic amphibolite and metagranodiorite unit that crops out adjacent to its northwestern contact may represent a gradational contact.

Lenoir Quarry migmatite. A heterogeneous assemblage of well-foliated, medium- to coarse-grained, intensely migmatized intermediate to mafic metaigneous rocks dominate the immediate footwall of the Brindle Creek fault in the southwestern Brushy Mountains. This heterogeneous migmatitic unit was recognized by previous workers (Reed, 1964a; Rankin et al., 1972; Goldsmith et al., 1988) as migmatitic biotite granodiorite, biotite-hornblende quartz diorite, and migmatitic granitic gneiss with frequent elongate blocks of massive amphibolite. Detailed geologic mapping during this study revealed a similar assemblage. Migmatite is exposed in a 6 km-wide, northeast-striking band that contains large (mappable) disconnected, elliptical amphibolite bodies that parallel the regional structural trend (Fig. 2). The amphibolite bodies in this unit are chemically similar to Poor Mountain Amphibolite (Kalbas, in progress). The internal structure, chemical composition, age, and petrogenesis of the migmatitic metagranodiorite and amphibolite are discussed in greater detail by Kalbas (in progress).

The migmatite unit is dominated by interlayered, continuous and discontinuous biotite gneiss, biotite-hornblende metagranodiorite, amphibolite, leucogranitoid and pegmatite and the textural variations of migmatite defined by Mehnert (1968). Amphibolite boudins are common in outcrop; large exposures of leucogranitoid are also typical. Amphibolite weathers to reddish-brown- to ochre-colored saprolite while more felsic fractions weather to gray to light orange or tan saprolite.

Modal abundances of the migmatitic metagranodiorite and amphibolite are reported by Kalbas (in progress), and will be summarized here. Meso- to leucocratic, migmatitic metagranodiorite contains hornblende, biotite, quartz and plagioclase. Muscovite, K-feldspar, myrmekite, and epidote are also variably present. Quartz-muscovite-biotite gneiss and micaceous quartzite are also present. Amphibolite layers and boudins are composed of hornblende, plagioclase, and quartz; biotite and epidote are common. Leucosomes are quartz and K-feldspar rich, and diatexite contains hornblende phenocrysts. Melanosomes are dominated by hornblende with variable amounts of plagioclase and other minor phases.

The Brindle Creek thrust sheet

Previous studies in the eastern IP have recognized variable lithologies. Overstreet et al. (1963) mapped seven different lithologic units based on sillimanite content. Giorgis (1999), Williams (2000), and Bier (2001) recognized an upper and lower metagraywacke units separated by an aluminous schist in the South Mountains. All of these workers also recognized intrusions of peraluminous Toluca Granite and Walker Top Granite. We mapped two sillimanite schist units separated by a metagraywacke unit. These units were then, similarly intruded by peraluminous granitoid (Toluca Granite) and megacrystic Walker Top Granite. The context of two units, the Hibriten gneiss and Barrett Mountain gneiss, is unknown at this point.

Hibriten granitoid. An inequigranular biotite gneiss was recognized at several locations in and to the southwest of the Brushy Mountains in the Charlotte 1˚ x 2˚ geologic map (Goldsmith et al., 1988). Detailed geologic mapping for this study revealed a garnet and locally amphibole-bearing, foliated, inequigranular biotite-quartz-plagioclase granitoid, and an amphibole bearing, quartz-plagioclase gneiss that crop out in the immediate hanging wall of the Brindle Creek thrust throughout most of the study area. Kalbas (in progress) informally named it the Hibriten granitoid for outcrops on the southeast slopes of Hibriten Mountain in the southwestern corner of the Kings Creek 7.5 minute quadrangle.

A characteristic texture of 0.25-1.0 cm diameter rounded and elongate plagioclase and less common quartz porphyroclasts in a dark gray, biotite-rich matrix is easily recognizable in outcrop. Moderately weathered exposures also retain a characteristic texture; plagioclase degrades first and creates a pattern of rounded dimples on surfaces. Complete weathering produces a reddish-brown schistose saprolite similar to decomposed exposures of adjacent metasedimentary rocks. The porphyroclastic biotite gneiss locally grades into porphyroclastic biotite schist. As with the adjacent metasedimentary rock units, local amphibolite layers and boudins are common and typically identified by sporadic float. Synthetic and discordant bands of hololeucocratic granitoid and pegmatite are common in outcrop.

The Hibriten granitoid is primarily composed of plagioclase (32-41%; An_{33-38}), quartz (2-29%), biotite (0-27%), and trace muscovite (0-1%). Accessory phases are hornblende, sericite (replaces plagioclase), garnet, rutile, sphene, apatite, epidote, sillimanite, chlorite, zircon, and opaque minerals. Rocks with either biotite- or amphibole-dominated matrices retain the characteristic porphyroclastic schistose texture. Amphibolite in the Hibriten granitoid is composed of hornblende (64%), quartz (19%), plagioclase (16%; An_{39}), and opaque minerals (4%). Accessory sericite, epidote, sphene, apatite, and zircon are also present.

Sillimanite schist. One of the two metasedimentary rock units that dominate the hanging wall of the Brindle Creek thrust is migmatitic, garnet-sillimanite-biotite-muscovite-quartz schist (here called sillimanite schist). The sillimanite schist unit contains three distinct lithologies: (1) coarse-grained, poikiloblastic muscovite, sillimanite schist; (2) migmatitic sillimanite schist (contains greater than 50% leucosome); and (3) garnet-biotite-sillimanite schist. Several bands of schist (undivided) are mappable in the southwestern Brushy Mountains; lithologies are similar, but a discernable stratigraphy is not evident. Most schist exposures are weathered along exposed surfaces and degrade to brown and purplish red saprolite. A well-developed foliation, pervasive throughout the sillimanite schist, is formed by the parallel alignment of biotite, muscovite, and fibrolitic sillimanite. Fibrolitic sillimanite is characteristic of the sillimanite schist and can usually be seen with 10x magnification. Meso-scale compositional banding of micaceous and quartzofeldspathic laminae is common. Amphibolite and calc-silicate float are also present, and several mappable bodies occur locally.

Both the sillimanite schist and metagraywacke (discussed below) contain variable percentages of medium- to coarse-grained, leucocratic granitoid and pegmatite. Granitoid and pegmatite can be divided into at least three structural/textural categories: (1) concordant deformed sills; (2) crosscutting deformed bodies; and (3) crosscutting, nondeformed (usually fracture-parallel) bodies. Evidence for anatectic and hydrothermally produced granitoid and pegmatite is pervasive throughout the Brindle Creek thrust sheet, but can be most easily seen in a series of outcrops along U. S. 64 (see Stop 14, Day 2, this guidebook).

Dominant minerals in the sillimanite schist are biotite (48-27%), quartz (13-45%), sillimanite (9-14%), muscovite (3-12%), plagioclase (0-7%; An_{20}), opaque minerals (trace-6%), and garnet (trace-7%). Accessory epidote, chlorite, apatite, and sericite are also present. Sillimanite schist has medium-grained, lepidoblastic texture.

Metagraywacke. The other metasedimentary rock unit in the Brindle Creek thrust sheet is migmatitic K-feldspar-plagioclase-biotite-quartz gneiss (metagraywacke). The metagraywacke is exposed as several northeast-trending bands that crop out adjacent to the sillimanite schist and Walker Top Granite (Fig. 2). It weathers to a reddish tan or light to dark greenish gray saprolite and frequently contains a significant percentage of quartzofeldspathic melt that weathers to a light tan to white, popcorn-textured saprolite with iron-oxide stain. As with the sillimanite schist, mesoscale compositional banding of micaceous and quartzofeldspathic laminae is common and amphibolite and calc-silicate float are variably present.

Variations in metagraywacke mineralogy may represent differences in protolith composition or degrees of migmatization. It is typically composed of quartz (37-49%), K-feldspar (2-32%), biotite (13-18%), plagioclase (13-28%; An_{25-31}), muscovite (trace-4%), hornblende (0-2%), and epidote (0-1%). Accessory phases are sillimanite, rutile, sphene, apatite, and opaque minerals.

Calc-Silicate. A mappable calc-silicate unit is located in the northeast corner of the Ellendale quadrangle and is closely related to the metagraywacke unit. It is a light gray to greenish gray, porphyroblastic to diablastic, hornblende-biotite-plagioclase-quartz granoblastite. It is often interlayered with minor amounts of quartzite and metagraywacke.

Dominant minerals in the calc-silicate are quartz (52%), biotite (20%), plagioclase (12%), hornblende (10%), and epidote (4%). Trace amounts of clinozoisite, tourmaline, monazite and opaque minerals are present. Dark green hornblende and epidote porphyroblasts are aligned to randomly oriented and range from 0.5 to 1 cm.

Walker Top Granite. The Walker Top Granite is easily recognized and is characterized by subhedral to euhedral K-feldspar phenocrysts/megacrysts in a medium-grained biotite, quartz, K-feldspar and plagioclase matrix (Giorgis, 1999; Vinson and Miller, 1999). It was first recognized by Goldsmith et al. (1988) as a poorly to moderately foliated, less-sheared, garnet-bearing version of the Henderson Gneiss. Both are dominated by large (2 cm to >10 cm) K-feldspar megacrysts with myrmekite rims. Megacrysts in Walker Top Granite, however, are typically subhedral to euhedral; aspect ratios range from 1:2 to 1:8 (Giorgis, 1999; Giorgis et al., this guidebook), whereas Henderson Gneiss megacrysts are sheared into an S-C fabric (Davis, 1993a). The matrix of the Walker Top Granite is darker (CI 40-50%) than Henderson Gneiss matrix (CI 20-40%). Geochronologic data preclude a genetic relationship between the Walker Top Granite and Henderson Gneiss. Mapes (2002) and Mapes et al. (2002) reported an Acadian (~370 Ma) ion microprobe U-Pb zircon crystallization age for the Walker Top Granite, in contrast with an Early Ordovician crystallization age of ~490 Ma for the Henderson Gneiss (Carrigan et al., 2001). Giorgis (1999) and Giorgis et al (this guidebook) defined the type area for the Walker Top Granite near Burkemont Mountain Road south of Kaylor Knob and Walker Top Mountain in the Morganton South 7.5 minute quadrangle.

Goldsmith et al. (1988) exaggerated the outcrop width of the Walker Top Granite in the South Mountains and southern Brushy Mountains in the Charlotte 1° x 2° sheet. Detailed mapping in the southwestern Brushy Mountians shows that it crops out as a series of linear, laterally extensive, and disconnected bodies that parallel the regional structural trend (Fig. 2). Similarly, more areally restricted outcrop belts of Walker Top Granite have been mapped in the South Mountains (Giorgis, 1999; Williams, 2000; Giorgis et al., this guidebook). In the southwestern Brushy Mountains, Walker Top Granite is bounded by metasedimentary units in the Brindle Creek thrust sheet (Fig. 2). Two disconnected bands of Walker Top Granite in the Kings Creek quadrangle coalesce into a uniform, continuous body in the Ellendale and Boomer quadrangles. In addition, several small (<0.1 km thick), discontinuous bodies of Walker Top Granite crop out southeast of the main bodies in the Brushy Mountains. Some outcrops in this band expose rocks with the characteristic megacrystic texture, while others contain mylonitic rocks with sheared or no megacrysts. The matrix weathers to an ochre-colored schistose saprolite similar to weathered metagraywacke.

The Walker Top Granite is a monzogranite to syenogranite to granodiorite (Giorgis, 1999; Bier, 2001; Giorgis et al., this guidebook). Its mineral assemblage consists of plagioclase (18-39%; An_{37-40}) and myrmekite, quartz (29-30%), microcline (16-30%), biotite (9-18%), muscovite (trace-5%), and garnet (0-1%). Trace amounts of epidote, sericite, apatite, zircon, and opaque minerals are present. A poorly to well-defined foliation in the Walker Top Granite consists of alignment of biotite crystals parallel to the c-axes of aligned microcline megacrysts.

Another unit mapped as biotite augen gneiss may actually be finer-grained Walker Top Granite. It is a garnet-bearing, megacrystic biotite-quartz-plagioclase-K-feldspar gneiss, except the subhedral to euhedral K-feldspar megacrysts range from 0.5 cm to 1 cm. This unit has an irregular outcrop pattern.

Mylonitic Walker Top Granite is a highly deformed augen gneiss that crops out in two bands within the Poplar Springs fault zone. The bands strike NE-SW and become disconnected pods and lenses to the SW. The extent and relationship of these units northeast of the study area is uncertain. Compositionally, these rocks are the same as the unsheared version, except for the rare occurrence of hornblende in the matrix. Rocks within these bands generally range from protomylonite to mylonite, with mantled K-feldspar porphyroclasts being sheared parallel to the strike of the unit.

Toluca Granite. Several disconnected bodies of peraluminous biotite granitoid intruded the paragneisses of the Brindle Creek thrust sheet. Reconnaissance mapping (Goldsmith et al., 1988) recognized some of these bodies and correlated them regionally with the Toluca Granite named by Griffits and Overstreet (1952). Mapes et al. (2001) reported a U-Pb ion microprobe zircon age of ~375 Ma. The Toluca Granite varies texturally from medium- to coarse-grained, massive to strongly foliated, and locally porphyritic. Typically, it is a garnet- and muscovite-bearing, uniform textured, weakly foliated biotite granitoid. The lack of a contact aureole, interfingering margins with the sillimanite schist and metagraywacke, elongate shape of bodies parallel to foliation, and continuation of foliation through the plutons suggest that these are catazonal plutons. Mapes (2002) concluded that the Toluca Granite is derived from partial anatexis of the surrounding country rocks based on the similarities of whole-rock chemistry and isotopic data (Sr, Nd, and O). Sharp contacts between the schist and Toluca Granite observed in the field preclude the idea of local generation of the Toluca Granite from country rocks. The granite, once formed, had to move into the metasedimentary assemblage.

Barrett Mountain Gneiss. Goldsmith et al. (1988) described two metamorphosed quartz diorite bodies near Barrett Mountain, in the southeast corner of the Ellendale quadrangle. This study refines the previous location of the bodies and recognizes several recumbent folds cored by this unit (Fig. 2). It is a dark gray, locally migmatitic, medium- to coarse-grained porphyroblastic, garnet-quartz-biotite-feldspar orthogneiss. The unit is well foliated with weak to moderate compositional banding. Stromatic migmatite is common; layers range from 1 cm to 1 m. No detailed isotopic or chemical data exist for this unit, so its age and origin are uncertain. The unit is in contact with sillimanite schist and appears to grade into mylonitic Walker Top Granite in the southeast corner of the Ellendale quadrangle. Goldsmith et al. (1988) mapped three other bodies of this unit where it often closely related spatially to the Walker Top Granite. Its occurrence near the Walker Top Granite may indicate consanguinity.

METAMORPHISM

The IP is one of the world's largest zones of sillimanite grade metamorphism. Although the grade of metamorphism is well established, the metamorphic history of these rocks remains enigmatic. Lemmon (1973) originally described two high-grade episodes of metamorphism in the western IP that were later refined to one prograde event by Davis (1993a, 1993b). Other studies in the South Mountains (e.g., Hill, 1999; Bier, 2001; Bream, this guidebook) have reconfirmed Davis' conclusions. Our study incorporates field and petrographic observations supplemented by electron microprobe data to document the metamorphic conditions.

Field indicators of metamorphic grade include index minerals in the aluminous schist and pervasive migmatite. Sillimanite is ubiquitous in the pelitic rocks of the Brushy Mountains, with few exceptions. The muscovite schist in the hanging wall of the Green Mountain fault lacks sillimanite, but the origin and composition of this schist is speculative (Kalbas, in progress). Kyanite is rare and occurs in a few outcrops of kyanite-garnet-biotite schist approximately 4 km (2 mi) south of Boomer, North Carolina, in the Brindle Creek thrust sheet. Careful examination of mineral abundances and textures in the field reveal two mineral assemblages for the aluminous schist. One assemblage is dominated by biotite, with little to no muscovite (garnet-biotite-sillimanite schist). Another assemblage contains little or no biotite, and possibly two generations of muscovite. Early muscovite is fine- to medium-grained and defines the dominant foliation. Later muscovite is postkinematic, coarse-grained, poikiloblastic, and frequently crosscuts the foliation. These differences may be related to differences in original bulk composition or variations in metamorphic conditions.

The rocks in the study area are pervasively migmatitic with more intense migmatization in the footwall of the Brindle Creek thrust. The migmatization associated with the rocks of the Mill Spring thrust sheet is intense near the Brindle Creek thrust, and documentation of diatexites containing 2 cm porphyroblasts of hornblende constrains the temperature of these rocks to greater than 630°C (Kalbas, in progress). Rocks of the Brindle Creek thrust sheet are also migmatitic and leucosomes consisting largely of quartz and feldspar are commonly interlayered with sillimanite schist and metagraywacke. Metamorphic conditions are greater than the wet-granite solidus defined by Luth et al. (1974).

Petrographic analyses of sillimanite schist confirm the field observations, including the metamorphic grade and assemblages. Two assemblages recognized were:

Garnet + biotite + sillimanite + quartz + muscovite ± plagioclase ± opaques ± melt (A1)

Garnet + biotite + sillimanite + quartz + K-feldspar + plagioclase + opaques (ilmenite and rutile) (A2)

The lack of reaction textures suggests equilibrium assemblages. The occurrence of sillimanite in both of the assemblages indicates that they mark near-peak metamorphic conditions. Sillimanite is the only aluminum silicate polymorph observed in thin section, but it occurs as both fibrolitic and prismatic varieties (Fig. 4b and 4c). Fibrolitic sillimanite along with biotite and muscovite define the domi-

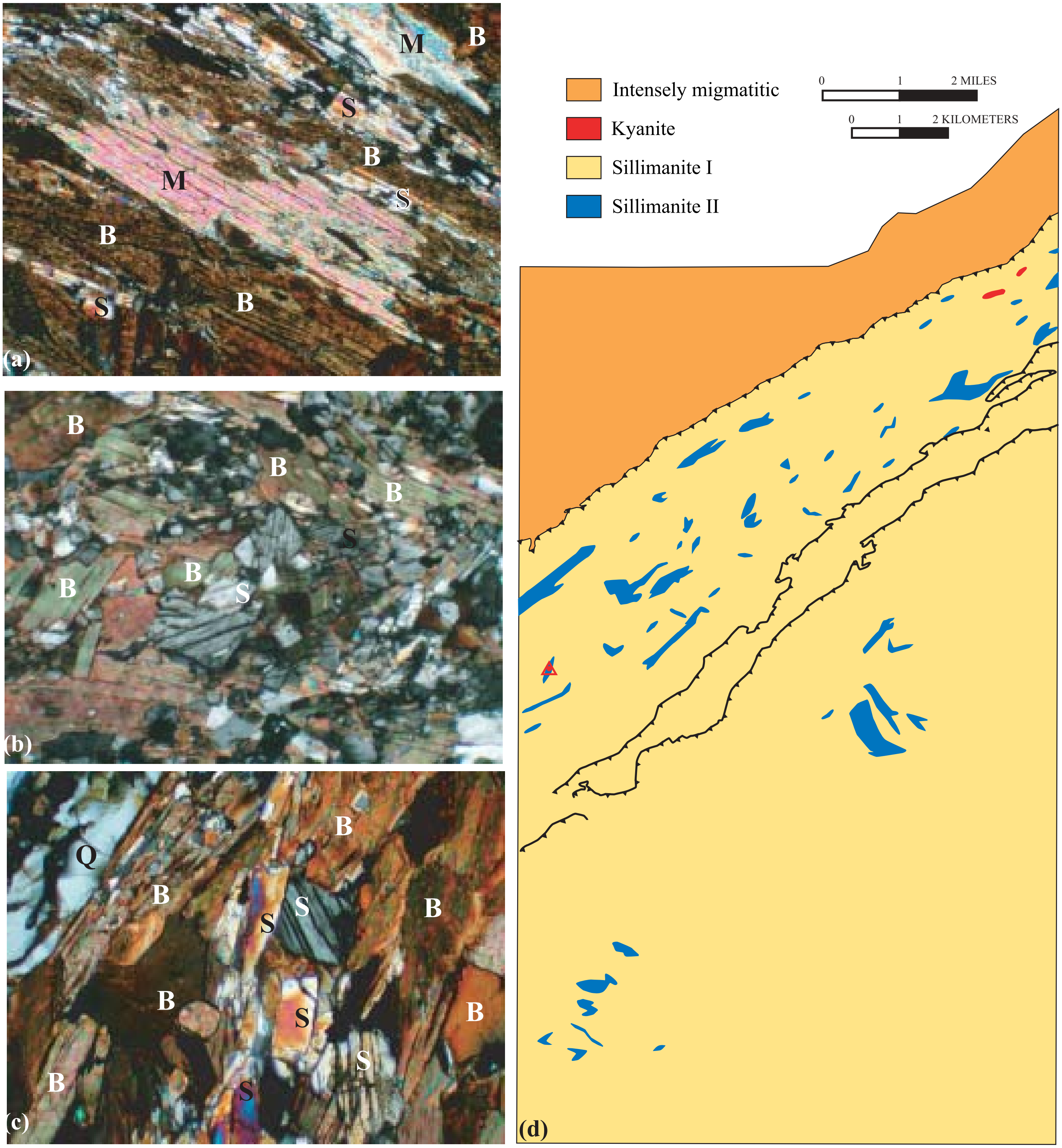

Figure 4. (a) Photomicrograph of sillimanite schist with assemblage A1 from the Kings Creek quadrangle. Fibrolitic sillimanite (S), muscovite (M), and biotite (B) are aligned in the S2 foliation. Field of view is 2 mm. (b) Garnet-biotite-sillimanite schist containing assemblage A2. Note that the assemblage is weakly foliated and prismatic sillimanite is the crystal habit represented. Field of view is 1 mm. (c) Coexisting prismatic and fibrolitic sillimanite in a garnet-biotite-sillimanite schist, assemblage A2. This schist is strongly foliated and contains bands of annealed quartz (Q). Fibrolitic sillimanite and biotite define the foliation in this sample. Field of view is 1 mm. (d) Metamorphic map of the Ellendale and a portion of the Boomer, NC 7.5-minute quadrangles. The second sillimanite isograd was mapped by the occurrence of garnet-biotite-sillimanite schist that lacks muscovite. The lenses and bands of second sillimanite rocks are concordant with the dominant foliation. Red triangle indicates location of electron microprobe sample pictured in Fig. 4b and 4c.

nant schistosity in the samples. Prismatic sillimanite is weakly aligned and is more common in A2. A2 contains both varieties of sillimanite and varies texturally from schistose to massive. Garnet porphyroblasts are subhedral to euhedral and range from 1 mm to 2 cm.

Minor retrograde assemblages were observed including: (R1) chlorite + quartz + sericite; (R2) sericite; and (R3) muscovite. In a sillimanite schist sample, garnets are replaced by chlorite, quartz, and sericite (R1). Muscovite and possibly sillimanite that originally defined the foliation are commonly replaced by sericite (R2). Development of muscovite fish in mylonite associated with Green Mountain fault is an amphibolite- to greenschist-facies retrograde overprint related to faulting. Finally, R3 is marked by the postkinematic poikilitic, coarse-grained muscovite that occurs locally in the Brushy Mountains. The development of coarse-grained poikiloblastic muscovite possibly represents either a late retrograde stage of the same event that produced A1 and A2 or a separate metamorphism postdating the event that produced assemblages A1 and 2.

Assemblage A1 is typical of the first sillimanite zone, upper amphibolite facies metamorphism, and is representative of the majority of the rocks in the southwestern Brushy Mountains. The coexistence of sillimanite and K-feldspar and absence of muscovite in A2 marks the second sillimanite isograd described by Evans and Guidotti (1966), and Chatterjee and Johannes (1974). Baker and Droop (1983) observed the same assemblage as A2 in pelitic schists from the Grampian Highlands granulite terrane in Scotland, and correlated this assemblage with granulite facies conditions. The lack of granulite facies index minerals in the study area, e.g., orthopyroxene, cordierite, or two pyroxenes in mafic rocks, suggests that A2 probably represents the transition between upper amphibolite and granulite facies metamor-

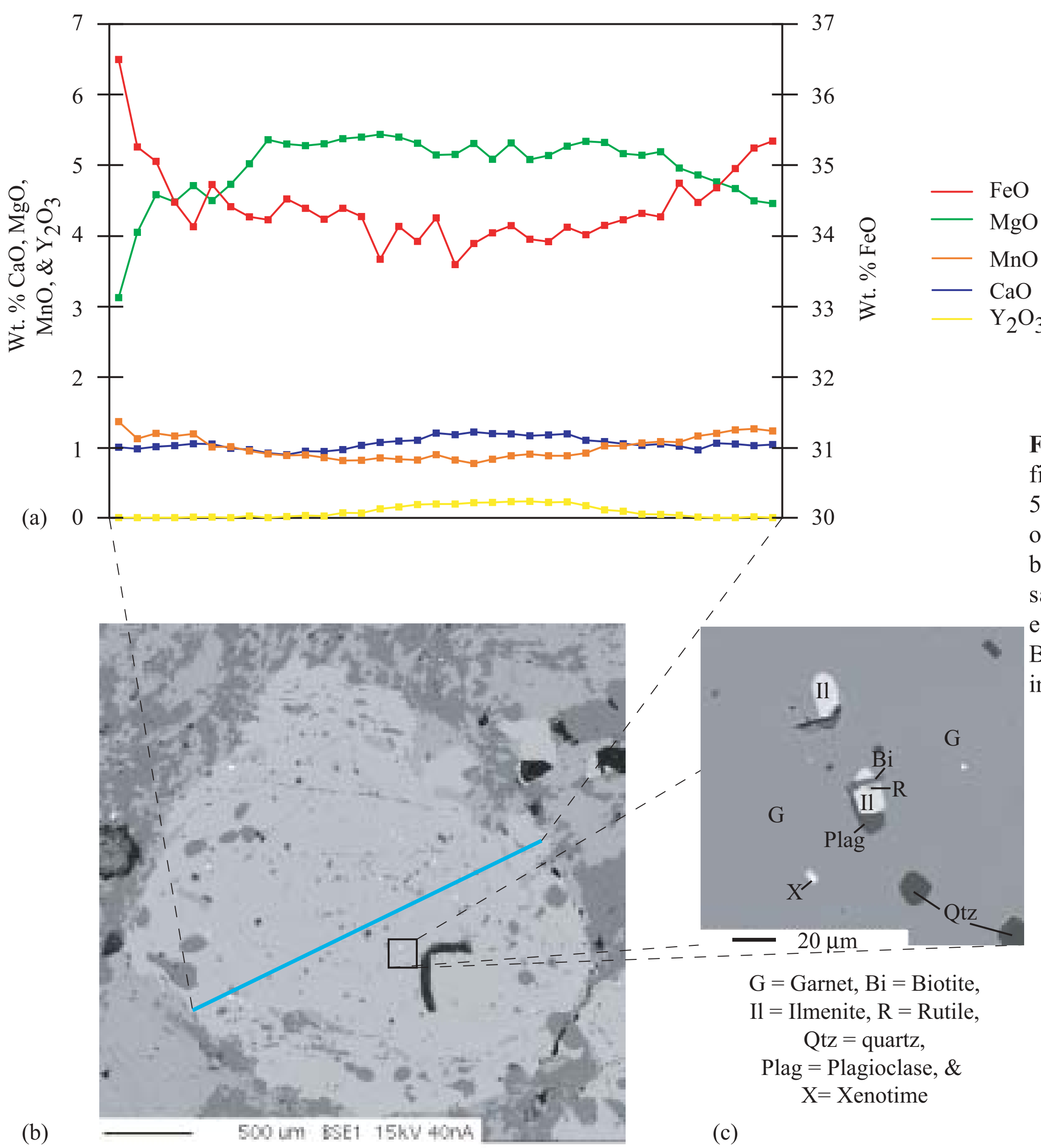

Figure 5. (a) Zoning profile across the garnet in Fig. 5b. (b) Back-scatter image of a garnet from the garnet-biotite-sillimanite schist sample analyzed with the electron microprobe. (c) Back-scatter image of some inclusions in the garnet.

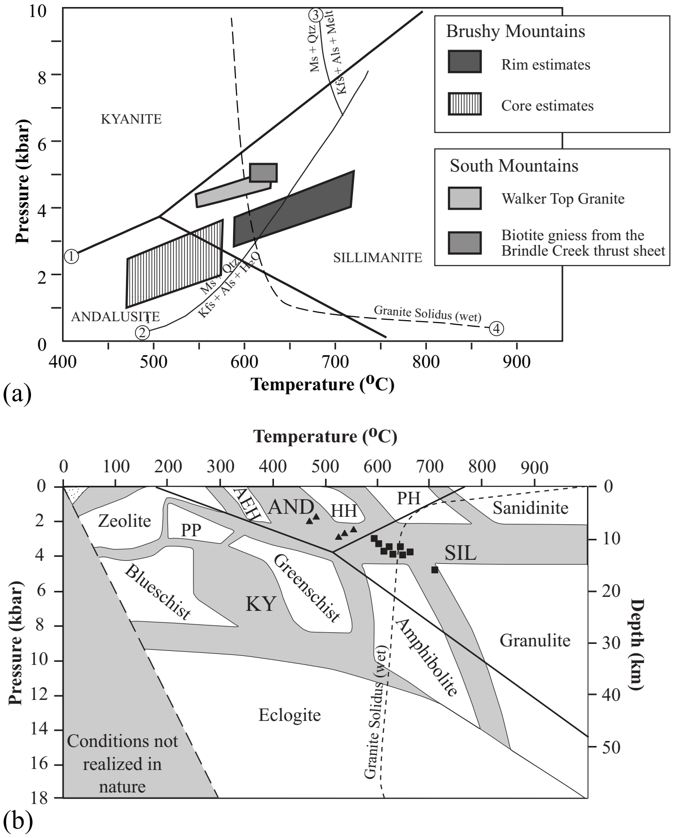

Figure 6. (a) P-T estimates from E1523, a sillimanite schist from the Brindle Creek thrust sheet in the southwestern Brushy Mountains. P-T estimates from rocks of the Brindle Creek thrust sheet in the South Mountains, NC are plotted for comparison (Bier, 2001). (1) Holdaway, 1971; (2) Chatterjee and Johannes (1974); (3) Thompson (1982); (4) Luth et al. (1964) Qtz – quartz, Ms – muscovite, Kfs – potassium feldspar, Als – aluminum silicate. (b) Petrogenetic grid, modified from Raymond (1995), with P-T estimates from E1523. Squares – rim estimates. Triangles – core estimates. This grid is oriented differently from the other P-T graphs. AEH – Albite-Epidote Hornfels, HH – Hornblende Hornfels, PH – Pyroxene Hornfels, PP – Prenite-Pumpellyite, AND – Andalusite, KY – Kyanite, SIL – Sillimanite.

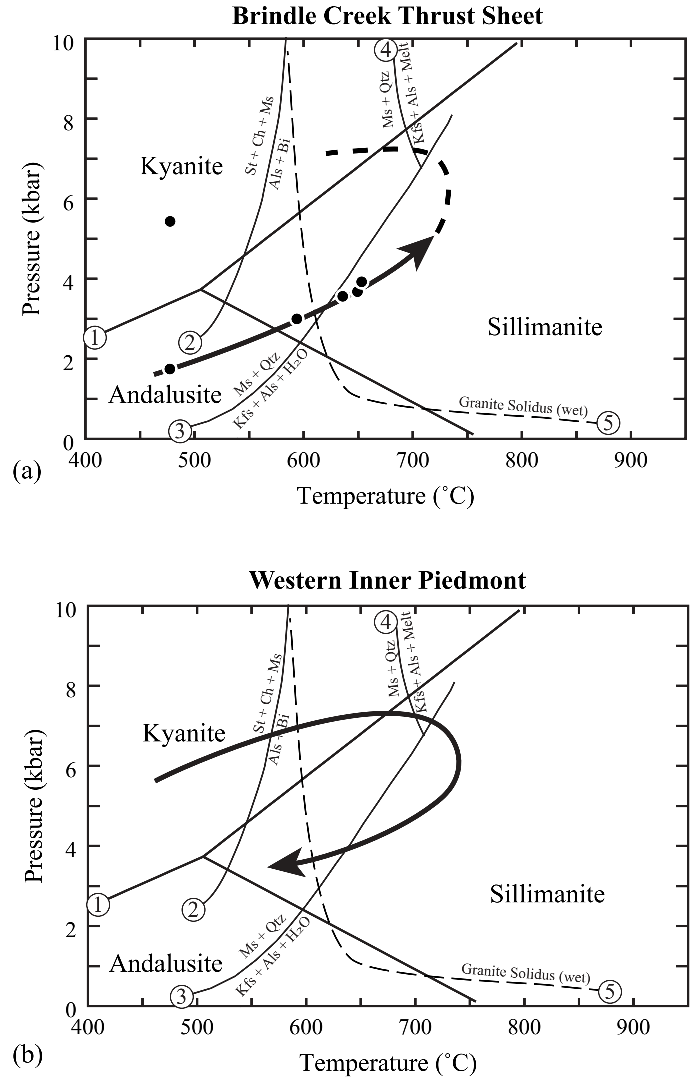

Figure 7. P-T paths for the Brindle Creek thrust sheet/eastern IP and western IP. (a) P-T path for the Brindle Creek thrust sheet constructed from representative P-T estimates from the garnet-biotite-sillimanite schist sample. The dashed line represents possible extensions of the path to explain the isolated occurrences of kyanite near the leading edge of the Brindle Creek thrust. (b) Possible P-T path for the western IP constructed from others (Bryant and Reed, 1970; Goldsmith et al., 1988; and Davis, 1993a). References for mineral reactions are as follows: (1) Holdaway (1971); (2)Albee (1965); (3) Chatterjee and Johannes (1974); (4)Thompson (1982); (5) Luth et al. (1964). Mineral abbreviations: Qtz – quartz; St – staurolite; Ch – chlorite; Ms – muscovite; Bi – biotite; Als – aluminum silicate; Kfs – potassium feldspar.

phism. Mapping of the second sillimanite isograd is based on the absence of muscovite corresponding with the distribution of garnet-biotite-sillimanite schist (Fig. 4d). This observation suggests that discontinuous bodies of second sillimanite grade rocks exist and are surrounded by first sillimanite grade rocks. These pods of second sillimanite rocks may represent areas where dehydration reactions progressed further, allowing conversion to the second sillimanite assemblage.

Geothermobarometry was employed to help decipher the thermal evolution of rocks in the Brindle Creek thrust sheet. Microprobe analyses of a garnet-biotite-sillimanite schist sample were preformed with the CAMECA-SX 50 fully automated electron microprobe at the University of Tennessee Microprobe Facility. Well-characterized synthetic compounds and minerals were used as standards. A potential of 15 KeV and 20 nA beam current were sufficient for all the analyses within this study, except for feldspar analyses (10 nA). Beam size and count time varied depending on the mineral or element being analyzed. Analyses performed on garnets utilized a 2 μm beam size, while a beam size of 5 μm was used for all other analyses. A count time of 20 seconds per element was used unless increased to 30-40 seconds for detection of minor elements (Mn, Cr, Na, Cl, Y, and Ba). All data were fully reduced using the CAMECA PAP software. The computer program of Spear and Kohn (1989) was used to plot the P-T estimates.

Garnets in assemblage A2 in a garnet-biotite-sillimanite schist sample (Figure 4b, 4c) were examined, and displayed distinct patterns. The sample is massive to weakly foliated, and prismatic sillimanite dominates (Fig. 4b). No reaction or retrograde textures or assemblages, as discussed above, were observed, and the phases present are interpreted to be in equilibrium. Garnets range from one to five mm in diameter. The garnets contain inclusions of quartz, biotite, plagioclase, rutile, ilmenite, and minor aluminum silicate. These inclusions are assumed to represent a mineral assemblage in equilibrium during garnet growth. The garnets are almandine-rich and display distinct chemical zonations. FeO and MnO increase toward the rims and MgO, CaO, and Y_2O_3 increase toward the cores (Fig. 5). Inclusions in the garnets mimic these trends. Biotite and ilmenite inclusions are enriched in MgO, and plagioclase inclusions are more calcic than similar phases in the matrix.

Pressure estimates were determined using the GASP (Hodges and Spear, 1982) and GRAIL (Bohlen et al., 1983) barometers. The geothermometers used were the garnet-biotite (Ferry and Spear, 1978) and garnet-ilmenite (Pownceby et al., 1987a, 1987b). P-T estimates for rim assemblages range from 585^{o} C, 2.8 kbar to 710^{o} C, 4.7 kbar, and several plot above the second-sillimanite reaction line (Fig. 6). These estimates agree with the observed mineral assemblage. Inclusions in the garnets yielded P-T estimates within the andalusite and kyanite stability fields. The GRAIL geobarometer yielded estimates for the cores that plot in the kyanite field. These estimates were discarded, because the same geobarometer did not predict equilibrium conditions for the rim assemblage. The estimates for conditions under which the garnet cores formed range from 450^{o}C, 1.3 kbar, to 570^{o}C, 2.5 kbar.

The continuous zoning profile and inclusions preserved in the garnet indicate a single continuous metamorphic event. The increase in temperature and pressure from garnet cores to rims indicates a prograde event reaching the second sillimanite zone. The locations of these estimates on a petrogenetic grid (Fig. 6) support the idea that assemblage A2 represents a transition assemblage between the upper amphibolite and granulite facies.

Using the estimates of metamorphic conditions associated with the growth of garnets in sillimanite schist, a P-T path can be constructed that constrains the thermal evolution of the Brindle Creek thrust sheet. The P-T estimates define a counterclockwise path representing crustal loading during metamorphism (Fig. 7). An explanation of this path involves the emplacement of nappes/thrust sheets containing hot rocks and Buchan-type metamorphism (Spear et al., 1984). The interpretation of Buchan-type metamorphism is based only on analytical evidence and contradicts the previously interpreted Barrovian-type metamorphism in the southern Appalachian Blue Ridge and IP (Butler, 1991). No relict andalusite or other Buchan facies index minerals were observed either in the field or petrographically. Bryant and Reed (1960), however, reported an outcrop of andalusite-bearing schist in the Mill Spring thrust sheet approximately 16 km (10 mi) northwest of Morganton, North Carolina. Conversely, excluding two occurrences of kyanite, no other Barrovian index minerals are present in the Brindle Creek thrust sheet. The P-T path that the Brindle Creek thrust sheet followed is unconstrained and either Buchan- or Barrovian-type metamorphism can explain its path.

Based on the P-T estimates reported above, and the counterclockwise P-T path, Buchan-type metamorphism is favored for the rocks of the Brindle Creek thrust sheet. This path is typical of thrust sheets that were emplaced while the rocks are still hot (Spear et al., 1984). The minor occurrences of kyanite and their location near the leading edge of the Brindle Creek thrust sheet can be explained by this path via an increase in pressure or decrease in temperature. The location of kyanite along the leading edge of the Brindle Creek thrust sheet could correspond to areas of increased crustal thickening producing high-pressure kyanite after sillimanite. This does not agree with the intense migmatitic rocks in the footwall of the Brindle Creek thrust. Alternatively, rocks in the footwall of the Brindle Creek thrust were cooler, and locally cooled the rocks in the frontal edge of the Brindle Creek thrust sheet, forming kyanite after sillimanite (Fig. 7). The latter possibility is favored because the emplacement of hot rocks onto cooler can also explain the increased migmatization in the footwall of the Brindle Creek thrust sheet.

Rocks of the Mill Spring and Marion thrust sheets followed an opposite path than the rocks of the Brindle Creek thrust sheet. From west to east, rocks of the western IP indicate prograde Barrovian-type metamorphic conditions. In the southwestern Brushy Mountains, rocks of the Mill Spring and Marion thrust sheets are sillimanite grade. Further to the west Bryant and Reed (1970), Goldsmith et al., (1988), and Butler (1991) observed the assemblages of sillimanite, kyanite, and kyanite + staurolite in rocks of the Marion thrust sheet. This assemblage defines a clockwise P-T path typical of prograde Barrovian-type metamorphism. Placement of hot Buchan facies rocks of the Brindle Creek thrust sheet onto cooler Barrovian facies rocks of the western IP helps explain the intense migmatization in the Brindle Creek thrust footwall, and the higher-pressure rocks in the Marion thrust sheet. Similar occurrences of terranes with opposing P-T paths are recognized in New England (Spear et al., 1984; Spear, 1993), and Scotland (Baker and Droop, 1983). These authors proposed similar models involving the emplacement of hot thrust sheets followed by rapid exhumation to explain metamorphic conditions in these terranes. More data are needed to fully understand IP metamorphism, but a preliminary model involving Buchan-type metamorphism is plausible with the present data.

Constraints on the timing of metamorphism are U-Pb ages of metamorphic rims on zircons, and U-Pb ages of monazite. Dennis and Wright (1997) and Mirante and Patino-Douce (2000) reported U-Pb monazite from the IP of South Carolina and Georgia. Mirante and Patino-Douce (2000) reported an age of ~330 Ma for migmatitic amphibolite in Georgia. Dennis and Wright (1997) reported ages of ~360 Ma and ~325 Ma from the South Carolina IP. Kalbas et al. (2002) presented a ~350 Ma ion microprobe U-Pb age date from metamorphic rims of several zircons from leucosome of the migmatitic metagranodiorite and amphibolite in the footwall of the Brindle Creek thrust in the southwestern Brushy Mountains (Fig. 2). They interpreted this data to mark the timing of near peak metamorphism and coeval migmatization in the footwall of the Brindle Creek thrust (Kalbas et al., 2002). Timing of metamorphism in the Brindle Creek thrust sheet is well within the range of ~360-330 Ma presented by these independent studies. Exact correlation of the timing of metamorphism across the Brindle Creek thrust can be debated. If the Brindle Creek thrust sheet was emplaced hot, peak metamorphism in the footwall of the Brindle Creek thrust may be younger than peak metamorphism in the Brindle Creek thrust sheet. The ~350 Ma age (Kalbas et al., 2002) presently is the best-reported age to date for timing of metamorphism in both the western and eastern IP.

STRUCTURE

Structural data and observations presented here are similar to those of earlier studies in the IP (e.g. Hatcher, 1974; Hopson and Hatcher, 1988; Davis, 1993a, 1993b; Bier, 2001; Hatcher, 2001). Three crystalline thrust sheets that

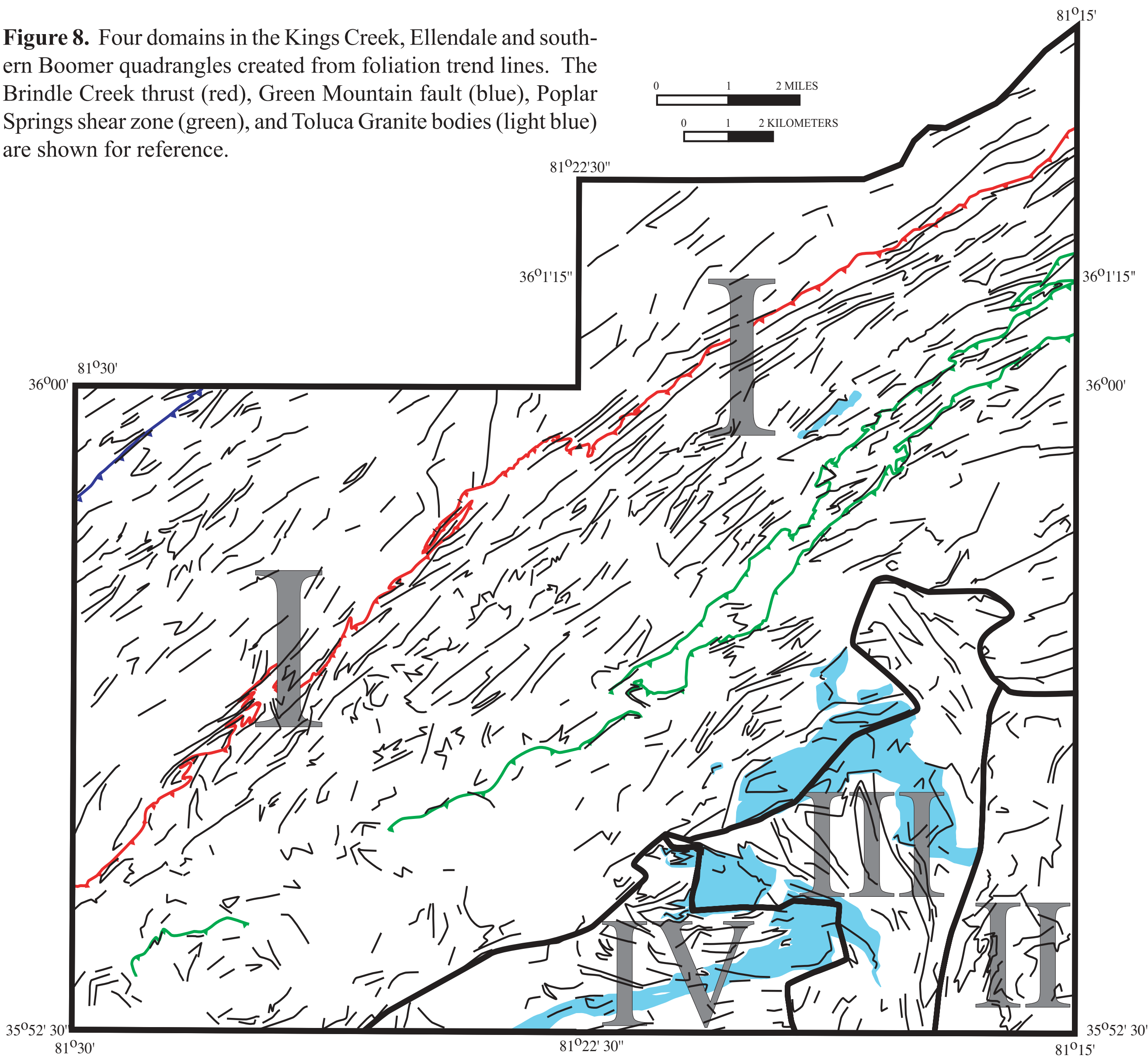

Figure 8. Four domains in the Kings Creek, Ellendale and southern Boomer quadrangles created from foliation trend lines. The Brindle Creek thrust (red), Green Mountain fault (blue), Poplar Springs shear zone (green), and Toluca Granite bodies (light blue) are shown for reference.

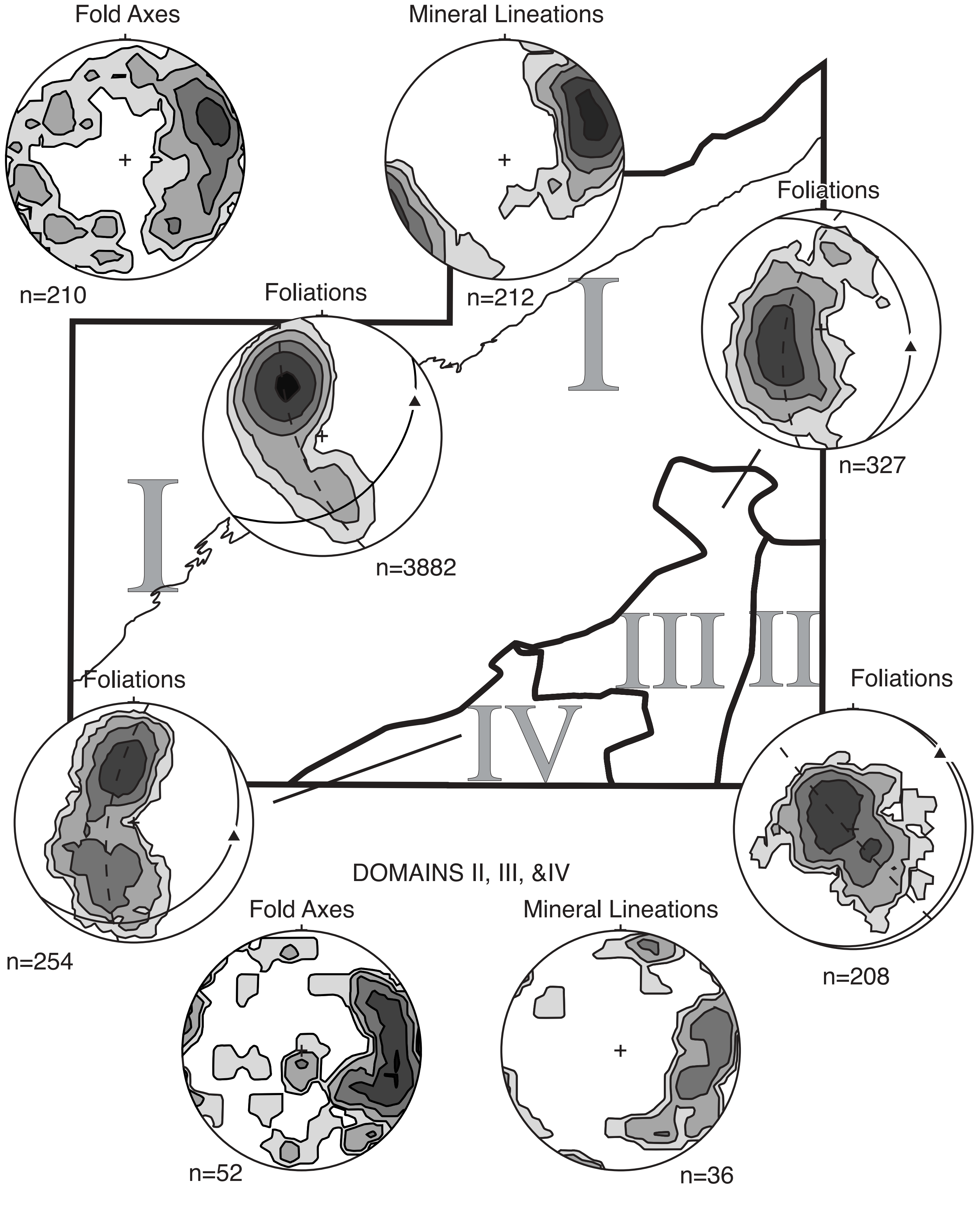

Figure 9. Contoured, lower-hemisphere, equal-area projections of poles to foliation, trend of fold axes and mineral lineations. Each domain is plotted on a separate stereonet except mineral lineations and fold axes are combined for domains II-IV. Plots of fold axes include all fold generations. Contour interval begins at 1%, and increases by a factor of two per interval (1%, 2%, 4%, 8%, 16%). Triangles – Beta axes. Solid great circle is the mean foliation, and the dashed great circle is the fold axis girdle.

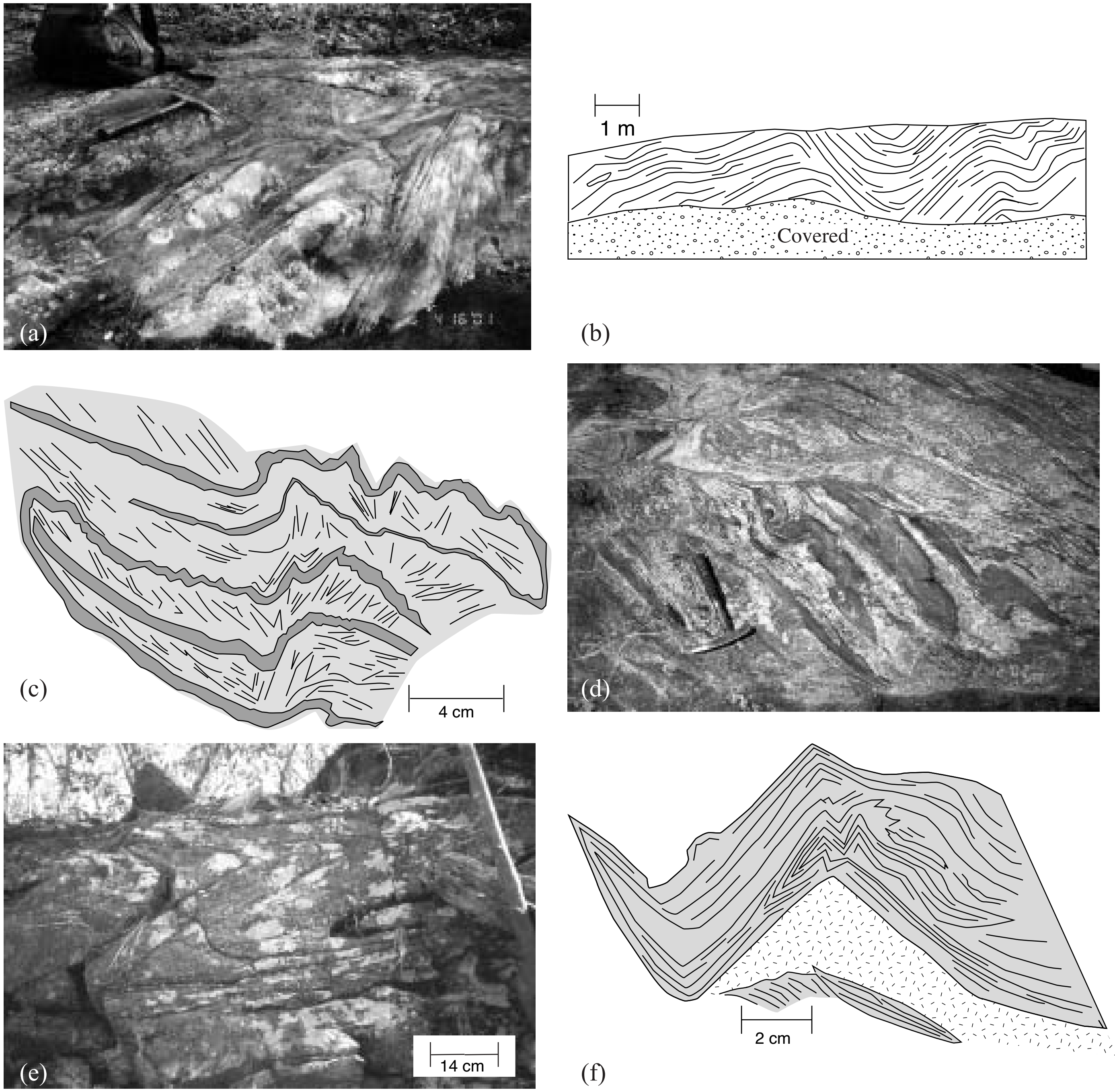

Figure 10. Photos and drawings of folds observed in the field. (a) Inclined isoclinal fold in metagraywacke from domain I. The fold plunges moderately to the NE. (b) NW-plunging open folds in thinly layered (2-10 cm) metagraywacke from domain I. (c) Refolded garnet-rich layers in garnet-biotite-sillimanite schist from domain III. A weak axial planar foliation is developing in the later folds. The later foliation is defined by sillimanite and biotite. (d) Refolded biotite gneiss xenoliths in Toluca Granite, domain III. The xenoliths preserve an earlier foliation but not folds. (e) Reclined isoclinal folds in interlayered metagraywacke and schist, domain II. Fold crests are sharp and hinges are significantly thickened. (f) Refolded migmatitic sillimanite schist, domain IV. Fold crests in sillimanite schist are very angular and even the fold crest containing the granitic material (cross-hatch pattern) is angular.

were nucleated plastically in a transpressional regime are recognized in the southwestern Brushy Mountains. They record a polyphase deformational history of early ductile deformations overprinted by later near-brittle to brittle conditions. A change in orientation of structures occurs in the Ellendale quadrangle: NE-SW-trending structures to the northwest give way to NW-SE- and N-S-trending structures to the southeast (Fig. 2), has important implications regarding the tectonic development of this terrane.

Domains

A form-line map of foliation trend (Fig. 8) emulates the geologic map pattern, but form lines cut lithologic contacts and major structures like the Brindle Creek thrust. Four domains can be separated and each displays a roughly triclinic symmetry common in polydeformed terranes (Turner and Weiss, 1963) (Fig. 9). The boundary between domain I and the other domains is an important structural break discussed below.

Domain I extends over two-thirds of the study area, encompassing parts of the western and eastern IP. It is a homogeneous containing NE-SW striking units and structures that dip moderately to steeply SE. The mean foliation is roughly orogen-parallel N 49° E, 42° SE. Stromatic migmatite layering is common and parallels the dominant foliation. The mean vector of mineral lineations defined by the alignment of sillimanite plunges 32°, N 69° E. Map-scale structures, overturned folds, and thrust faults verge NW. Major folds are inclined to reclined and tight to isoclinal. The fold axes plunge gently NE or SW. The mean foliation in this domain is axial planar to the macroscopic folds. The northwesternmost band of Walker Top Granite can be traced southwestward into an earlier fold hinge in the Kings Creek quadrangle. Amplitudes of map-scale folds are difficult to estimate, but may exceed 1000 m.

The three major ductile faults in the study area are located in domain I. They trend NE-SW and dip SE parallel to the mean foliation of the domain. The structurally lowest fault is the Green Mountain fault (Mill Spring thrust) located in the northwest corner of the Kings Creek quadrangle. The Brindle Creek thrust that bounds the western and eastern IP, is structurally above the Green Mountain fault. Finally, the highest faults are two closely related faults that comprise the Poplar Springs fault zone.

Three sets of mesoscopic folds were observed in domain I, reflected in concentrations of fold axes in Figure 9. Fold sets trend NE-SW, NNE to SSW, and NW-SE. The earliest and dominant fold set plunges gently to the NE and SW. It is inclined to recumbent, tight to isoclinal and verges NW (Fig. 10a). These folds have distinctly thickened hinges with moderately curved to angular crests. Folds in sillimanite schist have sharper crests than those in metagraywacke. An axial planar relationship exists between the penetrative foliation and these folds. Occasionally, the first set is superposed by a later north-northeast trending, inclined, closed to tight fold set. This later fold set commonly has thickened hinges and tight crests, with similar contrasts in crest shape relating to rheology as in the early fold set, but folds the dominant foliation. The latest fold set consists of upright open folds that trend NW-SE and plunge 10-40° (Fig. 10b).

Domain II is heterogeneous with dominant northerly trends and gentle dips. The mean foliation is oriented N 21° E, 8° SE and mineral lineations trend NNE and SE with an average of 22°, N 71° E. The map pattern in this domain is controlled by north-verging recumbent, gently E-NE plunging isoclinal folds. Recumbent folds are superposed by later NE-trending open folds. Mesoscopic folds are reclined to recumbent, tight to isoclinal and plunge gently ENE and SE. These folds have significantly thickened hinges and sharp, angular crests. The majority of these folds verge SW, but a few verge NW. The dominant foliation is axial planar to early recumbent folds. Later upright to inclined mesoscopic open folds plunge E to SE.

Domain III is homogenous with the average foliation oriented N 23° W, 29° NE and average mineral lineation of 32°, S 74° E. This zone may represent the eastern limb of an asymmetric, NE-plunging open antiform. The large asymmetric fold is defined by the linking of discontinuous bodies of Toluca Granite localized in the hinge of an earlier fold (Fig. 2). This fold can be traced into domains I and IV (Fig. 8). Mesoscopic folds display two episodes of deformation at near peak metamorphic conditions (Fig. 10c). Early inclined to recumbent isoclinal folds are superposed by later inclined to upright, tight-to-closed folds. First-generation folds in this domain generally verge SW. Foliations are axial planar to these early folds. A later closed to tight, upright fold set is often superposed on the earlier fold set. Rare foliations axial planar to the later fold set do occur here (Fig. 10c). Folded xenoliths of biotite gneiss in the Toluca Granite (Fig. 10d) are the only strain markers available to record deformations in the granite. They display two deformation episodes: early isoclinal folding followed by a later inclined open folding. Xenoliths are devoid of earlier internal folds. Late-stage crenulation cleavage was observed at several locations in the sillimanite schist plunging gently to moderately SE, and may be related to late stage open folding and growth of the coarse-grained poikiloblastic muscovite described above.

Domain IV is homogeneous and dominated by E-W trends. This domain contains the corresponding asymmetric synform and antiform of the asymmetric fold identified in domain III. The average foliation is oriented N 51° E, 24° SE and average mineral lineation 24°, S 84° E. Mesoscopic folds preserve a polyphase history with upright, tight-to-open folds superposed on earlier isoclinal folds. Early isoclinal folds plunge gently E or W, and later folds plunge NW or SE (Fig. 10f). These folds are geometrically similar to the earliest fold set in other domains with angular crests and thickened hinges. Late-stage open folds are common and plunge NW or SE. Crenulations are also present in the sillimanite schist unit and plunge gently SE.

Faults and Flow Kinematics

The Green Mountain fault is the best candidate for the northern extension of the Mill Spring thrust based on similar lithostratigraphy in the hanging wall and footwall. In the Kings Creek quadrangle, the fault strikes N 50° E, dips 30-50° SE, and contains mylonitic Tallulah Falls rocks in the footwall. Sillimanite lineations in footwall rocks are strike-parallel, and muscovite fish are similarly oriented with top to the SW shear sense indicating this fault has a major dextral strike-slip movement component. The limited exposure of this structure in the area mapped in detail (Fig. 2) provides insufficient data to confirm it is a Type F thrust, but the location of the upper member of the Tallulah Falls Formation in the footwall suggests a footwall syncline could be present, as along strike in the South Mountains. The amount of displacement cannot be determined in the study area. If the correlation of the fault observed in this study with the Mill Spring thrust is correct, the displacement may be greater than 100 km (Hatcher, in press).

The Brindle Creek thrust may be the most significant fault in the IP (Bream et al., 2001; Hatcher, this guidebook). The fault trends from N 45° E to N 60° E, and is folded and dips from 20° to 50° SE. Foliation form lines both parallel and crosscut the fault (Fig. 8). A footwall granitoid body and an amphibolite band are truncated by the Brindle Creek thrust in the northeastern part of the Kings Creek quadrangle (Fig. 2b). An overturned antiform in the hanging wall immediately adjacent to the trace of the fault is typical of Type F thrusts (Fig. 2e). Mineral lineations in the rocks on both sides of the fault trend NE-SW. The irregular trace of the Brindle Creek thrust in the Kings Creek quadrangle is the result of superposed tight to closed folds. The lack of correlative units across the fault hinders determination of displacement. A minimum estimate is >100 km, based on the trace length of the fault (Hatcher, this guidebook).

The Poplar Springs fault zone consists of two closely related ductile faults that strike N 50° to 60° E and dip from 30° to 65° SE. They are recognized by two bands of mylonitized Walker Top Granite occurring along the trace of the faults in the Ellendale quadrangle. These bands become macroscopic boudins in the Kings Creek quadrangle and the trace of the fault becomes discontinuous (Fig. 2). Reconnaissance mapping (Rankin et al., 1972) suggests that these faults continue northeast of the study area but their kinematic relationships to each other cannot be determined. The form-line map (Fig. 8) displays minor truncations of footwall foliations against the faults. Cross sections A-A' through F-F' (Fig. 2e) depict these faults evolving by the attenuation of northwestern limbs of antiforms cored by metagraywacke – classic Type-F faults. Kinematic indicators along these faults indicate two components of movement: (1) fault orientation coupled with vergence of early inclined isoclinal folds suggest significant NW-directed movement, and (2) mantled feldspar porphyroclasts, asymmetric folds, drag folds, and possibly the macroscopic outcrop pattern of the mylonitic Walker Top Granite indicate top-to-the-southwest, dextral strike-slip movement. Displacement varies on these faults from zero to at least 2 km.

Other mesoscopic shear zones occur throughout domain I. Several outcrop-scale shear zones were identified in the Walker Top Granite (see Stop 13). Several distinct minor dextral shear zones are present in an outcrop at the northeast end of the Walker Top Granite outcrop belt.

Orogen-parallel mineral lineations are problematic. Davis (1993a, 1993b) and Hatcher (2001) have interpreted mineral lineations in the IP to represent flow paths tracking the movement of thrust sheets. Orogen-parallel mineral lineations are observed in other orogenic belts and interpreted similarly (e.g., Burn and Burg, 1982; Coward and Potts, 1983; Lisle, 1984). Davis (1993a, 1993b) proposed that thrust sheets of the IP were buttressed against a NE-SW-trending, SE-dipping structure, the primordial Devonian to Early Mississppian BFZ. Hatcher (1971; 2001) suggested that the initial localization of the primordial BFZ coincides with a stratigraphically controlled crustal anisotropy. This model adequately described the structural patterns in the Columbus Promontory and the majority of the IP (Goldsmith, 1981; Hatcher, 2001) by buttressing ductile thrust sheets of the IP against a rigid structure SE-dipping, NE-SW-striking. West-directed thrusts were deflected to the SW along the primordial Devonian BFZ (Davis, 1993a, 1993b; Hatcher, 2001). The zone of constricted flow was identified by Hatcher (2001) to describe the area southeast of the BFZ that is characterized by strongly aligned NE-SW-trending structures and dominated by SW-directed transpressional flow. The zone extends from Georgia to North Carolina, ending at the Sauratown Mountains window (Hatcher, 2001).

With the exception of the Poplar Springs fault zone, the Green Mountain fault, and a few minor mesoscopic shear zones, the lack of shear sense indicators associated with the Brindle Creek thrust makes understanding the kinematics of this fault difficult. All of the faults in this study occur in strongly aligned domain I. Mineral lineations near the faults are parallel to sub-parallel to fault traces, and vergence of both macro- and mesoscopic structures is NW. Shear-sense indicators in the Poplar Spring fault zone yield-consistent top-to-the-SW shear sense, and is therefore interpreted to have significant dextral strike-slip movement. The attenuation of NW-verging antiforms by the fault suggest that initial movement of the fault zone was dip-slip and directed NW. The variation in displacement along the length of the fault, and discontinuous trace of the fault in

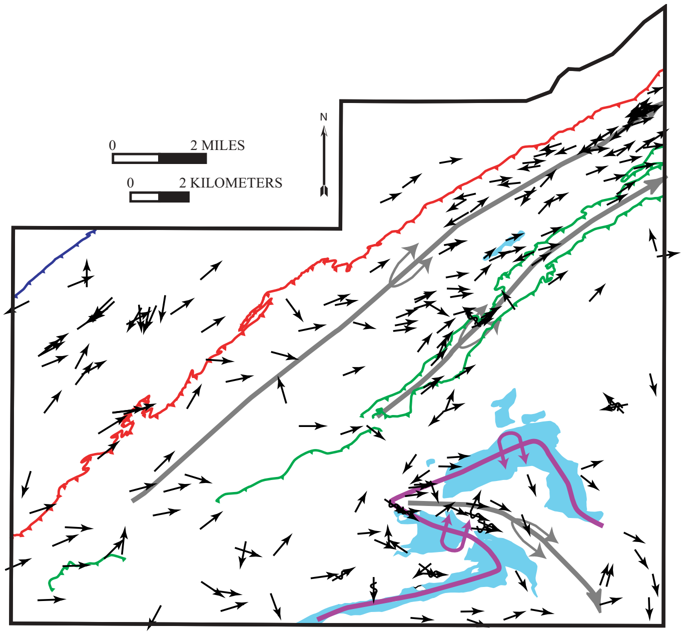

(a)

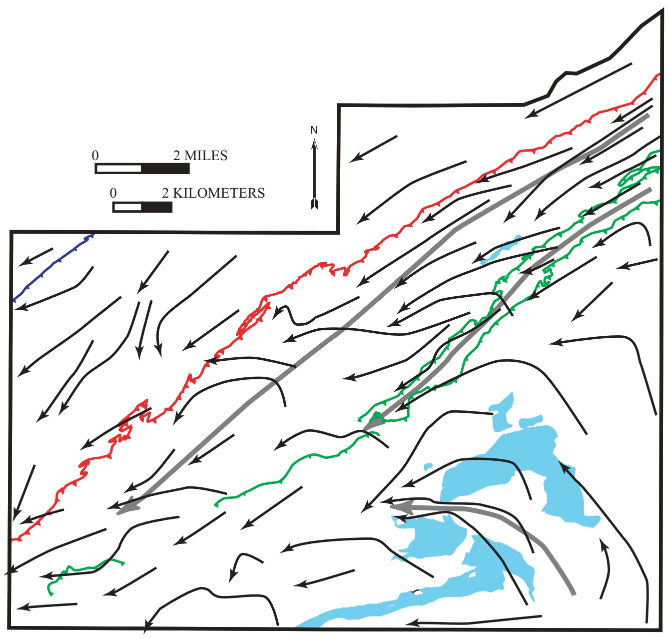

(b)

Figure 11. (a) Mineral lineation pattern and locations of possible sheath fold axes (gray) in the southwestern Brushy Mountains. The bodies of Toluca Granite (light blue), Green Mountain/Mill Spring fault (blue), Brindle Creek thrust (red), and Poplar Springs fault zone (green) are shown for reference. (b) Flow paths constructed from mineral lineations (black) and sheath folds (gray) are interpreted to track thrust sheet movement. Major faults and bodies of Toluca Granite are shown for reference as in Fig. 11a and for comparison with the flow lines.

Kings Creek quadrangle may be related to the noncylindrical shape of the attenuated fold. Muscovite fish and mantled porhyroclasts in the mylonite near the Green Mountain fault indicate dextral strike-slip movement, while geometry and fold vergence suggest NW-directed dip-slip movement. Also we assumed that mineral lineations and vergence of early structures track thrust sheet movement in the Brushy Mountains. The NW vergence of structures in domain I suggests significant NW-SE shortening coupled with NW displacement on the faults. The kinematic history of the Brindle Creek thrust in the study area can be interpreted by making assumptions similar to those of Davis (1993a, 1993b), sillimanite growth is synkinematic and represents flow paths that track thrust sheet movements. The strongly aligned nature of domain I suggests flow was NE- or SW- directed (Fig. 11). Combining these interpretations about fault movements and shear sense indicators from the Poplar Springs fault zone, Green Mountain fault, and the primordial BFZ (Davis, 1993a, 1993b; Hatcher, 2001), the Brindle Creek thrust probably had two simultaneous movement components: (1) a NW-directed displacement from E-W contraction; and (2) dextral strike-slip movement resulting from SW-directed flow.

The boundary between domain I and the other domains also represents an important kinematic break. The strongly aligned structures in domain I mark the eastern extent of the zone of constricted flow. Material in this strongly aligned zone was transported SW along the primordial Devonian-Mississippian BFZ. The asymmetric, closed-to-tight folds, traceable by connecting the bodies of Toluca Granite in the hinge, may have developed as the result of buttressing against the primordial BFZ. In domain III the Toluca Granite body appears to occupy of the core of a NW-trending, SW-verging antiform that may represent the core of an earlier antiform. As the Brindle Creek thrust sheet advanced NW, the NW-trending fold cored by Toluca Granite was deflected with the front of the Brindle Creek thrust sheet to the SW by the Devono-Miss. BFZ, producing the refolded pattern preserved on the map. Alternatively, the collective anvil-shaped geometry of the bodies of Toluca Granite can be interpreted as a map-scale sheath fold plunging SE. Although the first explanation is viable, the interpretation of the bodies of Toluca Granite in the Ellendale quadrangle as a map-scale sheath fold is favored because it is more compatible with other kinematic indicators in domain III. Ductile flow has been documented parallel to sheath fold axes (e.g. Cobbold and Quinquis, 1980; Alsop and Holdsworth,1999). The anvil shape coupled with the SE-plunging axis of the sheath fold suggests that the nose of the sheath fold is located to the NW and flow in domain III was NW-directed, parallel to the flow lines in domain III constructed from mineral lineations (Fig. 11). Similarly, the two bands of both nonmylonitic and mylonitic Walker Top Granite can be interpreted as NE-plunging sheath folds resulting from SW flow in domain I (Fig. 11). Flow lines constructed mineral lineations and sheath fold axes systematically rotate counterclockwise from NNW to NW and W in domains II-IV as the NW verging Brindle Creek thrust sheet advances and is buttressed against the primordial BFZ and deflected to the SW in domain I.

Table 1. Deformation characteristics and chronological order in the southwestern Brushy Mountains, NC.

DEFORMATION EVENTS	STRUCTURES: Fabrics	STRUCTURES: Folds	STRUCTURES: Faults	METAMORPHIC CONDITIONS	REGIONAL EVENTS	OROGENY & TIMING
D_1	S_1 Early foliation preserved in boudins	F_1 Map-scale folds associated the Walker Top and Toluca Granites	———	Moderate to high pressure and temperature	———	Pre- to early Neoacadian
D_2	S_2 Penetrative foliation L_2 Mineral lineation	F_2 Inclined to recumbent, tight to isoclinal passive and flexural flow folds, andmap-scale sheath folds; trend NE, SW, & SE	Intial NW and then SW deflected movement of the BCT, PSFZ, and GMF	Peak metamorphism, upper amphibolite facies, sillimanite I & II grade	Emplacement of crystalline thrust sheets of the IP, and SW deflection along primordial BFZ	Neoacadian ~350 Ma
D_3	S_3 Rare, secondary foliation	F_3 Inclined to upright, closed to open folds, trend NNE, N, & NW	Continued SW and NW(?) movement on the BCT,GMF, and PSFZ	Decreasing conditions, high to moderate pressure and temperature	Final emplacement and exhumation of IP thrust sheets,	Late Neoacadian or early Alleghanian
D_4	S-C and related fabrics in the BFZ	F_4 Upright, open folds, trend NW- SE & SE plunging crenulations	Ductile reactivation of BFZ	Low pressure and temperature – greenschist facies	Initial emplacement of the composite Blue Ridge-IP thrust sheet	Alleghanian
D_5	Joints	Regional broad, open folds	Brittle movements associated with the Rosam Fault	Brittle conditions	Continued emplacement of the composite Blue Ridge-IP thrust sheet	Late Alleghanian
$D_{6...}$	Joints	Regional broad, open folds	Meso- and macroscale normal faults, not observed in study area.	Brittle conditions	Rifting — ? — Uplift	Mesozoic extension — ? — Cenozoic uplift

*Modified from Davis (1993a, 1993b).
BCT = Brindle Creek thurst sheet, GMF = Green Mountain fault, PSFZ = Poplar Springs fault zone, and BFZ = Brevard fault zone

Until now the primordial BFZ has not been shown to affect eastern IP crystalline thrust sheets (Giorgis, 1999; Williams, 2000; Bier, 2001). Recognition of the zone of constricted flow in the southwestern Brushy Mountains has several key implications, many of which confirm earlier interpretations of Davis (1993a, 1993b) and Hatcher (2001). The reconstructed geometry of the primordial BFZ by (Davis, 1993a, 1993b) suggests that the zone of constricted flow here marks the extent of buttressing by the Devono-Miss. BFZ. The highly aligned nature of this zone, together with the occurrence of mylonite throughout the zone, suggest it is a crustal shear zone. The width of the zone in the Brushy Mountains is ~15 km (9 mi), compatible with the ~20 km reported by Hatcher (2001) for the thickness of a crustal scale shear zone. If the zone maintained a uniform thickness and orientation during the Neoacadian, then it can be used to measure the relative displacement on Neoacadian faults in the IP.

The decreased distance between the Brindle Creek thrust sheet and the BFZ at the current erosion level can be explained in various ways. (1) Product of erosion of a low-angle SE-dipping fault. As the Brindle Creek thrust sheet continues to be eroded, the distance between it and the BFZ will increase. To the south where the distance from the Brindle Creek thrust and BFZ is greater correspond to greater amounts of erosion. (2) Rocks in domain I dip more steeply than in the Columbus Promontory and South Mountains, possibly accounting for some of the decreased outcrop width of the western IP in the Brushy Mountains. It is more likely that the steeper orientations in the study area are a consequence of the greater component of strike-slip movement on faults than the same faults elsewhere in the IP. (3) Increased displacement along the Brindle Creek thrust northward from where the fault was originally recognized by Giorgis (1999) in the South Mountains, our favored interpretation. Assuming the thickness of the zone of constricted flow does not vary appreciably suggests the Brindle Creek thrust may have greater displacement of the Brindle Creek thrust in the Brushy Mountains.

Deformation Scheme

The structures described above can be summarized into chronological order recognizing six distinct deformations (Table 1). D_1, D_2, and D_3 were ductile deformations that may be related to one prolonged tectonothermal event. A contrasting view to other workers that interpreted D_1 as

Taconic (Bream , 1999; Hatcher, 2001). The Silurian age of metasedimentary rocks (Bream, this guidebook) Devonian magmatism in the eastern IP/Brindle Creek thrust sheet and Neoacadian – early Alleghanian timing of metamorphism, ~350 Ma (Kalbas et al., 2002) provide a reference frame to delimit the early ductile deformation observed in the southwestern Brushy Mountains. Deformation that postdates this reference frame are linked with the most probable documented tectonic event. The post Neoacadian events, D_4, D_5, and D_6 are linked to Alleghanian reactivation of the BFZ and Mesozoic or Cenozoic tectonism, respectively.

Regionally, D_1 structures are recognized as isoclinal folds preserved in boudins, rootless isoclinal folds, and map-scale patterns (Hatcher, 1974; Hopson and Hatcher, 1988; Davis, 1993a, 1993b). Boudins and xenoliths in the southwestern Brushy Mountains commonly preserve an earlier foliation, S_1(?), but no earlier folds. Bryant and Reed (1970) observed a polydeformed boudin of biotite-hornblende gneiss in a weakly foliated, leucocratic biotite granitoid near Lenoir, North Carolina. The intensely migmatitic nature of the rocks obscured earlier compositional layering, making it impossible to identify rootless intrafolial folds. Map-scale patterns of the Toluca and Walker Top Granites supply the best evidence for D_1. The outcrop patterns of both units can be linked to define earlier fold axes, F_1, that were transposed into the later S_2 foliation. Alternatively, these structures could be the result of a single progressive ductile event as described by Griffin (1969), or as favored here, F_2 map-scale sheath folds. It is likely that D_1 is the early stage of a large progressive tectonothermal event that postdates intrusion of the Walker Top Granite and Toluca Granite, ~370 Ma. The younger dates constraining the timing of deformation in the Brindle Creek thrust sheet suggests that D_1 across the study area and the IP is potentially diachronous. D_1 in the thrust sheets of the western IP could be Taconic (Bream, 1999; Hatcher, 2001), but D_1 in the eastern IP must be early Neoacadian.

D_2 is characterized by the S_2 penetrative foliation, commonly axial planar to the recumbent to inclined, isoclinal to tight folds, F_2. Development of stromatic migmatite parallel to transposed S_2 compositional layering and the preferred orientation of fibrolitic sillimanite, L_2 parallel to F_2 fold hinges, within the S_2 fabric suggest that D_2 occurred at near peak metamorphic conditions. The combination of F_2 fold geometries and metamorphic conditions suggests F_2 folds developed as result of passive and flexural flow folding (Hatcher, 1995). Macroscopic structures associated with this event include the development of inclined, isoclinal folds, sheath folds and faulting associated with the Green Mountain fault/Mill Spring thrust, Brindle Creek thrust, and Poplar Spring fault zone. Map patterns of the Walker Top and Toluca Granites provide a strong argument for F_2 sheath folds and support a kinematic model involving NW flow deflected to the SW by the primordial BFZ. D_2 is constrained to a ~10 Ma interval, 360 Ma to 350 Ma, corresponding to metamorphic peak and interpreted to mark peak Neoacadian deformation in the southern Appalachians.

Regional D_3, was postmetamorphic peak but was still ductile. It incorporates the development of later inclined, tight to open F_3 folds and rare axial planar foliation, S_3, associated with these folds. Mechanisms that may be responsible for the development of these folds include: passive flow, and a combination of flexural flow and buckling. Cooling of the thrust sheets probably increased their strength, so they gained coherence, partially transforming to Type-C sheets permitting greater displacement to occur (Hatcher and Hooper, 1992). The trace of the Brindle Creek thrust in the Kings Creek quadrangle is superposed by F_3 folds suggesting greatest displacement was achieved prior to D_3. Yanagihara (1993) documented that D_3 is a continuation of D_2, delimiting the event to a similar interval of time as D_2 and in the late Neoacadian or early Alleghanian.

Earlier structures were superposed by low P-T D_4 and D_5 Alleghanian structures. D_4 defined by the development of upright open F_4 buckle folds and a crenulation cleavage interpreted to be related to the F_4 open buckle folds based on similar orientations. These low P-T structures are interpreted to be associated with the retrograde reactivation of the BFZ under greenschist facies conditions during the Alleghanian (Hatcher, 2001). A substantial amount of joints may have developed synchronous to the brittle deformation associated with the Rosman Fault, D_5, but they are difficult to differentiate from later joints.

The last deformation, D_6, is represented by jointing that could be related to either Mesozoic rifting and strike-slip faulting (Hooper, 1990; Garihan et al., 1993) or Cenozoic uplift (Dennison and Stewart, 2001; Knapp, 2001). No brittle normal faults were observed but Goldsmith et al. (1988) observed several near the study area and throughout the IP. Cenozoic uplift might be expressed as very broad folding of the crust into domes corresponding to the location of regional topographic highs and lows (Dennison and Stewart; 2001).

CONCLUSIONS

1. The southwestern Brushy Mountains contain parts of three NW- and SW-verging crystalline thrust sheets: the Marion, Mill Spring, and Brindle Creek thrust sheets each containing a distinct lithostratigraphy. The Marion thrust sheet contains Tallulah Falls/Ashe Formation rocks, Early Ordovician Henderson Gneiss, and Middle Ordovician Poor Mountain Formation. The Mill Spring sheet thrust migmatitic Ordovician-age intermediate and mafic metaigneous rocks and muscovite schist over the Marion thrust sheet. The Brindle Creek thrust sheet and eastern IP contain an unique

assemblage of Silurian aluminous schist and metagraywacke intruded by Devonian Walker Top and Toluca Granites.

2. Rocks of the southwestern Brushy Mountains are pervasively migmatitic and contain upper amphibolite facies assemblages. Local second sillimanite zone rocks are enveloped by first sillimanite zone rocks. Independent geochronologic data indicate the timing of metamorphism is ~ 350 Ma, constrained by metamorphic rims on zircons.
3. Pressure and temperature estimates from sillimanite schist in the Brindle Creek thrust sheet are 585^{o} C, 2.8 kbar to 710^{o} C, 4.7 kbar for garnet rim assemblages. Garnet cores yield 450^{o}C, 1.3 kbar, to 570^{o}C, 2.5 kbar estimates. The increase in pressure and temperature from garnet cores to rims, continuous zoning profiles across garnets and occurrence of phases within the garnets similar to those in the matrix suggest that rocks of the Brindle Creek thrust sheet were subjected to only one prograde metamorphic event.
4. Eastern IP/Brindle Creek thrust sheet rocks record a contrasting thermal evolution from western IP rocks. P-T paths constructed from the estimates above define a counterclockwise path for the Brindle Creek thrust sheet/eastern IP. The trajectory of this path indicates Buchan metamorphism. Western IP P-T paths suggest Barrovian metamorphism.
5. Intense footwall migmatite indicates the Brindle Creek thrust sheet was emplaced hot.
6. The distinctive transition from strongly aligned fabrics to more randomly oriented fabrics on all scales may define the eastern limit of the primordial BFZ. It is also interpreted to be the break where NW-verging crystalline thrust sheets and sheath folds are transposed into SW-directed flow.
7. Displacement along the Brindle Creek thrust may be greater in the Brushy Mountains than in the South Mountains. Faults here may preserve greater component of dextral strike-slip.
8. Six deformations affected the southwestern Brushy Mountians. D_1, D_2 and D_3 were all ductile and may result from one prolonged tectonothermal event, ~360-330 Ma, and are early Neoacadian to early Alleghanian. D_1 is preserved as an early S_1 foliation in boudins, and as possible map-scale F_1 folds. D_2 marks peak Neoacadian, ~350 Ma, deformation and metamorphism, marked by development of the dominant S_2 foliation, inclined to recumbent tight to isoclinal F_2 folds, sheath folds, Type-F faults and the prominent L_2 mineral lineation. D_3 involved the development map-scale to mesoscale, inclined to upright tight to open F_3 folds, and rare S_3 foliations. D_4 involved lower temperatures and pressures and the development of open buckle folds and crenulations during the late Paleozoic, possibly during the Alleghanian orogeny. D_4 deformation was synchronous with greenschist retrograde deformation of the BFZ. D_5 and D_6 are recognized by brittle jointing related to brittle deforamtion associated with the late Alleghanian Rosman Fault ($D_{5)}$ and Mesozoic extension or Cenozoic uplift ($D_{6)}$.

ACKNOWLEDGMENTS

This research was supported by the U.S. Geological Survey, EDMAP component of the National Cooperative Geologic Mapping Program, under grant 01HQAG0176 to Robert D. Hatcher, Jr. Hatcher provided important advice, and insight regarding geologic mapping, and structural and petrographic analysis. He also reviewed several drafts of this paper, leading to numerous improvements. Dr. Larry Taylor, at the University of Tennessee, Knoxville, provided guidance on the interpretations of electron microprobe data and by reviews of the manuscript. Assistance of Allen Patchen is gratefully appreciated in operating the CAMECA-SX 50. We would also like to thank Mark W. Carter and Carl E. Merschat of the North Carolina Geological Survey for several field reviews. Finally, we would like to thank the dedicated students that comprise the "Hatchery" for their constant flux of ideas about the tectonics of the southern Appalachians.

REFERENCES CITED

Albee, A. I., 1965, Distribution of Fe, Mg, and Mn between garnet and biotite in natural mineral assemblages: Journal of Geology, v. 73, p. 155-164.

Baker, A. J., and Droop, G. T. R. 1983, Grampian metamorphic conditions deduced from mafic granulites and sillimanite–K-feldspar gneisses in the Dalradian of Glen Muick, Scotland: Journal of the Geological Society of London, v. 140. p. 489-497.

Bier, S. E., 2001, Geology of the southeastern South Mountains, North Carolina [M.S. thesis]: Knoxville, University of Tennessee, 162 p.

Bohlen, S. R., Wall, V. J., and Boetcher, A. L., 1983, Experimental investigations and geological applications of equilibria in the system $FeO-TiO_2-Al_2O_3-SiO_2-H_2O$: American Mineralogist, v. 68, p. 1049-1068,

Bream, B. R., 1999, Geology of the Glenwood and Sugar Hill quadrangles, North Carolina, and the structure of the northeast end of the Henderson Gneiss [M.S. thesis]: Knoxville, University of Tennessee, 155 p.

Bream, B. R., Hatcher, R.D., Jr., Miller, C.F., and Fullagar, P.D., 2000, Paragneiss geochemistry and preliminary ion microprobe geochronology of detrital zircons from the southern Appalachian crystalline core: Geological Society of America Abstracts with Programs, v. 32, p. 31.

Bream, B. R., Hatcher, R.D., Jr., Miller, C.F., and Fullagar, P. D., 2001, Geochemistry and provenance of Inner Piedmont paragneisses, NC and SC: Evidence for an internal terrane boundary?: Geological Society of America Abstracts with Programs, v. 33, p. 65.

Brown, P. M., Burt, E. R., II, Carpenter, P.A., Enos, R. M., Flynt, B. J., Jr., Gallagher, P. E., Horrman, C. W., Merschat, C. E., Wilson, W. F., and Parker, J. M., III, 1985, Geologic map of North Carolina: North Carolina Geological Survey, scale 1:500,000.

Bryant, B., and Reed, J. C. Jr., 1960, Road log of the Grandfather Mountain area, North Carolina: Carolina Geological Society Annual Meeting, Field Trip Guidebook, 10 p.

Bryant, B., and Reed, J. C., Jr., 1970, Geology of the Grandfather Mountain window and vicinity, North Carolina and Tennessee: U.S. Geological Survey Professional Paper 615, 190 p.

Brun, J. P., and Burg, J. P., 1982, Combined thrusting and wrenching in the Ibero-Armorican arc: A corner effect during continental collision: Earth and Planetary Science Letters, v. 61, p. 319-332.

Butler, J. R., 1991, Metamorphism, *in* Horton, J. W., Jr., and Zullo, V. A., eds., The geology of the Carolinas: Knoxville, University of Tennessee Press, p. 127-141.

Carrigan, C. W., Bream, B. R., Miller, C. F., and Hatcher, R. D., Jr., 2001, Ion microprobe analyses of zircon rims from the eastern Blue Ridge and Inner Piedmont, NC-SC-GA: Implications for the timing of Paleozoic metamorphism in the southern Appalachians: Geological Society of America Abstracts with Programs, v. 33, p. A42.

Chatterjee, N. D., and Johannes, W., 1974, Thermal stability and standard thermodynamic properties of synthetic 2M1 muscovite, $KAl_2AlSi_3O_{10}(OH)_2$: Contributions to Mineralogy and Petrology, v. 48, p.119-126.

Coward, M. P., and Potts, G. J., 1983, Complex strain patterns developed at the frontal tips and lateral tips to shear zones and thrust zones: Journal of Structural Geology, v. 5, p. 383-399.

Davis, G. L., Tilton, G. R., and Wetherill, G. W., 1962, Mineral ages from the Appalachian province in North Carolina and Tennessee: Journal of Geophysical Research, v. 67, p. 1987-1996.

Davis, T. L., 1993a, Lithostratigraphy, structure, and metamorphism of a crystalline thrust terrane, western Inner Piedmont, North Carolina [Ph.D. dissertation]: Knoxville, University of Tennessee, 245 p.

Davis, T. L., 1993b, Geology of the Columbus Promontory, western Piedmont, North Carolina, southern Appalachians, *in* Hatcher, R. D., Jr., and Davis, T. L., eds., Studies of Inner Piedmont geology with a focus on the Columbus Promontory: Carolina Geological Society Guidebook, North Carolina Geological Survey, p. 17-43.

Dennis, A. J., and Wright, J. C., 1997, Middle and late Paleozoic monazite U-Pb ages, Inner Piedmont, South Carolina: Geological Society of America Abstracts with Programs, v. 29, p. 12.

Dennison, J. M., and Stewart, K. G., 2001, Regional structural and stratigraphic evidence for dating Cenozoic uplift of southern Appalachian Highlands: Geological Society of America Abstracts with Programs, v. 33, p. 6.

Espenshade, G. H., Rankin, D. W., Shaw, K. W., and Neuman, R. B., 1975, Geologic map of the east half of the Winston-Salem quadrangle, North Carolina-Virginia: U.S. Geological Survey Map I-709-B, scale 1:250,000.

Evans, B. W. and Guidotti, C. V., 1966, The sillimanite-potash feldspar isograd in western Maine, USA: Contributions to Mineralogy and Petrology, v. 12, p. 25-62.

Ferry, J. M., and Spear, F. S., 1978, Experimental calibration of the partitioning of Fe and Mg between biotite and garnet: Contributions to Mineralogy and Petrology, v. 66, p. 113-117.

Garihan, J. M., 2001, Observations of the Seneca fault and their implications for thrust sheet emplacement in the Inner Piedmont of the Carolinas: South Carolina Geology, v. 43, p. 1-13.

Garihan, J. M., Ranson, W. A., Orland, K. A., and Preddy, M. S., 1990, Kinematic history of faults in northwestern South Carolina and adjacent North Carolina: South Carolina Geology, v. 33, p. 18-31.

Garihan, J. M., Preddy, M. S., and Ranson, W. A., 1993, Summary of mid-Mesozoic brittle faulting in the Inner Piedmont and nearby Charlotte belt of the Carolinas, *in* Hatcher, R. D., Jr., and Davis, T. L., eds., Studies of Inner Piedmont geology with a focus on the Columbus Promontory: Carolina Geological Society Guidebook, North Carolina Geological Survey, p. 55-65.

Giorgis, S. D., 1999, Inner Piedmont geology of the northwestern South Mountains near Morganton, North Carolina [M.S. thesis]: Knoxville, University of Tennessee, 191 p.

Goldsmith, R., 1981, Structural patterns in the Inner Piedmont of the Charlotte and Winston-Salem 2-degree quadrangles, North Carolina and South Carolina, *in* Horton, J. W., Jr., Butler, J. R., and Milton, D. M., eds., Geological investigations of the Kings Mountain belt and adjacent areas in the Carolinas: Carolina Geological Society Field Trip Guidebook, p. 19-27.

Goldsmith, R., Milton, D. J., and Horton, J. W. Jr., 1988, Geologic map of the Charlotte 1-degree x 2-degree quadrangle, North Carolina and South Carolina: U.S. Geological Survey Map I-1251-E, scale 1:250,000.

Griffin, V. S. Jr., 1969, Migmatitic Inner Piedmont belt of northwestern South Carolina: South Carolina Division of Geology, Geologic Notes, v. 13, p. 87-104.

Griffin, V. S., Jr., 1974a, Analysis of the Piedmont in northwest South Carolina: Geological Society of America Bulletin, v. 85, p. 1123-1138.

Griffin, V. S., Jr., 1974b, Progress report on a geologic study in Anderson County, South Carolina: South Carolina Divison of Geology, Geologic Notes, v. 18, p. 13-23.

Griffits, W. R., and Overstreet, W. C., 1952, Granitic rocks of the western Carolina Piedmont: American Journal of Science, v. 250, p. 777-789.

Hatcher, R. D. Jr., 1969, Stratigraphy, petrology, and structure of the low rank belt and part of the Blue Ridge of northwestern South Carolina: South Carolina Division of Geology, Geologic Notes, v. 13, p. 105-141.

Hatcher, R. D., Jr., 1972, Developmental model for the southern Appalachians: Geological Society of America Bulletin, v. 82, p. 2735-2760.

Hatcher, R. D., Jr., 1974, Introduction to the tectonic history of northeast Georgia: Georgia Geological Society Guidebook 13-A, 59 p.

Hatcher, R. D., Jr., 1978, Tectonics of the western Piedmont and Blue Ridge: Review and speculation: American Journal of Science, v. 278, p. 276-304.

Hatcher, R. D., Jr., 1987, Tectonics of the southern and central Appalachian internides: Annual Review Earth Planetary Science, v. 15, p. 337-362.

Hatcher, R. D., Jr., 1989, Tectonic Synthesis of the U.S. Appalachian, Chapter 14 *in* Hatcher, R. D., Jr., Thomas, W. A., and Viele, G. W., eds., The Appalachian Ouachita orogen in the United States: Boulder, Colorado, Geological Society of America, The geology of North America, v. F-2, p. 511-535.

Hatcher, R. D., Jr., 1993, Perspective on the tectonics of the Inner Piedmont, southern Appalachians, *in* Hatcher, R. D., Jr., and Davis, T. L., eds., Studies of Inner Piedmont geology with a focus on the Columbus Promontory: Carolina Geological Society Guidebook, North Carolina Geological Survey, p. 17-43.

Hatcher, R. D., Jr., 1995, Structural geology: Principles, concepts, and problems, 2nd ed.: Engle Cliffs, New Jersey, Prentice Hall Inc., 525 p.

Hatcher, R. D., Jr., 2001, Rheological partitioning during multiple reactivation of the Palaeozoic Brevard Fault Zone, southern Appalachians, USA, *in* Holdsworth, R. E., Strachan, R. A., Magloughlin, J. F., and Knipe, R. J., eds., The nature and tectonic significance of fault zone weakening: London, Geological Society of London Special Publication 186, p. 255-269.

Hatcher, R. D., Jr., in press, Properties of thrusts and upper bounds for the size of thrust sheets, *in* McClay, K. R. ed., Thrust tectonics: American Association of Petroleum Geologists Memoir

Hatcher, R. D., Jr., and Butler, J. R., 1979, Guidebook for southern Appalachian field trip in the Carolinas, Tennessee, and northeastern Georgia: International Geological Correlation Program, (IGCP), Field Conference and Symposium on the Caledonide Orogen, Raleigh, North Carolina Geological Survey, 117 p.

Hatcher, R. D., Jr., and Hooper, R. J., 1992, Evolution of crystalline thrust sheets in the internal parts of mountain chains, *in* McClay, K.R., ed., Thrust tectonics: London, Chapman and Hall, p. 217-234.

Hatcher, R. D., Jr., and Zietz, I., 1980, Tectonic implications of regional aeromagnetic and gravity data from the southern Appalachians, *in* Wones, D., Ed., Proceedings, The Caledonides in the USA, IGCP Project 27-Caledonide orogen, 1979 Meeting: Blacksburg, Virginia Polytechnic Institute and State University, Department of Geological Sciences, Memoir 2, p. 235-244.

Hill, J. C., 1999, Geology of the Marion East quadrangle, North Carolina, and the stratigraphy of the Tallulah Falls Formation in the Chauga belt [M.S. thesis]: Knoxville, University of Tennessee, 188 p.

Hodges, K. V., and Spear, F. S., 1982, Geothermometry, geobarometry and the Al_2SiO_5 triple point at Mt. Moosilauke, New Hampshire: American Mineralogist, v. 67, p. 118-1134.

Holdaway, M. J., 1971, Stability of andalusite and the aluminum silicate phase diagram: American Journal of Science, v. 271, p. 97-131.

Hooper, R. J., 1990, Effects of late Mesozoic(?), brittle faults on Paleozoic tectonic configurations: Central Georgia Piedmont: Geological Society of America Programs with Abstracts, v. 22, p. 232.

Hopson, J. L., and Hatcher, R. D., Jr., 1988, Structural and stratigraphic setting of the Alto allochthon, NE Georgia: Geological Society of America Bulletin, v. 100, p. 339-350.

Horton, J. W., Jr., and McConnell, K. I., 1991, The western Piedmont, *in* Horton, J.W., Jr., and Zullo, V.A., The geology of the Carolinas: Knoxville, University of Tennessee Press, p. 59-78.

Kalbas, J. L., Bream, B. R., Hatcher, R. D., Jr., and Maybin, A. H., 2002, Evidence for mafic Ordovician magmatism in the Brushy Mountains, western Inner Piedmont of North Carolina: Geological Society of America Abstracts with Programs, v. 34, p. 119.

Keith, A., 1905, Description of the Mount Mitchell quadrangle (North Carolina-Tennessee): U. S. Geological Survey geologic atlas, Folio 124, 10 p.

Keith, A., 1907, Description of the Pisgah quadrangle (North Carolina-South Carolina): U. S. Geological Survey geologic atlas, Folio 147, 10 p.

King, P. B., 1955, A geologic cross section across the southern Appalachians: An outline of the geology in the segment in Tennessee, North Carolina, and South Carolina, *in* Russell, R. J., ed., Guides to southeastern geology: New Orleans, Geological Society of America, p. 332-373.

Knapp, J. H., 2001, Cenozoic tectonic evolution of southeastern North America: Evidence for passive margin uplift?: Geological Society of America Abstracts with Programs, v. 33, p. 5.

Kohn, M. J., 2001, Timing of arc accretion in the southern Appalachians: Perspectives from the Laurentian margin: Geological Society of America Abstracts with Programs, v. 33, p. 262.

Lemmon, R. E., 1973, Geology of the Bat Cave and Fruitland quadrangles and the origin of the Henderson Gneiss, western North Carolina [Ph.D. dissertation]: Chapel Hill, University of North Carolina, 145 p.

Lemmon, R. E., and Dunn, D. E., 1975, Origin and geologic history of the Henderson Gneiss from Bat Cave and Fruitland quadrangles, western North Carolina: Geological Society of America Abstracts with Programs, v. 7, p. 509.

Lisle, R. J., 1984, Strain discontinuities within the Seve-Koli Nappe complex, Scandanavian Caledonides: Journal of Structural Geology, v. 6, p. 101-110.

Luth, W. D., Jahns, R. H., and Tuttle, O. F., 1964, The granite system at pressures of 4 to 10 kilobars: Journal of Geophysical Research, v. 69, p. 759-773.

Mapes, R. W., 2002, Geochemistry and geochronology of mid-Paleozoic granitic plutonism in the southern Appalachian Piedmont terrane, North Carolina-South Carolina-Georgia [M.S. thesis]: Nashville, Vanderbilt University, 150 p.

Mapes, R. W., Miller, C. F., Fullagar, P. D., and Bream, B. R., 2001, Acadian plutonism in the Inner Piedmont and eastern Blue Ridge, North Carolina and northern Georgia: Geological Society of America Abstracts with Programs, v. 33, p. 30.

Mapes, R.W., Maybin, A. H., III, Miller, C. F., Fullagar, P. D., and Bream, B.R., 2002, Geochronology and geochemistry of mid Paleozoic granitic magmatism, central and eastern Inner Piedmont, North Carolina and South Carolina: Geological Society of America Abstracts with Programs, v. 34, p. A-94.

Mirante, D. C., and Patino-Douce, A. E., 2000, Melting and migmatization in the southern Appalachian Inner Piedmont of northeast Georgia; the Athens gneiss: Geological Society of America Abstracts with Programs, v. 33, p. 297.

Odom, A. L., and Fullagar, P. D., 1973, Geochronological and tectonic relationship between the Inner Piedmont, Brevard zone, and Blue Ridge belts, North Carolina: American Journal of Science, v. 273-A, p. 133-149.

Odom, A. L., and Russell, G. S., 1975, The time of regional metamorphism of the Inner Piedmont, North Carolina, and Smith River allochthon: Inference from whole-rock ages: Geological Society of America Abstracts with Programs, v. 7, p. 522-523.

Overstreet, W. C., Yates, R. G., and Griffits, W. R., 1963, Geology of the Shelby quadrangle, North Carolina: U.S. Geological Survey Miscellaneous Geological Investigations, Map I-384, Scale 1:62,500.

Pownceby, M. I., Wall, V. J., and O'Niel, H. S. C., 1987a, Fe-Mn partitioning between garnet and ilmenite: Experimental calibrations and applications: Contribution to Mineralogy and Petrology, v. 97, p. 116-126,

Pownceby, M. I., Wall, V. J., and O'Niel, H. S. C., 1987b, Fe-Mn partitioning between garnet and ilmenite: Experimental calibrations and applications (corrections): Contribution to Mineralogy and Petrology, v. 97, p. 539.

Rankin, D. W., Espenshade, G. J., and Neuman, R. B., 1972, Geologic map of the west half of the Winston-Salem quadrangle, North Carolina, Virginia, and Tennessee: U. S. Geological Survey Map I-709-A, scale 1:250,000.

Raymond, L. A., 1995, Petrology: The study of igneous, sedimentary, and metamorphic rocks: Dubuque, Iowa, Wm. C. Brown Communications, Inc, 742 p.

Reed, J. C., 1964a, Geology of the Lenoir quadrangle, North Carolina: U. S. Geological Survey Map I-709-A, scale 1:62,500.

Reed, J. C., 1964b, Geology of the Linville Falls quadrangle North Carolina: U.S. Geological Survey Bulletin 1161-B, 53 p.

Reed, J. C., and Bryant, B., 1964, Evidence for strike-slip faulting along the Brevard zone in North Carolina: Geological Society of America Bulletin, v. 75. p. 1177-1195.

Sinha, A. K., Hund, E. A., and Hogan, J. P., 1989, Paleozoic accretionary history of the North American plate margin (central and southern Appalachians): Constraints from the age, origin, and distribution of granitic rocks, *in* Hillhouse, J., ed., Deep structure and past kinematics of accreted terranes: American Geophysical Union Monograph Series, p. 219-238.

Spear, F. S., 1993, Metamorphic phase equilibria and pressure-temperature-time paths: Chelsea, Michigan, Book Crafters, Inc., 799 p.

Spear, F.S., Selverstone, J., Hickmott, D., Crowley, P., and Hodges, K. V., 1984, P-T paths from garnet zoning: A new technique for deciphering tectonic processes in crystalline terranes: Geology, v. 12, p 87-90.

Spear, F.S., and Kohn, M., 1989, Thermobarometry, v. 1.9, computer program.

Thompson, A. B., 1982, Dehydration melting of pelitic rocks and generation of H_2O-undersaturated granitic liquids: American Journal of Science, v. 282, p. 1567-1595.

Turner, F. J., and Weiss, L. E., 1963, Structural analysis of metamorphic tectonites: New York, New York, McGraw-Hill Book Company, Inc., 545 p.

Vinson S. B., 2001, Ion probe geochronology of granitoid gneisses of the Inner Piedmont, North Carolina and South Carolina [M.S. thesis]: Nashville, Vanderbilt University, 84 p.

Vinson, S. B., and Miller, C. F., 1999, Constraints on timing of Inner Piedmont plutonism, NC–SC, from ion microprobe U-Pb zircon analysis: Geological Society of America Abstracts with Programs, v. 31, p. A77.

Werner, C. D., 1987, Saxonian granulites-igneous or lithogenous? A contribution to the geochemical diagnosis of the original rocks in high-metamorphic complexes, *in* Gerstenberger, H., ed., Contributions to the geology of the saxonian granulite massif: Sachsisches Granulitegebire, Zfl-Mitteilungen Nr, v. 133, p. 221-250.

Williams, P. F., 1970, A criticism of the use of style in the study of deformed rocks: Geological Society of America Bulletin, v. 81, p. 3283-3296.

Williams, S. T., 2000, Structure, stratigraphy, and migmatization in the southwestern South Mountains, North Carolina [M.S. thesis]: Knoxville, University of Tennessee, 111 p.

Yanagihara, G. M., 1993, Evolution of folds associated with D_2 and D_3 deformation and their relationship with shearing in a part of the Columbus Promontory, North Carolina, *in* Hatcher, R.D., Jr., and Davis, T.L., eds., Studies of Inner Piedmont geology with a focus on the Columbus Promontory: Carolina Geological Society Guidebook, North Carolina Geological Survey, p. 45-54.

Yanagihara, G. M., 1994, Structure, stratigraphy, and metamorphism of a part of the Columbus Promontory, western Inner Piedmont, North Carolina [M.S. thesis]: Knoxville, University of Tennessee, 214 p.

Field Trip Stop Descriptions

INTRODUCTION

This field guide contains 16 stops in the western and eastern Inner Piedmont of central-western North Carolina (Fig. 1). On Day 1 we will examine representative exposures of characteristic western Inner Piedmont rocks and structures south of Marion and gradually move eastward into the eastern Inner Piedmont of the South Mountains (Fig. 2), then begin Day 2 in the western Inner Piedmont and spend the remainder of the Sunday morning trip in the eastern Inner Piedmont of the southwestern Brushy Mountains (Fig. 3). While we have not constructed a detailed roadlog for the trip, we have provided instructions for getting from one stop to another along with GPS (global positioning satellite) locations at each stop to aid those wanting to find any of the stops again. In the future when you return to any stops requiring permission from landowners, please honor the requests made herein to do so to enable those who may come along later to have similar access.

SAFETY

2002 Carolina Geological Society field trip stops will be mostly along roads and highways, with one along an active railroad track, but there will be a few stops that will involve some walking and one (Stop 4) that will require a very steep descent into a river gorge. At all stops we request that everyone exercise extreme care in getting onto and off the buses, walking along and crossing roads and highways, crossing the railroad track, and in walking during stops. We strongly recommend that, if you have any difficulty whatsoever in descending or ascending steep slopes, you *NOT* go down the steep trail into the Second Broad River gorge at Stop 4. There are some rocks that are worth looking at highway level about 50 m south of the trailhead.

We wish everyone a safe, educational, and enjoyable 2002 Carolina Geological Society field trip.

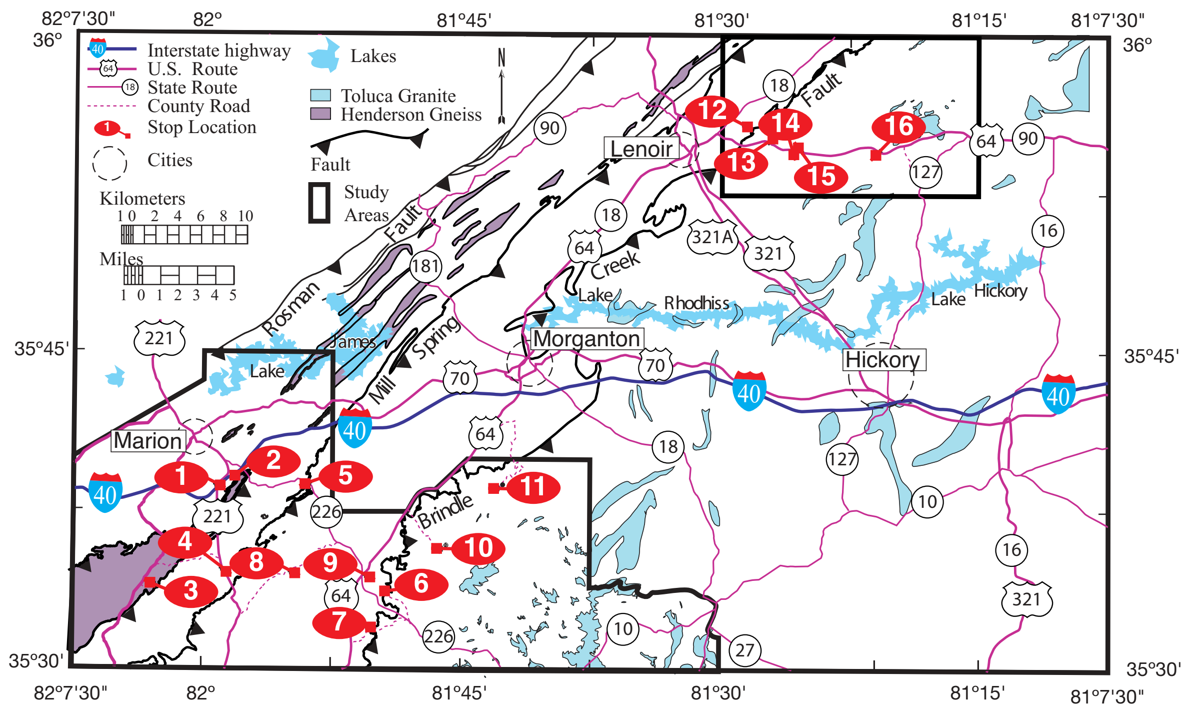

Figure 1. Reference map for the 2002 CGS field trip showing stop locations, roads, cities, simplified geology and areas of detailed studies in the Brushy and South Mountains.

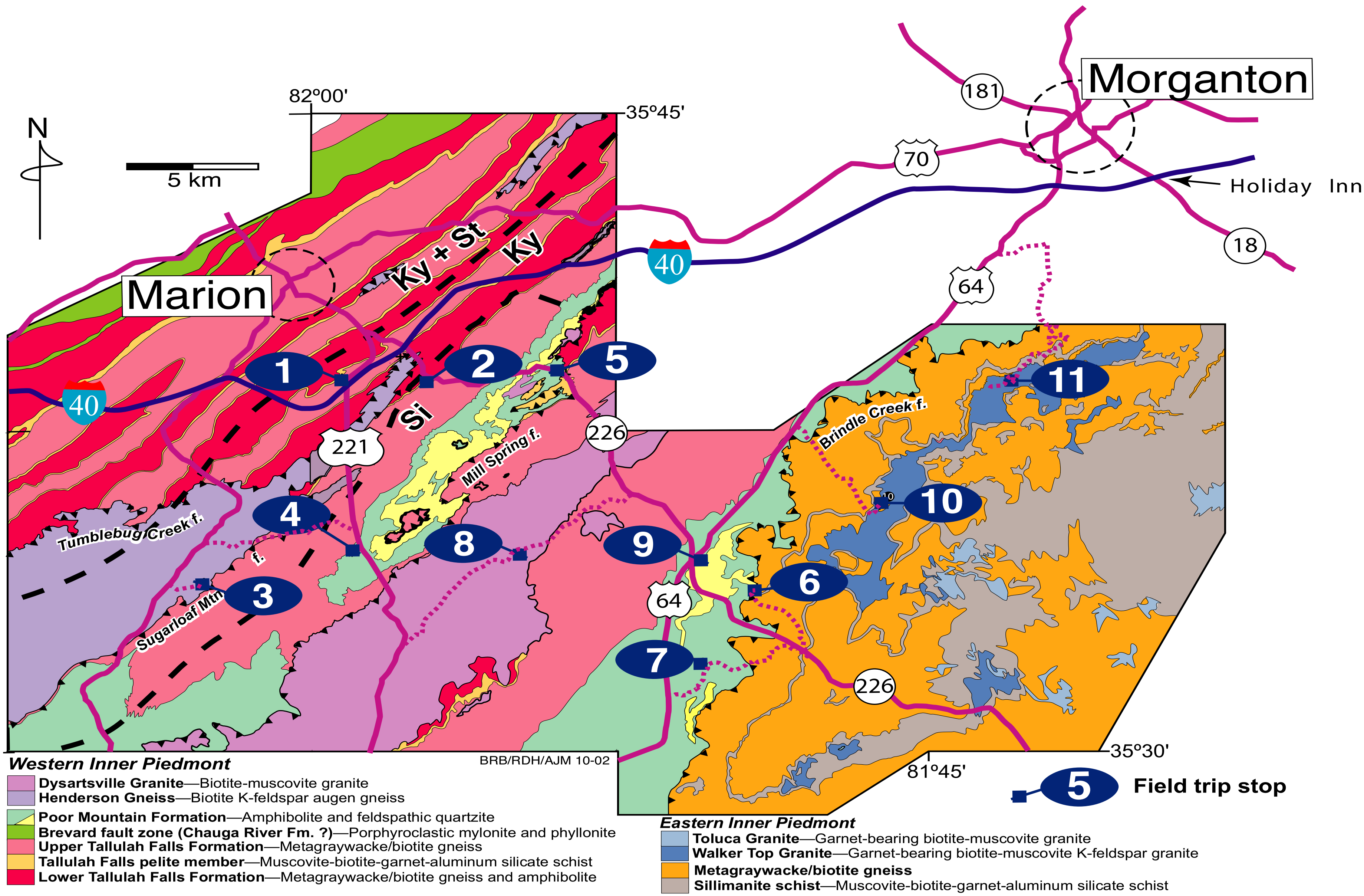

Figure 2. Field trip stop locations and critical roads for Day 1 superposed on the geologic map of the Marion-South Mountains area.

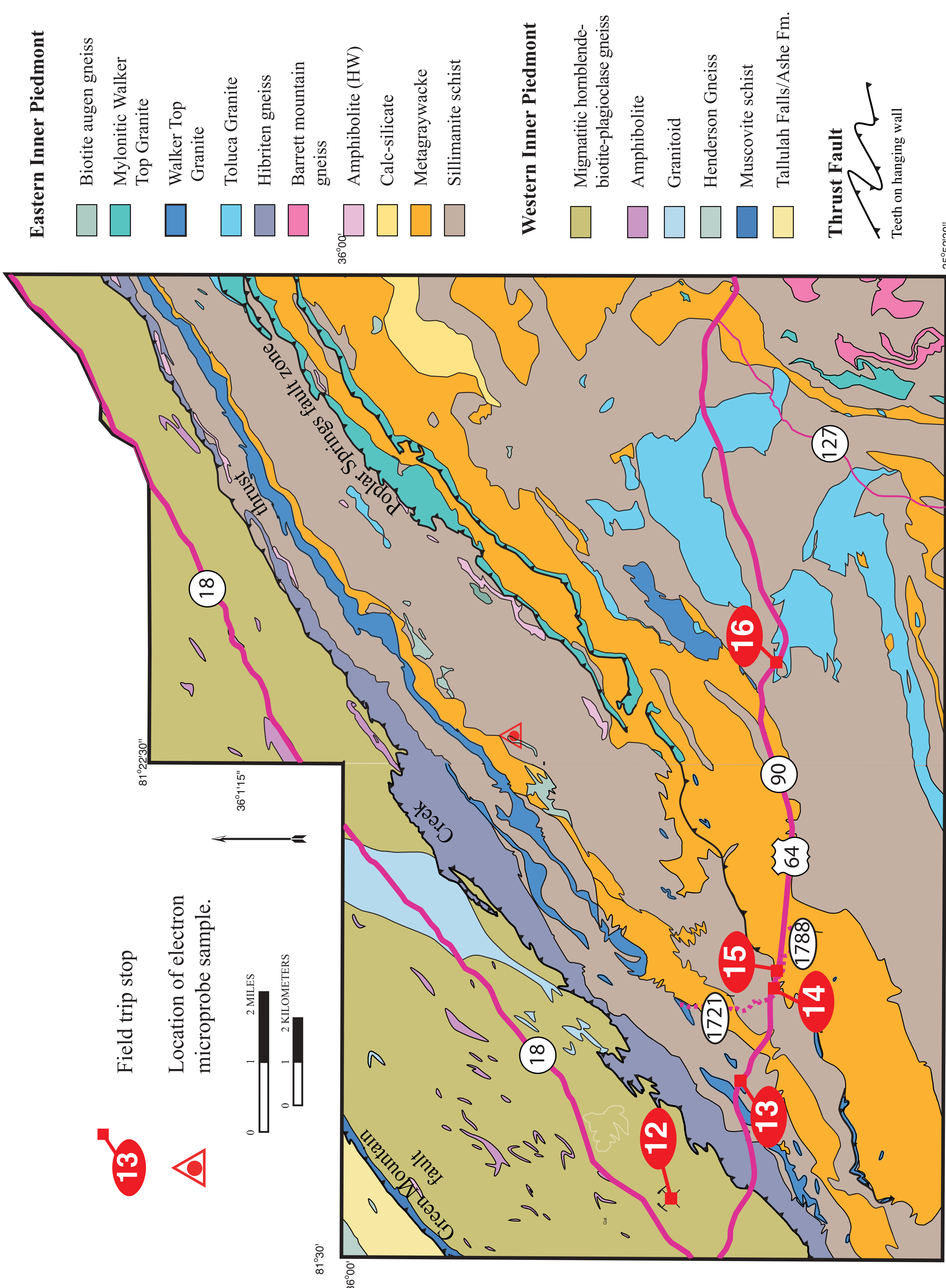

Figure 3. Field trip stop locations and critical roads for Day 2 superposed on the geologic map of the Brushy Mountains area.

DAY 1

8 a.m. Depart Holiday Inn parking lot, turn left (N) onto NC 18, then left again (0.1 mi) onto I-40 westbound. Drive 20 mi west to Exit 85 (U.S. 221),exit, and turn right. Take a left 0.1 mi (N) at Rockwell Drive, park on shoulder.

STOP 1: Upper Tallulah Falls Formation on Rockwell Drive north of I–40 Exit 85. ***Leader: Joe Hill.***
Location: 35˚38.75' N, 81˚59.15' W, Marion East 7.5-minute quadrangle.

PURPOSE: To examine Upper Tallulah Falls Formation metagraywacke and schist. (20 minutes)
DESCRIPTION: This stop is located approximately in the geographic center of one of the NE-SW trending belts of upper Tallulah Falls Formation (TFF). The unit is bounded both a few hundred meters NW (on the back side of the ridge) and approximately 700 m SE by belts of garnet aluminous schist member of the TFF. The upper member of the TFF is relatively fresh and well exposed here and contains little to no amphibolite, a distinguishing characteristic that separates the upper from the lower TFF. It is slightly migmatitic. See Bier et al. (this guidebook) for general description of the TFF. This is one of Bream's (this guidebook) detrital zircon sample localities.

Upper TFF rocks here consist dominantly of dark gray medium-grained metagraywaqcke and minor muscovite-biotite schist (containing retrograde chlorite), with veins and layers of quartz and quartz-feldspar. Metagraywacke layers range from 5 to 15 cm thick, schist layers range from a few millimeters to a few centimeters thick, and compositional layering and dominant foliation (S_2) are parallel. Orientation of S2 ranges from N37E, 15˚ SE to N10E, 56˚ SE. Several veins contain the assemblage quartz + feldspar + biotite -$\pm$ muscovite $\pm$ epidote $\pm$ garnet. Minor sulfide minerals are also present in the metagraywacke and in veins.

Return 0.2 mi to I-40 eastbound. Drive east ~2 mi and get off at Exit 86 (NC 226). Turn left (S) onto NC 226, then almost immediately right onto College Drive. Drive ~0.2 mi, cross railroad track, and park on shoulder or in small pull off next to tracks.

NOTE: STAY OFF RAILROAD TRACKS. CROSS QUICKLY AND CAREFULLY—THIS IS AN ACTIVE TRACK!

STOP 2: Tallulah Falls Formation Aluminous (Sillimanite) Schist on CSX Railroad. ***Leader: Joe Hill.***
Location: 35˚39.28' N, 81˚57.77' W, Marion East 7.5-minute quadrangle.

PURPOSE: To examine the garnet aluminous schist member of the Tallulah Falls Formation. (20 minutes)
DESCRIPTION: Stratigraphically, the garnet aluminous schist member of the TFF occurs below the upper graywacke-schist member and above the lower graywacke-schist-amphibolite member. It is arguably the most important rock unit in the western Inner Inner Piedmont at this latitude because it serves as the most recognizable and traceable lithologic marker thus permitting resolution of the structural geometry.

The aluminous schist here consists of sillimanite (abundant fibrolite) schist with some metagraywacke and amphibolite layers and boudins. This locality is in the Sugarloaf Mountain thrust sheet a few kilometers west (and in the footwall) of the Mill Spring thrust. The sillimanite-in isograd is between this and Stop 1. Compositional layering and the dominant S_2 foliation are parallel here, with an average orientation of N48E, 36˚SE. A weak S_3 (?) foliation has an orientation of N61E, 64˚SE. A coarse pegmatite (quartz, K-spar, muscovite) occurs parallel to the S_2 foliation.

The contact between metagraywacke and Henderson Gneiss is present about 150 m west near the old disposal plant. The contact was well exposed, but is now covered by slope excavation.

Backtrack to Exit 86 on I-40, cross overpass, and turn left onto westbound lane. Drive W to Rest Area, exit, and pull in. This will be our MORNING COFFEE BREAK (20 minutes). Get back onto I-40 (W) and drive ~3.9 mi to Exit 81 (Sugar Hill Exit, SR 1001). Drive S 4.7 mi, veer right remaining on SR 1001,then 1.5 mi to intersection in downtown Sugar Hill. Continue straight (S) 2.8 mi and turn left onto SR 1144, Hensley Road. Drive 0.6 mi to end of road and park. Walk N to exposure on mountainside.

NOTE: PERMISSION MUST BE OBTAINED FROM THE PROPERTY OWNERS PRIOR TO ENTRY!!!

STOP 3: Henderson Gneiss. ***Leader: Brendan Bream.***
Location: 35˚33.93' N, 82˚02.84' W, Sugar Hill 7.5-minute quadrangle.

PURPOSE: To observe the Henderson Gneiss near the NE termination of the main outcrop body, and examine the deformational fabric(s) in the Henderson Gneiss. (35 minutes)

DESCRIPTION: This stop is located less than 400 m northwest of the Sugarloaf Mountain fault. At this lattitude, displacement on the Sugarloaf Mountain fault is minimal and it terminates ~2 km to the northeast. This exposure is typical of Henderson Gneiss in this area. The impressive relief to the immediate NE is part of the same Henderson Gneiss body located just SE of the Brevard fault zone and contains the highest peak in the greater South Mountains area, Hickorynut Mountain (just over 1000 m, 3200 ft). Exfoliation surfaces are common in this area. The main body extends along strike to the NE through the Glenwood 7.5-minute quadrangle into the Marion East 7.5-minute quadrangle where it terminates (Bream, 1999; Hill, 1999). Further northeast along strike, Henderson Gneiss occurs as small elliptical outliers up to several kilometers long but mostly less than ~0.5 km (Reed, 1964; Bryant and Reed, 1970; Hill, 1999).

The Henderson Gneiss has an areal extent of more than 5,000 km^2 and its present geometry is a result of folding and shearing of the original granitic pluton (see Hatcher, this guidebook, his Fig. 9). Strain within the rock unit is dominantly flattening, S-L tectonite with Flinn's k~0.75, but may also be constrictional forming L-tectonites with k~10.1 in some fold hinges. Here the Henderson Gneiss is an S-tectonite and the augen are elongate in the S_2 foliation surface. The Henderson Gneiss here is a biotite, quartz, plagioclase, K-feldspar augen gneiss. Augen are dominantly microcline with myrmekite rims and have long axes up to 2 cm long. Both K-feldspar and plagioclase occur in the groundmass. A rare fold is preserved beneath the overhang and another is present in the saprolite near the old dirt road (back toward the vehicles).

Return to SR 1001 and turn right, drive 1.4 mi N to SR 1135 and turn right (E). Drive 3.6 mi to U.S. 221; turn right (S) and drive 0.8 mi to exposure of Poor Mountain Amphibolite on west side of road; park in pulloff on east side of road, then carefully cross the highway.

STOP 4: Unconformity between upper Tallulah Falls Formation and Poor Mountain Amphibolite. ***Leader: Brendan Bream.***
Location: 35˚34.80' N, 81˚58.80' W, Glenwood 7.5-minute quadrangle.

PURPOSE: To observe the contact between the basal Poor Mountain Amphibolite and upper Tallulah Falls metagraywacke in the Second Broad River. (45 minutes).

WARNING: TRAIL DOWN TO THE SECOND BROAD RIVER IS VERY STEEP AND SLIPPERY, ESPECIALLY WHEN WET. DO NOT GO DOWN IF YOU HAVE DIFFICULTIES WITH STEEP SLOPES OR HOPPING ROCKS IN CREEKS.

DESCRIPTION: This is the best accessible fresh exposure of the TFF-Poor Mountain Amphibolite contact in this area. The contact is interpreted as stratigraphic and unconformable.

The Tallulah Falls-Poor Mountain Amphibolite contact is located at the base of the thin-bedded yellowish-tan muscovite schist (total thickness is less than 30 cm) (Fig. 4). Because much of the actual contact is cut by a granitoid intrusion, the following support the unconformable contact interpretation: (1) no truncation of foliation exists between the rock units; (2) lack of mylonite deformation and shear-sense indicators in either unit near the contact; and (3) regional stratigraphic relationships (see Hatcher, this guidebook, his Fig. 8) throughout the western Inner Piedmont.

The muscovite schist exposed near the contact in the Second Broad River is coarser grained than the Poor Mountain Quartzite that, in places, is muscovite-rich. Exposure of this layer is limited and its extent along strike is unknown. The mineralogy of the layer suggests that it represents the uppermost part of the Tallulah Falls Formation or that it is a thin layer of the Brevard-Poor Mountain transitional unit, which further supports interpretation of this contact as an unconformity.

Poor Mountain Amphibolite here is finely laminated nonmigmatitic amphibolite (Fig. 4d) interlayered with feldspathic quartzite (and metatuff?) with lesser amounts of amphibole gneiss. Amphibole gneiss occurs as thin to thick bands within the more dominant laminated amphibolite. A mineral lineation is defined by alignment of hornblende in the laminated amphibolite and less commonly in amphibole gneiss. Layering in the laminated amphibolite varies from a few mm to approximately 30 cm thick. The interlaying in the laminated amphibolite and feldspathic quartzite (or metatuff?) is interpreted as a primary sedimentary (volcaniclastic?) feature of the Poor Mountain Formation. Laminated amphibolite here is mostly fine-grained, and rarely contains mesoscopic folds, in contrast with exposures found in the Columbus Promontory and in South Carolina. The unit is dark- to medium-gray and weathers to an orange ochre saprolite. Epidote and clinozoisite occur mostly in quartzofeldspathic layers, as either hydrous alterations or prograde metamorphic products of recrystallization of Ca-rich components. Recrystallized quartz with 120˚ grain boundaries occurs in the laminated amphibolite but is more common in the amphibole gneiss and quartzite layers. The hornblende is prismatic and has strong green pleochroism. Nematoblastic and sometimes poikiloblastic textures are found in this unit.

The roadcut exposure ~50 m S on U.S. 221 is typical of the finely laminated nonmigmatitic Poor Mountain Amphibolite where it is preserved in the northwest, upright limb of a large isoclinal reclined syncline in the footwall of the Mill Spring thrust sheet. A later open fold, the Rockhouse Mountain syncline, overprints this fold here and the Mill Spring thrust ~1.5 km to the NE on Rockhouse Mountain.

Turn around and head N on U.S. 221 toward I-40; at I-40 (~4.7 mi) turn right onto eastbound ramp; get off at exit 86 (NC 226); turn left (S) onto NC 226. Head S on NC 226 ~5 mi and pull into parking lot of Victory Temple Full Gospel Church.

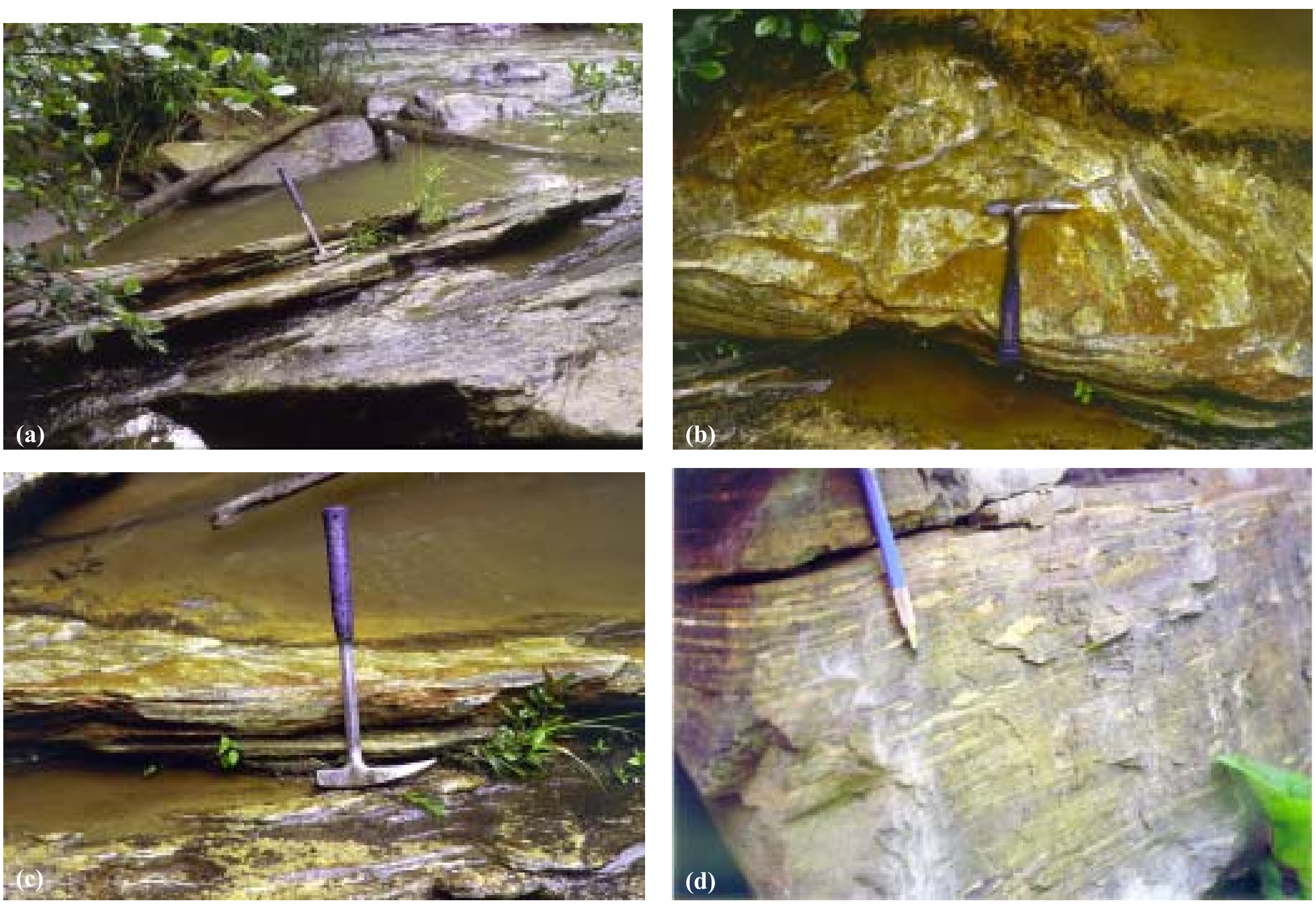

Figure 4. Contact between the upper Tallulah Falls Formation and Poor Mountain Amphibolite. (a) through (c) are located in the Second Broad River south of Spooky Hollow Road in the Glenwood 7.5-minute quadrangle. (d) Typical Poor Mountain Amphibolite outcrop along U.S. 221 near Stop 4.

STOP 5: Migmatitic Sillimanite Schist at Victory Temple Full Gospel Church. ***Leader: Joe Hill.***
Location: 35˚ 38.80' N, 81˚53.82' W, Marion East 7.5-minute quadrangle.

PURPOSE: To examine the structure of the sillimanite schist and amphibolite immediately beneath the Mill Spring fault. (25 minutes)
DESCRIPTION: The Mill Spring fault is exposed at the east end of the parking lot and is marked by the occurrence of a garnet and sillimanite bearing quartzite, which is interpreted to be equivalent to the garnet-aluminous-schist member of the Tallulah Falls Formation. At this locality, migmatitic Poor Mountain Amphibolite saprolite is exposed in the footwall behind the church annex building.

Numerous tight to isoclinal folds and refolds occur here. Intense deformation and migmatization here may be related to the location of these rocks immediately beneath the (eroded) Mill Spring thrust sheet.
The Mill Spring fault is a gently folded, relatively planar structure that dips gently (12-19˚) southeast. This fault emplaces a hanging-wall antiform of TFF over an isoclinal footwall synform. These isoclinal folds are overprinted by a later upright open folds including the Rockhouse Mountain syncline. The refolding of preexisting isoclinal folds at this locality is likely either late syn- to post-thrust sheet emplacement. Detailed mapping has revealed that attitudes of faults and other contacts in the Inner Piedmont do not always parallel measured foliations, an observation also made in other parts of the southern Appalachians (R. D. Hatcher, pers. comm., 1997). Faults here have shallow (~15˚) dip and are folded by broad open folds. The dominant foliation (S_2) generally dips 10˚ to 15˚ greater than the calculated attitudes of major D_4 structures. This discrepancy can be explained here if one set of structures formed at a different time under different P-T conditions than the other. Hence, the S_2 foliation is interpreted to have developed earlier than the map-scale structure.

Continue S on NC 226 just over 10 mi past U.S. 64 intersection; turn left onto Camp McCall Road; follow ~2 mi to camp office. This will be our LUNCH STOP. Feel free to use camp tables and restrooms.

NOTE: PERMISSION MUST BE OBTAINED FROM CAMP MANAGEMENT PRIOR TO ENTRY.

STOP 6: Intensely migmatitic Poor Mountain (and Tallulah Falls?) Formation at Camp McCall in the Brindle Creek fault footwall. ***Leader: Scott Giorgis.***
Location: 33˚33.65' N, 81˚49.18' W, Dysartsville 7.5-minute quadrangle.

PURPOSE: To observe intensely migmatitic rock units in the Brindle Creek fault footwall. (1 hour).
DESCRIPTION: After parking near the caretaker's house walk upstream (north) along Somey Creek away from McCall Lake. The water in the falls ahead flows over migmatitc Poor Mountain Formation (and possibly upper TFF). The transition between the Quartzite and Amphibolite members of the Poor Mountain Formation is everywhere gradational. Both units contain hornblende, quartz, biotite, and feldspar. This outcrop is predominantly metasandstone and has been mapped as part of the Poor Mountain Quartzite member, but the metasandstone here is much more biotite rich and contains large (~1 cm) hornblende porphyroblasts and tailed 1-to-3 cm feldspar and composite feldspar-quartz porphyroclasts in more amphibole-poor layers (Fig. 5). Good F_2 folds of pre-F_2 veins occur in some of the thicker layers. Compositional layering and S_2 foliation are parallel and oriented N62W, 24˚ E to N75 W, 15˚ NE in the falls area.
Cropping out downstream from the waterfall is migmatitic quartzofeldspathic biotite gneiss and. the ridge to the east is capped by the sillimanite schist, both of the Brindle Creek thrust sheet. The contact here between Poor Mountain Formation and the sillimanite schist is interpreted as the Brindle Creek fault for two reasons: (1) The sillimanite schist unit can be traced throughout the South Mountains. The sillimanite schist in the hanging wall is truncated at the contact. (2) The contact places a different lithologic assemblage over the upper Poor Mountain Formation.

Backtrack to NC 226 and U.S. 64 intersection; take U.S. 64 W (S) past the McDowell-Rutherford County line (2.1 mi). Continue 1.6 mi to SR 1706 (Cane Creek Road) and turn left. Drive 1.7 mi to gated road on left. Park on shoulder of road.

Figure 5. Early folded veins in migmatitic porphyroclastic (composite feldspar-quartz) Poor Mountain Quartzite at the bottom of Somey Creek Falls at Camp McCall. Large hornblende porphyroblasts occur a few meters downstream in other layers.

STOP 7: Agmatite in intense migmatite in the Brindle Creek fault footwall *Leader: Scott Williams.*
Location: 35˚31.91' N, 81˚50.42' W, Dysartsville 7.5-minute quadrangle.

PURPOSE: To examine several well-exposed migmatite structures preserved in saprolite.
(30 minutes)

DESCRIPTION: From Cane Creek Mountain Road, walk north along the gated logging road. Agmatite saprolite is located in the roadcuts approximately 50 m from the gate around a right bend. Amphibolite blocks up to 1-m long, probably Poor Mountain Amphibolite protolith, are present in the migmatite. A block of coarse augen granitic gneiss that resembles a xenolith is also present here. Biotite selvages surround several of the amphibolite blocks in the agmatite (Fig. 4). Other migmatitic structures are also present here including opthalmitic (augen/eyed) and schollen (raft/disoriented) structures.

Backtrack to U.S. 64; turn right onto U.S. 64 W (N); at U.S. 64-NC 226 intersection (5.5 mi) take NC 226 N; turn left onto SR 1802 (Vein Mountain Road) 2.3 mi from U.S. 64. Drive 3.1 mi to Lost Dutchmen's Mining Association campground on right (N). Carefully cross Vein Mountain Road onto the gravel road and continue past the gate.

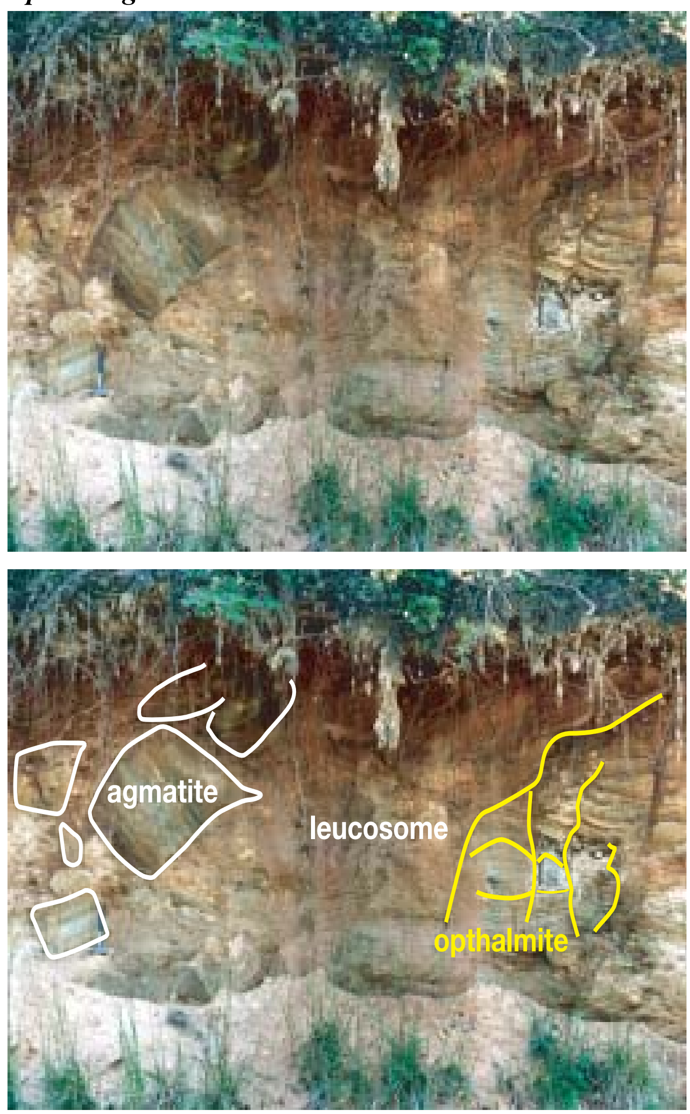

Figure 6. Saprolite exposure of extensive migmatite just north of Cane Creek Mountain Road, approximately 1 mile east of U.S. 64. (a) Well-preserved Poor Mountain Amphibolite migmatite saprolite. Note rock hammer to lower left. (b) Outline of some structures within migmatite exposure. White outlines are agmatite paleosome blocks of Poor Mountain Amphibolite. Yellow outlines are opthalmitic structures within stromatic migmatite.

STOP 8: Dysartsville Tonalite northwest of Turkey Mountain. ***Leaders: Brendan Bream and Scott Williams. Location: 35˚34.62' N, 81˚54.82 W, Glenwood 7.5-minute quadrangle.***

PURPOSE: To examine the Dysartsville Tonalite. (30 minutes).
DESCRIPTION: The Dysartsville Tonalite is locally known as "blue granite" and limited gold production has been associated with veins and placer deposits in and near the body. Several small gold panning camps and a single larger failed gold mine are located in the Dysartsville tonalite near Vein Mountain in the Glenwood quadrangle. Small fresh to semiweathered outcrops of the Dysartsille tonalite occur along the dirt road located on the NE edge of Turkey Mountain. At this stop we are structurally located in the overturned limb of an isoclinal synform located just SE of the South Muddy Creek anticline first documented by Goldsmith et al. (1988). Several map-scale amphibolite bodies, one containing an altered ultramafic body, are present within the Dysartsville Tonalite. Smaller lenses and layers of amphibolite are also present but not mappable at 1:24,000-scale (Bream, 1999; Williams, 2000). The Dysartsville Tonalite is one of numerous Early to Middle Ordovician granitoids found throughout the western Inner Piedmont in the Carolinas and northeastern Georgia. Perhaps unique though is its presence in the Mill Spring thrust sheet proximal to the Brindle Creek fault. In outcrop, Dysartsville Tonalite is usually massive, foliated, and light gray to gray. Biotite, quartz, and feldspar can be easily identified in hand specimen. Foliation here is oriented N41E, 25˚ SE Outcrops are best found where the unit is dissected by streams and in only a few locations does the unit occur on hill- or ridgetops. The South Muddy Creek basin in underlain entirely by Dysartsville Tonalite.

The Dysartsville Tonalite contains 40-55 percent plagioclase (An_{20-25}), 30-43 percent quartz, 4-15 percent biotite, and 0-10 percent muscovite. Muscovite where abundant is coarse-bladed and overgrown by biotite. Biotite occurs as subhedral and euhedral pleochroic grains from 0.1 to 1 cm long that define the foliation. Epidote is colorless, commonly present as aggregates, and often forms bands with bioite and accessory minerals along the foliation. Common accessory minerals are magnetite, pyrite, sphene, zircon, apatite, and allanite. The Dysartsville Tonalite is massive to foliated, fine to medium grained, and leucocratic (Fig. 7). The granitoid exhibits both granoblastic and lepidoblastic textures, often in the same outcrop. Trace element discriminant diagrams (Bier, 2001) point to a volcanic-arc granite origin.

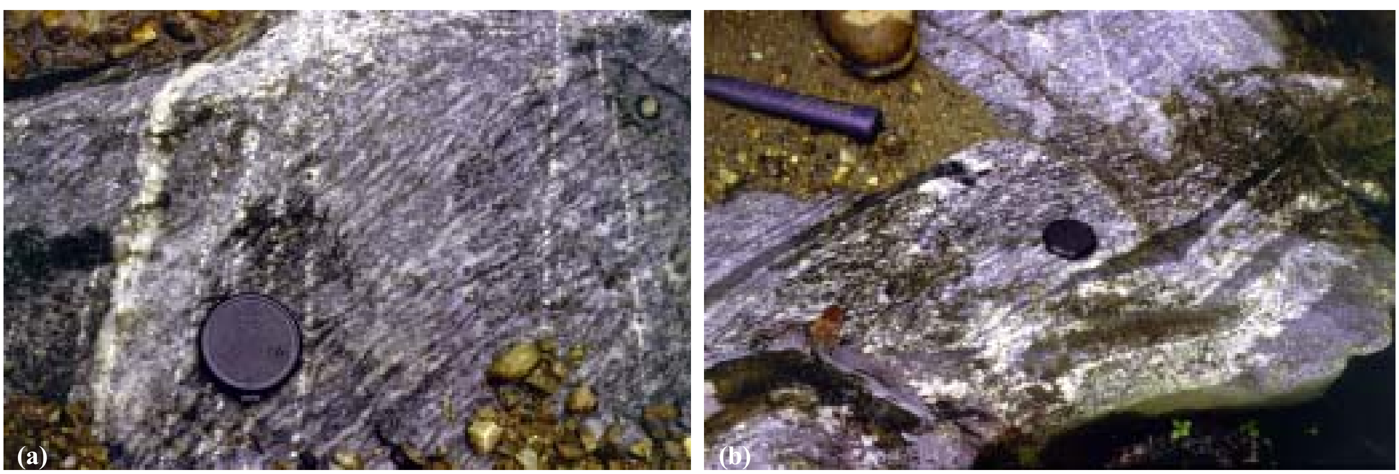

Figure 7. (a) and (b) Dysartsville Tonalite outcrops in South Muddy Creek north of Vein Mountain Road (Glenwood 7.5-minute quadrangle).

Return to Camp McCall for afternoon break. Backtrack to NC 226; turn right onto NC 226 (S); continue on NC 226 just over 10 mi past U.S. 64 intersection; turn left onto Camp McCall Road; follow ~2 mi to camp office. This will be our ***AFTERNOON COFFEE BREAK (30 minutes)****. After the break retrace route 2.5 mi to NC 226, turn right (N) on NC 226 and follow 4 mi, take exit for U.S. 64 E. Turn into Houston House Retirement Home parking lot.*

NOTE: PERMISSION MUST BE OBTAINED FROM HOUSTON HOUSE RETIREMENT HOME PERSONNEL PRIOR TO ENTRY.

STOP 9: (ALTERNATE) Poor Mountain Amphibolite Migmatite at Houston House. ***Leader: Scott Giorgis. Location: 35˚34.47' N, 81˚50.60' E, Dysartsville 7.5-minute quadrangle.***

PURPOSE: To examine intensely migmatitic Poor Mountain Amphibolite. (20 minutes)
DESCRIPTION: Migmatitic Poor Mountain Amphibolite saprolite occurs in an excavated bank behind the rest home, and is easily recognized by its characteristic yellow to orange ochre color. Some fresh to partially weathered blocks of coarse-grained migmatite consist of alternating layers of amphibolite (paleosome, locally biotite rich) and feldspar-quartz-biotite-hornblende granitoid (leucosome; Fig. 8). Migmatitic layering is parallel to S_2 (oriented N34E, 31˚ SE). The intensely migmatitic Poor Mountain Amphibolite here is typical of that in the Brindle Creek thrust footwall throughout the South Mountains and southwestern Brushy Mountains.

Figure 8. Block of intensely migmatitic Poor Mountain Amphibolite at Houston House retirement home. Note that migmatitic layering is parallel to the domnant foliaton and that it is folded by passive to flexural-flow F_3(?) folds.

Exit parking lot, turn right onto U.S. 64 and drive 4 mi E. Turn right onto SR 1969 (Roper Hollow Road), drive 1.2 mi toward Sisk Gap then another 0.5 mi to Sisk Gap, then turn left onto the upper road and continue to the higher gap, park in wide area available and begin downhill walk back to Sisk Gap.

STOP 10: Sillimanite Schist–Walker Top Granite contact above Sisk Gap. ***Leader: Scott Giorgis. Location: 35˚35.58' N, 81˚46.21' W, Dysartsville 7.5-minute quadrangle.***

PURPOSE: To examine the contact between the Walker Top Granite and sillimanite schist in the Brindle Creek fault hanging wall. (30 minutes)
DESCRIPTION: Along the northwestern side of the road are saprolite exposures of an inequigranular, feldspar megacrystic biotite granite (the Walker Top Granite). This unit can be traced to the northeast along the road, where the contact with sillimanite schist saprolite is visible in the upper parts of the almost continuous roadcut. The undulose nature of this contact led to early suggestions of an unconformable relationship between the two units, but subsequent geochronologic data argue strongly against this interpretation (Giorgis et al., this guidebook). High grade metamorphism here has led to development of sillimanite, reduction in the amount of garnet, and absence of kyanite. Sillimanite schist holds up this

NE-SW striking ridge. The high sillimanite and quartz content of the schist unit make the unit resistant to chemical weathering, but the high mica content is very susceptible to mechanical weathering. The result is that sillimanite schist in the western portion of the South Mountains tends to hold up ridges, but with very little outcrop.

Backtrack to U.S. 64 and turn right (NE) onto U.S. 64. Drive ~3.9 mi to SR 1945 (Salem Church Road) and turn right. Drive 1.2 mi to Salem and turn right (SE) onto SR 1956 (Burkemont Road). Drive 1.2 mi and turn left onto SR 1957 (Burkemont Mountain Road). Follow SR 1957 for 4.9 mi to exposures of Walker Top Granite.

NOTE: EVEN THOUGH THIS IS A PUBLIC ROAD, PLEASE ASK PERMISSION OF THE LANDOWNERS BEFORE EXAMING THESE ROCKS.

STOP 11: (ALTERNATE) Walker Top Granite near Walker Top Mountain. ***Leader: Scott Giorgis.***
Location: 35˚38.62' N, 81˚42.81' E, Morganton South 7.5-minute quadrangle.

PURPOSE: To examine the type area Walker Top Granite in the type area. (20 minutes)
DESCRIPTION: Rocks exposed here are typical Walker Top Granite (Fig. 9; also see Giorgis et al., this guidebook, their Fig. 3) that contain subhedral to euhedral 1- to 8-cm K-spar megacrysts with myrmekite rims. Possible quartzite xenoliths are are present. Foliation here is oriented N78E, 55˚SE. Small outcrops of fresh Walker Top Granite occur along Burkemont Mountain Road driving toward Walker Top Mountain. The best exposures are present on the northwest flanks of Walker Top and Burkemont Mountains as minor cliffs and exfoliation whalebacks. Many saprolite exposures of sillimanite schist and Walker Top Granite along Burkemont Mountain Road, unfortunately, have been seeded by the North Carolina Department of Transportation.

Board buses and return to Morganton Holiday Inn via U.S. 64. Backtrack to Salem and turn right on SR 1956. Drive 1 mi to U.S. 64. Turn right and follow U.S. 64 to I-40 (Exit 103). Get onto I-40 eastbound and drive 2.2 mi to Exit 105 (NC 18).

Figure 9. Typical Walker Top Granite on Burkemont Mountain Road in the type area immediately south of Walker Top Mountain.

END OF DAY 1

DAY 2

8 am Depart Holiday Inn-Morganton. Turn left out of Holiday Inn and follow NC 18 to intersection in Morganton with U.S. 64. Follow U.S. 64 21.1 mi from Holiday Inn to U.S. 64-U.S. 321 intersection and continue east on U.S. 64 1.4 mi to traffic light where U.S. 64 turns right (E). Continue 2.6 mi N on NC 18 to Vulcan Materials Company Lenoir Quarry entrance and 0.3 mi additional to quarry office. This stop will also serve as our MORNING COFFEE BREAK (when we come out of the quarry).

SAFETY WARNING: DO NOT GO NEAR QUARRY FACES FOR ANY REASON!!!! There will be adequate loose material for sampling.

STOP 12: Vulcan Materials Company, Lenoir Quarry. ***Leaders: Jay Kalbas and Vulcan Materials Company Hosts, Geologists Jim Stroud and Marion Wiggins, and Plant Manager Brad Allison.***
Location: (35˚55.92' N, 81˚29.01' W, Kings Creek 7.5-minute quadrangle.

PURPOSE: To examine fresh exposures of the Lenoir Quarry migmatite (1 hour total).
DESCRIPTION: A zone of intense migmatization up to 10 km wide exists in the Brindle Creek fault footwall. Reed (1964) in the Lenoir 15-minute quadrangle and Goldsmith et al. (1988) in the Charlotte 1˚ x 2˚ quadrangle first mapped an extensive migmatite from the Brushy Mountains to the South Mountains in the footwall of the Brindle Creek fault. Although the Brindle Creek fault has not been mapped southwest of the South Mountains, a belt of migmatite has been mapped southward by Goldsmith et al. (1988). This and recent mapping raise the possibility that both the Brindle Creek fault and its intensely migmatitic footwall continue at least 110 km southward into South Carolina (Nelson et al., 1987; Curl, 1997a, 1997b; Niewendorp et al., 1997; Maybin, 1998; Maclean and Blackwell, 2001) (also see Hatcher, this guidebook, his Fig. 1b).

Stop 12 highlights N 50-60˚E-striking, 30-40˚SE- dipping, intensely migmatitic amphibolite, hornblende-biotite granodiorite, and biotite granitoid characteristic of the Brindle Creek footwall and Mill Spring thrust sheet in the Brushy Mountains. The Brindle Creek thrust is exposed on the north-facing slope directly to the southeast of the quarry and parallels the Brushy Mountain ridgeline. The quarry contains well-exposed intense migmatite in the footwall of the Brindle Creek thrust.

Lenoir Quarry Migmatite. Texture and composition of migmatite in the Brindle Creek footwall are variable. Melanosome consists of 1.5 to 11 cm thick continuous and discontinuous layers and boudins of fine- to coarse-grained amphibolite and biotite-hornblende gneiss (Fig. 9). Corresponding sympathetic and crosscutting leucosome is typically coarse-grained granite and granodiorite. Leucosome and melanosome layers are folded (F_3; Merschat and Kalbas, this guidebook). Both metatexitic and diatexitic neosomes indicate differential or fractional partial melting. Prominent > 4 mm hornblende and biotite porphyroblasts occur in leucocratic mobalizates. Foliated granitic and granodioritic leucosome with only minor melanocratic layers dominate some exposures.

Migmatitic structures are well developed in the Brindle Creek footwall. Folded stromatic (layered) and schollen (raft) structures dominate; phlebitic (vein), and schlieren (flow fabric) structures and boudins are also common (terminology from Mehnert, 1968). Tight to isoclinal fold axial surfaces parallel foliation in stromatite. Incipient transposition of earlier (S_2) surfaces occurs in some diktyonitic (reticulated, vein-like) migmatite (Fig. 9). Gradational transitions from stromatic migmatite to more homogeneous granitoid were recognized at several localities; beaded leucosome surrounded by amphibolite and biotite-hornblende granodiorite grade into lenticular hornblende- and biotite-rich pods engulfed by quartz- and feldspar-rich leucosome. Sharp contacts between melanosomes and leucosomes were also documented.

Northeast-striking foliation, gently northeast- or southwest-plunging fold axes, and coaxial mineral lineation in migmatite neosome are consistent with the regional structural trend and are orogen parallel. Poorly developed foliations in some granodiorite and early pegmatite also parallel the dominant, northeasterly structural trend. Similarly, foliation in leucocratic and diatexite neosome surrounding amphibolite boudins is typically layer parallel. At least two generations of granitic pegmatite are also present: an axial planar generation that likely resulted from syndeformational migmatization, and later, less deformed to undeformed crosscutting pegmatite.

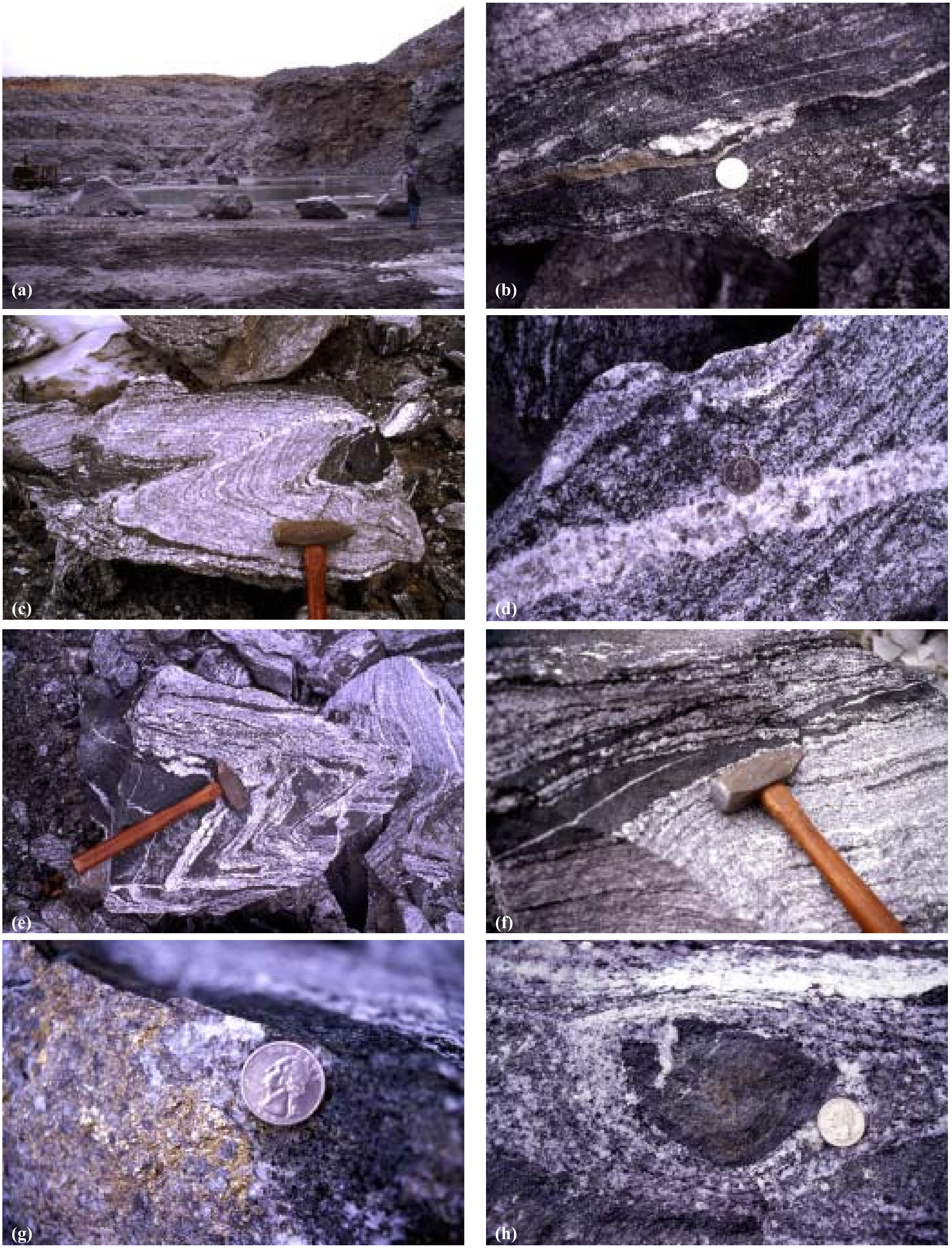

Figure 9. Intensely migmatitic Poor Mountain Amphiblite in the Vulcan Materials Company Lenoir quarry. (a) View of main pit. (b) Layered amphibolite. (c) Folded leucosome. (d) Pegmatite. (e) Folded leucosome. (f) Leucosome-paleosome contact. (g) Sulfides. (h) Amphibolite boudin.

The migmatite typically has a lepidoblastic to nematoblastic foliation defined by parallel orientation of hornblende, plagioclase, biotite, and quartz. Leucosome consists of medium- to coarse-grained quartz (38-68 %), plagioclase (32-36 %; An_{24-34}), biotite (12-14 %), + microcline (< 10 %), hornblende (< 5 %), myrmekite (2-3 %), and epidote/clinozoisite (1-2 %), with accessory chlorite, garnet, apatite, and opaque minerals. Melanosome consists of fine- and medium-grained hornblende (33-99 %), quartz (0-27 %), plagioclase (< 1-27 %; An_{24-44}), biotite (0-12 %), and epidote/clinozoisite (< 1-7 %), with accessory muscovite, sericite, apatite, sphene, and opaque minerals. Both prograde and retrograde epidote/clinozoisite are present in migmatite melanosome. As noted by Davis (1993), prograde epidote consists of coarse, foliation-parallel, tabular crystals; retrograde epidote is identified by randomly oriented, fine-grained hornblende and plagioclase replacements. Melanosome is hypersthene- or olivine-normative (up to 25 %, and 18 %, respectively); minor amounts of normative nepheline or quartz are also intermittently present.

Petrogenesis & Tectonic Implications. Mesoscopic migmatite structures denote partial melting. The presence of both deformed metatexite and diatexite indicates partial melting above 630 ˚C (Sawyer, 1999) during penetrative deformation, consistent with estimated temperatures from mineral assemblages and compositions. Moreover, schlieren imply some melt fractions were at or above the melt escape threshold (Sawyer, 1999). Any plausible model for migmatization in the Brindle Creek footwall must account for at least local anatexis and melt migration. Complementary trends in REE data from Brushy and South Mountains migmatite may represent metamorphic segregation or partial melting (e.g., Holtz, 1989). Metamorphic segregation at subsolidus conditions, however, typically produces leucosomes with marked positive Eu anomalies (Sawyer and Barnes, 1988; Barbey et al., 1989). This was not observed in the leucosome; therefore, subsolidus metamorphic segregation is not favored. Supercritical hydrous fluids do not readily dissolve REE (Flynn and Burnham, 1978; Johannes et al., 1995); thus metasomatism likely had little effect on the immobile trace element chemistry of the migmatite. Likewise, consistent chemical relationships among all migmatite samples rule out large-scale intrusion of foreign magma.

Geochronologic data from the Lenoir Quarry samples support a Poor Mountain Formation protolith for the migmatite. Ordovician (~450 Ma) core ages of migmatite zircons are nearly coeval with Poor Mountain Quartzite felsic tuff crystallization ages (Kalbas et al., 2002; Bream, unpublished data). Contributions from numerous western Inner Piedmont Ordovician granitoids (Vinson and Miller, 1999; Bream, unpublished data), however, cannot be ruled out on the basis of geochronology. Sensitive high resolution ion microprobe zircon rim U-Pb ages indicate subsequent metamorphism at 342 and 330 Ma.

Geochronologic evidence, based in part on rocks from the Lenoir Quarry, indicates diachronous relationships and Neoacadian or Alleghanian emplacement of the hot Brindle Creek thrust sheet. Specifically, western Inner Piedmont thrust sheets contain primarily Ordovician-age granitoids (Vinson and Miller, 1999; Bream, unpublished data). Eastern Inner Piedmont granitoids have Devonian and early Mississippian crystallization ages (Mapes, 2002); therefore, it is likely that the eastern and western Inner Piedmont were spatially separated from early to middle and late Paleozoic granitoid intrusion. If the Acadian and Neoacadian plutonic suites are restricted to the Brindle Creek thrust sheet and zircon overgrowths date migmatization, the timing of thrust emplacement is confined to an ~30 million year interval between the crystallization age of the Walker Top Granite (~377 Ma; Giorgis et al., this guidebook) and the oldest metamorphic overgrowths on zircons in the migmatite (~340 Ma). Thus rocks from the quarry provide a critical piece of the tectonic puzzle for both the western and eastern Inner Piedmont.

COFFEE BREAK AT LENOIR QUARRY PARKING AREA

Return to NC 18 and turn left (S). Drive 1.2 mi to intersection of NC 18 and U.S. 64. Turn left and drive 3.0 mi to Walker Top Granite exposure on left. Park on shoulder to right of highway.

CAREFULLY CROSS HIGHWAY.

STOP 13: Devonian Walker Top Granite east of St. Johns Lutheran Church on U.S. 64. ***Leaders: Arthur Merschat, Jay Kalbas, and Russ Mapes***
Location: 33˚55.02' N, 81˚27.27' W, Kings Creek 7.5-minute quadrangle.

PURPOSE: To examine a fresh exposure of Walker Top Granite in the southwestern Brushy Mountains. (20 minutes).
DESCRIPTION: Goldsmith et al. (1988) was the first to recognize this unique unit but they thought it is less deformed Henderson Gneiss. Giorgis et al. (this guidebook) formally proposed a type area on Walker Top and Burkemont Mountains, along the western front of the South Mountains naming the unit the Walker Top Granite. Its characteristic K-feldspar megacrysts and fine, dark groundmass (Fig. 10) makes it a distinct marker unit in the sea of sillimanite schist and biotite gneiss of the eastern Inner Piedmont. This outcrop is part of one of the larger disconnected bodies located at the southwestern end of the outcrop belt of the Walker Top Granite in the Kings Creek quadrangle. It is located nearly 2 km (~1 mi) southeast of the Brindle Creek thrust and may be the southeast part of the limb of a macroscopic F_1 antiform or an F_2 sheath fold (Merschat and Kalbas, this guidebook, their Figs. 2b and 2e).

The Walker Top Granite is a garnet-bearing, megacrystic biotite, quartz, plagioclase, microcline granite to granodiorite (Giorgis, 1999; Bier, 2001; Giorgis et al., this guidebook). Megacrysts occur in a fine- to medium-grained groundmass of quartz, biotite, K-feldspar, and plagioclase. Foliation strikes N 78˚ E and dips 81˚ NW in the western part of the outcrop and rolls over to N 59˚ E, 28˚ SE dip to the east in the best part of the exposure. The weak to moderate foliation is defined by the alignment of microcline feldspar megacrysts and matrix biotite. Euhedral to subhedral Carlsbad-twinned microcline megacrysts contain garnet and biotite inclusions, and range from 1 to 8 cm with long axes preferentially aligned parallel to the foliation. Some megacrysts are randomly oriented or define a possible second steeper foliation. Garnet is more common at this stop than in other outcrops (see Stops 10 and 11, this guidebook) and occurs in the matrix as well as inclusions in microcline feldspar megacrysts. Garnets in both settings range from 0.5 to >1 cm in diameter; some are flattened into the foliation. Bier (2001) determined that these garnets are magmatic based on irregular geochemical zoning patterns, and concur with this interpretation. Myrmekite rims are common on all microcline feldspars and some garnets in the matrix consist of symplectite.

Interesting structures here are upright open to closed folds at the western part of the outcrop, two minor shear zones that verge NW, and two sets of granitoid dike intrusions. Shear zones are approximately 10 cm wide and marked by a decrease in groundmass grain size and sheared megacrysts. An earlier quartzofeldspathic dike has irregular margins and is foliated. One dike located near the center of the outcrop is folded into a NW-verging, reclined drag fold associated with one of the shear zones (Fig. 10b). The other later dike set is unfoliated medium- to coarse-grained biotite granitoid with very planar margins.

Finally, a comparison should be made with the paucity of migmatite textures in the Walker Top Granite here and at Stops 10 and 11 to the plethora of migmatite textures in other lithologies observed at Stops 11, 13, 14, and 15 (this guidebook). One possibility a syn- to post-metamorphic intrusion of the Walker Top Granite in the Brindle Creek thrust sheet. This would require that timing of metamorphism in the eastern Inner Piedmont be ~370 Ma, in contrast with most data that suggest metamorphim occurred at 350 Ma (Kalbas et al., 2002). Also, if this hypothesis were valid, Walker Top Granite should be found in the western Inner Piedmont, and it is not.

Continue east 1.3 mi on U.S. 64. Just past the intersection of SR 1788 and U.S. 64, park on should of road at large saprolite exposure to the right (S).

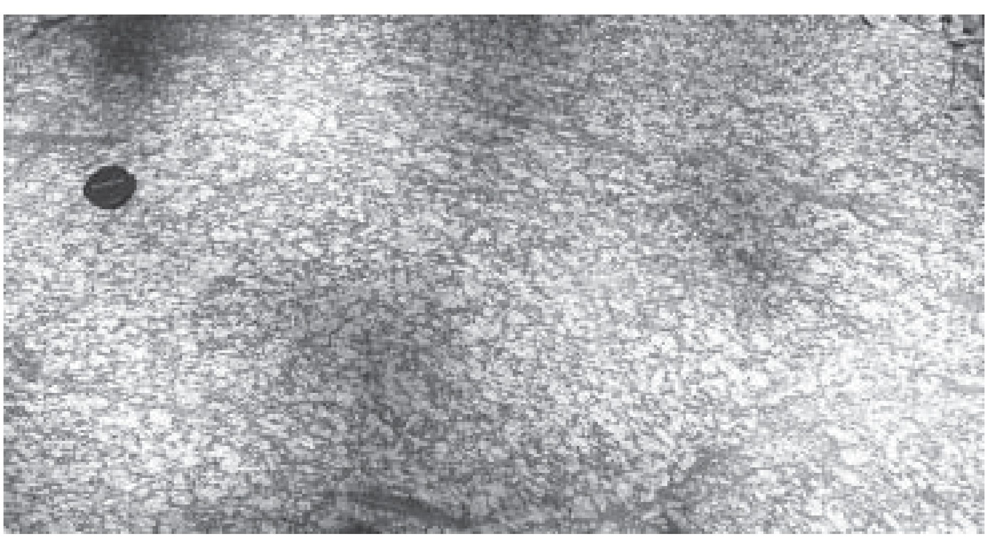

Figure 10. Weakly mylonitic Walker Top Granite from the Poplar Springs fault zone along Duck Creek in the Ellendale quadrangle. The megacrystic texture of this unit makes it easily recognizable in the eastern Inner Piedmont.

STOP 14: Migmatitic Sillimanite schist saprolite. ***Leaders: Arthur Merschat and Jay Kalbas. Location: 35˚54.630' N, 81˚25.902' W, Kings Creek 7.5-minute quadrangle.***

THIS OUTCROP IS LOCATED ON PRIVATE PROPERTY AND PERMISSION FROM MCGEE AND HONEYCUT CONSTRUCTION COMPANY SHOULD BE OBTAINED BEFORE EXAMINING THE OUTCROP.

PURPOSE: To examine the relationship between migmatitic sillimanite schist and biotite granitoids. (25 minutes)
DESCRIPTION: This saprolite outcrop is a microcosm of eastern Inner Piedmont structure (Fig. 11), where many textures and structures associated with the sillimanite schist occur and their relationships to small syntectonic biotite granitoid intrusions can be observed. Sillimanite schist is the most abundant lithology in the eastern Inner Piedmont. Ages of detrital zircons (Bream, this guidebook) and igneous intrusions, ~375 Ma (Mapes, 2002), constrain the age of the sillimanite schist and other paragneisses of the eastern Inner Piedmont to between Middle Ordovician and Early Devonian.

Several lithologies present in this outcrop represent the variation frequently observed in this rock unit. Sillimanite schist, the dominant lithology, is fine- to medium-grained, garnet-sillimanite-biotite-muscovite schist. It weathers to a bright purplish red to light yellowish orange and is strongly foliated with stromatic migmatite (Mehnert, 1968) layering parallel to the dominant foliation. The lower meter of the outcrop contains abundant light brown weathering metagraywacke/biotite gneiss interlayered with sillimanite schist. Ocher-weathering calc-silicate boudins commonly occur in both sillimanite schist and metagraywacke. Coarse-grained, weakly to moderately foliated leucocratic biotite granitoid intruded the sillimanite schist, and weathers white with minor light orange-brown stains. The granitoid interfingers with the sillimanite schist, but both concordant and discordant contacts are distinct. This suggests that these are not in situ melts, but have risen from greater depth.

All of these lithologies are transposed into the regional S_2 foliation, oriented N 48˚ E, 49˚ SE. The sillimanite schist and biotite granitoids are deformed by later folds. The east side of the outcrop contains several inclined folds of sillimanite schist and granitoid, while the northern part of the north-south trending face is dominated by a shear zone verging WSW. Sillimanite schist and granitoid are folded into an inclined, closed drag fold that plunges 23, S20E. Several polished black surfaces probably represent nontectonic adjustments during saprolite formation.

Drive 0.2 mi east on U.S. 64. Park on right shoulder of highway.

CAREFULLY CROSS HIGHWAY.

STOP 15 Metagraywacke/biotite gneiss on U.S. 64 just west of Southern Star gas station. ***Leaders: Arthur Merschat and Jay Kalbas. Location: 35˚54.58' N, 81˚25.64' W, Kings Creek 7 1/2-minute quadrangle.***

PURPOSE: To examine the mineralogy, textures, and structures of the metagraywacke/biotite gneiss. (20 minutes).
DESCRIPTION: The metagraywacke/biotite gneiss is the other principal metasedimentary unit of the Brindle Creek thrust sheet in this area. This outcrop of metagraywacke is located in the core of a map-scale NE-trending isoclinal antiform that is plastically attenuated by the Poplar Springs fault zone (Merschat and Kalbas, this guidebook). Detailed mapping indicates that this portion of the antiform is not truncated. The exposure contains a large SE-verging antiform with a NE-dipping west limb, and the exposed portion of the east limb dips steeply NE. An amphibolite boudin occurs in the core of the fold in the eastern part of the outcrop. The vergence of this fold is not typical of other F_2 folds in domain I of Merschat and Kalbas (this guidebook) and may be part of a larger sheath fold or the product of fold interference.

The metagraywacke occurs in sequence with sillimanite schist, but the metagraywacke is areally subordinate to the sillimanite schist in this area. Metagraywacke consists of garnet-bearing, fine- to medium-grained plagioclase, biotite, quartz paragneiss with trace amounts of muscovite and hornblende. Compositional layering ranges between 1 cm and 1 m but averages 10-40 cm thick. Some smaller layers (1-2 cm thick) contain greenish-black hornblende. The amphibolite boudin at the east end of the outcrop is medium- to coarse-grained and contains hornblende, plagioclase, and quartz. It varies texturally from gneissose to granoblastic. Stromatic migmatite textures are more common in the metagraywacke while vein-type migmatite occurs in the amphibolite. Migmatitic layers and pods in metagraywacke range from 3 cm to greater than 1 m. Vein-type migmatite associated with the amphibolite boudins is only a few cm thick.

Drive 4.5 mi east on U.S. 64 to a roadcut on the left (north) side of the highway just east of the bridge over the Middle Little River. Park on the right shoulder.

CAREFULLY CROSS HIGHWAY.

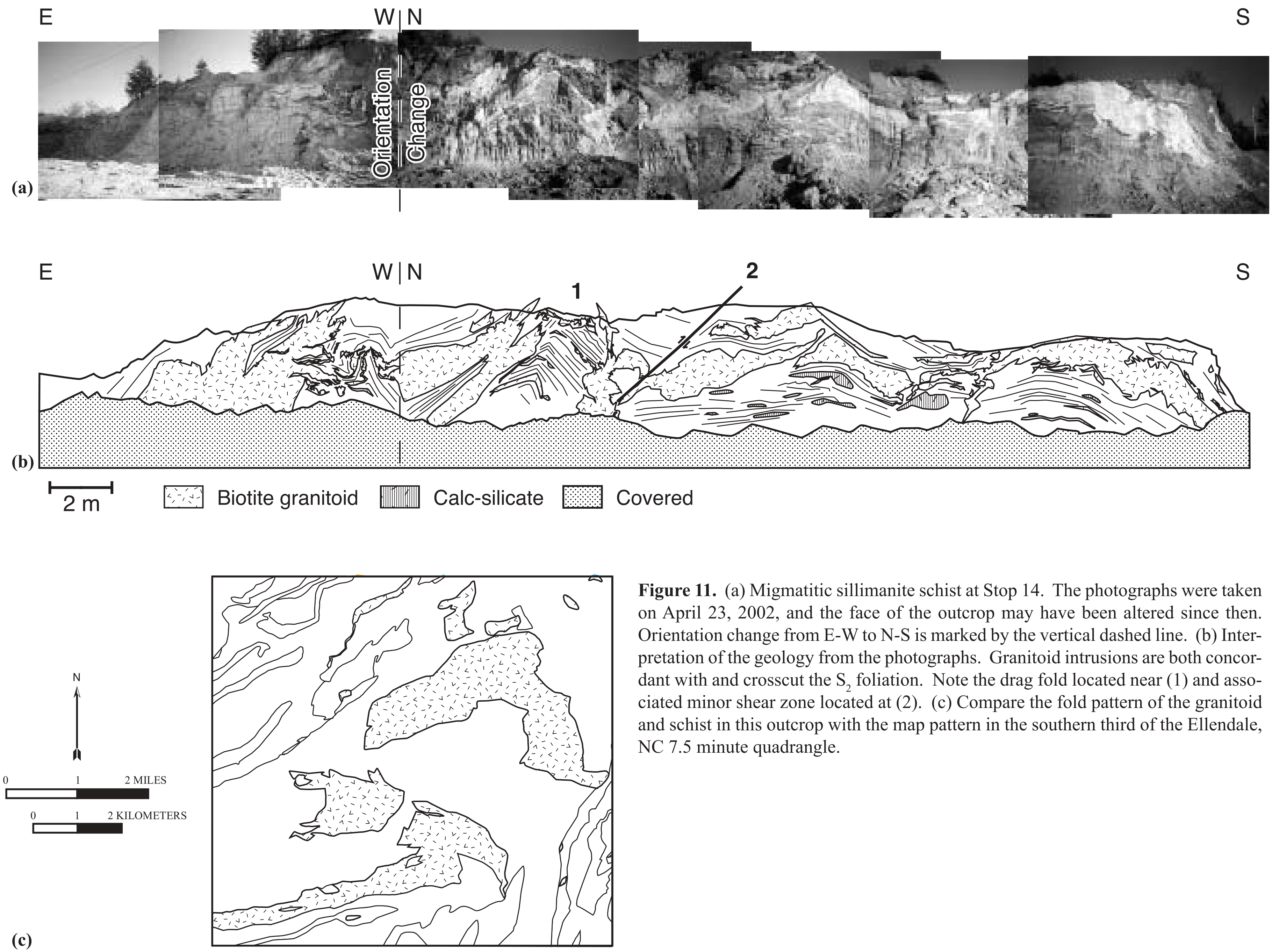

Figure 11. (a) Migmatitic sillimanite schist at Stop 14. The photographs were taken on April 23, 2002, and the face of the outcrop may have been altered since then. Orientation change from E-W to N-S is marked by the vertical dashed line. (b) Interpretation of the geology from the photographs. Granitoid intrusions are both concordant with and crosscut the S_2 foliation. Note the drag fold located near (1) and associated minor shear zone located at (2). (c) Compare the fold pattern of the granitoid and schist in this outcrop with the map pattern in the southern third of the Ellendale, NC 7.5 minute quadrangle.

STOP 16: Toluca Granite and sillimanite schist on U.S. 64. ***Leaders: Arthur Merschat and Russ Mapes. Location: 35˚54.576' N, 81˚20.902' W, Ellendale 7.5-minute quadrangle.***

PURPOSE: To examine an exposure of the Toluca Granite and fresh sillimanite schist. (20 minutes).
DESCRIPTION: The Toluca Granite was originally described near Shelby, NC, by Griffits and Overstreet (1952). Goldsmith et al., (1988) correlated it with many of the other small peraluminous catazonal granitoid bodies in the Inner Piedmont. Mapes et al. (2002) reported a U/Pb age of ~375 Ma for the Toluca Granite and first recognized an important trend in the Inner Piedmont: ~370 Ma magmatism in the Inner Piedmont is partitioned into the eastern Inner Piedmont/ Brindle Creek thrust sheet. Toluca Granite is thus diagnostic of the Brindle Creek thrust sheet, but not all of the small granitoid plutons have been studied petrographically, geochemically, or dated to determine if they are Toluca Granite. Several small exposures of Toluca Granite occur closeby near U.S. 64. The Toluca Granite exposed here is allanite-bearing, medium-grained, moderately to well-foliated biotite granite. These small bodies are located on the northwestern margin of a larger body of Toluca Granite that dips 52˚ NE. While nonmigmatitic, weakly to moderately foliated equigranular texture is typical of Toluca Granite, it can be locally banded and migmatitic.

Several exposures of sillimanite schist occur on eastward U.S. 64 between the outcrop of Toluca Granite and the Middle Little River bridge on U.S. 64. The outcrops are 3-5 m above the level of the road with abundant fresh sillimanite schist float on the lower slopes of the cut. The sillimanite schist float is fresher than the rock present at Stop 14, and contains many interesting textures. It is possible to find sillimanite schist float with garnets greater than 1 cm in diameter, coarse-grained, poikiloblastic muscovite containing biotite inclusions, and crenulations.

END OF TRIP. BOARD BUSES AND RETURN TO MORGANTON.

REFERENCES CITED

Barbey, P., Bertrand, J. M., Angoua, S., and Dautel, D., 1989, Petrology and U/Pb geochronology of the Telohat migmatites, Aleksod, Central Hoggar, Algeria: Contributions to Mineralogy and Petrology, v. 101, p. 207-219.

Bier, S. E., 2001, Geology of the southeastern South Mountains, North Carolina [M.S. thesis]: Knoxville, University of Tennessee, 162 p.

Bryant, B., and Reed, J. C., Jr., 1970, Geology of the Grandfather Mountain window and vicinity, North Carolina and Tennessee: U.S. Geological Survey Professional Paper 615, 190 p.

Curl, D. C., 1997a, Bedrock geologic map of the Reidville 7.5 minute quadrangle, Spartanburg and Laurens Counties, South Carolina: South Carolina Geological Survey Open File Report 94, scale 1:24,000.

Curl, D. C., 1997b, Bedrock geologic map of the Welford 7.5 minute quadrangle, Spartanburg County, South Carolina: South Carolina Geological Survey Open File Report 95, scale 1:24,000.

Davis, T. L., 1993, Lithostratigraphy, structure, and metamorphism of a crystalline thrust terrane, western Inner Piedmont, North Carolina [unpublished Ph.D. dissertation]: Knoxville, University of Tennessee, 245 p.

Flynn, R. T., and Burnham, C. W., 1978, An experimental determination of rare earth partition coefficients between chloride-containing vapor phase and silicate melts: Geochimica et Cosmochimica Acta, v. 42, p. 685-701.

Giorgis, S. D., 1999, Inner Piedmont geology of the northwestern South Mountains near Morganton, North Carolina [M.S. thesis]: Knoxville, University of Tennessee, 191 p.

Goldsmith, R., Milton, D. J., and Horton, J. W., 1988, Geologic map of the Charlotte 1˚x 2˚ quadrangle, North Carolina and South Carolina: U.S. Geological Survey Map I-125-E, scale 1:250,000.

Griffits, W. R., and Overstreet, W. C., 1952, Granitic rocks of the western Carolina Piedmont: American Journal of Science, v. 250, p. 777-789.

Hill, J. C., 1999, Geology of the Marion East quadrangle, North Carolina, and the stratigraphy of the Tallulah Falls Formation in the Chauga belt [M.S. thesis]: Knoxville, University of Tennessee, 188 p.

Holtz, F., 1989, Importance of melt fraction and source rock composition in crustal granitoid genesis: The example of two granitic suites north of Portugal: Lithos, v. 24, p. 21-35.

Johannes, W., Holtz, F., and Möller, P., 1995, REE distribution in some layered migmatites: Constraints on their petrogenesis: Lithos, v. 35, p. 139-152.

Kalbas, J. L., Bream, B. R., Hatcher, R. D., Jr., and Maybin, A. H., III, 2002, Evidence for mafic Ordovician magmatism and Acadian metamorphism in the Brushy Mountains, Western Inner Piedmont of North Carolina: Geological Society of America Abstracts with Programs, v. 34, A-119.

Maclean, J. S., and Blackwell, S. S., 2001, Paris Mountain Project: Part 1, Geology of the Taylors 7.5 minute quadrangle, Greenville County, South Carolina, *in* Garihan, J. M., Ranson, W. A., and Clendenin, C. W., eds., South Carolina Geology: South Carolina Department of Natural Resources, v. 43, p. 25-35.

Mapes, R. W., 2002, Geochemistry and geochronology of mid-Paleozoic granitic plutonism in the southern Appalachian Piedmont terrane, North Carolina-South Carolina-Georgia [M.S. Thesis]: Vanderbilt University, 140 p.

Maybin, A. H., III, 1998, Bedrock geologic map of the Greer 7.5 minute quadrangle, Greenville and Spartanburg Counties, South Carolina: South Carolina Geological Survey Open File Report 113, scale 1:24,000.

Mehnert, K. R., 1968, Migmatites and the origin of granitic rocks: Amsterdam. Elsevier. 393 p.

Nelson, A. E., Horton, J. W., Jr., and Clarke, J. W., 1998, Generalized tectonic map of the Greenville 1˚ x 2˚ quadrangle, Georgia, South Carolina, and North Carolina: U. S. Geological Survey Miscellaneous Field Studies Map I-2175, Scale

Niewendorp, C. A., Clendenin, C. W., Dorr, W. R., III, and Maybin, A. H., III, 1997, Geologic map of the Paris Mountain 7.5 minute quadrangle: South Carolina Geological Survey Open–File Report 99, scale 1:24,000.

Reed, J. C., 1964, Geology of the Lenoir quadrangle, North Carolina: U. S. Geological Survey Map I-709-A, scale 1:62,500.

Sawyer, E. W., 1999, Criteria for the recognition of partial melting: Physics and Chemistry of the Earth, v. 24, p. 269-279.

Sawyer, E. W., and Barnes, S. J., 1988, Temporal and compositional differences between subsolidus and anatectic migmatite leucosomes from the Quetico metasedimentary belt, Canada: Journal of Metamorphic Geology, v. 6, p. 437-450.

Vinson, S. B., and Miller, C. F., 1999, Constraints on the timing of Inner Piedmont plutonism, N.C.–S.C., from ion microprobe U-Pb zircon analysis: Geological Society of America Abstracts with Programs, v. 31, p. A-77.

ADDENDUM:
Figure intended for insertion on page 80 of the guidebook (Bier et al.).

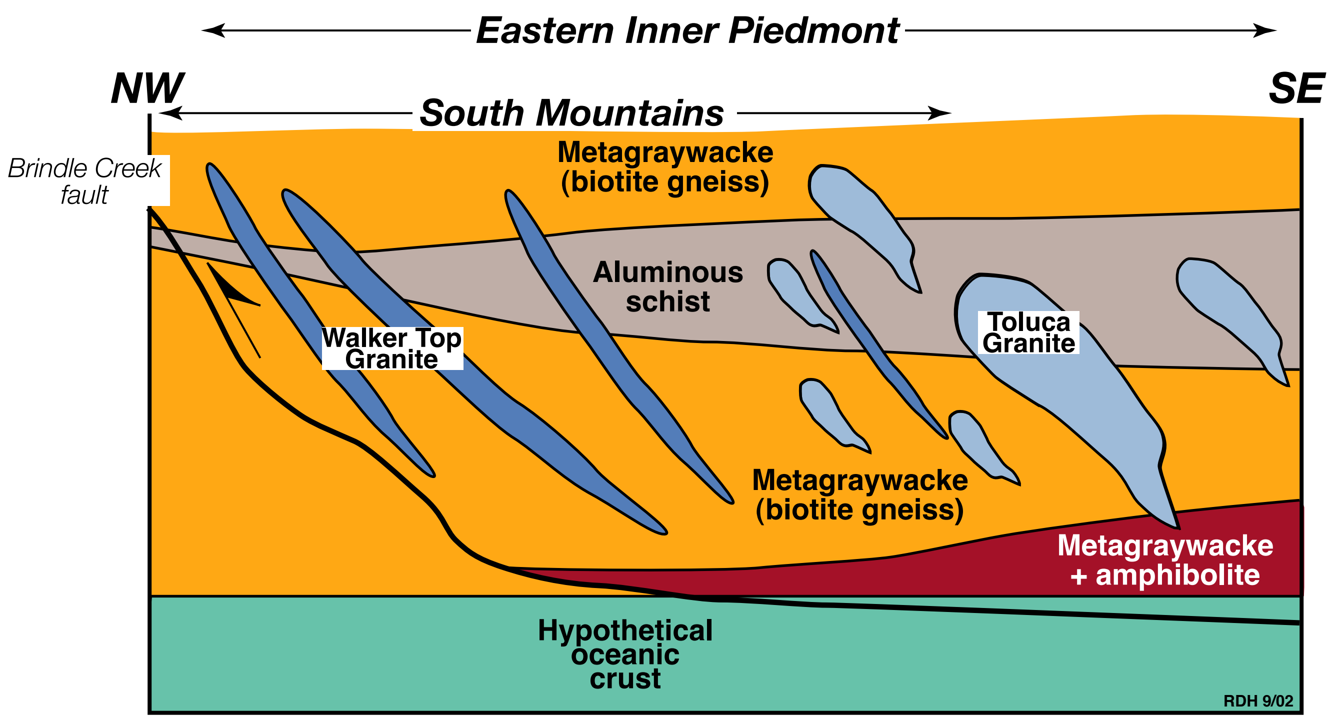

Figure 17.5. Lithologic assemblage of the eastern Inner Piedmont (Brindle Creek thrust sheet).